# TARGETING INTERSTRAND CROSSLINK REPAIR TO IMPROVE CHEMOTHERAPEUTIC STRATEGIES

**Lianne Castle**
Weatherall Institute of Molecular Medicine
and
St Catherine's College

A thesis submitted to the University of Oxford for the degree of Doctor of Philosophy
Trinity Term 2017



# Abstract

Many clinically effective chemotherapeutic agents exert their toxicity through formation of DNA interstrand cross-links (ICL). These prevent the replication and transcription of DNA and if unrepaired lead to cell death.

Despite the success of ICL inducing agents in treating cancers, issues remain with a lack of sensitivity in some tumours, therapy-limiting toxicity and acquired resistance and tumour recurrence. The modulation of ICL repair could improve chemotherapy outcomes and the specific targeting of ICL repair in quiescent cells may selectively target cancer stem cells and ameliorate issues with recurrence. This thesis seeks to identify potential druggable targets that may sensitise cancer cells to ICL inducing agents and elucidate the role of ICL repair in quiescence.

Previous studies have suggested ICL repair occurs chiefly in S-phase when DNA replication forks collide with ICLs. However, recent research in budding yeast, using *Xenopus* cell-free extracts and using genetic reporter assays in mammalian cells suggests that ICL repair can occur in the G1 phase of the cell cycle via the nucleotide excision repair (NER) and translesional synthesis (TLS) pathways. Previously this G1 pathway had not been well explored in mammalian cells.

In this thesis a model for G1 ICL repair was created using a mammalian cell line. Flow cytometry analysis (FACS) of cell cycle dynamics following ICL induction in phase G1 demonstrated that repair of ICL can occur in G1 and this appears time dependent. Further analysis by FACS, comet assays and cell survival analysis confirmed repair of ICL in G1 and suggested that the NER factors XPF, XPB and

XPD and the exonucleases SNM1A and EXO1 may be required for ICL repair in G1 but not the XPG, FAN1 or CSB repair proteins.

Along-side these studies, a large-scale siRNA screen of 640 DNA damage repair genes was performed in a lung cancer cell line utilising colony formation assays to identify potential cisplatin and radiotherapy sensitising genes. Following a secondary screen, eight potential radiation and cisplatin sensitising genes were identified and examined in further detail, with the gene PIF1 finally confirmed in CRISPR/Cas9 knockout cells as a potential cisplatin sensitising gene.

The findings in this thesis confirm ICL repair can occur in G1 in mammalian cells and identify PIF1 as a potential cisplatin sensitiser in human cells. In the future, targeting of the specific endonucleases responsible for G1 ICL repair or PIF1 may offer a potential clinical cancer treatment option.

# Acknowledgements

I would like to thank my supervisors Peter McHugh and Geoff Higgins for their unending support during this D.Phil. In particular, I'd like to thank them for their support and enthusiasm for my initial application to commence this body of work and I am grateful for their continued support during my time in the laboratory through their encouragement, scientific advice, proof reading and guidance.

I am grateful to Cancer Research UK for their funding and support in my Clinical Fellowship allowing submission of this D.Phil thesis.

I am also extremely indebted to the other members of the McHugh and Higgins' Laboratories, in particular, to Lonnie Swift at the Weatherall Institute for his expert help and advice with experimental techniques and his general life advice and gossip administered at tea breaks. I would also like to thank Remko Prevo, Dorine Bax and Patsy Adamo for their invaluable help and support at the Target Discovery Institute with the large-scale genetic screens.

I'd also like to thank the other member of both laboratories: Anna for her assistance with comet assays, Gagan for his help and sympathy with the screen, Hannah for sport breaks, tea and hugs, Sook Lee for thesis editing advice, Ghadir for western blot expertise and Giocamo, Gonzalo, Kate and Ummi.

Finally, I'd like to thank my family for their support and encouragement.

# List of Abbreviations

| | |
|---|---|
| ALK | anaplastic lymphoma kinase |
| ATCC | American Type Culture Collection |
| ATR | Ataxia telangiectasia and Rad3 related |
| BER | base excision repair |
| BrdU | 5-bromo-2-deoxyuridine |
| BSA | bovine serum albumin |
| CFA | colony formation assay |
| CHO | Chinese Hamster Ovary |
| $CO_2$ | carbon dioxide |
| CPD | cyclobutane-pyrimidine dimers |
| CRISPR | clustered regularly interspaced short palindromic repeat |
| CSA | Cockaine Syndrome A |
| CSB | Cockaine Syndrome B |
| CSCs | cancer stem cells |
| DHJ | double Holliday junction |
| DMEM | Dulbecco's Modified Eagle Medium |
| DMSO | dimethyl sulfoxide |
| DNA | deoxyribonucleic acid |
| DNA-PKcs | DNA-dependent protein kinase, catalytic subunit |
| DPC | DNA-protein cross-link |
| DSB | double strand break |
| dsRNA | double-strand RNA |
| DTM | decrease in tail moment |
| EDTA | ethylenediaminetetraacetic acid |
| EGFR | epidermal growth factor receptor |
| FA | Fanconi Anaemia |
| FACS | fluorescence activated cell sorting |
| FBS | fetal bovine serum |
| GAPDH | glyceraldehyde 3-phosphate dehydrogenase |
| GG-NER | global genome nucleotide excision repair |
| HCl | hydrochloric acid |
| HJ | Holliday Junction |
| HN1 | 2-dimethylaminoethylchloride (mono nitrogen mustard) |
| HN2 | mechlorethamine hydrochloride (nitrogen mustard) |
| HR | homologous recombination |
| HTS | high-throughput screening |
| ICL | interstrand Crosslink |
| ILF | isoleucine free media |
| IMDM | Iscove's Modified Dulbecco's Medium |
| IR | ionising radiation |
| KD | knockdown |
| kDa | kiloDalton |
| KO | knockout |
| LP-BER | long patch base excision repair |
| MEF | mouse embryonic fibroblasts |
| miRNA | microRNA |

| | |
|---|---|
| MMC | mitomycin C |
| MMR | mismatch repair |
| MTT | 3-(4,5-Dimethylthiazol-2-yl)-2,5-diphenyl tetrazolium bromide |
| NER | nucleotide excision repair |
| NHEJ | non-homologous end joining |
| NSCLC | non-small cell lung cancer |
| NT | non-targeting |
| PBS | phosphate buffered saline |
| PCNA | proliferating cell nuclear antigen |
| PCR | polymerase chain reaction |
| PE | plating efficiency |
| PI | propidium iodide |
| PLK-1 | polo-like kinase 1 |
| PUVA | psoralen and ultraviolet A light |
| qRT-PCR | quantitative real-time polymerase chain reaction |
| RAS | Rat Sarcoma |
| RIR | replication independent repair |
| RNA | ribonucleic acid |
| RNAi | RNA interference |
| RPA | replication protein A |
| rpm | revolutions per minute |
| RPMI | Roswell Park Memorial Institute |
| SABR | stereotactic ablative radiotherapy |
| SCID | severe combined immunodeficiency |
| SCGE | single cell gel electrophoresis |
| sd | standard deviation |
| SDS | sodium dodecyl sulphate |
| SDS PAGE | sodium dodecyl sulphate polyacrylamide gel electrophoresis |
| SEM | standard error of mean |
| SF | surviving fraction |
| siRNA | small interfering RNA |
| SP-BER | short patch base excision repair |
| TC-NER | transcription coupled nucleotide excision repair |
| TCR | transcription coupled repair |
| TLS | translesion synthesis |
| UV | ultra violet light |
| UVA | ultra violet A light |
| WT | wild type |
| XP | Xeroderma Pigmentosum |
| 5FU | 5 fluorouracil |

# Table of Contents

**ABSTRACT** ..... **I**

**ACKNOWLEDGEMENTS** ..... **III**

**LIST OF ABBREVIATIONS** ..... **IV**

**TABLE OF CONTENTS** ..... **VI**

**LIST OF FIGURES** ..... **XII**

**LIST OF TABLES** ..... **XVII**

**CHAPTER 1 - INTRODUCTION** ..... **1**

1.1 DNA Damage ..... 2

1.1.1 Endogenous DNA Damage ..... 2

1.1.2 Exogenous DNA Damage ..... 2

1.2 DNA Damage Repair Pathways ..... 4

1.2.1 Base Excision Repair ..... 4

1.2.2 Nucleotide Excision Repair ..... 7

1.2.3 Mismatch Repair ..... 11

1.2.4 Translesion Synthesis ..... 14

1.2.5 Double Strand Break Repair ..... 16

1.2.5.1 Non-Homologous End Joining ..... 17

1.2.5.2 Homologous Recombination ..... 21

1.3 Interstrand cross-links ..... 25

1.3.1 Endogenous formation of ICL ..... 26

1.3.2 Exogenous formation of ICL ..... 29

1.3.2.1 Nitrogen mustards ..... 29

1.3.2.2 Platinum compounds ..... 32

1.3.2.3 Mitomycin C ..... 34

1.3.2.4 Psoralen ..... 36

1.4 Repair of interstrand cross-links ..... 38

1.4.1 Recognition of ICL ..... 38

1.4.1.1 ICL recognition in non-replicating cells ..... 38

1.4.1.2 ICL recognition during transcription ..... 39
1.4.1.3 ICL recognition by replication forks ..... 40
1.4.2 Basic model of ICL repair ..... 42
1.4.2.1 Single fork stalling ..... 45
1.4.2.2 Converging fork model for replication-dependent ICL repair ..... 46
1.4.2.3 Unhooking of ICLs ..... 47
1.4.2.4 Translesion synthesis and ICL repair ..... 50
1.4.2.5 Homologous recombination and ICL repair ..... 52
1.4.2.6 Involvement of base excision repair DNA glycosylases in ICL repair. ..... 53
1.5 Current understanding of replication independent repair in G1 ..... 54
1.5.1 Basic model of ICL repair in G1 ..... 54
1.5.2 Unhooking of ICL in G1 ..... 56
1.5.3 TLS bypass of ICL in G1 ..... 57
1.5.4 HR and ICL repair in G1 ..... 58
1.6 RNA interference ..... 60
1.6.1 siRNA and miRNA silencing ..... 61
1.6.2 Off-target effects ..... 63
1.6.2.1 Sequence dependent suppression of unintended targets ..... 63
1.6.2.2 Inflammatory effects ..... 65
1.6.2.3 Saturation of RNAi machinery ..... 66
1.7 siRNA screens ..... 67
1.7.1 siRNA screening in mammalian cells ..... 67
1.7.1.1 Cisplatin siRNA screens ..... 68
1.7.1.2 Radiation siRNA screens ..... 70
1.7.2 End-points for siRNA screens ..... 72
1.7.2.1 Cell growth and survival assays ..... 72
1.7.2.2 DNA damage foci quantification ..... 73
1.7.2.3 Cell proliferation ..... 73
1.7.2.4 Micronuclei assays ..... 74
1.7.2.5 Colony Formation Assays ..... 74
1.8 Cancer stem cell theory and its role in resistance to cancer treatment ..... 75
1.8.1 Origins of stem cell theory ..... 75
1.8.2 Evidence for cancer stem cells from the haematopoietic system ..... 76

1.8.3 Evidence for solid tumour cancer stem cells ..... 77
1.8.4 The role of cancer stem cells in resistance to cancer treatment ..... 79
1.9 Objectives of this thesis ..... 80

**CHAPTER 2 - METHODS ..... 81**

2.1 Materials and Reagents ..... 81
2.2 Drug Preparation ..... 81
2.3 Mammalian Cell Culture ..... 81
2.3.1 Mammalian cell lines ..... 81
2.3.2 Culture medium ..... 82
2.4 High-throughput siRNA screen ..... 83
2.4.1 siRNA libraries ..... 83
2.4.1.1 Primary siRNA screening library ..... 83
2.4.1.2 Secondary siRNA screening library ..... 83
2.4.1.3 Positive and negative controls for the siRNA screens. ..... 83
2.4.2 High-throughput siRNA transfection in 96 well plates ..... 84
2.4.3 Assessment of cell viability using Resazurin ..... 85
2.4.4 Re-plating of transfection plates ..... 85
2.4.5 Cisplatin and irradiation treatment ..... 86
2.4.6 Colony staining and counting ..... 87
2.4.7 Statistical analysis of screens ..... 87
2.5 Transient transfection of mammalian cell lines ..... 90
2.5.1 siRNA transfection (6 well format) for confirmation of siRNA screen hits . 90
2.5.2 siRNA transfection (10cm dish) for CHO cell knockdown ..... 90
2.6 Clonogenic Survival Assay ..... 92
2.6.1 6-well clonogenic survival assays for confirmation of siRNA screen hits .... 92
2.6.2 10cm dish clonogenic survival assay for CRISPR knock-out cells ..... 93
2.6.3 10cm dish clonogenic survival assays of DNA damage mutant in G1 ..... 93
2.6.4 Statistical analysis for 6-well and 10cm dish colony forming assays ..... 94
2.7 Assessment of gene expression ..... 95
2.7.1 Determination of mRNA expression by quantitative real-time PCR ..... 95
2.7.1.1 Total RNA preparation ..... 95
2.7.1.2 cDNA preparation ..... 95

2.7.1.3 qRT-PCR ..... 95
2.8 Cell Cycle Analysis ..... 97
2.8.1 Synchronisation of Chinese Hamster Ovary (CHO) cells to G1 using isoleucine starvation ..... 97
2.8.2 5-bromo-2-deoxyuridine incorporation assay and propidium iodide staining ..... 97
2.9 Modified alkaline comet assay ..... 99
2.9.1 Sample collection for modified alkaline comet assay ..... 99
2.9.2 Alkaline comet assay ..... 99
2.9.3 Comet assay analysis ..... 100

**CHAPTER 3 - RESULTS: REPAIR OF ICL IN G1 MAMMALIAN CELLS. ..... 102**

3.1 Introduction ..... 102
3.2 Flow cytometry assessment of repair of ICL in G1 ..... 105
3.2.1 Wild-type CHO cells can be synchronised to G1 and early S-phase ..... 105
3.2.2 Cell cycling is stalled in asynchronous cells to allow repair of ICL ..... 108
3.2.3 Treatment in early S-phase causes cell cycle stalling ..... 110
3.2.4 ICL repair occurs in G1 and is time dependent ..... 112
3.2.4.1 Repair of ICL in G1 with immediate release to cell cycle ..... 112
3.2.4.2 Repair of ICL in cells held in G1 for 12 hours ..... 114
3.2.4.3 Repair of ICL in cells held in G1 for 24 hours ..... 116
3.2.5 Assessment of ICL repair in DNA Damage Repair Mutants ..... 120
3.3 Determination of exonuclease involvement in G1 ICL repair ..... 126
3.4 Comet assay analysis of ICL induction and unhooking in G1 cells. ..... 134
3.4.1 Comet assay analysis of ICL induction and unhooking in G1 WT cells. ..... 134
3.4.2 Comet Assay analysis of ICL unhooking in mutant and siRNA KD CHO cells. 140
3.5 Assessment of survival following treatment in G1 or in asynchronous state 144
3.6 Conclusions ..... 152

**CHAPTER 4 - RESULTS: A LARGE-SCALE SIRNA SCREEN TO IDENTIFY CISPLATIN AND RADIATION SENSITISING GENES. ..... 158**

4.1 Introduction ..... 158
4.2 Results ..... 161
4.2.1 Large scale primary siRNA screen ..... 161
4.2.1.1 Initial optimisation of siRNA screen conditions ..... 161
4.2.1.2 Optimisation of siRNA transfection conditions ..... 162
4.2.1.3 Z-factor testing of optimal conditions ..... 165
4.2.1.4 Results from primary DNA damage siRNA screen ..... 168
4.2.2 Secondary screen of 40 potential radiation and cisplatin sensitisers. ..... 175
4.2.3 Confirmation of sensitising genes with further colony survival assays. ..... 179
4.2.3.1 siRNA suppression of LIG1 causes cisplatin sensitisation. ..... 179
4.2.3.2 siRNA suppression of DCLRE1C does not appear to sensitise to radiation in H460 cells ..... 182
4.2.3.3 siRNA suppression of CHD4 results in sensitisation to cisplatin and radiation ..... 184
4.2.3.4 siRNA suppression of CHD5 leads to sensitisation to cisplatin and radiation ..... 186
4.2.3.5 siRNA suppression of LIG3 leads to sensitisation to cisplatin but not radiation ..... 188
4.2.3.6 siRNA suppression of KDM2B induces weak sensitisation to cisplatin but not radiation ..... 190
4.2.3.7 siRNA suppression of TAL1 induces sensitisation to cisplatin but not radiation ..... 192
4.2.3.8 siRNA suppression of PIF1 causes sensitisation to cisplatin. ..... 194
4.2.4 Clonogenic assay confirmation of cisplatin sensitisation in a HAP1 knock out cell line ..... 196
4.3 Conclusions ..... 200
4.3.1 Assessment of primary and secondary siRNA screens ..... 200
4.3.2 Assessment of potential cisplatin and radiation sensitisers from the siRNA screen. 202
4.3.3 Further analysis of PIF1 as a cisplatin sensitiser. ..... 203

**CHAPTER 5 - GENERAL DISCUSSION AND FURTHER WORK ..... 205**

5.1 Investigation of ICL repair in G1 phase of the cell cycle ..... 206

5.1.1 General findings from study of ICL repair in G1 phase ..... 206
5.1.2 Further areas for study in ICL repair in G1 phase ..... 211
5.2 Large-scale siRNA screen of DNA damage response and repair targets ..... 212
5.2.1 General findings from large-scale siRNA screen ..... 212
5.2.2 Further area for study related to large-scale screen ..... 214

**APPENDIX ..... 217**

**REFERENCES ..... 262**

# List of Figures

Figure 1.1: Base Excision Repair Pathway ..... 6
Figure 1.2: Nucleotide Excision Repair Pathway ..... 10
Figure 1.3: Mismatch Repair Pathway ..... 13
Figure 1.4: Non-Homologous End Joining Repair Pathway ..... 20
Figure 1.5: Homologous Recombination Repair Pathway ..... 24
Figure 1.6: Structure of nitrogen mustards HN1 and HN2 ..... 30
Figure 1.7: Nitrogen mustard interstrand cross-link formation ..... 31
Figure 1.8: Cisplatin interstrand cross-link formation ..... 33
Figure 1.9: Mitomycin C interstrand cross-link formation ..... 35
Figure 1.10: Psoralen interstrand cross-link formation ..... 37
Figure 1.11: Proposed model of ICL repair in replicating cells. ..... 44
Figure 1.12: Proposed model for repair of ICL in G1 ..... 55
Figure 1.13: siRNA and miRNA silencing ..... 62
Figure 2.1: Layout of control siRNA for high throughput screen. ..... 85
Figure 2.2: Equations used in the statistical analysis of siRNA screens ..... 89
Figure 2.3: Formulae for calculating % decrease in tail moment (DTM) and % unhooking ..... 101
Figure 3.1: Timing of entry of synchronised WT CHO cells into early S-phase ..... 107
Figure 3.2: Cell cycle dynamics of asynchronous WT CHO cells following treatment with 50μM HN1 and 5μM HN2. ..... 109
Figure 3.3: Cell cycle dynamics of S-phase synchronised WT CHO cells following treatment with 50μM HN1 and 5μM HN2. ..... 111
Figure 3.4: Cell cycle dynamics of G1 synchronised WT CHO cells following treatment with 50μM HN1 and 5μM HN2 and immediate release to cell cycle. ..... 113
Figure 3.5: Cell cycle dynamics of G1 synchronised WT CHO cells following treatment with 50μM HN1 and 5μM HN2 and holding in G1 for 12 hours prior to release to cell cycle. ..... 115
Figure 3.6: Cell cycle dynamics of G1 synchronised WT CHO cells following treatment with 50μM HN1 and 5μM HN2 and holding in G1 for 24 hours prior to release to cell cycle. ..... 118

Figure 3.7: Flow cytometry assessment of Live/Dead Stain ..... 119
Figure 3.8: Cell cycle dynamics of G1 synchronised NER mutant CHO cells following treatment and holding in G1 for 24 hours prior to release. ..... 122
Figure 3.9: Cell cycle dynamics of G1 synchronised XPG mutant CHO cells following treatment in G1 and release to cell cycle. ..... 123
Figure 3.10: Cell cycle dynamics of G1 synchronised CSB mutant CHO cells following treatment in G1 and release to cell cycle..... 123
Figure 3.11: Cell cycle dynamics of G1 synchronised mutant NHEJ and HR CHO cells following treatment and holding in G1 for 24 hours prior to release.... 125
Figure 3.12: Cell cycle dynamics of G1 synchronised CHO-K1 WT CHO cells following treatment and holding in G1 for 24 hours prior to release. ..... 125
Figure 3.13: Cell cycle dynamics after siRNA knockdown of XPF, synchronisation to G1 and treatment in G1 with 5μM HN2 for 1 hour followed by further incubation in G1 for 24 hours prior to release to cell cycle. ..... 130
Figure 3.14: Cell cycle dynamics after siRNA knockdown of FAN1, synchronisation to G1 and treatment in G1 with 5μM HN2 for 1 hour followed by further incubation in G1 for 24 hours prior to release to cell cycle. ..... 131
Figure 3.15: Cell cycle dynamics after siRNA knockdown of SNM1A, synchronisation to G1 and treatment in G1 with 5μM HN2 for 1 hour followed by further incubation in G1 for 24 hours prior to release to cell cycle..... 132
Figure 3.16: Cell cycle dynamics after siRNA knockdown of EXO1, synchronisation to G1 and treatment in G1 with 5μM HN2 for 1 hour followed by further incubation in G1 for 24 hours prior to release to cell cycle. ..... 133
Figure 3.17: Comet Assay assessment of ICL formation. ..... 135
Figure 3.18: Change in comet tail moment with increasing doses of HN2 ..... 138
Figure 3.19: Unhooking of WT CHO cells after treatment with HN2 in G1 ..... 139
Figure 3.20: ICL unhooking in WT and DNA damage mutant CHO cells ..... 141
Figure 3.21: ICL unhooking in SNM1A siRNA and NT KD CHO cells..... 143
Figure 3.22: Survival of WT CHO cells following treatment in G1. ..... 145
Figure 3.23: Survival of XPF mutant CHO cells following treatment in G1. ..... 147
Figure 3.24: Survival of XPB mutant cells following treatment in G1. ..... 149
Figure 3.25: Survival of XPD mutant cells following treatment in G1..... 151

Figure 4.1: Screening protocol for primary and secondary screens using 96-well colony formation assay ..... 160
Figure 4.2: Optimisation of transfection reagent concentrations ..... 163
Figure 4.3: qPCR analysis of optimisation of controls with 0.05% and 0.075% INTERFERin ..... 164
Figure 4.4: Z-factor test of final conditions for large-scale siRNA screen. ..... 167
Figure 4.5: Cell viability of screen control wells 72 hours after transfection. ..... 169
Figure 4.6: Plating efficiencies for control wells in the siRNA screen. ..... 169
Figure 4.7: Surviving fractions of control wells and Z-Factor results ..... 171
Figure 4.8: Z-score distributions from primary siRNA screen ..... 174
Figure 4.9: Quality control parameters for secondary screen ..... 176
Figure 4.10: Z-scores for secondary screen genes ..... 178
Figure 4.11: Validation of LIG1 knockdown as potential cisplatin and radiation sensitiser. ..... 181
Figure 4.12: Validation of DCLRE1C knockdown as potential radiation sensitiser. ..... 183
Figure 4.13: Validation of CHD4 knock down as a potential radiation and cisplatin sensitiser ..... 185
Figure 4.14: Validation of CHD5 knockdown as potential cisplatin and radiation sensitiser ..... 187
Figure 4.15: Validation of LIG3 knockdown as potential cisplatin and radiation sensitiser. ..... 189
Figure 4.16: Validation of KDM2B knockdown as potential cisplatin and radiation sensitiser. ..... 191
Figure 4.17: Validation of TAL1 knockdown as potential cisplatin and radiation sensitiser. ..... 193
Figure 4.18: Validation of PIF1 knockdown as potential cisplatin sensitiser. ..... 195
Figure 4.19: Clonogenic survival assay comparing WT HAP1 and PIF1 KO HAP1 cells ..... 199
Figure 5.1: Model of G1 HN2 ICL repair based on experimental findings in this thesis ..... 210
Figure 5.2: Cell cycle assessment with BrdU and PI staining of asynchronous WT CHO cells following treatment with 5μM HN2. ..... 218

Figure 5.3: Cell cycle assessment with BrdU and PI staining of S-phase synchronised WT CHO cells following treatment with 5μM HN2. ..... 219
Figure 5.4: Cell cycle assessment with BrdU and PI staining of G1 synchronised WT CHO cells following treatment with 5μM HN2 and immediate release to cell cycle. ..... 220
Figure 5.5: Cell cycle assessment with BrdU and PI staining of G1 synchronised WT CHO cells following treatment with 5μM HN2 and holding in G1 for 12 hours prior to release to cell cycle. ..... 221
Figure 5.6: Cell cycle assessment with BrdU and PI staining of G1 synchronised WT CHO cells following treatment with 5μM HN2 and holding in G1 for 24 hours prior to release to cell cycle. ..... 222
Figure 5.7: Cell cycle assessment with BrdU and PI staining of G1 synchronised XPB mutated CHO cells following treatment with 5μM HN2 and holding in G1 for 24 hours prior to release to cell cycle. ..... 223
Figure 5.8: Cell cycle assessment with BrdU and PI staining of G1 synchronised XPD mutated CHO cells following treatment with 5μM HN2 and holding in G1 for 24 hours prior to release to cell cycle. ..... 224
Figure 5.9: Cell cycle assessment with BrdU and PI staining of G1 synchronised XPF mutated CHO cells following treatment with 5μM HN2 and holding in G1 for 24 hours prior to release to cell cycle. ..... 225
Figure 5.10: Cell cycle assessment with BrdU and PI staining of G1 synchronised CSB mutated CHO cells following treatment with 5μM HN2 and holding in G1 for 24 hours prior to release to cell cycle. ..... 226
Figure 5.11: Cell cycle assessment with BrdU and PI staining of G1 synchronised CSB mutated CHO cells following treatment with 5μM HN2 and immediate release to cell cycle. ..... 227
Figure 5.12: Cell cycle assessment with BrdU and PI staining of G1 synchronised XPG mutated CHO cells following treatment with 5μM HN2 and holding in G1 for 24 hours prior to release to cell cycle. ..... 228
Figure 5.13: Cell cycle assessment with BrdU and PI staining of G1 synchronised XPG mutated CHO cells following treatment with 5μM HN2 and immediate release to cell cycle. ..... 229

Figure 5.14: Cell cycle assessment with BrdU and PI staining of G1 synchronised and EXO1 siRNA suppressed CHO cells following treatment with 5μM HN2 and holding in G1 for 24 hours prior to release to cell cycle. ..... 230
Figure 5.15: Cell cycle assessment with BrdU and PI staining of G1 synchronised and FAN1 siRNA suppressed CHO cells following treatment with 5μM HN2 and holding in G1 for 24 hours prior to release to cell cycle. ..... 231
Figure 5.16: Cell cycle assessment with BrdU and PI staining of G1 synchronised and SNM1A siRNA suppressed CHO cells following treatment with 5μM HN2 and holding in G1 for 24 hours prior to release to cell cycle. ..... 232
Figure 5.17: Cell cycle assessment with BrdU and PI staining of G1 synchronised and XPF1 siRNA suppressed CHO cells following treatment with 5μM HN2 and holding in G1 for 24 hours prior to release to cell cycle. ..... 233

# List of Tables

Table 2.1: Chinese Hamster cell lines used for experiments in this thesis. ..... 82
Table 2.2: siRNA sequences for siRNA knockdown experiments ..... 91
Table 2.3: Cell numbers plated for different treatment modalities ..... 92
Table 2.4: qRT-PCR primer forward (F) and reverse (R) sequences ..... 96
Table 4.1: Genes selected from secondary screen for further analysis. ..... 179
Table 5.1: List of genes from primary siRNA screen and their respective Z scores for sensitisation to radiation. ..... 234
Table 5.2: List of genes from primary siRNA screen and their respective Z-scores for cisplatin treatment. ..... 247
Table 5.3: List of genes included in secondary screen and their respective Z-scores ..... 260

# Chapter 1 - Introduction

The DNA of cells is continually susceptible to damage as a consequence of exposure to environmental agents, reactive species from cellular metabolic processes and exogenous agents such as chemotherapeutic agents. These insults lead to chemical modifications to DNA such as strand breaks or base modifications, usually on one strand of the DNA, and covalent adducts between DNA bases on opposing strands of the DNA leading to interstrand cross-links (ICL).

The replication of DNA containing unrepaired damage to bases can lead to mutations resulting in modified cell phenotype or cell death. Accurate cellular detection and repair of DNA damage is essential to remove lesions and avoid genetic instability. This is achieved through direct reversal repair of lesions and by eliciting damage responses that are able to moderate the effects of the DNA damage.

An undamaged DNA template strand is essential for the repair of DNA lesions via the base excision repair (BER) and nucleotide excision repair (NER) pathways. Both of these pathways require cleavage of the DNA lesion and gap filling by DNA polymerases. Double-strand breaks (DSB) caused by ionising radiation (IR) are particularly cytotoxic lesions that are mainly repaired through two distinct mechanisms- homologous recombination (HR) or non-homologous end joining (NHEJ). Interstrand cross-links (ICL) require the repair of damage to both strands of the DNA helix making the agents that cause these lesions particularly deleterious and the lesions are more complex to repair requiring the contribution of several DNA damage pathways.

If DNA lesions are left unrepaired and cellular processes, such as transcription and replication, are impaired by this damage, cell death may result. It is this cytotoxic response that is utilised by chemotherapy agents and further understanding of the repair of this damage is essential to understand potential resistance to chemotherapy agents.

## 1.1 DNA Damage

### 1.1.1 Endogenous DNA Damage

DNA is constantly exposed to cellular chemicals that may lead to DNA damage. These cellular chemicals include derivatives of oxygen, water and lipid peroxidation products. For example, intracellular respiration produces reactive oxygen species (ROS), such as hydroxyl radicals, that are able to react with guanine bases to form the mutagenic base 8-hydroxyguanine (8-oxoG) (Dizdaroglu and Jaruga, 2012). Hydrolysis of glycosylic bonds by water can cause DNA depurination and can lead to deamination of cytosines (Lindahl and Karlstrom, 1973). Lipid peroxidation produces alkylating species that can react with DNA to form adducts and S-adenosylmethionine (SAM) present in all cells can cause methylation of DNA (Lindahl and Barnes, 2000). Finally, erroneous physiological DNA replication can lead to base mispairing, deletions and duplications.

### 1.1.2 Exogenous DNA Damage

There are a wide variety of exogenous DNA damaging agents. The two most common exogenous DNA damaging agents are ionising (IR) and ultra-violet (UV) radiation. UV irradiation from sunlight causes photoadducts as covalent linkages between pyrimidines, cyclobutane pyrimidine dimers (CPDs) and pyrimidine-(6-

4)-pyrimidone photoproducts (6-4PPs). These can both block DNA replication and transcription (Sinha and Hader, 2002). IR can damage DNA by generating ROS that react with DNA to form adducts and by causing single-strand and double-strand breaks (SSBs and DSBs).

Other exogenous sources of DNA damage include reactive chemicals from tobacco smoke, aldehydes and formaldehyde from alcohol consumption and chemotherapeutic drugs. Chemotherapeutic drugs damage DNA by forming a variety of lesions including monoadducts, intrastrand cross-links, interstrand cross-links and DNA-protein cross-links.

## 1.2 DNA Damage Repair Pathways

The majority of DNA lesions can be repaired by directly reversing the damage or by using the undamaged DNA template strand to achieve error-free repair. An example of direct reversal of a lesion is the action of DNA photolyases, such as cyclobutane pyrimidine dimer photolyase, that can reverse UV-induced pyrimidine dimers (Sancar, 2003). Complex DNA damage requires the actions of multistep pathways, which may act in co-ordination, and are discussed further below.

### 1.2.1 Base Excision Repair

Base excision repair (BER) is the pathway responsible for correcting the most common forms of endogenous DNA damage that result from single base deamination, oxidation and alkylation. The BER pathway, illustrated in Figure 1.1, consists of the following steps: initial excision of a chemically altered base moiety, incision at the resulting abasic site, replacement of the excised nucleotide, clean up of the terminal ends and finally sealing of the nick in the DNA backbone. Each step can be performed in isolation but studies suggest the proteins involved in BER act in a co-operative fashion (Wilson and Kunkel, 2000).

Initial recognition and excision of chemically modified bases is carried out by the DNA glycosylases which recognise specific base modifications and catalyse hydrolysis of the N-glycosylic bond (Dizdaroglu, 2005). This results in an abasic (AP) site with an intact phosphodiester backbone.

Monofunctional DNA glycosylases, such as uracil DNA glycosylase (UDG), are able to catalyse the hydrolysis of the glycosylic bond and remove the damaged base from the DNA backbone. Bifunctional glycosylases, such as 8-guanine glycosylase

(OGG1), are able to both excise substrate bases and incise the DNA backbone immediately 3' to the AP site (Hazra et al., 2001). The resulting single strand break contains a 3'-α,β-unsaturated aldehyde or 3'-phosphate. This is "cleaned up" and resolved to a 3'hydroxyl.

Following the actions of the Monofunctional glycosylases, apuric endonuclease 1 (APE1) makes an incision 5' to the AP site and generates a single nucleotide gap (Wiederhold et al., 2004). If the initial excision was performed by a bifunctional glycosylase APE1 acts to restore a 3'-hydroxyl from a 3'-α,β-unsaturated aldehyde. End processing in humans is also performed by polynucleotide kinase-phosphatase (PNKP), which phosphorylates 5' hydroxyl ends and removes phosphates from 3' ends. DNA polymerase β (POLβ) then replaces the excised damaged nucleotide and removes the 5'-terminal abasic fragment left behind by APE1 incision (Wilson, 1998). To complete repair the DNA is ligated by either a complex of X-ray cross-complementing 1 (XRCC1) protein and DNA Ligase 3α (LIG3α) or DNA Ligase 1 (LIG1) (Tomkinson and Mackey, 1998).

This pathway, which involves replacement of a single nucleotide and POLβ, is referred to as short patch BER (SP-BER). If the 5'-moiety is refractory to POLβ then strand displacement synthesis is required and an alternative long patch BER (LP-BER) pathway occurs which involves the recruitment of proliferating cellular nuclear antigen (PCNA) (Gary et al., 1999), replication factor C (RFC) and the polymerases Polε and Polδ to insert multiple nucleotides. The resulting 5'-flap is excised by the flap endonuclease, FEN1 and LIG1 seals the nick in the DNA backbone to complete repair (Tomkinson et al., 2001) (Figure 1.1).

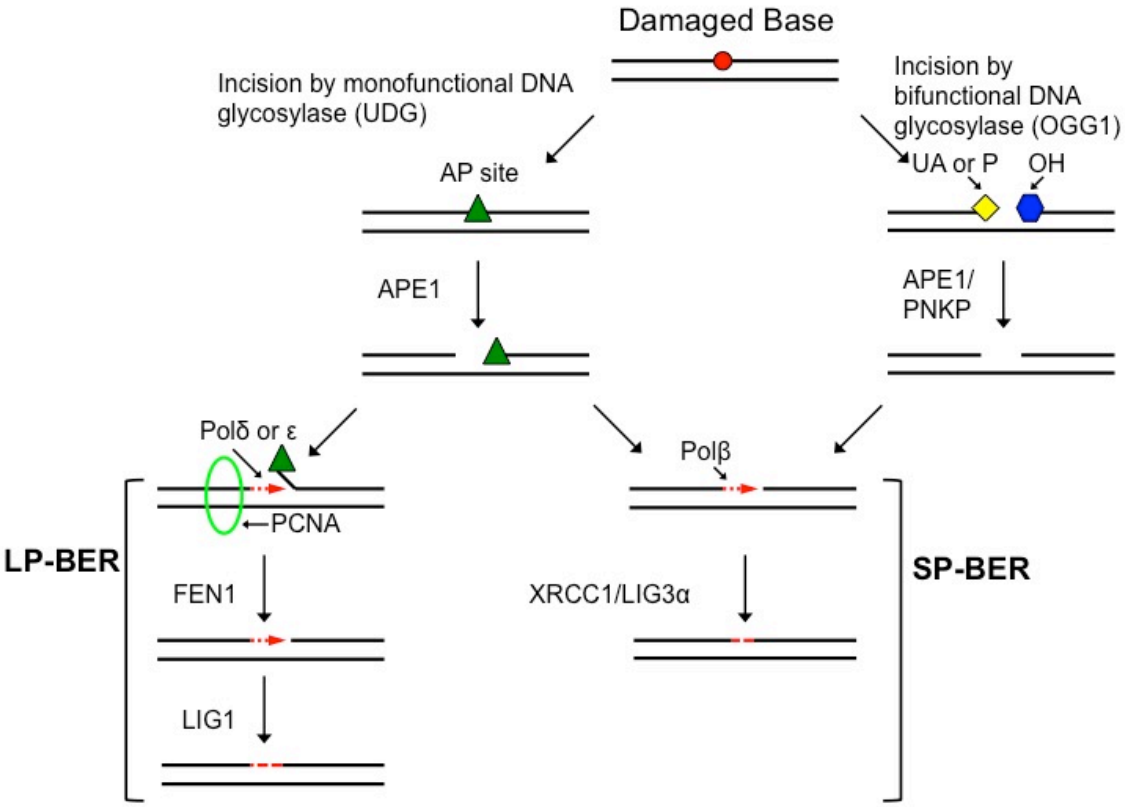



**Figure 1.1: Base Excision Repair Pathway**

A damaged base is shown by a red circle, the AP site and 5'deoxyribose phosphate by a green triangle, the α,β-unsaturated aldehyde (UA) or phosphate (P) by a yellow diamond, hydroxyl by a blue hexagon, and the newly incorporated nucleotides by a red dashed line.

LP-BER: long patch base excision repair.
SP-BER: short patch base excision repair.

### 1.2.2 Nucleotide Excision Repair

Nucleotide excision repair (NER) is the main repair pathway responsible for removal of bulky helix distorting lesions caused by environmental mutagens, UV irradiation and chemotherapeutic agents. It can eliminate lesions by a multistep 'cut and patch' type reaction. This repair involves at least 30 polypeptides within two different sub-pathways, the global genome repair (GG-NER) sub-pathway, which prevents mutations by continually scanning the entire genome for helix distorting lesions, and the transcription coupled repair (TC-NER) pathway, which removes transcription-blocking lesions to allow unperturbed gene expression. Defects in GG-NER result in cancer predisposition, in contrast defects in TC-NER can cause a variety of diseases such a ultra-violet sensitivity syndromes and severe premature aging syndromes such as Cockayne syndrome.

As illustrated in Figure 1.2, in GG-NER the DNA damage sensor XPC, in association with UV excision repair protein RAD23B (Masutani et al., 1994) and centrin 2 (Nishi et al., 2005), scans the genome for DNA structures which cause DNA helix distortion. It then binds to the small single strand DNA (ssDNA) gap caused by disrupted base pairing opposite the lesion (Min and Pavletich, 2007). Some UV cyclobutane-pyrimidine dimers (CPDs) only mildly distort the DNA complex (Reardon and Sancar, 2003). To allow repair of these lesions the UV-DDB (ultraviolet radiation-DNA damage-binding protein) complex, comprised of DDB1 (also known as XPE-binding factor) and the protein DDB2 (Chu and Chang, 1988) binds to UV lesions and stimulates the subsequent binding of XPC (Wakasugi et al., 2002). Once the XPC complex binds to the DNA damage RAD23B dissociates.

In the TC-NER pathway damage is directly recognised when RNA Polymerase II is stalled by a DNA lesion (Laine and Egly, 2006) (Figure 1.2). RNA Pol II interacts with UV-stimulated scaffold A (UVSSA), ubiquitin-specific-processing protease 7 (USP7) and Cockayne syndrome protein B (CSB) transiently during transcript elongation (Schwertman et al., 2012). On stalling the affinity of CSB for RNA Pol II increases and the Cockayne syndrome WD repeat protein A (CSA)-CSB complex is formed. This may result in backtracking of RNA Pol II allowing the DNA lesion to become accessible for repair (Sigurdsson et al., 2010).

Following damage recognition the TFIIH (transcription initiation factor IIH) complex is recruited to the DNA lesion in both GG-NER and TC-NER (Riedl et al., 2003; Yokoi et al., 2000). TTFIIH is a transcription initiation and repair factor consisting of 10 protein subunits (Compe and Egly, 2012). The two helicase subunits of TFIIH XPB and XPD have different polarities and unwind the DNA to create a bubble structure (Tapias et al., 2004). Assessment of archaeal XPD orthologues has demonstrated that undamaged ssDNA but not damaged DNA can pass through the Arch and Fe-S cluster domains of XPD (Fan et al., 2008; Wolski et al., 2008). If XPD does not detect any damage the repair reaction may be aborted (Mathieu et al., 2013). Following unwinding of the DNA around the lesion, XPA binds and forms a pre-incision complex with XPG and replication protein A (RPA). XPA promotes the release of the cyclin-dependent kinase (CDK)-activating kinase (CAK) complex from the TFIIH complex which assists in the recruitment of XPF-excision repair cross complementing 1 (XPF-ERCC1) and XPG endonuclease (Coin et al., 2008). RPA binds to the ssDNA opposite the DNA lesion and is thought to

help guide XPF-ERCC1 and XPG and also protect the undamaged DNA strand (Overmeer et al., 2011).

Following DNA damage verification dual incisions are first made by XPF-ERCC1 and then XPG, each incising the damaged strand 5' and 3' to the lesion respectively. A single strand gap is formed and undergoes gap filling, after recruitment of PCNA and RFC, by the polymerases DNA Polδ, ε or κ (Ogi et al., 2010). Finally, LIG1 or LIG3 seals the nick in the DNA backbone. The specific involvement of polymerases depends on the proliferative stage of the cell. In replicating cells DNA Polε and LIG1 operate and non-replicating cells perform gap filling with DNA Polκ and ligation with LIG3 (Moser et al., 2007) (Figure 1.2).

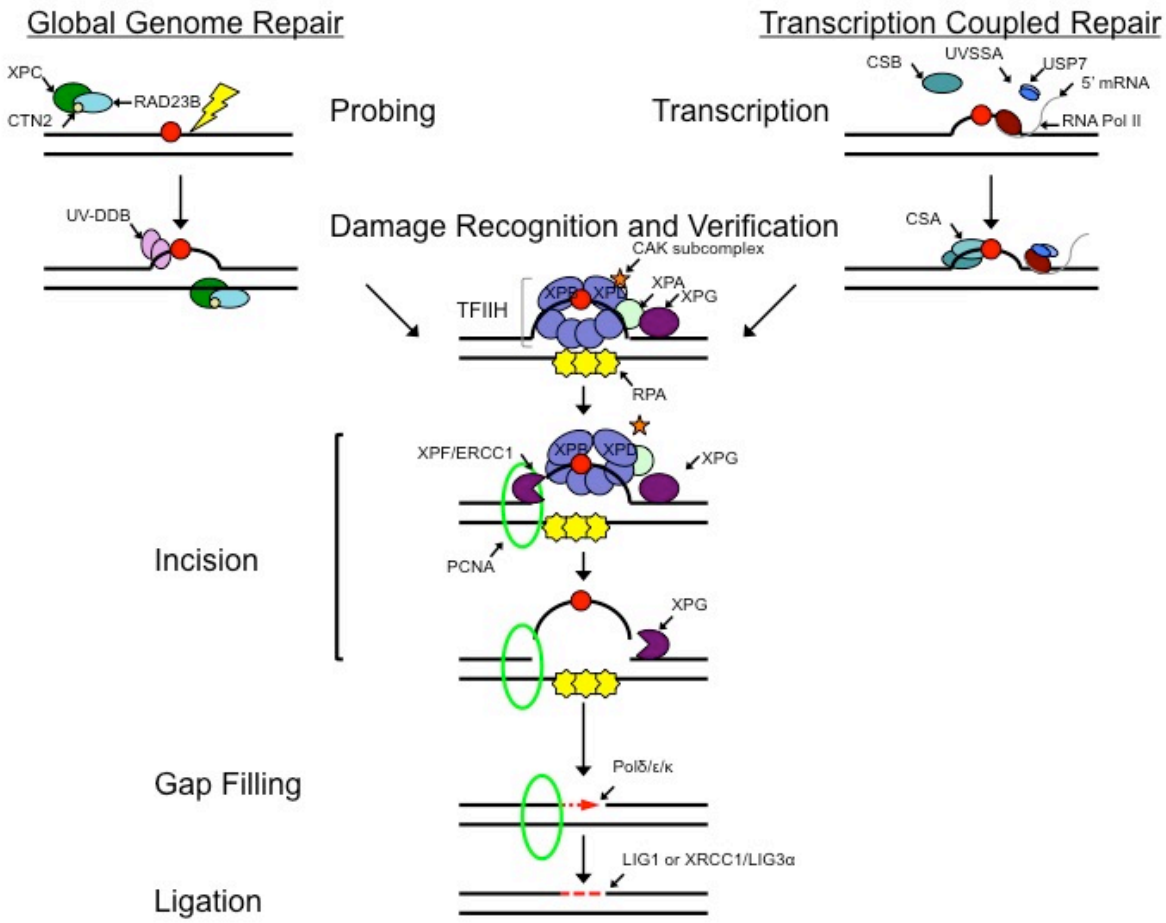



**Figure 1.2: Nucleotide Excision Repair Pathway**

The key proteins in both the GG-NER and TC-NER pathways are illustrated. Damaged nucleotide illustrated with a red circle, newly synthesised DNA labelled with red dashed line. Figure adapted from Marteijn *et al* (Marteijn et al., 2014).

### 1.2.3 Mismatch Repair

Mismatch repair (MMR) is responsible for correcting DNA mismatches created during DNA replication and preventing these from becoming permanently fixed in dividing cells (Kunkel and Erie, 2005). Therefore, defects and deficiencies in MMR lead to increased mutation rates (Tiraby and Fox, 1973) and sporadic and hereditary cancers (Lynch and la Chapelle, 1999). MMR has an important role in the DNA damage response pathway in eliminating severely damage cells and preventing mutagenesis and tumorigenesis.

MMR is a highly conserved pathway between prokaryotes and eukaryotes (Modrich and Lahue, 1996). In eukaryotes, repair is initiated when MutSα or MutSβ bind to a mismatch (Figure 1.3). MutSα is a heterodimer of MSH2 and MSH6 and primarily repairs single base mismatches and insertion-deletion loops (IDLs) that are 1-2 bases long. MutSβ is a heterodimer of MSH2 and MSH3 and repairs IDLs with mismatches containing up to 16 nucleotides in one strand (Genschel et al., 1998; Palombo et al., 1996). Crystal studies of these heterodimers show they form a clamp-like structure that is similar to PCNA around the DNA (Warren et al., 2007). They are able to move along the DNA helix and pause when a mismatch is sensed.

Following binding of MutS to dsDNA a further heterodimer, MutL, is recruited to the mismatch. MutL also has a number of isoforms including MutLα, MutLβ and MutLγ which are heterodimers of MLH1 and PMS2, PMS1 and MLH3 respectively (Kunkel and Erie, 2005). MutLα is involved in post replicative MMR, MutLγ plays a role in meiosis and no specific biological role has been identified for MutLβ

(Cannavo et al., 2005). Like MutS, MutLα also forms a clamp-like structure around the DNA helix (Guarne, 2012). It is not clear if MutLα slides along DNA with MutS or if it is only loaded onto DNA after the mismatch is identified.

In order to preserve genome integrity MMR must selectively occur on the strand of DNA that contains the mismatch. In eukaryotic cells one study found that the MMR machinery interacted with the replication apparatus and therefore this helps discriminate strands (Wagner and Meselson, 1976).

More recent studies in yeast have identified that ribonucleotides, incorporated into DNA by Pol ε during leading strand synthesis, may play an important role in signalling sites of mismatch repair (Ghodgaonkar et al., 2013; Lujan et al., 2013).

Ribonucleotides are incorporated by RNA primases (Kuchta and Stengel, 2010) and primase-polymerases (Martinez-Jimenez et al., 2015) during TLS (Goodman and Woodgate, 2013), specialised DNA repair and during R-loops formation (Sollier and Cimprich, 2015). They are efficiently removed by RNase H2 via 5' nicks; which may also provide a mechanism to discriminate between newly synthesised and template strands in MMR. MutLα can load at these nicks and perform a further incision through activation by PCNA(Pluciennik et al., 2010). This allows removal of the mismatch (Ghodgaonkar et al., 2013; Lujan et al., 2013). On the lagging strand the presence of frequent DNA termini prior to completion of Okazaki fragments may provide a similar entry point for MutLα.

Following excision of the mismatch, RPA stabilises the single stranded DNA region and the gap formed is filled by polymerase δ (Polδ) and repair is completed by DNA ligase 1 (LIG1) (Iyama and Wilson, 2013) (Figure 1.3).

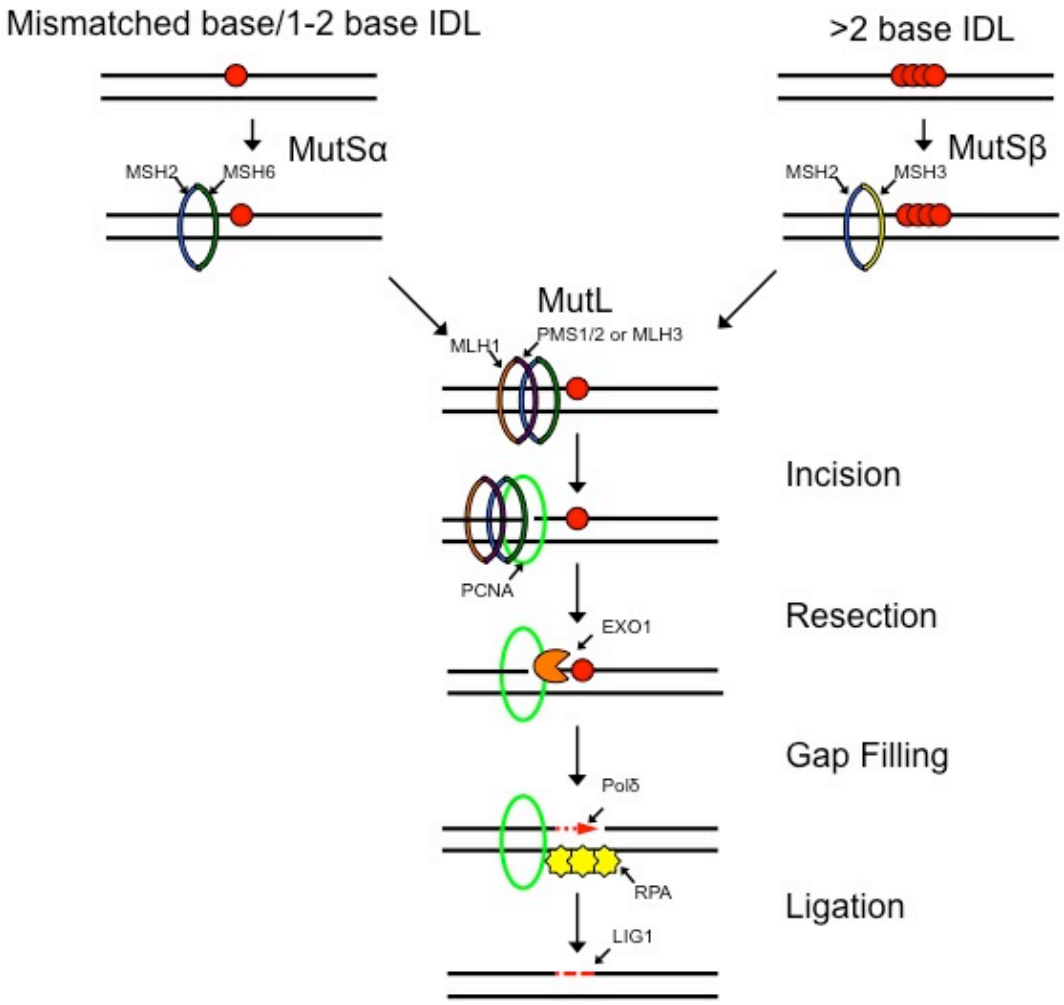



**Figure 1.3: Mismatch Repair Pathway**

Schematic diagram of mismatch repair pathway with mismatched bases shown as red circles. Key proteins in pathway are as labelled in figure. Newly synthesised DNA is illustrated with red dashed line.

### 1.2.4 Translesion Synthesis

Cellular DNA is replicated with high efficiency and fidelity. This replication is easily disturbed by damage to the DNA template and replication polymerases are intolerant of most DNA lesions leading to DNA synthesis arrest. To tolerate this, DNA is synthesised past the damaged bases by a process known as translesion synthesis (TLS). This process is completed by specialised DNA polymerases, the most abundant of which belong to the Y-family (Ohmori et al., 2001), which have poor processivity and lack proof-reading exonuclease activity leading to low fidelity (Friedberg et al., 2001). This mechanism of replication past DNA damage was first noted in the 1960s when UV irradiation of *E. coli* was discovered to cause gaps in DNA which could subsequently be sealed resulting in the suggestion that an error-prone DNA polymerase path existed (Rupp and Howard-Flanders, 1968).

The basic steps of TLS are as follows: initially a stalled replicative polymerase is replaced with a TLS polymerase that inserts a correct or incorrect base opposite the DNA lesion. Extension then occurs from the inserted base by the same or a second polymerase. Once base pairing is completed beyond the lesion a replicative polymerase then continues DNA copying (Johnson et al., 2000; Woodgate, 2001; Shachar et al., 2009).

The initial step of 'polymerase switching', when replicative polymerases are displaced and specialised TLS polymerases recruited, appears to be activated by the monoubiquitination of PCNA. On encountering DNA damage replication stalls leading to exposure of ssDNA, which is coated by the ssDNA binding protein RPA. RPA recruits Rad18 (Davies et al., 2008), a E3 ubiquitin ligase, which is able to collaborate with Rad6, an E2 ubiquitin conjugating enzyme, to monoubiquitinate

PCNA at its lysine-164 residue (Lehmann et al., 2007; Hoege et al., 2002). TLS polymerases possess ubiquitin binding motifs (UBZ and UBM) (Bienko et al., 2005) which increase their affinity for ubiquitylated PCNA at the blocked replication site leading to base insertion opposite the DNA lesion. The switch to TLS polymerases also involves Rev1 which is able to interact with TLS polymerases and PCNA through its C-terminus and N-terminus respectively (Friedberg et al., 2005).

It is possible, in some cases, that lesion bypass can occur in a single step by a single DNA polymerase, for example the bypass of CPDs by Polη. However, in mammalian cells evidence suggests a two-step mechanism exists for TLS bypass (Sale, 2013; Prakash et al., 2000). Initially a base is inserted opposite the lesion possibly by Polη, ι or κ. Following this a second extender polymerase, such as Polζ extends beyond the base pair involved in the lesion until the replicative polymerase takes over DNA synthesis (Livneh et al., 2010).

### 1.2.5 Double Strand Break Repair

Double-strand breaks (DSB) occur when the phosphate backbones of two complementary DNA strands are broken simultaneously in close proximity. They are one of the most cytotoxic DNA lesions and can cause genome rearrangements and cell death. Defective DSB repair is a major driver for cancer (Jackson and Bartek, 2009) and is also associated with developmental, immunological and neurological disorders (McKinnon, 2009).

DSB can arise following exposure to exogenous agents such as ionising radiation (IR) but a major endogenous cause of one sided DSB occurs when replication forks encounter DNA damage leading to fork collapse (Pfeiffer et al., 2000).

DSB are also generated in a programmed fashion by cells in some specific situations. For example, meiotic DSB repair is required to allow chromosome segregation at the first meiotic division and generation of unique gametes (Keeney and Neale, 2006). DSB-induced rearrangements of immunoglobulin genes are also essential to maintain antigen receptor diversity (Dudley et al., 2005).

There are two major DSB repair pathways: homologous recombination (HR, Figure 1.5) and non-homologous end joining (NHEJ, Figure 1.4). These pathways are discussed in more detail below. NHEJ acts independently of the cell cycle but is error-prone whereas HR functions in S-phase and G2 phase of the cell cycle (Rothkamm et al., 2003). It appears that the choice through which pathway the DSB is repaired depends on the nature of the DSB and the accessibility of the DNA ends to resection.

### 1.2.5.1 Non-Homologous End Joining

NHEJ allows the modification and ligation of broken DSB ends with very little homology. This often creates small deletions or insertions and accordingly NHEJ is considered an error-prone mechanism of DSB repair. NHEJ can occur at any point in the cell cycle but appears to be more important in G1 when the 5' to 3' end resection that initially occurs in HR is inhibited.

Canonical-NHEJ (c-NHEJ) proceeds in three steps: DNA damage recognition and recruitment of repair proteins, DNA termini processing and a third step of DNA ligation. These steps are illustrated in Figure 1.4.

Initial recognition of DSB is performed by the Ku heterodimer, Ku70 and Ku80 (Mari et al., 2006; Mimori and Hardin, 1986). The binding of the Ku heterodimer blocks any non-specific processing of the DSB and keeps the broken strands closely opposed to allow for ligation (Pang et al., 1997). Ku is able to rapidly localise to DSB and acts as a protein scaffold (Zhang et al.) forming a Ku:DNA complex at which the nucleases, polymerases and ligases of NHEJ (Lieber, 2008) can dock. As there are two DNA ends, two Ku:DNA complexes form and allow modification of each DNA end in preparation for re-joining. Binding of the Ku heterodimer to the DNA ends allows the assembly of DNA-dependent protein kinase catalytic subunit (DNA-PK*cs*) (Uematsu et al., 2007), X-ray repair complementing protein 4 (XRCC4) (Costantini et al., 2007), XRCC4-like factor (XLF) (Yano et al., 2008; Yano and Chen, 2014), DNA Ligase IV (LIG4) (Costantini et al., 2007) and aprataxin-and PNK-like factor (APLF) (Grundy et al., 2013). It is presumed that Ku changes conformation on binding to DNA as it is unable to form stable complexes with DNA-PK*cs* when DNA ends are absent (Yaneva et al., 1997).

DNA-PK*cs* kinase activity is activated by the Ku heterodimer and it assists in bridging the ends of the DNA strands together (Cary et al., 1997). XRCC4 is able to form a multimeric protein complex with LIG4 which interacts with the Ku heterodimer (Mari et al., 2006). XLF also interacts with the Ku heterodimer and XRCC4 (Yano et al.). It has been proposed that XRCC4-XLF forms filaments that are used to help bridge the opposing DNA strands together (Malivert et al., 2010).

Recent work has also identified a novel XRCC4 superfamily member, Paralog of XRCC4 and XLF (PAXX) (Ochi et al., 2015). Assessment of this protein by immunoprecipitation and western blotting revealed that PAXX interacts with Ku and depletion of PAXX increased cellular sensitivity to IR suggesting a role in DSB repair. Depletion of PAXX and XRCC4 or PAXX and XLF did not induce IR sensitivity greater than depletion of PAXX, XRCC4 or XLF alone suggesting PAXX functions epistatically with XRCC4 and XLF as a NHEJ factor.

To allow ligation the DNA ends need processing to allow them to possess the appropriate 5' phosphate or 3' hydroxyl ends. The chemical nature of the DSB determines which enzyme performs this role. Artemis (DNA cross-link repair enzyme 1C, DCLRE1C) is the major protein that repairs DSB ends produced by IR and its activity is mediated by DNA-PK*cs* (Woodbine et al., 2011). Polynucleotide 3' phosphate (PNKP) is able to phosphorylate 5' ends (Coquelle et al., 2011) and dephosphorylate 3' ends and aprataxin-PNKP-like factor (APLF) can perform end resection of 3' overhangs through its exonuclease activity (Li et al., 2011). Prior to ligation any gaps are filled by DNA polymerases μ or λ and the XRCC4-LIG4 complex re-joins the ends of DNA (Ahnesorg et al.).

An alternative NHEJ pathway (alt-NHEJ or microhomology-mediated end joining (MMEJ) also exists which operates in the absence of c-NHEJ (Figure 1.4). This pathway performs much slower DSB repair than c-NHEJ (Wang et al., 2003) and is considered to be more error-prone than c-NHEJ as sequence alterations at the DSB junctions and translocations can occur more frequently and extensively than c-NHEJ leading to genetic instability (Lieber, 2010). Alt-NHEJ can function throughout the cell cycle (Iliakis, 2009) but is thought to be enhanced in S and G2 (Wu et al., 2008a; b). It has been proposed that alt-NHEJ may function when both c-NHEJ and HR have failed to proceed.

This pathway is dependent on signalling by poly(ADP-ribose) polymerase 1 (PARP1) (Audebert et al., 2006) and involves limited resection of DNA ends by MRN (MRE11-RAD50-NBS1) and CtIP (carboxy-terminal binding protein (CtBP) interacting protein) (Rass et al., 2009). This leads to regions of homology that are able to base pair and drive ligation of opposing DNA ends. The annealed DNA ends undergo fill-in synthesis by the DNA polymerase θ (Polθ) (Mateos-Gomez et al., 2015) which stabilises the annealed intermediates and promotes end joining by LIG3 (Audebert et al., 2004).

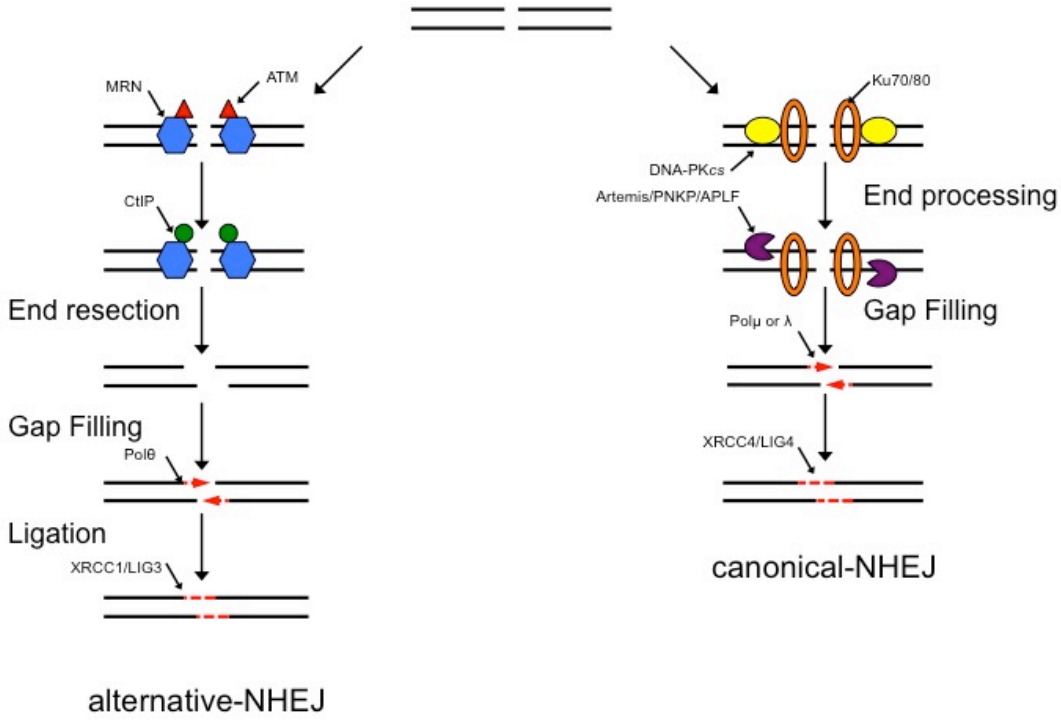



**Figure 1.4: Non-Homologous End Joining Repair Pathway**

Schematic representation of NHEJ with newly synthesised DNA represented by red dashed line.

### 1.2.5.2 Homologous Recombination

Homologous recombination (HR) is a largely error-free DSB repair pathway which requires a sister chromatid as a template for DNA synthesis. This pathway principally functions in S and G2 phases of the cell cycle (Symington and Gautier, 2011). HR involves several steps to repair DSB. The initial step involves the recognition, resection and coating of the DNA ends by proteins with high affinity for ssDNA and the formation of nucleoprotein filaments. This is followed by filament invasion of the sister chromatid DNA leading to the formation of a crossover Holliday junction (HJ). Branch migration is co-ordinated by the helicases allowing alignment of DNA strands, further expansion of the Holliday junction and polymerase synthesis of the missing DNA occurs. Finally, nuclease incision and ligation of DNA occurs to reverse the Holliday junction. These steps and the proteins involved are illustrated in Figure 1.5.

The MRN complex of MRE11-RAD50-NSB1 detects the DSB and recruitment of CtIP and ATM occurs. CtIP activates the exonuclease activity of MRE11 leading to end resection producing 3' overhangs and ssDNA (Mimitou and Symington, 2008; Buis et al., 2008).

More recently, the exonuclease 3'-5' domain containing 2 (EXD2) has been identified as also contributing to end resection (Broderick et al., 2016). EXD2 is a recently identified exonuclease which appears conserved across vertebrates, it interacts with the MRN complex and depletion of EXD2 was shown to impair DNA end resection following DSB formation suggesting this exonuclease may play a role in the initial steps of end resection, promoting HR and DSB repair.

The MRN complex also recruits RPA and activates the DNA damage checkpoint kinases. The initial CtIP-dependent resection is common to alt-NHEJ and HR (Rass et al., 2009) but the pathways diverge when further 5' to 3' resection occurs by either exonuclease 1 (EXO1) or DNA2 exonuclease/helicase in collaboration with Bloom syndrome helicase (BLM) (Nimonkar et al., 2011).

The resulting ssDNA is coated by RPA, which protects the ssDNA from further end processing. RPA triggers ATR and the intra-S/G2/M checkpoint response. This leads to phosphorylation of Chk1 and RAD51, promoting repair of DSB by HR (Sorensen et al., 2005). Breast cancer susceptibility gene 2 (BRCA2) promotes the displacement of RPA from ssDNA and the formation of RAD51 nucleoprotein filaments (Jensen et al., 2010). These RAD51 nucleoprotein filaments are required for strand invasion and homology searching of sister chromatid DNA to allow template repair (Baumann et al., 1996). Several RAD51 paralogues are able to form nucleoprotein filaments these include XRCC2, XRCC3, RAD51B and RAD51C. RAD51C is able to form a structure that keeps the DNA strands separate, the displacement loop (D-loop). The DNA polymerase η (Polη) may be responsible for extending the invading DNA strand to form a D-loop (Moldovan et al., 2010).

Following D-loop formation repair proceeds via two main pathways, synthesis dependent strand annealing (SDSA) or DSB repair (DSBR). SDSA occurs if the nascent strand is displaced after a limited amount of DNA synthesis. The nascent synthesised strand then anneals to the original complementary DNA (Ferguson and Holloman, 1996), following further DNA synthesis and removal of flap products, a non-cross over product is created. This is the major pathway in mitotic cells.

In DSBR, invasion of two D-loops occurs into the sister chromatid resulting in the creation of a double Holliday junction (DHJ) (Schwacha and Kleckner, 1995). These require cleavage and the manner of resolution results in differing genetic outcomes. Resolution is achieved by the combined actions of the different structure specific endonucleases MUS81-EME1, SLX1-SLX4 and GEN1. These cut the DHJ in different orientations leading to 50% crossover products (Moynahan and Jasin, 2010). The cut ends are then re-joined by DNA ligase 1.

Alternatively, the two Holliday junctions can be brought together by branch migration by BLM in association with BLAP75 and topoisomerase IIIα resulting in dissolution of the Holliday junction and the generation of non-crossover products (Wu and Hickson, 2003).

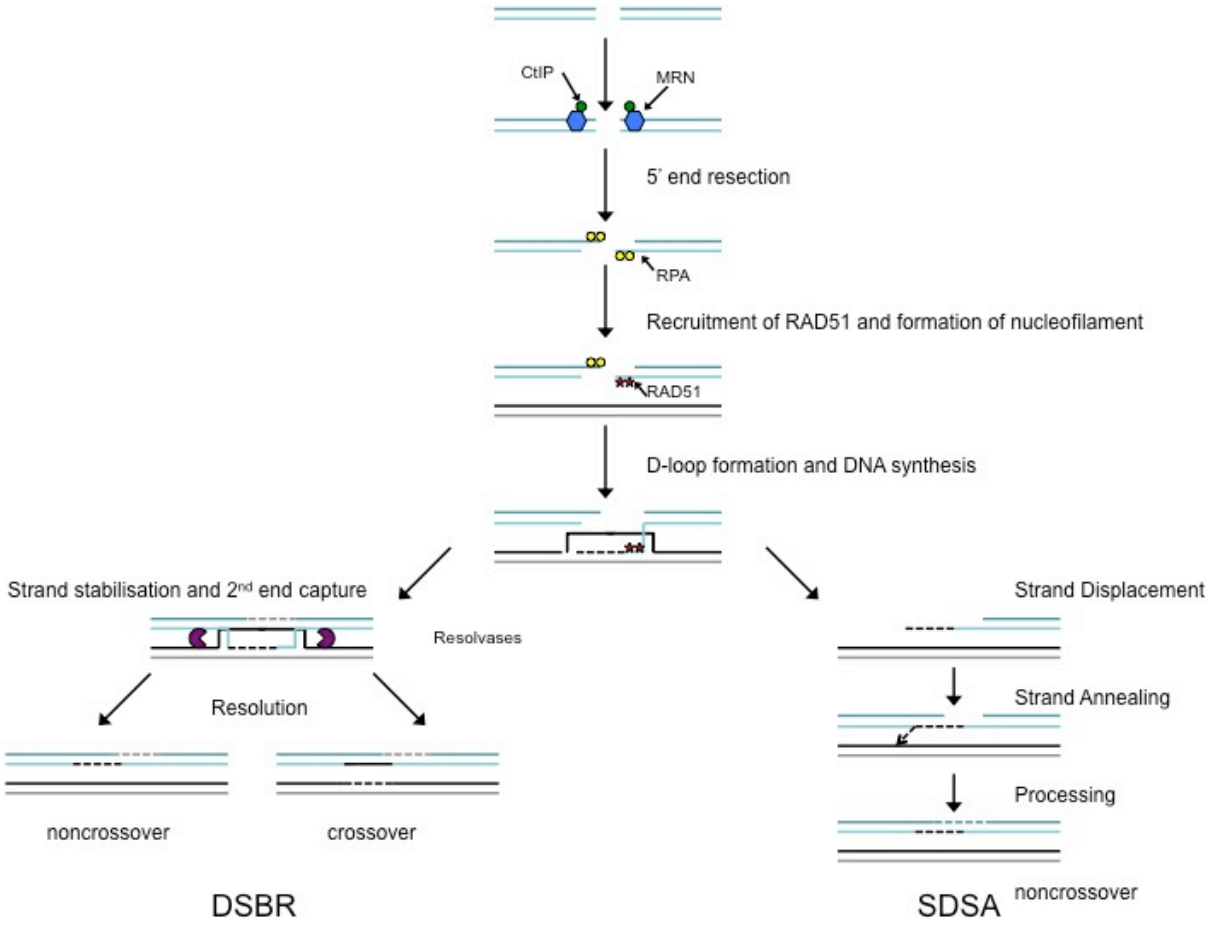



**Figure 1.5: Homologous Recombination Repair Pathway**

Schematic diagram of homologous recombination repair with newly synthesised DNA represented by dashed lines.

DSBR: double strand break repair
SDSA: synthesis dependent strand annealing

## 1.3 Interstrand cross-links

Interstrand cross-links (ICL) are covalent links between bases of opposing DNA strands. They prevent the separation of DNA necessary for essential processes such as replication and transcription (Niedernhofer et al., 2005). Unrepaired, as few as 20 ICL in a mammalian genome can lead to cell death (Lawley and Phillips, 1996). A comparative analysis ranked ICL agents as the most genotoxic in vitro and in vivo chemical compounds (Lohman, 1999; Mendelsohn et al., 1992). Within the top 20 genotoxic agents, 16 were bifunctional alkylating agents (Vogel et al., 1998).

There are multiple sources for ICL formation including environmental exposures, by-products of metabolism and exogenous drug sources (Schärer, 2005). Exogenous agents that can induce ICL include bifunctional alkylating agents, psoralen and platinum compounds. Both alkylating drugs, such as nitrogen mustards and mitomycin C (MMC), and platinum compounds react with the N7 of guanine bases to form interstrand cross-links. Psoralen and its related compounds form ICL when activated by UV light. Endogenous ICL may form due to the reaction of DNA with unsaturated aldehydes that form following lipid peroxidation.

Early studies compared the range of DNA lesions caused by bifunctional compounds that can form ICL, with their point mutation forming monofunctional analogues (Yaghi et al., 1998; Wijen et al., 2000). These confirmed, in Chinese hamster ovary (CHO) cells, that the majority of mutations caused by monofunctional alkylating agents are point mutations. Comparatively a bifunctional alkylating agent, chlorambucil, caused lesions that were consistent DNA strand breakage and recombination (Yaghi et al., 1998). Furthermore, studies

have demonstrated that ICL forming agents are clastogenic causing damage at a chromosomal level such as chromosomal loss, breaks and deletions (Vogel et al., 1996). They also cause more sister chromatid exchanges than their monofunctional analogues (Tokuda and Bodell, 1987).

One of the key reasons for studying ICLs stems from the use of ICL forming agents in cancer treatment. Chemotherapeutic agents such as cisplatin, mitomycin C (MMC) and the nitrogen mustards (HN2) all exploit the toxicity of ICL to cells to induce cancer cell death. Tumour sensitivity to ICL drugs can be enhanced by defects in recognition or repair of ICL. Conversely tumours with enhanced ICL repair can develop clinical drug resistance (Wynne et al., 2007). As ICL agents are currently some of the most successful chemotherapies it is clear that manipulation and targeting of ICL repair offers a potential therapeutic target to improve cancer treatment regimes.

### 1.3.1 Endogenous formation of ICL

The clinical syndrome Fanconi Anaemia (FA) illustrates the threat caused by endogenous ICL formation. FA is a rare disease that results from genetic defects in the proteins responsible for DNA repair. Patients with FA are exquisitely sensitive to ICL agents and the diagnostic test for the disorder involves cytogenetic analysis of chromosome breakage and radial chromosome formation caused by addition of ICL agents to lymphocytes (Auerbach, 1988). It is widely thought that the clinical features of FA result from a failure to repair endogenously produced ICL. Which metabolites produce the ICL causing FA is still widely debated but recent work has suggest that endogenously produced aldehydes may be a key candidate.

Reactive aldehydes are known to cause a number of DNA adducts including ICL (Voulgaridou et al., 2011). There are a number of sources of aldehydes to humans. Acetaldehyde is a major metabolite of ethanol oxidation and intermediate of carbohydrate metabolism (Brooks and Zakhari, 2014). Exposure to acetaldehyde may also occur via environmental pollution, as acetaldehyde is one of the most common carcinogens in cigarette smoke. Acetaldehyde is able to form ICL by reacting with guanines (Matsuda et al., 1998). It reacts with the exocyclic amine of deoxyguanine to form $N^2$-ethylidene-2'-deoxyguanine adducts (Wang et al., 2000). A further reaction with a second acetaldehyde molecule can result in the formation of 1,$N^2$-proprano-2'-deoxyguanine (Garcia et al., 2011) which is able to exist in both open and ring forms. The ring form can react with another dG on the complementary DNA strand to form ICL (Kozekov et al., 2003).

Formaldehyde has also been implicated in the formation of ICL. Formaldehyde is required in the synthesis of amino acids including purines and is formed endogenously by histone demethylation and dealkylation of methylated DNA. Formaldehyde is able to form ICL by reacting with the amines of DNA bases to form a methylol adduct. Following dehydration a Schiff base intermediate is formed which can react with another DNA base to form an ICL or can react with lysine to form a DNA-protein cross-link (DPC).

Other reactive aldehydes include crotonaldehyde, acrolein and malondialdehyde which occur as products of lipid peroxidation (Chung et al., 1996). Crotonaldehyde is also found in cigarette smoke. These form ICL in 5'CpG sequence (Kozekov et al., 2001) (Kozekov et al., 2003) (Cho et al., 2006).

Recent *in vivo* work has reiterated the possible link between aldehydes and FA. Studies in mice examining the interaction of aldehyde metabolism and the Fanconi Anaemia repair proteins have demonstrated that mice deficient in both FANCD2, an essential Fanconi anaemia protein, and the acetaldehyde detoxifying enzyme, aldehyde dehydrogenase 2 (ALDH2), when challenged with ethanol develop severe bone marrow failure (Langevin et al., 2011). The authors also found the majority of FANCD2 and ALDH2 deficient mice developed acute lymphoblastic anaemia within 6 months of birth (Garaycoechea et al., 2012) and proposed that the FA repair proteins were essential for preventing aldehyde mediated toxicity to haematopoietic stem cells.

Further studies have confirmed that formaldehyde causes significant toxicity *in vivo.* Following suppression of alcohol dehydrogenase 5 (ADH5), a formaldehyde catabolising enzyme, mice that were also deficient in FANCD2 developed bone marrow failure (Pontel et al., 2015). This bone marrow failure developed earlier than in ALDH2/FANCD2 deficient mice suggesting that endogenous formaldehyde is more toxic than acetaldehyde.

These studies elegantly illustrate the toxicity of aldehydes *in vivo*, however, it is not clear if ICLs are entirely responsible for the toxicity seen since aldehydes lead to the formation of both ICL and DPC lesions and similarly many exogenous ICL agents such as cisplatin also form a mixture of lesions.

### 1.3.2 Exogenous formation of ICL

#### 1.3.2.1 Nitrogen mustards

Nitrogen mustards are clinically important bifunctional alkylating drugs that contain a *N*,*N*-bis-(2-chloroethyl)amine reactive functional group Figure 1.6 B. Several chemotherapeutic drugs belong to this class of ICL agent including nitrogen mustard (HN2) or mechlorethamine, chlorambucil, melphalan and phosphoramide mustard, which is derived from the metabolism of cyclophosphamide. These drugs all vary in their structure and mechanism of reaction with DNA but share a common principle of ICL formation (reviewed in (McHugh et al., 2001), (Hartley and Wyatt, 1997)

The initial step in ICL formation by nitrogen mustards is the displacement of a chloride ion by water (Figure 1.7). This results in a positively charge aziridinium intermediate which can react with guanine residues in the major groove of DNA to form an N7-alkylated guanine derivative. In the majority reactions (90-95%), following formation of a second aziridinium intermediate, the N7-alkylated guanine derivative reacts with water to form a stable 2-hydroxyethyl monoadduct. However, in a minority of reactions (approximately 5%) the aziridinium intermediate can react with a second guanine residue on the opposite strand to form an interstrand cross-link (reviewed in (Kohn et al., 1987; Williamson and Witten, 1967)).

The majority of ICL formation appears to occur with guanine residues in 5'GNC-3' sequences in DNA (Ojwang et al., 1989). As the distance between the guanines in this sequence in B form DNA is 6.8 Å and the distance that the 5 atom cross-link spans is 5.1 Å (Rajski and Williams, 1998), a distortion of the DNA helix in the

region is created resulting in a bend of approximately 14° (Rink and Hopkins, 1995).

It has been demonstrated that only 5-10% of the lesions caused by HN2 are ICL with the majority of lesion being monoadducts (Larminat et al., 1993). Intrastrand cross-links may also form between consecutive guanine residues in 5'-GGC-3' sequences (Bauer and Povirk, 1997). The variety in lesions created by HN2 can complicate study of nitrogen mustard ICL repair.

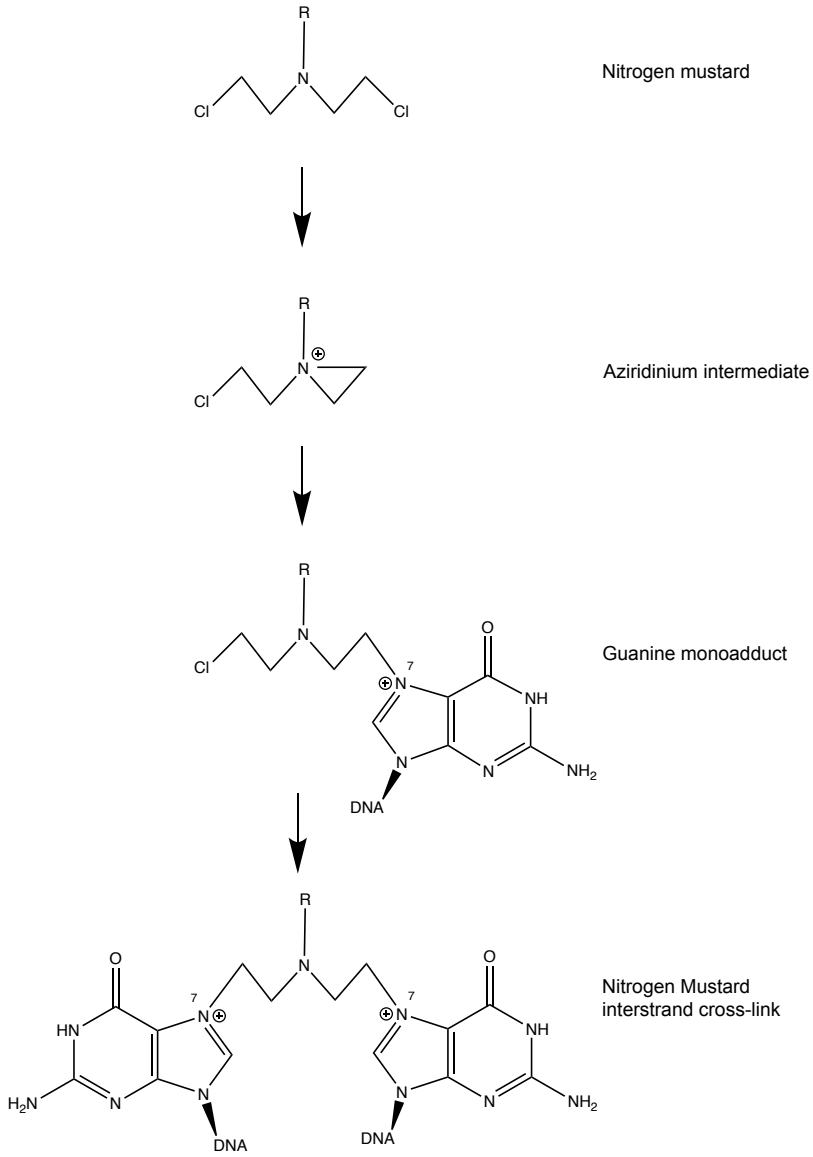
2-dimethylaminoethylchloride hydrochloride (HN1 or monofunctional nitrogen mustard) is a chemical analogue of HN2 and a monofunctional alkylating agent. It is capable of forming *N*-alkylpurine monoadducts but does not form ICL. Its chemical structure is illustrated in Figure 1.6 A and contains only a single reactive site capable of generating monoadducts (Kohn et al., 1966).




**Figure 1.6: Structure of nitrogen mustards HN1 and HN2**

A: Bis(2-chloroethyl)ethylamine (HN1)

B: Bis(2-chloroethyl)methylamine (HN2)




## Figure 1.7: Nitrogen mustard interstrand cross-link formation

Displacement of a chloride ion from nitrogen mustard results in a positively charged aziridinium intermediate. This is able to react with guanine to form a monoadducts. Further chloride ion displacement and formation of a second aziridinium intermediate leads to either a nitrogen mustard ICL forming with an opposing guanine or a 2-hydroxyethyl monoadducts with water.

### 1.3.2.2 Platinum compounds

*Cis*-Diamminedichloroplatinum, (*cis*-DDP or cisplatin) is a chemotherapeutic agent that is used in the treatment of solid tumours particularly lung, ovarian and testicular cancer.

Rosenberg *et al*, first identified that electrolysis of platinum electrodes within media resulted in production of a platinum complex that was capable of inhibiting cell division in *Escherichia Coli* (*E. coli*) bacteria resulting in the bacteria growing as filaments (ROSENBERG et al., 1965). Further studies by the authors confirmed that the square planar Pt(II) complex, *cis*-$[PtCl_2(NH_3)_2]$ could inhibit cell division in *E. coli* (ROSENBERG et al., 1967) and was also capable of causing regression of sarcoma and leukaemia in mice (ROSENBERG et al., 1969).

Within the cellular environment, *cis*-DDP becomes aquated by sequential displacement of two chloride ions by water molecules resulting in the formation of bifunctional electrophilic sites (Figure 1.8). This activated form of the drug is able to react with bases on DNA strands, in particular the N7-nitrogen of purines favouring guanine (Noll et al., 2006). The most commonly formed lesions by *cis*-DDP with DNA are intrastrand cross-links between guanine residues in 5'-GG-3', 5'-GNG-3' and between adenine and guanine in 5'-AG-3' sequences. Intrastrand cross-links account for more 90% of lesions formed by *cis*-DDP. The remaining 2-5% of lesions are interstrand cross-links which form between guanines in 5'-GC-3' sequences (Kartalou and Essigmann, 2001).

*Cis*-DDP interstrand cross-links result in significant deformation of the DNA helix. Studies using gel-shift mobility assays, NMR and X-ray crystallography have

identified that *cis*-DDP ICL result in 79˚ unwinding and 45˚ bending of the DNA helix (Coste et al., 1999; Huang et al., 1995; Malinge et al., 1994; Gelasco and Lippard, 1998).

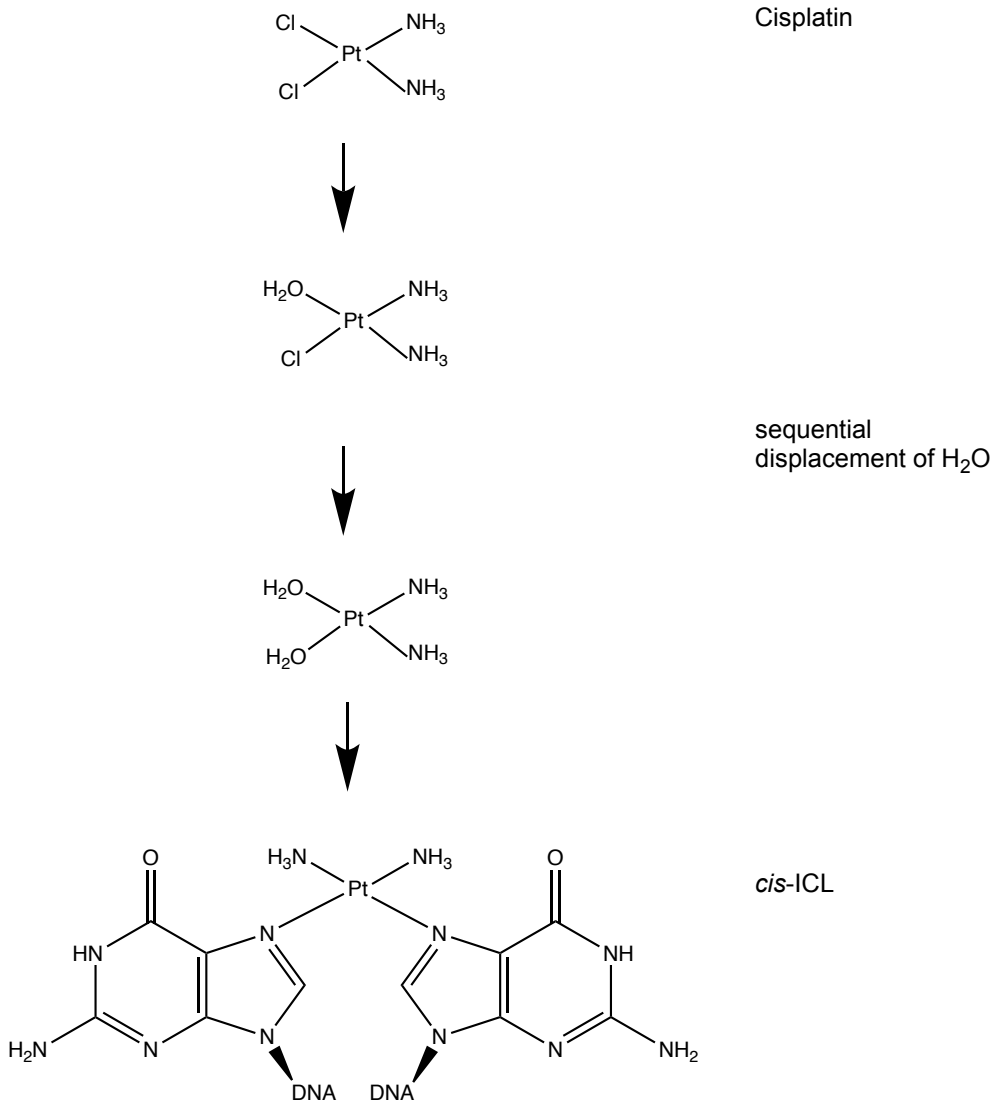



**Figure 1.8: Cisplatin interstrand cross-link formation**

Formation of cisplatin interstrand cross-link by sequential displacement of water to form *cis*-ICL between opposing guanine bases

#### 1.3.2.3 Mitomycin C

Mitomycin C (MMC) is a product of the mould *Streptomyces caespitosis* and was originally identified for its antibiotic activity against bacteria mediated through formation of ICL (Lawley and Phillips, 1996). It is used in the treatment of upper gastrointestinal, breast and anal cancers intravenously and bladder cancers topically.

MMC requires reduction of its quinone ring to initiate alkylation. The formation of ICL by MMC is illustrated in Figure 1.9. Initially the quinone ring undergoes 2 electron reduction resulting in the loss of methyoxygroup and allowing formation of a hydroquinone intermediate (Watanabe et al., 2004). This hydroquinone intermediate undergoes tautomerization and reacts with the $N^2$-amino group of the guanine to produce a monoadducts (Cummings et al., 1998). Following elimination of a carbamoyl group, a reactive vinylogous hydroquinone methide intermediate is produced which, following oxidation, is able to alkylate the opposing strand guanine to form an ICL.

Mitomycin C, unlike nitrogen mustards, reacts with guanine residues in the minor groove of DNA in 5'-CG-3' sequences to form ICL (Rajski and Williams, 1998). MMC is also able to form intrastrand cross-links between adjacent guanine sequences (Norman et al., 1990). The ICL formed by MMC are accommodated within the minor groove of DNA with minimal alteration of structure. Analysis of electrophoretic mobility shift gels and NMR studies have shown no significant unwinding or distortion of the DNA helix by MMC ICL despite MMC intrastrand cross-links causing significant bending (Rink et al., 1996). This lack of deformation

of helical DNA may alter the detection of ICLs induced by MMC and be relevant to understanding of ICL repair.

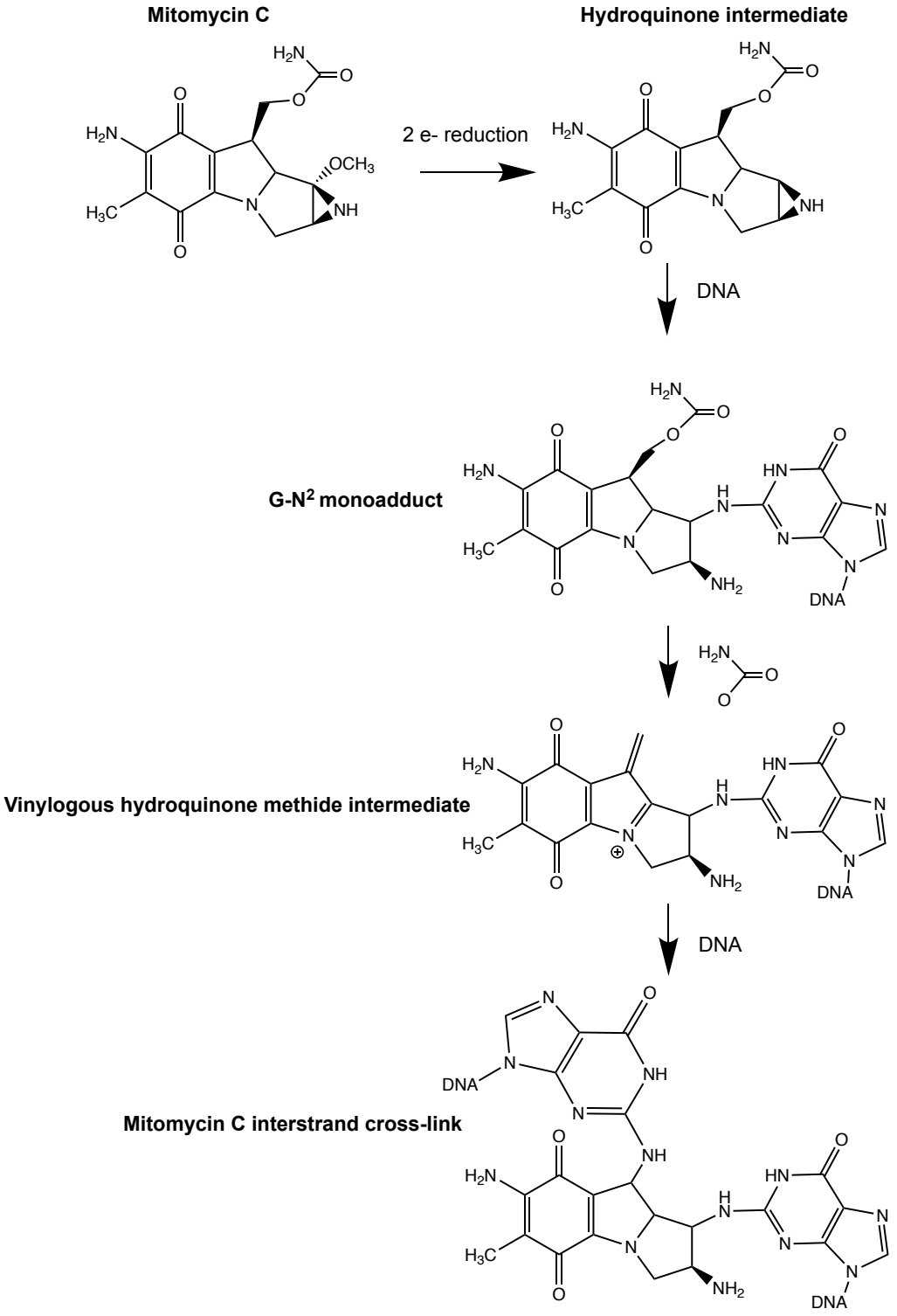



**Figure 1.9: Mitomycin C interstrand cross-link formation**

Formation of MMC ICL adapted from Noll *et al* (Noll et al., 2006).

#### 1.3.2.4 Psoralen

Psoralen is a compound found in a family of natural products called furocoumarins. Furocoumarins are produced by a variety of plants and consist of a furan ring fused with coumarin. Psoralen occurs naturally in many plants such as parsley, celery, citrus fruits and figs and is used extensively in the treatment of skin diseases such as eczema, psoriasis and T-cell lymphoma with ultraviolet A light (UVA) as PUVA.

Psoralens are able to form covalent adducts with DNA following irradiation with UV light (Hearst, 1981). Planar tricyclic psoralens that intercalate with DNA are orientated so that the 3,4-pyrone ring and 4',5' furan ring double bonds are directly above or below the 5,6-double bonds of thymines. Following absorption of UV light a cycloaddition reaction occurs either between the furan or pyrone ring and the adjacent thymine to lead to the formation of a monoadduct containing a cyclobutane bridge. Monoadducts formed on the furan-side are able to absorb a second UV dose resulting in a second cycloaddition between the pyrone double bond and an opposing DNA strand thymine to form an interstrand cross-link. Monoadducts formed on the pyrone-side cannot absorb a second UV quantum of light and they remain as monoadducts (Noll et al., 2006).

NMR studies have shown psoralen ICL do not cause significant bending of the DNA helix but at the site of the ICL approximately 25° of duplex unwinding and distortion occurs (Haran and Crothers, 1988).

Psoralen ICL are relatively easy to synthesise, in particular, irradiation of 8-methoxypsoralen results in ICL formed as 40% of lesions (Stern, 2007). Due to

UVA being a specific requirement for induction, studies utilising specific localised irradiation of cells can also be performed.

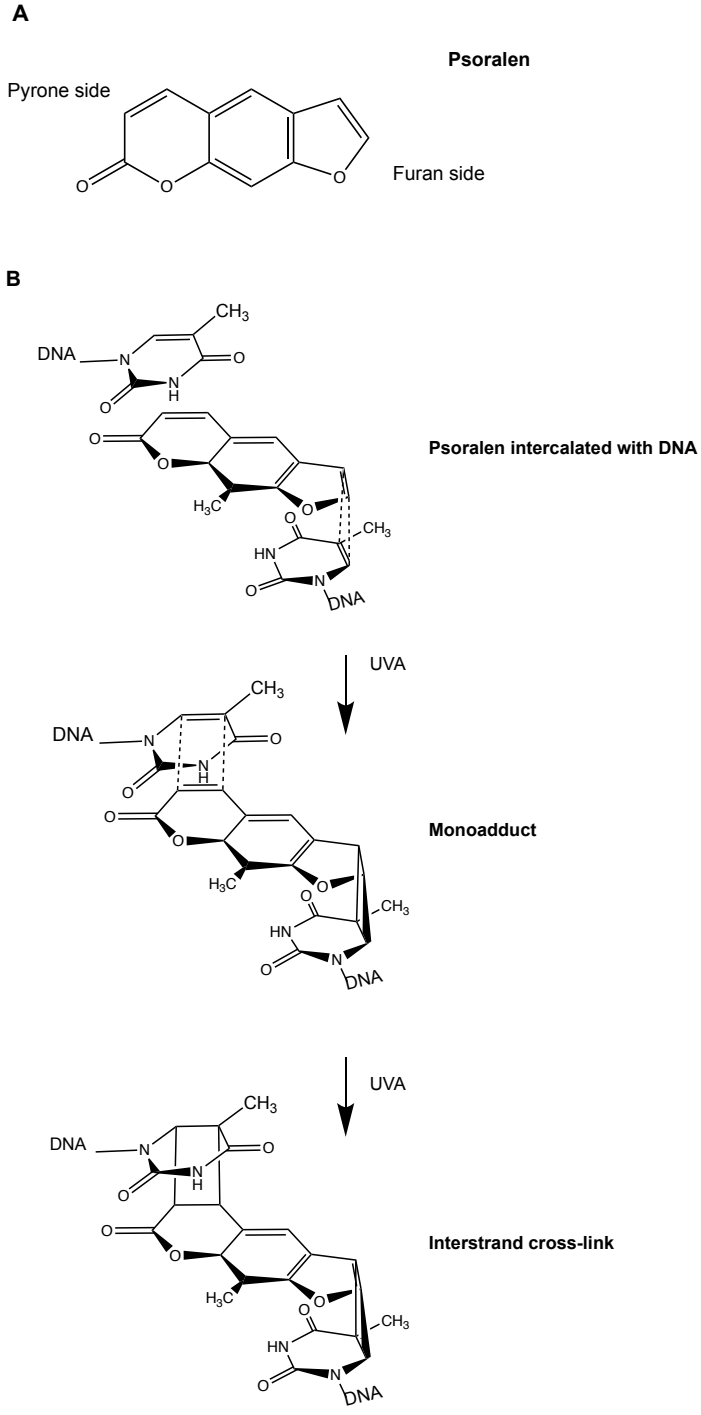



**Figure 1.10: Psoralen interstrand cross-link formation**

A: Structure of Psoralen demonstrating furan and pyrone rings.
B: Formation of ICL with thymine by UVA excitation.

## 1.4 Repair of interstrand cross-links

### 1.4.1 Recognition of ICL

In mammalian cells ICL can be recognised in three potential situations. ICL can be recognised in the unperturbed duplex DNA, in the absence of replication, by factors that recognise DNA damage. Alternatively, ICL can be sensed by transcription machinery, again without the need for replication. Finally, ICL can be identified after causing blockage to progression of replication forks.

Understanding how ICL recognition occurs is complicated by the varying effects different ICL have on DNA structure and helical distortion. This, alongside disparity in the assay systems used to study cross-links, has resulted in a lack of consensus in the understanding of mechanisms of ICL recognition.

#### 1.4.1.1 ICL recognition in non-replicating cells

The repair of ICL in the absence of either a transcription bubble or a replication fork has been demonstrated in *Xenopus* cell-free extracts (Williams et al., 2012) (Ben-Yehoyada et al., 2009). The main candidates for ICL recognition in this situation are the NER or mismatch repair (MMR) proteins. The MMR pathway was implicated by the finding that cells deficient in MSH2 were sensitive to both MMC and psoralen (Fiumicino et al., 2000) (Wu et al., 2005). *In vitro* studies have also demonstrated that MMR and NER proteins can bind to ICL duplexes in experiments using purified components. MutSβ has been demonstrated to recognise and bind to psoralen ICL in *in vitro* gel shift assays (Zhao et al., 2009; Zhang et al., 2002). Psoralen ICL placed within a plasmid substrate required the interaction of MutSβ, XPF/ERCC1 and RPA but not XPC/XPG for incision (Zhang et

al., 2002). Recent studies have identified that MutSβ, PARP-1, DNA Ligase III, XRCC1 and Ku70-80 are able to bind to a cisplatin ICL (Zhu and Lippard, 2009). PCNA has also been implicated in stimulating the binding of MutSβ complexes to ICL (Li et al., 2000).

#### 1.4.1.2 ICL recognition during transcription

In the absence of a stalled replication fork, recognition of ICL during transcription may play an important role. This may be particularly important during G1 phase of the cell cycle where transcription coupled nucleotide excision repair (TC-NER) may play an important role in recognising ICL. This recognition could occur via the collision of a transcribing RNA polymerase with an ICL.

Several previous studies have suggested ICL are preferentially repaired in actively transcribed genes. Studies using renaturing agarose gel electrophoresis assessing ICL repair in CHO cells suggested that HN2 ICL induced in the actively transcribed gene dihydrofolate reductase (DHFR) were preferentially repaired compared to HN2 ICL induced in a downstream inactive region (Larminat et al., 1993). Similar studies inducing psoralen ICL in DHFR and the inactive *fms* proto-oncogene gene demonstrated reduced cross-linking removal in the inactively transcribed genes (Islas et al., 1991). These findings in mammalian cells appear to be supported by studies in yeast that have demonstrated that psoralen ICL are repaired more rapidly at the transcriptionally active MATα locus compared to those at the transcriptionally inactive HMLα locus (Zheng et al., 2003).

Despite the evidence of TC-NER appearing to contribute to ICL recognition there are conflicting findings relating to the contribution of global-genome nucleotide

excision repair (GG-NER). Previous studies of cisplatin ICL have identified a requirement for XPA, XPF and XPG (Xeroderma Pigmentosum complementation groups A, F and G all required for TC-NER) but not XPC to repair ICL (Enoiu et al., 2012). However, assessment of repair of MMC ICL in the actively transcribed region of a luciferase reporter plasmid has suggested the transcription-coupled repair genes CSA and CSB are required. However, cells with mutations to Xeroderma Pigmentosum complementation group C (XPC), a NER protein that is only required for GG-NER, also showed impaired ICL repair suggesting for MMC ICL that both TC-NER and GG-NER may play a role (Zheng et al., 2003). The differences in the required pathways may result from the differences in distortion of the DNA helix caused by these different ICL. MMC ICL cause minimal distortion and these results suggest that less distorting ICL may rely on XPC more extensively for detection.

#### 1.4.1.3 ICL recognition by replication forks

In cells undergoing division the collision of one or two replication forks with an ICL blocks helicase progression and leads to initiation of replication-dependent ICL repair.

Specific direction into the ICL repair pathway appears to be orchestrated by the FANCM/FAAP24 sub-complex, which is able to identify stalled replication forks and recruit downstream components of the ICL repair pathway. Evidence for FANCM/FAAP24 involvement in identifying ICL stalling of replication stems from its preference for branched DNA structures *in vitro* (Ciccia et al., 2007; Yan et al., 2010) and the finding that FANCM-depleted cells do not recruit the Fanconi anaemia (FA) core complex or mono-ubiquitylate the FANCD2-FANCI heterodimer

as usually occurs in ICL repair (Kim et al., 2008). Furthermore, it appears that FANCM may act to protect the replication fork, and prevent its collapse, by promoting replication fork regression (Gari et al., 2008). Using plasmid-based DNA replication structures Gari *et al* demonstrated FANCM could convert a replication fork to a four-way structure. FANCM performs this regression by displacement and annealing of the nascent and parental DNA strands. Fork reversal may prevent the replication fork from encountering the ICL and allow for repair by translesion bypass without the need for fork collapse and DSB formation that can potentially lead to chromosomal aberrations through recombination.

It is not clear if FANCM is unique in its interaction with stalled replication forks several studies have suggested that FANCA and MutS may also play roles. Studies in cells with biallelic mutations in FANCA used to study the interactions of FANCM have revealed that correction of FANCA defects leads to rescue of FANCD2 monoubiquitation but not sensitivity to MMC (Singh et al., 2009). Deletion of FANCM in DT40 chicken cell lines does not cause complete abolition of FANCD2 ubiquitylation (Rosado et al., 2009; Wang et al., 2013). These studies suggest that FANCM is not solely acting as a sensor in this pathway.

Several studies have suggested that MutS homologues (MSH) that are involved in the recognition of mismatched bases in MMR may also play a role in recognising ICLs. Cells that are depleted of MSH2, 3 or 6 lack FANCD2 ubiquitylation and do not recruit the FA core complex after treatment with MMC. The effects of co-depleting FANCM and MSH2 were additive in further studies (Huang et al., 2011). It has been suggested that MutSβ is required for ICL-induced DNA synthesis

(Zhang et al., 2002) and cells lacking MSH2, part of MutSβ, are sensitive to ICL drugs (Fiumicino et al., 2000).

Despite these findings, several recent studies (Hlavin et al., 2010; Enoiu et al., 2012) have not identified any ICL repair defect in MSH2 deficient cells suggesting that MSH2 may play a redundant role in particular types of ICL and this may explain the lack of sensitivity to ICL seen in some experiments.

### 1.4.2 Basic model of ICL repair

ICL affect the physical structure of DNA and therefore require the involvement of multiple repair pathways for their resolution. The basic model for ICL repair in replicating cells was developed from studies by Cole *et al* in bacteria in the 1970s.

These studies examined strains of *E.coli* that were deficient in nucleotide excision repair (NER), homologous recombination (HR) or both. Strains deficient in RecA, a component of HR, and strains deficient in NER activity demonstrated decreased resolution of ICL formed by psoralen and UV light. The strains appeared to tolerate fewer ICL (5-20) compared to wild-type cells. Cells that were deficient in NER and HR were unable to tolerate more than one ICL per genome suggesting that both the NER and HR pathways are involved in ICL repair (Cole, 1973) (Cole et al., 1976).

This resulted in the development of the "Cole" model. In this scheme the initial step involves the recognition of ICL by NER proteins with subsequent incision on one strand of DNA either side of the ICL (Van Houten et al., 1986a; b). This leads to the production of an unhooked substrate with the excised fragment still attached to the un-incised DNA strand by the cross-link. At this point the unhooked ICL-

repair intermediate can undergo further processing by two independent pathways that involve either HR or translesion synthesis (TLS). In the HR mediated pathway in bacteria, the exonuclease DNA pol I performs end resection at the 3' side of the cross-link and RecA mediated strand exchange can occur with the unaffected homologous chromosome (Sladek et al., 1989). The remaining cross-linked oligonucleotide can then be removed by NER.

Alternatively, in the absence of a functional homologous recombination pathway the gap formed by dual incisions around the ICL can be filled by lesion bypass. This is performed by Pol II in N7-N7 guanine cross-links caused by nitrogen mustard (Berardini et al., 1997) and Pol IV in acrolein N2-N2 guanine cross-links (Kumari et al., 2008).

This basic pathway of unhooking, gap formation, followed by gap repair by recombination or gap bypass synthesis leading to the formation of a monoadducts that undergo a second round of repair is found in all organisms although there are significant differences between non-vertebrate and vertebrate cells (Figure 1.11). Further discussion in this section will detail ICL repair pertaining to replicating cells in eukaryotes.

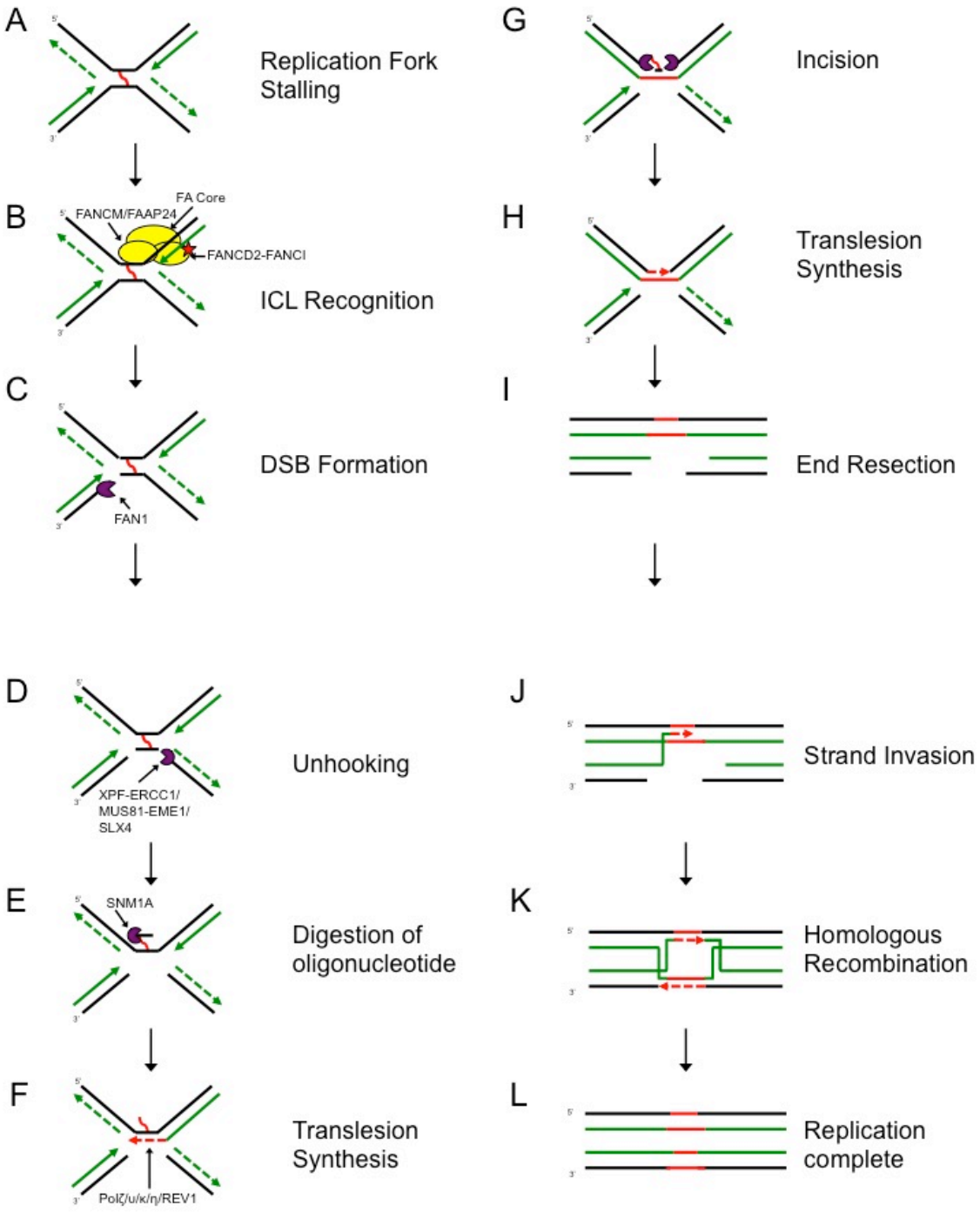



**Figure 1.11: Proposed model of ICL repair in replicating cells.**

Model for repair of ICL during replication adapted from Huang *et al* (Huang and Li, 2013)
A and B: Replication forks converge on ICL and stall leading to the recruitment of FANCM/FAAP24 complex.
C and D: Incisions occur 5' and 3' to ICL leading to formation of a DSB and unhooking of the ICL
E and F: Digestion of the unhooked oligonucleotide by SNM1A and translesion bypass across strand gap.
G and H: Further dual incisions occur around the unhooked ICL followed by a further TLS bypass.
I and J: 5' end resection by MRN complex occurs followed by strand invasion.
K and L: Homologous recombination occurs to complete replication.

#### 1.4.2.1 Single fork stalling

It was previously proposed by a number of groups that repair of ICL occurred principally in S-phase when replication fork arrest at ICL triggered recognition and cellular repair responses. This was based on work by Akkari *et al* that demonstrated synchronised human skin fibroblast cells treated with psoralen/UVA needed to pass through S-phase to elicit any cell cycle delay or chromosomal breakage (Akkari et al., 2000). These effects were independent of where in the cell cycle ICLs were induced and lead to the proposal that the initial recognition of ICL and repair of ICL occurred in S-phase.

Further identification that DSB were generated in S-phase following treatment with ICL agents lead to the development of a model of replication-dependent repair that involved formation of a DSB followed by unhooking by ERCC1-XPF and recombinational repair of the gap created (De Silva et al., 2000). This was supported by evidence that replicating, but not stationary, yeast cells accumulated DSB after treatment with cisplatin and HN2 (McHugh et al., 2000). CHO cells treated with HN2 also accumulated DSB (De Silva et al., 2000). Two different explanations of the timing of this repair were proposed. The first suggested that unhooking could occur in G1 phase cells and in S-phase when the replication fork encountered these unrepaired gaps generated by unhooking, a second incision would occur leading to a DSB (Rothfuss and Grompe, 2004). A second proposal suggested that during S-phase replication forks encountered cross-links and at this point, incision and unhooking of the ICL occurred, with further incision upstream of the ICL to generate of a DSB. This second proposal is supported by evidence from cross-linked replicating plasmids (Kuraoka et al., 2000) .

#### 1.4.2.2 Converging fork model for replication-dependent ICL repair

An alternative model of fork repair has been proposed based on studies of repair of ICL in *Xenopus* egg extracts. This has suggested that repair of ICL occurs when two replication forks converge on a single ICL. This model has been developed from electron microscopy studies of replication of ICL plasmid substrates incubated in the presence of *Xenopus* egg extracts (Räschle et al., 2008). In this system replication was initiated at a random location within the plasmids and the two replisomes converged on the ICL. This model of ICL was initially studied for a cisplatin ICL and a nitrogen mustard analogue (Angelov et al., 2009) and the progress of replication and the length of the daughter strands assessed by $^{32}$P-α-dATP incorporation. Further studies have demonstrated that the leading strand stalls approximately 20 bases from the cross-link due to the steric obstruction of CMG helicase, a complex of Cdc45, MCM2-7 and GINS (Fu et al., 2011). CMG helicase is then unloaded via a mechanism that is still not clear but requires ubiquitin signalling and the BRCA1 (FANCS)-BARDI complex (Long et al., 2014). Following unloading the leading strand is extended to within 1 nucleotide of the ICL possibly by the leading strand DNA Polymerase ε (Budzowska et al., 2015). Following this, the ubiquitylated heterodimer of FANCI and FANCD2 (ID2) localises to the ICL and allows dual incisions either side of the ICL allowing unhooking of the ICL (Knipscheer et al., 2009). ID2 recruits the scaffold protein SLX4 via its ubiquitin binding domains (Yamamoto et al., 2011).

More recently work by Seidman and colleagues has identified that single forks colliding with an ICL are capable of bypassing ICLs without unhooking them. This phenomenon, termed replication traverse by the investigators, was identified

using fluorescently labelled psoralen ICLs and DNA fibre studies (Huang et al., 2013). Repair of ICL is thought to occur after the traversed fork has moved beyond the lesion. It has been proposed that traverse of the ICL can occur after transient opening of the CMG helicase ring (reviewed in (Trakselis et al.)) and is promoted by the translocase activity of FANCM in association with PCNA (Rohleder et al., 2016) and BLM helicase (Ling et al.).

Similar bypass of DNA-Protein cross-links (DPCs) has also been demonstrated by the large T antigen DNA helicase (Yardimci et al., 2012). This form of lesion bypass creates a similar X-shaped product as the convergence of two replication forks. This structure may be critical in the instigation of ICL unhooking.

#### 1.4.2.3 Unhooking of ICLs

SLX4 is a structure specific endonuclease that is a FA protein (FANCP) (Kim et al., 2011) and acts as a scaffold for the recruitment of nucleases that incise the ICL. The precise nucleases responsible for incision are still not clear and will be discussed below. SLX4 is able to interact with both XPF-ERCC1 and MUS81-EME1. SLX4 forms a dimeric nuclease with SLX1 in which SLX4 acts as the regulatory subunit and SLX1 provides catalytic activity (Kim et al., 2011). SLX4 involvement in recruitment to ICL is demonstrated by the evidence that SLX4-null cells are sensitive to ICL agents and PARP inhibitors, a surrogate marker for homologous recombination defects (Fekairi et al., 2009). The PARP sensitivity, but not MMC sensitivity, of SLX4-null cells can be abrogated by complementation with SLX4 mutants that do not interact with XPF (Kim et al., 2013). SLX4 defective DT40 cells sensitivity to ICL agents cannot be rescued by complementation with mutants that lack the domain required for interaction with ubiquitylated FANCD2 (Yamamoto

et al., 2011). These experimental findings suggest that SLX4, XPF and FANCD2 co-operate in resolution of ICL.

The XPF-ERCC1 heterodimer has been identified as a key nuclease for the incision step of ICL repair. Biochemical studies have identified XPF-ERCC1 as a structure specific endonuclease that can incise splayed-arm, 3' flap structures, bubble and stem and loop structures (Ciccia et al., 2008). Both XPF and ERCC1 deficient CHO cells are more sensitive to HN2 and cisplatin than other NER deficient CHO cells (De Silva et al., 2000; Andersson et al., 1996). Comet assay analysis of replicating CHO cells has demonstrated decreased ICL unhooking in XPF and ERCC1 deficient CHO cells suggesting a role for XPF-ERCC1 in ICL incision (De Silva et al., 2000). In these studies DSB formation was normal in XPF-ERCC1 deficient cells leading to the initial suggestion that the incision made by XPF-ERCC1 was 5' to the ICL. Contrary to these findings other studies have suggested that XPF-ERCC1 may also be able to make 3' incisions. Studies assessing incision of psoralen ICL have suggested that XPF-ERCC1 is able to make incisions on both the 5' and 3' sides of the ICL (Kuraoka et al., 2000).

MUS81-EME1 (MUS81 structure specific subunit-essential meiotic structure specific endonuclease 1) is an endonuclease that incises 3' flap and replication fork-like structures (Ciccia et al., 2008). Previous studies have suggested that MUS81-EME1 may also play a role in ICL repair as MUS81-EME1 deficient mouse embryonic stem cells are sensitive to MMC (Hanada et al., 2006). MUS81-EME1 has been implicated in the formation of DSB in ICL resolution suggesting a redundant role with XPF-ERCC1 (Hanada et al., 2006). MUS81-EME1 is also involved in the resolution of Holliday junctions in HR (Chen et al., 2001) suggesting it could

perform incisions at stalled replication forks. Recent studies have identified that MUS81-EME2 (MUS81 structure specific subunit-essential meiotic structure specific endonuclease 2) is more efficient at incising 3' flap DNA and is also able to incise 5' flap structures (Pepe and West, 2014) suggesting that MUS81-EME2 could potentially complete the dual incisions in the initial stages of ICL resolution. MUS82-EME2 has decreased efficiency in Holliday junction resolution compared to MUS81-EME1. This suggests MUS81-EME2 plays a more important role in in initial incision, whilst MUS81-EME1 is more effective in HJ resolution (Pepe and West, 2014).

Fanconi anaemia-associated nuclease 1 (FAN1) is a 5'-3' exonuclease and structure specific endonuclease. As an endonuclease it incises 5' flap structures in preference to splayed arm or 3-way junction substrates (Kratz et al., 2010; Smogorzewska et al., 2010; MacKay et al., 2010). FAN1 also interacts with monoubiquitinated FANCD2. FAN1 deficient cells are sensitive to MMC and cisplatin. FAN1 depleted cells show persistence of the DSB markers γH2AX, RPA and Rad51 after treatment with cisplatin suggesting FAN1 may be involved in the resolution of DSB (Kratz et al., 2010; Smogorzewska et al., 2010; MacKay et al., 2010). Further studies have suggested FAN1 can incise 5' to ICLs and digest past the site of the ICL (Pizzolato et al., 2015).

Sensitive to nitrogen mustard 1A and 1B (SNM1A and SNM1B) are 5'-3' exonucleases (Sengerová et al., 2012) that may be involved in repair of ICL. Human SNM1A is an ortholog of yeast Pso2 (Cattell et al., 2010) and ectopic expression of human SNM1A can partially restore yeast sensitivity to ICL agents (Hazrati et al., 2008). Previous work in our lab has demonstrated that human SNM1A is able to

digest past site specific SJG-136 ICLs. siRNA depletion of SNM1A increased mammalian cell sensitivity to MMC. The co-depletion of XPF-ERCC1 and SNM1A was not found to be additive suggesting these enzymes play epistatic roles. Co-depletion of SLX4 and SNM1A was also not additive suggesting that SLX4 acts in the same pathway as SNM1A. It was proposed that SNM1A might digest the oligonucleotide tethered to the ICL post incision by FAN1, XPF-ERCC1 or MUS81-EME1 (Wang et al., 2011).

SNM1B depleted cells show sensitivity to MMC and co-depletion of SNM1A and SNM1B in DT40 chicken cells caused increased sensitivity to cisplatin (Ishiai et al., 2004) suggesting that SNM1A and SNM1B play redundant roles.

The findings from the studies of XPF-ERCC1, MUS81-EME1, SLX1-SLX4, FAN1 and SNM1A suggest that several nucleases may be involved in ICL repair. The precise role of individual enzymes during replication dependent repair has yet to be unravelled and as specific enzymes might be involved in not only incision of ICL but repair of intermediates downstream this makes assignment of each nuclease to a specific task more difficult.

Following dual incision and unhooking a two-ended DSB is created in one chromatid and the sister chromatid is left with a DNA adduct. The adducted chromatid is repaired in a two-step process involving TLS and the DSB is repaired by HR these mechanisms are discussed below.

#### 1.4.2.4 Translesion synthesis and ICL repair

Following ICL unhooking, the TLS polymerases play an essential role in gap filling to allow full repair of one strand of the DNA duplex. Initially a nucleotide is

inserted opposite the damaged base by an unknown replicative polymerase and then the template is extended by TLS polymerases (Johnson et al., 2000; Prakash et al., 2000; Prakash and Prakash, 2002).

There are contrasting opinions regarding the regulation of translesional synthesis. Initial studies by Kannouche *et al* suggested the monoubiquitination of PCNA at lysine 164 allowed this switch from replicative polymerases to TLS polymerases (Kannouche et al., 2004). However, more recent studies by Budzowska *et al* using *Xenopus* egg extracts found that, whilst PCNA was ubiquitylated during DNA replication, levels of ubiquitylated PCNA were not higher than on undamaged DNA and the peak of ubiquitylated PCNA binding did not coincide with the peak of TLS and REV1/REV7 binding suggesting that PCNA ubiquitylation is not essential for bypass of ICL (Budzowska et al., 2015).

Despite debate over the regulation of translesional synthesis, it is clear that lesion bypass requires the sequential action of two different TLS polymerases (Johnson et al., 2000; Prakash and Prakash, 2002; Prakash et al., 2000). Several TLS polymerases have been suggested to play a role in this step of ICL repair. REV1 and Polζ are thought to play a key role in TLS. Similarly to yeast, vertebrate cells deficient in Polζ are sensitive to ICL agents (Gan et al., 2008; Nojima et al., 2005). Previous mechanistic studies in *Xenopus* egg extracts have shown Polζ does not play a role in the initial nucleotide insertion opposite a cisplatin ICL but is responsible for strand extension (Räschle et al., 2008). DT40 cells and MEFs defective in Rev1 are defective in repairing psoralen and MMC cross-links (Shen et al., 2006).

The role for other TLS polymerases appears less significant and this may in part be due to redundancy with Polζ. Polη-deficient XP-V (a variant of *Xeroderma pigmentosum*) cells are hypersensitive to platinum based compounds (Albertella et al., 2005). In host cell reactivation assays cells deficient in Polη also showed reduced repair of MMC and psoralen ICL (Wang et al., 2001b; Zheng et al., 2003). Polη deficient XP-V cells were also found to have higher levels of γH2AX foci following treatment with psoralen than wild-type cells (Mogi et al., 2008). As DSB are formed in replication-dependent ICL repair this suggests Polη may play a role in replication-dependent repair.

Polκ and Polυ deficient cells are sensitive to MMC (Zietlow et al., 2009). Polκ has been shown to bypass minor groove ICLs more efficiently than major groove ICL (Minko et al., 2008). In comparison Polυ can by bypass major groove ICL but not psoralen induced ICL and also interacts with FANCD2-FANCI suggesting a role in replication dependent repair (Moldovan et al., 2010).

#### 1.4.2.5 Homologous recombination and ICL repair

In ICL repair occurring during replication, following dual incisions, a DSB is formed. The availability of a homologous template for HR makes repair via this pathway over NHEJ more likely. This is also supported by findings that cells deficient in BRCA1, BRCA2 and Rad51 are sensitive to ICL agents (Bhattacharyya et al., 2000; Moynahan et al., 2001) whereas cells deficient in NHEJ proteins are not (De Silva et al., 2000).

Studies in *Xenopus* cell-free extracts have identified that inhibition of Rad51 leads to suppression of repair of a single site-specific ICL. In these studies Rad51 also

appeared to bind to replication forks stalled at ICL suggesting Rad51 may help stabilise stalled forks and promote strand invasion (Nakanishi et al., 2011). These findings support resolution of the DSB intermediates by HR in ICL repair during replication.

#### 1.4.2.6 Involvement of base excision repair DNA glycosylases in ICL repair.

Recent experimental work has suggested that the BER DNA glycosylases may play a role in resolution of ICL (reviewed in (Yang et al., 2017)) via *N*-glycosyl bond cleavage.

Previous studies have demonstrated that mouse embryonic stem cells deficient in murine 3-methyladenine glycosylase (Aag) are sensitive to psoralen induced ICL (Maor-Shoshani et al., 2008). Work by Couvé *et al* demonstrated that the DNA glycosylase NEIL1 was capable of excising unhooked psoralen ICLs providing an alternative to NER in the removal of ICL in the final stages of ICL repair (Couvé-Privat et al., 2007; Couvé et al., 2009).

More recently, Semlow *et al* (Semlow et al., 2016) demonstrated, using *Xenopus* egg extracts, that the DNA glycosylase NEIL3 was able to initiate ICL unhooking by cleaving one of the *N*-glycosyl bonds that form psoralen ICL. Investigations by this group demonstrated that this reaction required replication fork convergence but did not require FANCI-D2 or CMG unloading. Inhibition of *N*-glycosyl cleavage caused psoralen ICL unhooking to proceed via incisions around the ICL.

This pathway of repair of ICL, via *N*-glycosyl cleavage, does not require the Fanconi pathway or result in the generation of DSB. This results in rapid repair with potentially reduced occurrence of the chromosomal rearrangements

associated with ICL repair via the classical pathway of DSB and HR. To date this pathway of repair has only been demonstrated specifically with psoralen ICL.

## 1.5 Current understanding of replication independent repair in G1

ICL repair has been extensively studied in rapidly proliferating cells and there is increasing evidence that ICL repair can also occur in non-replicating or quiescent cells. Studies in bacteria have illustrated that a replication independent repair (RIR) pathway for ICL exists (Berardini et al., 1999; 1997) and this is conserved from yeast to mammals (Hlavin et al., 2010; Sarkar et al., 2006; Shen et al., 2006; Zheng et al., 2003). Repair of ICL in non-dividing cells is critical for cellular homeostasis particularly in post-mitotic cells such as neurons and may also be relevant to the repair of ICL in stem cells.

### 1.5.1 Basic model of ICL repair in G1

A basic model for ICL repair has been proposed based on studies in yeast, *Xenopus* extracts and mammalian cells (Figure 1.12) (reviewed in (Williams et al., 2012; McHugh and Sarkar, 2006)). As discussed previously, in section 1.4.1.1 and 1.4.1.2, in non-dividing cells recognition of ICL could occur either due to detection of DNA helix distortion caused by ICL by repair proteins (Williams et al., 2012; Ben-Yehoyada et al., 2009) or by RNA polymerase collision during transcription (Larminat et al., 1993; Islas et al., 1991; Zheng et al., 2003). Following recognition of ICL, incisions by NER proteins occur on either side of the ICL on one strand. XPF/ERCC1 is a key nuclease implicated in this process (Wang et al., 2001a; Zheng et al., 2003) and SNM1A is also thought to play a role in digesting the DNA around an unhooked ICL (Wang et al., 2011).

After unhooking of the ICL translesion synthesis is thought to occur past the gap created. Studies in yeast have suggested that monoubiquitination of PCNA at the K164 residue occurs leading to recruitment of Polζ and synthesis bypass occurs (Sarkar et al., 2006). Alternative studies suggest, in the absence of transcription, Polκ may be recruited and essential in this step (Williams et al., 2012).

Following TLS bypass and gap filling a second round of NER and TLS occurs to completely excise the lesion.

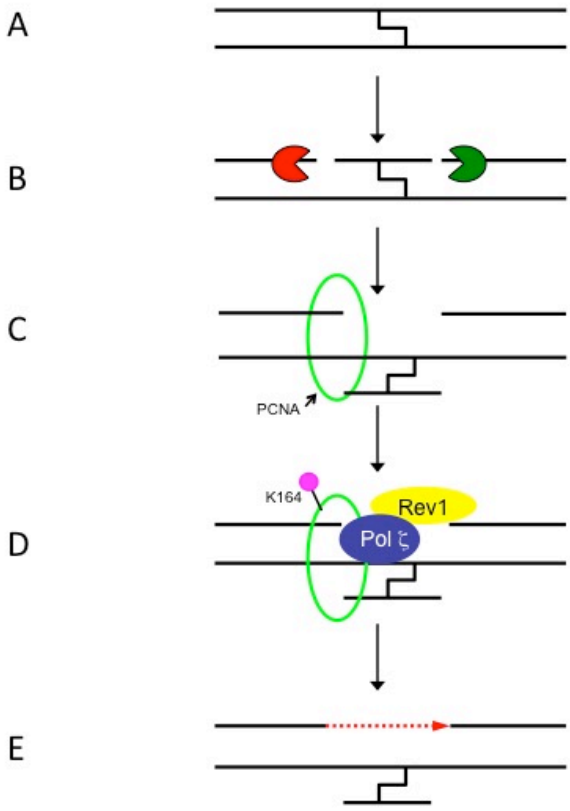



**Figure 1.12: Proposed model for repair of ICL in G1**

A: ICL is detected during transcription or due to the helix distortion caused by the ICL.

B: Dual incisions occur on each side of the ICL.

C: Recruitment of PCNA

D: Following monoubiquitination of PCNA, Rev1 and Polζ are recruited

E: Gap undergoes translesion synthesis bypass.

### 1.5.2 Unhooking of ICL in G1

Following recognition of ICL, incisions are made 5' and 3' to the lesion. In replication dependent repair this leads to formation of a DSB, collapse of the replication fork and repair by DSB-dependent recombination. In replication independent repair (RIR) DSB will not occur if incision occurs on one strand or on both strands but widely separated. This is supported by studies in yeast which observed minimal formation of DSB in stationary cells treated with HN2 (McHugh et al., 2000).

The nucleases involved in replication dependent repair have been discussed in section 1.4.2.3 and it is not clear if the same nucleases operate in RIR. XPF-ERCC1 has been demonstrated to be able to incise differing shaped structures, some in vitro studies have suggested XPF-ERCC1 can only incise 5' and 3' to ICL in Y-shaped structures and therefore might only operate at stalled replication forks (Kuraoka et al., 2000; Fisher et al., 2008). However, there is evidence that XPF-ERCC1 is able to incise duplex DNA (Wang et al., 2011) and in non-replicating mammalian cell free extracts XPF-ERCC1 could incise linear substrates (Smeaton et al., 2008).

Two separate studies by the same group have used a recombination-independent host reactivation assay that examines the repair of site-specific psoralen and MMC ICL to assess the involvement of NER proteins in a G1 type ICL repair (Wang et al., 2001b; Zheng et al., 2003). Their findings support the involvement of XPF-ERCC1 in the G1 repair of psoralen and MMC ICLs. These studies also noted that repair of both psoralen and MMC ICL was impaired in XPG deficient cells suggesting XPG may be involved in the second incision around the ICL. This may be aided by the

helicase XPD causing unwinding of the DNA around the ICL since cells deficient in XPD also showed reduced repair of psoralen and MMC ICL.

It appears that the FA pathway is not required for RIR and the nucleases involved in RIR are recruited independently of FANCD2-FANCI. This has been illustrated by studies of ICL in *Xenopus* extracts that identified depletion of FANCI had no effect on ICL repair in the absence of replication and similarly curcumin, a small molecule inhibitor of the FA pathway did not alter RIR of ICL (Williams et al., 2012).

### 1.5.3 TLS bypass of ICL in G1

Following incisions around the ICL translesion synthesis occurs across the gap formed. Studies in bacteria have illustrated that repair of an ICL-containing plasmid occurred via NER and the TLS polymerase PolB. In yeast detailed studies in G1 have illustrated that following incisions by the NER apparatus further TLS is performed by Polymerase ζ (Sarkar et al., 2006). This study found that initially polymerase Polδ attempts gap-filling but is stalled, possibly by the remaining cross-linked oligonucleotide, leading to monoubiquitination of PCNA and the subsequent recruitment of Polζ which completes gap filling.

These findings have been reiterated in studies using reporter plasmids in mammalian cells. These plasmids were not able to replicate and their repair was biased towards to transcription-coupled repair. In this reporting system REV1 and Polζ were identified as essential for RIR (Shen et al., 2006; Enoiu et al., 2012).

Work in *Xenopus* extracts has supported the involvement of PCNA in G1 TLS bypass. Depletion of PCNA in *Xenopus* extracts reduced repair of an ICL and re-

complementation with a PCNA K164 mutated form of PCNA did not significantly reverse this impaired repair supporting monoubiquitination of PCNA as key to the recruitment of TLS polymerases. In contrast, this study suggested that in the absence of both replication and transcription Polκ may be required for TLS (Williams et al., 2012). This is supported by the findings suggesting that Polκ is required for NER in quiescent cells (Ogi et al., 2010) and Polκ deficient mouse embryonic fibroblasts are highly sensitive to MMC (Enoiu et al., 2012). Therefore, Polκ may be required for TLS in the absence of replication and when levels of transcription are low.

Polη may also be involved in TLS bypass in G1. Studies of psoralen and MMC lesions in a recombination independent host reactivation assay demonstrated a minor role for repair of psoralen ICL and a more extensive role in MMC ICL (Zheng et al., 2003; Wang et al., 2001b). Both these studies used an XP-variant mutant cell line (XPV), XP30RO, which is deficient for Polη. However, there appeared to be no effect on repair of a cisplatin ICL in a human fibroblast XPV cell line in G1 (Enoiu et al., 2012). It is possible that the differing structure of the ICLs may alter the ability of Polη to perform TLS bypass.

### 1.5.4 HR and ICL repair in G1

Repair of ICL in G1 does not appear to generate DSB and it has been surmised that G1 ICL repair would not require HR proteins. This has been confirmed in studies utilising a single cisplatin ICL within a reporter assay system and psoralen and MMC ICL in a host reactivation assay. These demonstrated no difference in ICL repair in XRCC2/3 deficient cells in G0/G1 conditions (Enoiu et al., 2012; Zheng et al., 2003; Wang et al., 2001b). Depletion of Rad51 in *Xenopus* extracts also had no

effect on RIR of ICL (Williams et al., 2012). This supports the proposed model of G1 ICL repair and provides evidence that repair of ICL outside of S-phase is possible.

## 1.6 RNA interference

The discovery of RNA interference (RNAi) has revolutionised the understanding of gene regulation. RNAi refers to a group of related pathways in which small, less than 30 nucleotide long, noncoding RNAs and their associated proteins are able to control genetic expression through post-transcriptional gene silencing (Carthew and Sontheimer, 2009).

RNAi was initially discovered following the observation that injection of double stranded RNA could cause gene silencing in *Caenorhabditis elegans* (*C.elegans*) (Fire et al., 1998). Subsequently RNAi was found to be conserved across species. It has been demonstrated that 5% of the human genome is dedicated to encoding more than 1000 microRNA (miRNA) that regulate 30% of human genes (Jinek et al., 2012). RNAi controls vital cellular processes such as cell growth, tissue differentiation and cell proliferation. Subsequently RNAi dysfunction is associated with cardiovascular and neurological disease and cancer (Lu et al., 2008).

miRNA and siRNA (small interfering RNA) have differing cellular origins, miRNA are derived from the genome, in contrast siRNA can be endogenous or may be derived from viral infections or other exogenous sources (Jinek et al., 2012). In particular, siRNA are widely synthetically created and used in biomedical research. Endogenous sources of siRNA include repetitive sequences (transposons) (Lippman and Martienssen, 2004) and endogenous dsRNA (Watanabe et al., 2008). The dsRNA precursors also differ, with siRNA duplexes demonstrating precise base pairing whereas miRNA contain mismatches and extended terminal loops.

miRNA synthesis occurs in the nucleus where a primary miRNA (pri-miRNA) is created. This is at least 1000 nucleotides long and contains both single or double-stranded hairpins with 5' and 3' terminal overhangs and 10 nucleotide distal loops (Saini et al., 2007). This pri-miRNA is cropped by a microprocessor complex, comprising an RNase family enzyme Drosha and the protein DiGeorge syndrome critical region gene 8 (DGCR8) (Kim et al., 2014), to a 65 to 70 nucleotide precursor miRNA (pre-miRNA) which is exported to the cytoplasm (Han et al., 2006) (Figure 1.13). In the cytoplasm the processing pathways for miRNA and siRNA converge and are described below.

### 1.6.1 siRNA and miRNA silencing

Both RNAi precursors undergo cleavage by the enzyme Dicer (Liu et al., 2006), an endoribonuclease dsRNA-specific RNAse III, to form dsRNA duplexes that are 21 to 25 nucleotides in length that contain 5'phosphate and 3' overhangs (Bernstein et al., 2001). Dicer then assists the dsRNA duplex to bind to an argonate 2-containing RNA-induced silencing complex (RISC) (Liu et al., 2006). This step is assisted by a dsRNA-binding protein (dsRBP) such as TAR RNA-binding protein (TRBP).

The RISC complex is composed of Dicer, TRBP and argonaute-2 (Argo2) (Gregory et al., 2005) and is responsible for creating siRNA from diced dsRNA, loading siRNA and degradation of the 'passenger strand' (MacRae et al., 2008). At RISC loading strand selection occurs and the 'guide strand' is bound to Argonaute to direct silencing and the 'passenger strand' is discarded. It is not clear how strand selection occurs but it is thought to be determined by the thermodynamic stabilities of the siRNA (Elbashir et al., 2001).

The RISC is able to perform cellular surveillance and binds to single-strand RNA (ssRNA), such as mRNA, that is complementary to the guide strand. If there is perfect complementarity Argo2 uses its endonucleolytic activity to degrade the target mRNA by interaction with its PIWI domain, leading to slicing of the complementary mRNA and gene silencing (Tuschl et al., 1999) (Figure 1.13). The RISC and guide strand can repeat this targeted suppression in multiple cycles (Echeverri and Perrimon, 2006).

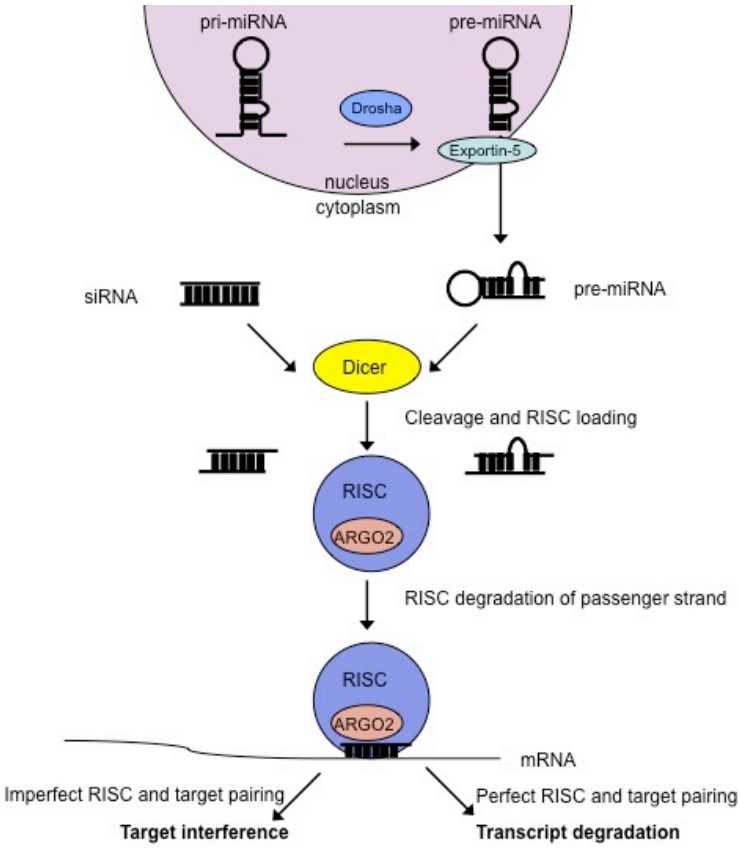



**Figure 1.13: siRNA and miRNA silencing**

miRNA are processed in the nucleus and exported to the cytoplasm. Both miRNA and siRNA are cleaved by Dicer in the cytoplasm and loaded onto the RISC complex. Following degradation of the passenger strand, the RISC is able to bind single stranded RNA that is complementary to the guide strand and depending on the level of complementarity either transcript degradation or interference occurs.

### 1.6.2 Off-target effects

Initially, gene silencing induced by siRNA suppression was considered to be highly specific but several studies have suggested that non-specific effects can be induced both at protein and mRNA level (Jackson et al., 2003). siRNA suppression used in an experimental setting can be challenging since ineffective siRNA suppression can lead to false negative experimental conclusions and non-specific siRNA suppression can produce false-positive experimental conclusions as to the role of gene function. These false-positive effects are termed "off-target" effects.

siRNA off-target effects can be divided into three categories: siRNA-induced sequence dependent suppression of unintended targets through partial sequence complementarity; inflammatory effects through activation of Toll-like receptors by siRNA (interferon response) or their transfection reagents and saturation of the endogenous RNAi machinery leading to effects on microRNA processing and function.

#### 1.6.2.1 Sequence dependent suppression of unintended targets

Previous studies, using microarray analysis, have revealed that siRNAs targeting the same sequence are able to induce differing unique gene silencing profiles (Jackson et al., 2003). Assessment of the transcripts of the suppressed genes revealed that the 3'UTR of the transcripts were complementary to the 5' end of the transfected siRNA guide strand (Jackson et al., 2006b; Birmingham et al., 2006). When siRNA were altered creating mismatches at the 5' end, the original off-target suppressive effects were reduced but also created a new panel of off-target transcripts that matched the new mismatched guide strand (Jackson et al., 2006b). It therefore appears that the 5' end of the siRNA guide strand is particularly

important in defining off-target silencing. This region of the guide strand appears to mimic the seed region of microRNA. microRNA are able to regulate multiple mRNA targets which possess 3'UTR sequences that are complementary to the 5' end of the microRNA strand (Brennecke et al., 2005; Farh et al., 2005) and it appears that siRNA are able to function in a similar fashion.

These microRNA like off-target effects can be mitigated through several methods. Chemical modification of siRNA to include a 2'-O-methyl ribosyl substitution in the second position in the guide strand has been shown to reduce off-target effects by 66% at transcript level (Jackson et al., 2006a). Studies have also illustrated that a similar modification to the passenger strand also reduces its activity and chance of causing off-target effects.

There have been conflicting findings with regards to the optimal concentration of siRNA to decrease off-target effects. Microarray profiling has suggested higher concentrations of siRNA lead to increased off-target activity (Persengiev et al., 2004). However, other studies have suggested off-target effects do not correlate with target gene silencing and therefore off-target effects cannot be specifically reduced by decreasing siRNA concentration (Jackson et al., 2003; 2006b). Current best practice appears to be to use the lowest concentration of siRNA that produces maximal silencing.

The use of pooled siRNA that target the same transcript, may reduce off-target effects by introducing competition for the target site (Kittler et al., 2007). Within the pool of siRNA particular siRNA will have higher affinity for the target mRNA leading to optimal silencing. Off-target effects can be minimalised, as the concentration of each individual siRNA strand is reduced leading to reduced

targeting of unwanted genes. One previous study identified that a pool of 10 synthetic siRNAs reduced off-target effects compared to a single siRNA (Kittler et al., 2007).

#### 1.6.2.2 Inflammatory effects

The immune system of cells detects infectious non-self agents such as lipopolysaccharide, bacterial DNA and viral RNA. Initially siRNA were thought to be too small to trigger the immune system and an interferon response. However, siRNA have been demonstrated to trigger the innate immune system through activation of Toll-like receptors (TLRs) (Judge and MacLachlan, 2008), in particular TLR7 and TLR8. siRNA stimulate monocytes and dendritic cells through TLR8 to produce inflammatory cytokines and activate plasmacytoid dendritic cells through TLR7 to produce interferon-α (IFNα) (Judge and MacLachlan, 2008; Hornung et al., 2005).

TLR7 and TLR8 appear to preferentially recognise siRNA sequences that are rich in uridine(U) and guanosine (G) and selecting sequences that lack GU-rich regions may reduce immunostimulatory activity (Heil et al., 2004). The length of the siRNA also appears to determine immunostimulation. siRNA that were 12 or 16 nucleotides in length and contained an immunostimulatory motif (GUCCUUCAA) resulted in less cytokine induction than siRNA that were 19 or more nucleotides in length (Hornung et al., 2005). Furthermore, it appears that the use of cationic lipids as a delivery vehicle to facilitate uptake and protect siRNA may also potentially stimulate the immune system via the endosomal pathway (Sioud, 2005).

#### 1.6.2.3 Saturation of RNAi machinery

It has been identified that co-transfection with multiple siRNAs can reduce the efficiency of each individual reagent and this may be due to saturation of components of the RNAi machinery. Studies have shown saturation of RISC may lead to competition between exogenous siRNA and microRNA potentially leading to disruption of endogenous microRNA regulation of gene expression (Khan et al., 2009). This may potentially result in exogenous siRNA having global effects on genes that are usually under the control of endogenous microRNA.

## 1.7 siRNA screens

### 1.7.1 siRNA screening in mammalian cells

The technique of RNAi has been adapted to allow screening on a genome-wide basis for varying cell properties. In particular within cancer medicine it has been used to screen for radiosensitivity (Higgins et al., 2010; Tiwana et al., 2015), drug sensitivity (Postel-Vinay et al., 2013) and mechanisms of cancer cell drug resistance (Iorns et al., 2008).

To facilitate large-scale screens, genome-wide libraries have been developed of one or more types of RNAi agent. Large-scale screens have been successfully performed in a number of cell lines including *Drosophila*, mouse and human cells. RNAi screens have also been performed *in vivo* in species such as *C.elegans* (Sin et al., 2014), *D. melanogaster* (Perrimon et al., 2010), trypanosomes (Mony et al., 2014) and mice.

As discussed previously, RNAi screens can be associated with false positive and false negative effects. A common strategy to validate RNAi screens is to test multiple reagents for each gene since different reagents will have different seed sequences, which as noted previously, can lead to off-target effects. If multiple independent reagents are able to reproduce the desired phenotype then there can be more confidence that a true positive result has been identified (Sigoillot and King, 2011).

Another technique for validating screen results is to perform rescue experiments. This involves expressing an RNAi-resistant version of the targeted gene within cells and assessing whether the phenotypic change identified with RNAi is re-

complemented. This can be time consuming and difficult to achieve if rescue constructs are not expressed at physiological levels (Zhou et al., 2008).

Recently with the advent of CRISPR-Cas9 technology and other genome-editing techniques it is possible to create complete knockout or loss of function alleles to assess functional screen results. A recent study used this approach after identifying FAT1 as a potential regulator of apoptosis in a siRNA screen in human glioblastoma cells. CRISPR-Cas9 mediated knockout of FAT1 confirmed sensitivity to death receptor-induced apoptosis consistent with the findings of the siRNA screen (Kranz and Boutros, 2014).

#### 1.7.1.1 Cisplatin siRNA screens

The identification of cisplatin drug response modulators could help to provide better understanding of the mechanisms of resistance to drug therapy, identify drug targets for combination therapy and provide biomarkers for treatment strategies. Several genetic screens have been performed in model organisms such as *S. cerevisiae* to identify cisplatin modulators (Wu et al., 2004; Simon et al., 2000; Lum et al., 2004). As there is a high level of genetic conservation between *S. cerevisiae* and humans this has been helpful in understanding response to cisplatin in human cells. These studies utilised yeast strains with defined genetic deletions and identified that strains which possessed deletions in the post-replication pathway (*rad6* and *rad18*), recombinational repair (*rad50, 51* and *52*), TLS (*rev1, rev3*) (Simon et al., 2000) and NER (*rad1,2,4,10* and *14*) had increased sensitivity to cisplatin.

siRNA screens have also been performed in human cells to identify potential cisplatin sensitisers (Nijwening et al., 2011). Linsley *et al* identified several cisplatin sensitisers that overlapped with previous yeast genetic screens in a screen performed in human TP53 deficient HeLa cells (Bartz et al., 2006). These included the DNA damage repair targets BRACA1, BRCA2, RAD51 and RAD18. Silencing of BRCA1, BRCA2 or associated BRCA1/2 genes resulted in a 4 to 7-fold increased sensitivity to cisplatin in TP53 deficient cells compared to wild-type TP53 cells.

RNAi libraries targeting kinases have also been used for analysis with both ovarian (SKOV3) (Arora et al., 2010) and colorectal (HCT-116), breast (MDA-MB-231) and lung cancer (A549) cell lines (Swanton et al., 2007). A 572 gene screen in ovarian cancer cells identified ATR, CHEK1 and PRKAB1 as potential cisplatin sensitisers (Arora et al., 2010). Further studies used small-molecule inhibitors of CHEK1 to confirm that suppression of CHEK1 resulted in increased sensitivity to cisplatin. Swanton *et al* utilised a siRNA library targeting kinases and proteins involved in ceramide lipid metabolism to examine sensitivity to a panel of 4 chemotherapeutic drugs including cisplatin. They identified that targeting of COL4A3BP resulted in marked multidrug sensitisation (Swanton et al., 2007). It was proposed this sensitivity might be due to ceramide accumulation in cells resulting in a synergistic effect.

These screens, whilst identifying cisplatin sensitivity, used differing durations of cisplatin treatment and measured phenotypic sensitisation by a variety of assays including resazurin and luciferase viability assays and nuclei staining with DAPI.

The form of end-point analysis used in a siRNA screen has potential to create differing results and this will be discussed further below.

#### 1.7.1.2 Radiation siRNA screens

Several large-scale siRNA screens have been previously performed to assess for radiosensitisation. As with cisplatin screens, these have utilised a variety of end-point assays and have been performed in a number of human cancer cell lines including laryngeal (Higgins et al., 2010), prostatic (Ni et al., 2011), lung (Nagel et al., 2015), cervical (Tiwana et al., 2015), glioblastoma (Zheng et al., 2008) and head and neck cancers (Ito et al., 2011).

Zheng *et al* successfully performed a large-scale siRNA screen in a glioblastoma cell line and identified that silencing of the gene tumour necrosis factor receptor-associated factor 2 gene (TRAF2) resulted in growth suppression and sensitised cells to radiation. Further experimental work confirmed suppression of this gene in both a radioresistant lung cancer and a head and neck cancer cell line also resulted in growth suppression and increased radiosensitisation.

Head and neck cancer cell lines were also used by Ito *et al* to identify uroporphyrinogen decarboxylase (UROD) as a potential radiosensitising target. The authors identified that UROD suppression and irradiation caused apoptosis and cell cycle arrest in cells and could also suppress the growth of tumour xenografts in mice. Further work suggested that UROD suppression also sensitised cancer cells to the chemotherapeutic agents cisplatin, paclitaxel and 5-fluorouracil (5FU).

A radiosensitivity screen performed by Higgins *et al* used parallel siRNA screens in tumour (SQ20B- laryngeal) and normal tissue (MRC5) cell lines. This screen of 200 DNA damage repair genes successfully identified several known radiosensitisers, validating the screen methods, and also POLQ (DNA polymerase θ) as a potential radiosensitiser. Further investigation revealed suppression of POLQ induced radiosensitisation in several other tumour cell lines.

Nagel *et al* performed an extensive siRNA radiosensitisation screen in a non-small cell lung cancer (NSCLC) cell line. This screen assessed 21,000 genes for induction of radiosensitivity and observed that suppression of both Forkhead box M1 (FOXM1) and microtubule-associated serine/threonine kinase-like (MASTL) caused radiosensitisation in panel of NSCLC but not in primary human fibroblasts. Further work suggested the sensitivity of MASTL suppressed cells was due to defects in cytokinesis leading to cell cycle arrest.

Finally, a major siRNA radiosensitivity screen was recently performed in HeLa cells by our laboratory. This utilised a high-throughput clonogenic formation assay to assess for radiosensitisation following suppression of a library of kinases. This screen successfully identified thiamine pyrophospkinase-1 (TPK1), a component of thiamine metabolism, as a potential target for radiosensitisation. The authors screen findings were confirmed by suppression with a thiamine analogue and by knockdown of the thiamine transporter-1 (THTR1) both of which also caused tumour specific radiosensitisation. This screen, unlike the others previously described, used clonogenic survival assays that are able to assess for long-term effects on clonality.

### 1.7.2 End-points for siRNA screens

Following siRNA suppression cells used in a screen are assessed for phenotypic changes by an appropriate assay. siRNA screens performed in cancer cell lines are principally interested in the effect of gene knockdown on tumour cell survival and susceptibility to a particular treatment. A variety of end-point assays have been utilised to assess cancer cell siRNA screens including cell viability assays, DNA damage foci quantification, micronuclei assays and colony formation assays

#### 1.7.2.1 Cell growth and survival assays

Cell viability assays have been used by several groups to assess the effects of siRNA suppression on sensitivity to chemotherapeutic agents or radiation. These include the use of the 3-(4,5-Dimethylthiazol-2-yl)-2,5-diphenyl tetrazolium bromide (MTT) (Bartz et al., 2006; Ni et al., 2011), Resazurin (also known as Alamar blue) and luciferase (Cell-Titer Glo) assays (Swanton et al., 2007; Arora et al., 2010; Zheng et al., 2008).

The MTT is a colorimetric assay assessing cell metabolic activity of NAD(P)H-dependent cellular oxidoreductase enzymes. These enzymes reduce tetrazolium dye in the MTT assay to insoluble formazan which can be assessed by spectrophotometer (Mosmann, 1983). MTT can be used to assess cytoxicity or cytostatic activity and has been used in siRNA screens to assess for radiosensitising and chemosensitising agents (Bartz et al., 2006; Ni et al., 2011).

Resazurin and luciferase assays are based on similar principles. NADH reduces Resazurin to resorufin in mitochondria and the assay can therefore assess mitochondrial metabolic activity and aerobic respiration. Luciferase assays such as

Titer-Glo assess the conversion of luciferin to oxyluciferin by ATP and therefore this assay also reflects cell viability.

These assays may be subject to technical issues with the solubilisation of the colorimetric stains leading to errors in absorbance readouts and the assay can also be effected by external factors that alter the growth of cells in culture. Importantly, cancer treatments such as radiation, initially may not lead to impaired cell proliferation but ultimately colony formation may be reduced (Price and McMillan, 1990). Thus viability assays may lead to false negative results.

#### 1.7.2.2 DNA damage foci quantification

DNA foci quantification has been successfully used in radiation siRNA screens (Higgins et al., 2010). Following irradiation DSB form and it is possible to assess recruitment of proteins to these breaks by fluorescent labelled antibodies. This technique has been used to assess γH2AX foci which have been shown to correlate with intrinsic radiosensitivity (Banath et al., 2004; Klokov et al., 2006). This is a useful technique to assess radiosensitivity but may only identify targets that interfere with the DNA damage response.

#### 1.7.2.3 Cell proliferation

A previous siRNA screen utilised Bromodeoxyuridine (BrdU) assays to assess cell proliferation (Ito et al., 2011) and assess for radiosensitivity. BrdU is a thymidine analogue which, when incubated with dividing cells, is incorporated into newly synthesised DNA. This technique was successfully adapted for use in a large-scale screen but only assesses for short-term effects and may not be able to accurately assess long-term effects of radiation on replication.

#### 1.7.2.4 Micronuclei assays

Micronuclei assays have been used to assess the outcome of radiation siRNA screens (Balmus et al., 2015). Micronuclei are formed when mis-segregation of chromosomes occurs during cell division. They consist of small fragments of chromosomes. Previous studies have suggested that there is a correlation between micronuclei formation and radiosensitivity (GUO et al., 2009; Liu et al., 2005). However this appears to be inconsistent and more recent studies suggest this may only be present at high doses of radiation (Bergqvist et al., 2001).

#### 1.7.2.5 Colony Formation Assays

Colony formation assays (CFA) are able to fully assess loss of replicative potential since they measure the ability of a single cell to replicate to a colony (Franken et al., 2006). This is particularly relevant to the assessment of cancer treatment since it is continued replicative potential that leads to recurrence of tumour or resistance. This technique is also useful in assessing response to radiation therapy as it can reveal the mitotic catastrophe that typically occurs some time after radiation. CFA are laborious to perform but our laboratory has recently successfully adapted the standard CFA technique to a 96-well format allowing it to be successfully used for a high-throughput radiation siRNA screen (Tiwana et al., 2015).

## 1.8 Cancer stem cell theory and its role in resistance to cancer treatment

It has been proposed that malignant tumours originate and are sustained by a population of cells that share characteristics with normal adult stem cells. This proposal, the cancer stem cell hypothesis, is based in part on the observation that tumour cells, like stem cells, possess the ability to self-renew and produce differentiated tissue cells. This theory is based on previous experimental findings in solid and haematological malignancies and will be discussed in more detail below.

### 1.8.1 Origins of stem cell theory

Stem cell theory proposes that cells can be divided into three basic functional groups: stem cells, progenitor cells and mature cells. Stem cells form only a small percentage of the cell population and rarely divide but are able to form descendent daughter stem cells or progenitor cells when they do. Stem cells possess traits of self-renew, self-protection and damage tolerance. Progenitor cells are able to proliferate intensively but have a limited capacity for self-renewal with a finite number of cell divisions. Mature cells represent the last stage of cellular development. Since tissue is characterised by a fixed number of cells, mature cells are replaced by new mature cells formed by progenitor cells and homeostasis is achieved (Fulawka et al., 2014).

Within this model, stem cells exist as a pool of long-lived cells that are able to continuously supply differentiated cells to tissue compartments. This is important for tissues such as the epithelium or blood that undergo continuous cellular turnover. This concept of adult stem cells fits with the classic model of

carcinogenesis that proposes that a long-lived cell undergoes multiple genetic hits resulting in malignant transformation (Vogelstein et al., 1988). An alternative proposal is that progenitor cells undergo aberrant transformation gaining the capacity to self renew and become the long-lived target cell that gains additional genetic mutations (Passegue et al., 2003).

### 1.8.2 Evidence for cancer stem cells from the haematopoietic system

Much of the evidence supporting the cancer stem cell theory has developed from experiments performed to examine normal and malignant haematopoiesis. These experiments initially identified the haematopoietic stem cell (HSC) and later leukaemic stem cells (LSC) that could be segregated by fluorescence-activated cell sorting (FACS).

Initial studies illustrated that grafted haematopoietic bone marrow cells could recapitulate in irradiated mice and differentiate towards mature blood cells demonstrating stem cells not only were self-renewing, but were able to differentiate into mature cells (Spangrude et al., 1988).

Further studies of haematological malignancies demonstrated, using myeloma and leukaemia cells, that only a small subset of cells were capable of forming colonies and extensively proliferating. Using colony forming assays and mouse myeloma, cells obtained from ascites and separated from normal haematopoietic cells, only 1 in 10,000 to 1 in 100 cells were able to form colonies (Park et al., 1971). Similarly, when leukaemic cells were transplanted into mice *in vivo* only 1-4% of cells could form spleen colonies (BRUCE and van der GAAG, 1963; Bergsagel and Valeriote, 1968). These results suggested that either all leukaemia cells could behave as stem

cells but had low proliferative capacity or that most leukaemic cells had a low proliferative ability but within the population of cells existed a subset that were extremely clonogenic.

To assess the second assumption it was necessary to prove that leukaemic cells could be separated into subsets and that one was highly enriched for clonogenicity. Seminal work was performed by Dick *et al* (Bonnet and Dick, 1997) who identified that a subset of AML cells could be purified that were $CD34^{+}CD38^{-}$. These cells represented only a small proportion (0.2% in one patient) of AML cells but when transplanted into immunodeficient mice they were capable of inducing AML suggesting that this subset of cells was enriched for proliferation and ability to transfer disease. Significantly cells that were $CD34^{+}CD38^{+}$ or $CD34^{-}$ were not able to initiate leukaemia and the engrafted leukaemia induced by $CD34^{+}CD38^{-}$ cells could be serial transplanted into secondary recipients supporting the cancer stem cell hypothesis.

### 1.8.3 Evidence for solid tumour cancer stem cells

The first evidence for solid tumour cancer stem cells (CSCs) was presented in the mid-$20^{th}$ century. A series of experiments demonstrated that a cancer cell population isolated from peritoneal fluid was present in every serially grafted tumour (MAKINO, 1956; Fiala, 1968) suggesting a self-renewing population of cells existed in the original tumour sample.

Most recently Al-Hajj *et al* (Al-Hajj et al., 2003) used similar techniques to those used in haematological malignancies to isolate a population of cells from human breast carcinoma that were able to form tumours in immunodeficient mice. The

authors used FACS to purify populations of breast cancer cells based on their expression of CD44 and CD24. Implanted samples that were $CD44^{+}CD24^{-}$ were able to initiate breast tumours when implanted into the mammary pads of immunodeficient mice whereas 100-fold more cells from $CD44^{+}CD24^{+}$ and $CD44^{-}$ populations when implanted could not form tumours. Significantly the engrafted tumours contained similar heterogeneity as the original sample containing $CD44^{+}CD24^{-}$, $CD44^{+}CD24^{+}$ and $CD44^{-}$ cells and could be serial engrafted demonstrating the self-renewal associated with stem cells.

Further evidence for cancer stem cells has also been identified in work in brain tumour cell lines. Two groups have independently isolated a stem-cell like population from human paediatric brain tumours (Singh et al., 2003; Hemmati et al., 2003). They identified that this population of cells was $CD133^{+}$ and, similar to the findings of Al-Hajj *et al* in breast cancer, $CD133^{+}$ transplanted cells gave rise to brain tumours in immunodeficient mice that contained heterogeneous cell types and these tumours could be serially transplanted.

These experimental findings all used xenotransplantation to demonstrate the presence of a self-renewing population of cells. This experimental model may introduce bias as engraftment may depend on other factors such as evasion of immune response and proliferative capacity. However, xenotransplantation appears to be the most physiologically comparative model for human malignancies and these studies appear to corroborate the concept of human cancer stem cells.

### 1.8.4 The role of cancer stem cells in resistance to cancer treatment

The classic strategy of anticancer treatment is to target intensively proliferating cells to reduce tumour burden and cause regression of malignant disease. The cancer stem cell hypothesis suggests that every tumour must contain a population of cancer stem cells (CSCs) and since these are quiescent or rarely dividing they are unlikely to be eradicated by treatments targeting rapid replication. This could potentially lead to persistence of CSCs leading to recurrence or metastatic disease. Furthermore, current and new therapies that are investigated are often identified by their ability to shrink tumours. This only eradicates cells with limited proliferative ability and will not target cancer stem cells. It is essential that cancer therapies are developed that target CSCs since many current therapies, whilst showing initial efficacy, only have a transient effect and recurrent disease eventually develops.

The targeting of cancer stem cells will remain elusive without further detailed study. Previous studies have identified that normal stem cells tend to be more resistant to chemotherapeutics than mature cell types from the same tissues (Harrison and Lerner, 1991). This reason for this is unclear but if cancer stem cells display the same traits then they too may be more chemoresistant. One area of study within this thesis will be the repair of ICL in quiescent cells. Better understanding of repair of ICL in non-dividing cells may reveal potential treatment targets for cancer stem cells and offer potentially translatable drug target for cancer treatment.

## 1.9 Objectives of this thesis

The primary objective of this thesis is to identify potential novel druggable targets to increase tumour sensitivity to cisplatin chemotherapy or radiation treatment. This will be addressed in two ways:

- Completion of a large-scale siRNA screen of a library of DNA damage repair genes to identify potential cisplatin and radiation sensitisers in a human lung cancer cell line.

- Creation of a model to study ICL repair in G1 using synchronised cells.

- Use of this model to analyse the potential role of candidate repair factors in repair of ICL in G1.

# Chapter 2 - Methods

## 2.1 Materials and Reagents

Unless otherwise stated all solvents and chemicals were purchased from Sigma-Aldrich, UK. Solutions were prepared with water purified using a Milli-Q system (Milli-Q purification system, Millipore Corporation, Billerica, MA).

## 2.2 Drug Preparation

Solutions of cisplatin, mechlorethamine hydrochloride (nitrogen mustard [HN2]) and 2-dimethylaminoethylchloride (mononitrogen mustard [HN1]) were prepared from powder for each experiment. Drugs were diluted to standard stock with water and then further diluted to the concentration required in fresh cell culture media.

## 2.3 Mammalian Cell Culture

### 2.3.1 Mammalian cell lines

Parental and DNA damage mutant Chinese Hamster Ovary cell lines (CHO, Table 2.1) were originally obtained from Clare Hall Cell Services, Cancer Research UK. Human H460 lung cancer cell lines were purchased from American Type Culture Collection (ATCC). HAP1 wild type and PIF1 CRISPR/Cas9 knockout cell lines were purchased from Horizon Discovery, Cambridge, UK. All cell lines were stored as frozen stocks in liquid nitrogen. New cultures were established from frozen stocks regularly and tested for *Mycoplasma* using MycoAlert (Lonza).

| Cell Line | Parental Cell Line | Defective Gene |
|---|---|---|
| **AA8** | | None WT |
| **UV23** | AA8 | XPB |
| **UV42** | AA8 | XPD |
| **UV47** | AA8 | XPF |
| **UV61** | AA8 | CSB |
| **UV135** | AA8 | XPG |
| **XRS5** | CHO-K1 | XRCC5 |
| **irs1SF** | AA8 | XRCC3 |

**Table 2.1: Chinese Hamster cell lines used for experiments in this thesis.**

### 2.3.2 Culture medium

All CHO cell lines were cultured in tissue flasks containing Roswell Park Memorial Institute (RPMI)-1640 media (Invitrogen, Carlsbad, CA) supplemented with 10% fetal bovine serum (FBS)(PAA Laboratories, Pasching, Austria). For G1 arrest experiments CHO cells were incubated in isoleucine free RPMI media prepared from powder (Invitrogen, Carlsbad, CA), this was supplemented with 10% dialysed FBS (Invitrogen, Carlsbad, CA).

H460 cells were cultured in Dulbecco's Modified Eagle Medium (DMEM, Sigma) also supplemented with 10% FBS. HAP1 cell lines were cultured in Iscove's Modified Dulbecco's Medium (IMDM, Invitrogen), again supplemented with 10% FBS.

All cell lines were incubated at 37°C in humidified 5% $CO_2$ cell culture incubators. Cells were sub-cultured when they reached 80% confluence by trypsinisation: media was removed from cultured cells and cells were washed in phosphate buffered saline (PBS) prior to the addition of trypsin-ethylenediaminetetraacetic acid (EDTA). Cells were then incubated for 10 minutes to allow disassociation of the adherent cells before re-suspension and dilution in the appropriate media.

## 2.4 High-throughput siRNA screen

### 2.4.1 siRNA libraries

#### 2.4.1.1 Primary siRNA screening library

A primary siRNA screen of a library of 640 genes involved in the DNA damage response was performed using a commercial siRNA library supplied by Qiagen, Germany. The "DNA damage" library consisted of genes involved in the duplication of the genome and also in repair of endogenous and exogenous damage. The library was laid out in eight 96-well plates with the two outer columns left empty to allow the addition of control siRNAs. Each well contained a pool of four separate siRNAs targeting a single gene.

#### 2.4.1.2 Secondary siRNA screening library

After analysis of the primary DNA damage screen results, a secondary screen was performed to reduce the possibility of false positive results from off-target siRNA effects. The secondary screen used a custom-made library of ON-TARGETplus siRNA supplied by Dharmacon (GE Lifesciences, USA) designed after selecting 40 genes of interest from the primary screen. Each well contained a pool of four separate ON-TARGETplus siRNAs targeting a single gene.

#### 2.4.1.3 Positive and negative controls for the siRNA screens.

Negative controls were a non-targeting (NT) siRNA and an un-transfected control using siBuffer only. The positive controls were ataxia telangiectasia and Rad3-related protein (ATR): a positive control for chemosensitisation, DNA-dependent protein kinase catalytic subunit (DNA-PK*cs*): a positive control for radiosensitivity

and polo-like kinase-1 (PLK-1): a positive control for transfection efficiency. Control siRNA were purchased from Qiagen, Germany.

### 2.4.2 High-throughput siRNA transfection in 96 well plates

Reverse transfection of H460 cells was performed in the Target Discovery Institute, Oxford using a Perkin Elmer Janus liquid handling workstation.

The siRNA libraries were diluted with the appropriate buffer or water to 0.4μM and kept at 4°C immediately before use. The Janus robot transferred 10μl siRNA stock from each library plate to new 96 well V-bottom plates and control siRNAs were subsequently added manually to these plates in columns 1 and 12 as illustrated in the plate diagram in Figure 2.1.

The transfection reagent INTERFERin-HTS (Polyplus, France) was diluted 1:100 with water and aliquoted across a V-bottom 96-well stock plate. Using the Janus robot 10μl INTERFERin-HTS was transferred to the 10μl siRNA and mixed. After 20 min incubation, 10μl of the INTERFERin-siRNA mix was transferred, using the JANUS robot, to flat-bottom 96 well plates already filled with 40μl culture medium. Finally 50μl of cell suspension (4000 cells total- concentration 8 x $10^4$ cells/ml) was then added manually to the siRNA/INTERFERin media, and incubated at room temperature for 20 minutes, to allow the cells to settle, prior to incubation at 37°C for 72 hours. The final concentration of siRNA was 20nM and final INTERFERin-HTS concentration was 0.05% for each transfection reaction.

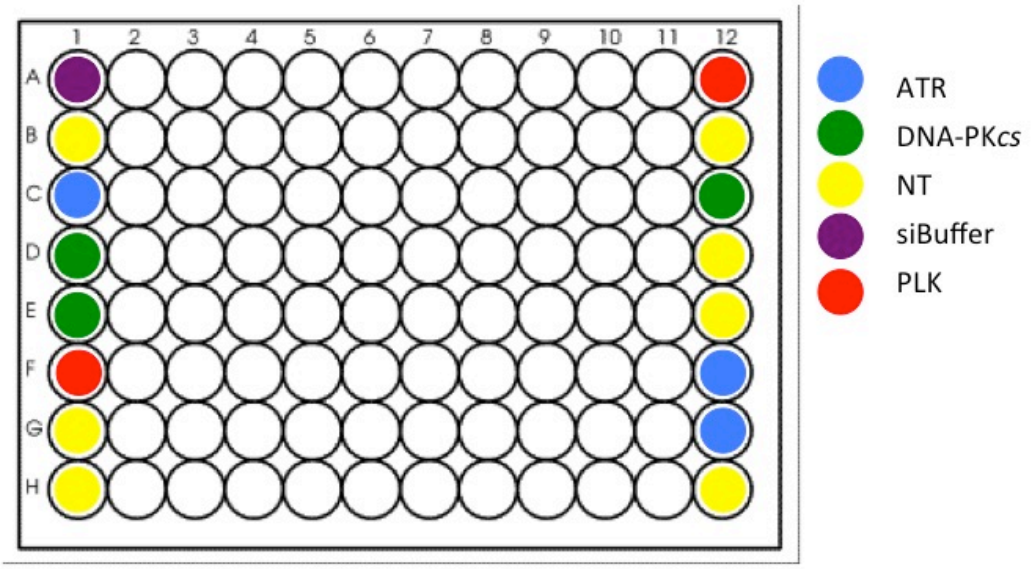



**Figure 2.1: Layout of control siRNA for high throughput screen.**

Control siRNA were placed around the edge of the 96-well plate in columns 1 and 2. Library siRNA were placed in columns 2 to 11.

### 2.4.3 Assessment of cell viability using Resazurin

The viability of H460 cells was assessed, 72 hours following siRNA transfection, by addition of resazurin sodium salt (Sigma), which is converted to the fluorescent resorufin by viable cells. To perform this assessment, 10µg/mL resazurin in PBS was added to cells in a 1/10 ratio. Cells were incubated for 1 hour at 37°C and the fluorescence activity of the cells measured using a POLARstar Omega plate reader at 560Ex/590Em. The efficiency of transfection could be assessed by cell viability as successful PLK-1 knockdown leads to cell death leading to a decreased fluorescent resorufin signal.

### 2.4.4 Re-plating of transfection plates

At 72 hour after transfection, the cells in the 96 well transfection plates were lifted, counted and split to treatment plates. To determine cell numbers, a single non-targeting siRNA well from each transfection plate was trypsinised, re-

suspended in a total volume of 200 µl, and counted to calculate the volume of cell suspension containing 12000 cells. This cell suspension volume was then applied for the transfer of all transfection plates as described below.

Medium was then removed from all wells of the transfection plates; each well was manually washed with 50µl PBS and incubated with 50µl trypsin for 10 minutes at 37°C. Using the Janus Robot, all wells were re-suspended in 200µl medium and the pre-determined volume transferred to a 96 deep-well plate to make a final concentration of 0.75 x $10^4$ cells/ml. The deep well plate was used as a stock to dispense 200µl (1500 cells) to each well of the 96 well plates undergoing 3Gy irradiation, 100µl (750 cells) to each well of cisplatin treatment plates and 40µl (400 cells) to control plates. The increased cell numbers for treated wells was to ensure adequate cell survival numbers to allow accurate assessment of the effects of siRNA knockdown. Plates had been prefilled with the appropriate volume of culture medium to ensure the final well volume was 200 µl across all treatment arms. After cell addition, plates were left to incubate at room temperature for 20 minutes before transfer to 37°C incubator.

Each transfection plate was replicated in quadruplicate plates for each condition (control, cisplatin treated and irradiated) and the entire screen was repeated a week after the initial experiment.

### 2.4.5 Cisplatin and irradiation treatment

Cells were treated with cisplatin or radiation 4 hours after plating. Cisplatin was dissolved in sterile water to make 2mM stock. This was diluted in DMEM with 10% FBS to make a 1µM medium-cisplatin solution. 100µl of this solution was added to

each well of cisplatin treated plates (final concentration 0.5μM) by JANUS robot. Cells were incubated with cisplatin for the duration of the experiment.

Plates were irradiated in batches of 24 inside a 2cm thick Perspex phantom. The irradiation was delivered by a Varian IX linear accelerator with 6 MV photons at a dose rate of 600MU/min, gantry angles of 0 and 180 degrees, to a total dose of 3Gy.

Following irradiation or addition of cisplatin all treatment plates were returned to the incubator to allow colony formation to occur.

### 2.4.6 Colony staining and counting

Seven days after radiation or cisplatin treatment, all plates were stained. Using the BioTek ELx405 microplate washer, the medium was aspirated from all wells and 25μl 0.5% crystal violet stain (10% ethanol, 50% methanol, 40% $H_2O$) added by MultiDrop 8-channel automated dispenser (Thermo Fisher). Plates were left to stain for 2 minutes at room temperature before each well was washed three times with water using the microplate washer and allowed to dry. Once dry, colonies were counted using a GelCount (Oxford Optronics) plate reader and counting software.

### 2.4.7 Statistical analysis of screens

In order to analyse the screen, averages were taken of the colony counts for each individual gene in both the untreated, cisplatin treated and irradiated quadruplicate plates. Using these averages a plating efficiency (PE, Figure 2.2 A) was calculated for each gene in the untreated and treated conditions. Surviving fractions (SF, Figure 2.2 B) were then calculated for each siRNA knockdown. The

SF for each gene of interest was normalised to the median NT control SF on each library plate. A standard score (Z-score, Figure 2.2 C) could then be calculated by comparing the library siRNA to the median of the normalised NT across all library plates.

Z-scores were ranked in ascending order and then a ranked product analysis carried out for each replicate run in both the primary and secondary siRNA screens.

Z-factor calculations (Figure 2.2) were also made for each library plate to assess the robustness of both primary and secondary screen.

**A**

$$PE = \frac{Average\ Colony\ Number}{Number\ of\ cells\ plated}$$

**B**

$$SF = \frac{PE_{treated}}{PE_{untreated}}$$

**C**

$$Z - score = \frac{(Normalised\ SF - median\ normalised\ NT\ SF)}{(Mean\ absolute\ deviation\ of\ normalised\ NT\ SF)}$$

**D**

$$Z - factor = 1 - \frac{3(\sigma SF_{NT} + \sigma SF_{treated})}{(\mu SF_{NT} - \mu SF_{treated})}$$

**Figure 2.2: Equations used in the statistical analysis of siRNA screens**

A: Equation for calculating plating efficiency (PE).
B: Equation for calculating surviving fraction (SF).
C: Equation for calculation of standard score (Z-score).
D: Equation for calculating Z –factor.
μ= Mean.
σ= standard deviation.
NT= Non-transfecting.

## 2.5 Transient transfection of mammalian cell lines

### 2.5.1 siRNA transfection (6 well format) for confirmation of siRNA screen hits

Targets identified in the secondary screen were validated by siRNA transfections and clonogenic survival assays performed in 6-well format. Each transfection was performed in triplicate wells to obtain sufficient cells for colony formation and confirmation of knock down by qRT-PCR or Western Blotting.

All confirmatory siRNA transfections were performed with siRNA from Ambion (Ambion Silencer Select siRNA, Life Technologies, Thermo Fisher, UK), a different supplier than both the primary and secondary screens. The siRNA used for these experiments were single siRNA strands.

Validation studies were performed with a reverse transfection protocol with a final siRNA concentration of 20nM and INTERFERin-HTS concentration of 0.05%. Briefly siRNA and INTERFERin-HTS were both diluted with sterile water to 2µM and 1 in 100 respectively. 100µl 0.4µM siRNA was added to 100µl 1% INTERFERin-HTS and incubated at room temperature for 20 minutes. 200µl of INTERFERin-siRNA complex were added to each well of a 6-well plate and 1.8ml of cell solution containing 1.5 $x10^5$ cells added to each well and the plate swirled before being incubated at 37˚C for 72 hours.

### 2.5.2 siRNA transfection (10cm dish) for CHO cell knockdown

siRNA knockdown of CHO cell lines was performed in 10cm dishes with a final siRNA concentration of 40nM and using 30µl of Lipofectamine 2000 (Thermo Fisher, UK) per reaction. Briefly siRNAs were diluted to 0.4µM with Opti-MEM (Thermo Fisher, UK). Lipofectamine 2000 was diluted 1 in 50 with Opti-MEM

(total solution 1500µl per reaction) and incubated for 5 minutes at room temperature. Equal volumes of diluted siRNA and Lipofectamine 2000 were combined (total reaction volume 3000µl), mixed gently and incubated for 20 minutes at room temperature. The reaction mixture (3000µl) was then added to a solution of 5 x $10^5$ cells and swirled gently. Plates were then incubated at 37˚C for 24 hours.

| Gene of interest (Species) | siRNA sequence |
|---|---|
| **EXO1 (CHO)** | GCAGUCGCAGUGGAUACAU<br>AUGUAUCCACUGCGACUGC |
| **FAN1 (CHO)** | UAUGGCAAAUUGAACAUGC<br>GCAUGUUCAAUUUGCCAUA |
| **SNM1A (CHO)** | UUAAAUUCUGACUGGAACC<br>GGUUCCAGUCAGAAUUUAA |
| **XPF (CHO)** | UUGCGAAUAUAAUACCACC<br>GGUGGUAUUAUAUUCGCAA |

**Table 2.2: siRNA sequences for siRNA knockdown experiments**

siRNA sense strand sequences for individual genes targeted in siRNA knockdown experiments.

## 2.6 Clonogenic Survival Assay

### 2.6.1 6-well clonogenic survival assays for confirmation of siRNA screen hits

At 72 hours post siRNA transfection, cells were lifted by trypsination and re-suspended and counted. A concentrated cell suspension was made and plated out in triplicate wells of 6-well plates at the cell densities required for the corresponding dose of radiation or cisplatin (Table 2.3). After incubating for 4 hours at 37°C to allow adherence of cells, plates were either irradiated at 2, 3 or 4 Gy (Caesium-137 irradiator, Gamma Service: GSR D1; dose rate 1.938 Gy/min) or cisplatin was added to a final concentration of 0.5μM, 0.75μM or 1μM. Cells were incubated with cisplatin for the duration of the experiment.

Plates were left to incubate for 14 days at 37°C to allow colonies to form and were then stained with crystal violet and counted with the GelCount colony counter (Oxford Optronix).

| Treatment | 6-well plate Number cells/well | 96-well plate Number of cells/well |
|---|---|---|
| **Untreated** | 500 | 400 |
| **0.5μM cisplatin** | 1500 | 750 |
| **0.75μM cisplatin** | 1800 | |
| **1μM cisplatin** | 3000 | |
| **2Gy** | 1000 | |
| **3Gy** | 1500 | 1500 |
| **4Gy** | 1800 | |

**Table 2.3: Cell numbers plated for different treatment modalities**

List of H460 cell numbers plated for different treatment doses and plate types for colony formation assays.

### 2.6.2 10cm dish clonogenic survival assay for CRISPR knock-out cells

To further confirm that the gene PIF1 was a cisplatin sensitiser CRISPR HAP1 knockout cells were purchased from Horizon (UK) and used to perform cisplatin clonogenic survival assays along side wild-type (WT) HAP1 cells.

Briefly, 3000 cells were seeded to each 10cm plate and allowed to adhere for at least 4 hours before application of cisplatin. A fresh 2mM stock solution of cisplatin was diluted using FBS free medium to concentrations of 5, 6, 7, 8 and 10μM and cells were incubated for 4 hours. Following treatment plates were washed twice in PBS, fresh media containing 10% FBS was applied and the plates were returned to a 37˚C incubator and allowed to form colonies for 7 days. Plates were then stained with crystal violet and counted with the GelCount colony counter (Oxford Optronix).

### 2.6.3 10cm dish clonogenic survival assays of DNA damage mutant in G1

Clonogenic survival assays were also performed to assess survival of CHO WT and DNA damage mutant cells after treatment with nitrogen mustard in G1.

Initially, 5 x $10^5$ cells were seeded to each 10cm plate and allowed to adhere for a minimum of 4 hours before standard media was exchanged for isoleucine free media. Cells were left to synchronise for 48 hours before being treated with varying doses of HN2 for 1 hour. After treatment with HN2 cells were either lifted immediately or left to repair ICL in G1 in isoleucine free media for 24 hours prior to harvesting.

At harvesting, media was aspirated from each dish and adherent cells were dissociated by trypsinisation and re-suspended in 10ml media. Cells were counted

using a Beckman Coulter Z2 Particle Count and Size Analyser and 4000 cells from each plate were reseeded in triplicate. Plates were incubated in isoleucine complete media at 37˚C for 7 days prior to staining with crystal violet and counting with a GelCount colony counter (Oxford Optronix).

### 2.6.4 Statistical analysis for 6-well and 10cm dish colony forming assays

Factorial 2-way ANOVA tests were performed with survival as the dependent variable and dose levels (dose of radiation or cisplatin) and treatment (gene siRNA/NT siRNA) as the two factors. Calculations were performed with GraphPad Prism and the *p*-values calculated represent the interaction between dose and treatment.

## 2.7 Assessment of gene expression

### 2.7.1 Determination of mRNA expression by quantitative real-time PCR

#### 2.7.1.1 Total RNA preparation

Total RNA was purified from cells using the Qiagen RNeasy Mini Kit according to the manufacturers instructions. Briefly, cell pellets were lysed in 350µl of lysis buffer and mixed with an equal volume of 70% ethanol. Lysates were then transferred to a RNA binding column, and following three washes the RNA was eluted RNA by addition of an elution buffer. The eluted RNA concentration of each sample was determined by NanoDrop spectrometer (Nanodrop Technologies, Wilmington, NC).

#### 2.7.1.2 cDNA preparation

Following RNA extraction, 500ng total RNA from each sample was reverse transcribed to produce cDNA using the AppliedBiosystems high capacity cDNA reverse transcription kit (Thermo Fisher Scientific, Lithuania). Each cDNA reaction was prepared as per the manufacturers protocol and incubated under the following conditions: 25˚C for 10 minutes, 37˚C for 120 minutes and 85˚C for 5 minutes using a Tetrad2 Thermal Cycler (BioRad)

#### 2.7.1.3 qRT-PCR

Following cDNA synthesis the mRNA levels of the genes of interest were quantified by real time PCR using the appropriate primers as listed in Table 2.4. Reactions were performed using the SensiMix SYBR kit (Bioline) and performed in triplicate. A Cas 1200 Corbett Robotics pipette robot (Corbett Life Science) was used to pipette all samples and all PCR reactions were carried out using a Corbett

Research Rotor Gene 3000 real-time thermal cycler (Corbett Life Science) using the cycling conditions: 95˚C for 15 minutes, 40 cycles of 95˚C 15 seconds followed by 60˚C 45 seconds. All data were normalised to GAPDH and analysed using the delta-delta CT method to determine the relative mRNA expression of the gene of interest.

| Gene of Interest | Sequence 5' to 3' |
|---|---|
| **GAPDH** | F: GCACCACCAACTGCTTAGC<br>R: AGTCTTCTGGGTGGCAGTGA |
| **FAN1** | F: TCGAATGTACGAGGAAGCCG<br>R: CTGATGCACCTAATTGCCGC |
| **EXO1** | F: AATTGAAAGGTCCCCGGCTG<br>R: CCAAGTGAGCCCAGGAGATCG |
| **SNM1A** | F: TTTCGAGTGTCTGGATTCTCC<br>R: TTTGAGCTAGCAGGAGGTGA |
| **XPF** | F: GAGTGATGAGGAACCTTTTTGTGA<br>R: TGTTGTTCCAAGAACGAFTTGACT |

**Table 2.4: qRT-PCR primer forward (F) and reverse (R) sequences**

## 2.8 Cell Cycle Analysis

### 2.8.1 Synchronisation of Chinese Hamster Ovary (CHO) cells to G1 using isoleucine starvation

5 x $10^5$ CHO cells were seeded to 10cm petri dishes in 10ml RPMI with 10% FBS and allowed to adhere for a minimum of 4hrs. Once adhered cells were washed twice with isoleucine free (ILF) RPMI media with no FBS before addition of 10mls ILF RPMI containing 10% ILF FBS. Cells were incubated for a further 48 hours to ensure synchronisation to G1 in the cell cycle.

### 2.8.2 5-bromo-2-deoxyuridine incorporation assay and propidium iodide staining

Cells were incubated with 10µl of 10µM BrdU for 30 minutes prior to harvesting. At the appropriate time point media was removed, cells washed once with PBS and incubated with trypsin for 5 minutes at 37°C prior to re-suspension in RPMI medium with 10% FBS. Each sample was centrifuged at 15000 rpm for 5 minutes (Beckman Allegra 6R centrifuge), excess media removed and the cell pellet obtained re-suspended in small amount of medium. Samples were washed twice with 1% bovine serum albumin (BSA) in PBS followed by a 10-minute 15000rpm centrifuge. Finally, each sample was re-suspend in 200µl cold PBS and added drop-wise to 5ml ice-cold 70% ethanol whilst vortexing. Samples were left to fix in 70% ethanol for a minimum 30 minutes on ice or stored at -20°C until required.

Samples of fixed cells were counted using a Beckman-Coulter cell counter and approximately 2 x $10^5$ cells per sample processed for FACS analysis.

Cells fixed in ethanol were spun for 10 minutes at 15000rpm and any excess ethanol removed and each cell pellet washed once in PBS prior to re-suspension

by drop-wise addition of 1ml 2M hydrochloric acid (HCl) containing 0.1mg/ml pepsin. Each sample was allowed to incubate, and then acid denatured at room temperature for 20 minutes with agitation.

After washing twice in PBS and once in 2% FBS in PBS, to ensure neutralisation of acid, the samples were incubated with rat anti-BrdU antibody (Abcam, Cambridge, UK), at a concentration of 1 in 500, for 30 minutes at room temperature with regular agitation. A further wash with 2% FBS in PBS was performed and samples were re-suspended in a secondary anti-Rat antibody conjugated to Alexafluor 488 fluorochrome (Abcam, Cambridge, UK) and incubated for 30 minutes with agitation in the dark. After a final wash with PBS samples were re-suspend in PBS containing 5μg/ml propidium iodide (PI) to stain nucleic acid.

All samples were analysed using a Cyan flow cytometer with Summit Software (Dako, Glostrup, Denmark). The PI signal was analysed using a FL2-H channel to detect emission of red fluorescence at 617nm wavelength. BrdU was detected by analysis of green fluorescence at a wavelength of 519nm using a FL1-H channel and FITC signal. For each sample at least 6000 events were collected and analysed. To determine the distribution of cells in each phase of the cell cycle log FITC was plotted against linear FL2-H (PI).

## 2.9 Modified alkaline comet assay

### 2.9.1 Sample collection for modified alkaline comet assay

A modified version of the standard alkaline comet assay was performed to detect the formation and resolution of ICL in cells (Hartley et al., 2011). Cells were seeded in 10cm petri dishes and allowed to adhere for 4 hours prior to incubation in isoleucine free media. Following incubation in isoleucine free media for 48 hours, to allow cells to synchronise to G1, cells were treated with 10μM HN2 for one hour and then re-incubated in isoleucine free media. Cells were harvested immediately, 4, 12 and 24 hours after treatment by trypsinisation. Following harvesting the samples were divided into two aliquots on 24 well plates. One aliquot was left untreated and the other irradiated with 10 Gy from a Caesium source (GAMMACELL 1000A irradiator, Atomic Energy of Canada Limited). Following this both aliquots were used to perform an alkaline comet assay.

### 2.9.2 Alkaline comet assay

Cells suspended in media were mixed with an equal volume of warmed 2% agarose (type VII) solution. Approximately 500μl of this solution was spread evenly over a microscope slide, which had previously been pre-coated in 1% (type II) agarose. Each sample was prepared in duplicate and immediately covered with a glass cover slip. Once each sample had set the glass cover slips were removed and the sample slides immediately immersed in ice-cold alkaline lysis buffer (30mM NaOH, 1M NaCl, 0.1% N-lauroylsarcosine) for one hour in the dark. Slides were then removed and washed twice in ice-cold electrophoresis buffer (30mM NaOH, 2mM EDTA) for 30 minutes in the dark. All slides were then placed in a flat bed electrophoresis chamber (GNA 200, Pharmacia Biotech) and covered in

electrophoresis buffer. Electrophoresis was performed for 30 minutes at 18V. Following electrophoresis, slides were removed and neutralised with 1M Tris-HCl, pH 7.5 solution for 10minutes before being allowed to dry overnight in the dark. The following day sample slides were allowed to rehydrate for 30 minutes in distilled water and then stained with SYBR gold solution (1:10000) for 10 minutes. Slides were briefly rinsed in distilled water and allowed to air dry.

### 2.9.3 Comet assay analysis

Air-dried slides were examined with a Zeiss Observer Z1 microscope. At least 8 fields of view were recorded for each sample slide. This allowed counting of at least 50 cells for each sample using Zen Pro software. Using OpenComet software (OpenComet, GNU General Public License version 3.0) the tail moment for 50 randomly sampled cells per sample was calculated.

Tail moment is a measure of DNA damage and is defined as the product of the percentage DNA in the comet tail and the distance between the means of the head and tail distributions (Olive et al., 1990)

Following calculation of the mean tail moment for each sample, the percentage decrease in tail moment (Figure 2.3A) and percentage unhooking (Figure 2.3B) were calculated using the formulae in Figure 2.3.

**A**

$$\%\ decrease\ in\ tail\ moment\ (DTM) = \left\{1 - \left[\frac{TM_{di} - TM_{cu}}{TM_{ci} - TM_{cu}}\right]\right\} \times 100$$

**B**

$$\%\ unhooking\ =\ \frac{DTM_{diT} - DTM_{di0}}{DTM_{di0}}$$

**Figure 2.3: Formulae for calculating % decrease in tail moment (DTM) and % unhooking**

$TM_{di}$ = tail moment of drug treated irradiated sample.
$TM_{cu}$ = tail moment of untreated unirradiated sample.
$TM_{ci}$ = tail moment of untreated irradiated sample.
$DTM_{diT}$ = % decrease in tail moment of drug treated irradiated sample at indicated time.
$DTM_{di0}$ = % decrease in tail moment of drug treated irradiated sample immediately after treatment with HN2.

# Chapter 3 - Results: Repair of ICL in G1 mammalian cells.

## 3.1 Introduction

ICL repair appears to be triggered by stalled replication forks in S-phase. However, there is increasing evidence that a second pathway of replication independent repair (RIR) is present in phases G0 and G1 of the cell cycle. This is supported by evidence that, in G0 or G1, cells ICL recognition may occur during transcription of DNA and involve the TC-NER and possibly GG-NER pathways (discussed in 1.4.1.2). Furthermore, recognition of ICL outside of transcription may also be possible and involve the MMR and NER pathways (discussed in 1.4.1.1)

The detailed proposed pathway for RIR has been described in Section 1.5. RIR was first described in bacteria (Berardini et al., 1997) and this pathway appears preserved in yeast and, potentially, mammalian cells. Similar to replication-dependent ICL repair, the initial step in repair is thought to involve incisions around the ICL on one DNA strand leading to unhooking of the ICL. Previous studies have suggested the NER apparatus is essential for recognition of ICLs and incision (Enoiu et al., 2012).

Following unhooking, PCNA may be involved in the recruitment of TLS polymerases (Williams et al., 2012), which then synthesise past the ICL lesion. Studies in yeast (Sarkar et al., 2006) and chicken DT40 (Shen et al., 2006) cells have implicated Polζ as essential to this process in G1. Despite conflicting results from different studies, Polκ (Enoiu et al., 2012; Williams et al., 2012) and Polη (Zheng et al., 2003; Wang et al., 2001a) may also play a role in TLS bypass.

Following TLS bypass and gap filling the resulting substrate can undergo a second round of NER to completely excise the ICL (Figure 1.12).

To date there have been no major studies of G1 ICL repair in mammalian cells. Defining a G1 ICL repair pathway in mammalian cells would have important clinical implications. Current chemotherapy regimes principally target rapidly proliferating cells but selectively targeting tumour cells in G0/G1, including cancer stem cells, may offer more efficient treatment and the chance to reduce tumour recurrence. To target these cells a detailed understanding of the mechanisms of ICL repair in both stationary and replicating mammalian cells is required.

The aim of this chapter is to create a mammalian cell experimental model for ICL repair in G1. With this in mind, CHO cells were chosen as a potential cell line to use for experimentation. It was envisioned that in order to study ICL repair in G1, it would be necessary to synchronise populations of cells to specific points in the cell cycle. Previous studies have shown this can be achieved in CHO cells by isoleucine starvation in isoleucine free media, resulting in homogenous synchronisation of all cells to G1. Once held in G1 cells can be released to progress through the cell cycle in synchrony by re-incubating the cells in isoleucine containing media (Tobey and Crissman, 1972).

CHO cell lines have been extensively previously studied and multiple stable DNA damage mutant cell lines have been identified. These mutant CHO cell lines have been derived by mutagenisation of parental cell lines with radiation or alkylating agents. Following this CHO cells were screened and clones isolated that were sensitive to particular DNA damaging agents (Hickson and Harris, 1988) such as ultra violet light (UV), ionising irradiation (IR) (Fuller and Painter, 1988) and

cross-linking agents (Jones et al., 1987). Confirmation of specific genetic defects has been classified by genetic complementation analysis (reviewed (Collins, 1993)). In many cases, this was achieved by human genetic complementation of specific genes, the addition of which reverse the observed sensitivity (Sijbers et al., 1996). These mutant cell lines provide a useful panel of DNA damage mutant cell lines that can be used for experimentation in a model of G1 repair.

Within this chapter, flow cytometry will be used to assess cell cycle dynamics. Flow cytometry can assess position in the cell cycle by quantitation of DNA. Traditionally, this is be performed by use of fluorescent dyes, such as propidium iodide (PI), which bind stoichiometrically to the DNA. This allows identification of G1 and G2 phase cells since the G2 population of cells contain roughly twice the amount of DNA as G1 having undergone replication (Krishan, 1975). One issue with this type of staining is that it is hard to identify which cells are in S-phase since DNA content in early S-phase and G1 and similarly G2 and late S-phase is the same.

To accurately assess which cells are in S-phase bromodeoxyuridine (5-bromo-2-deoxyuridine, BrdU) staining can be used (Gratzner et al., 1975). BrdU is a synthetic thymidine analogue that becomes incorporated in new DNA produced in S-phase. If cells are pulsed with BrdU for short period of time only cells that are in S-phase will incorporate the BrdU. To detect BrdU incorporation, the DNA must first be rendered single-stranded by acid denaturation to allow an anti-BrdU antibody to access the BrdU. A secondary fluorochrome labelled antibody is then applied. By tandem labelling with PI the G1, S-Phase and G2 populations can be differentiated and quantified.

The aim of this chapter is to develop an experimental model using CHO cells that will verify if ICL repair can occur in G1. Once substantiated, a panel of mutant CHO cell lines will be assessed to attempt to identify which DNA damage repair factors are essential to G1 repair.

## 3.2 Flow cytometry assessment of repair of ICL in G1.

### 3.2.1 Wild-type CHO cells can be synchronised to G1 and early S-phase

As discussed, previous studies have demonstrated that CHO cells can be synchronised to G1 by isoleucine starvation (Tobey and Crissman, 1972). To initially assess this the optimal time for complete synchronisation to G1 was defined. Cells were seeded in 10cm petri dishes in isoleucine complete media and allowed to attach for 4 hours. After washing twice with isoleucine free media, plates were incubated for varying time periods in isoleucine free media containing 10% isoleucine free FCS. Analysis of cell cycle dynamics by flow cytometry, with BrdU and PI staining, suggested the optimal length of time for synchronisation was 48 hours and that over 90% of cells could be synchronised to G1 by 48 hours of isoleucine starvation (results not shown).

To define the time taken from release to reach early S-phase AA8 cells were synchronised to G1 by isoleucine starvation for 48 hours. Media was then changed to isoleucine containing media and the progression of cells through the cell cycle assessed at intervals by FACS analysis. Figure 3.1 demonstrates that WT CHO cells remained in G1 up to 4 hours post media change; they progressed to early S-phase by 8 hours and to late S-phase by 12 hours.

These findings illustrate that CHO cells can be easily synchronised to G1 and used as a model for assessment of G1 repair. It is clear that following synchronisation and release WT CHO cells enter early S-phase approximately 8 hours after release from G1 and this would be the optimal time point to treat a synchronised population of cells in early S-phase.

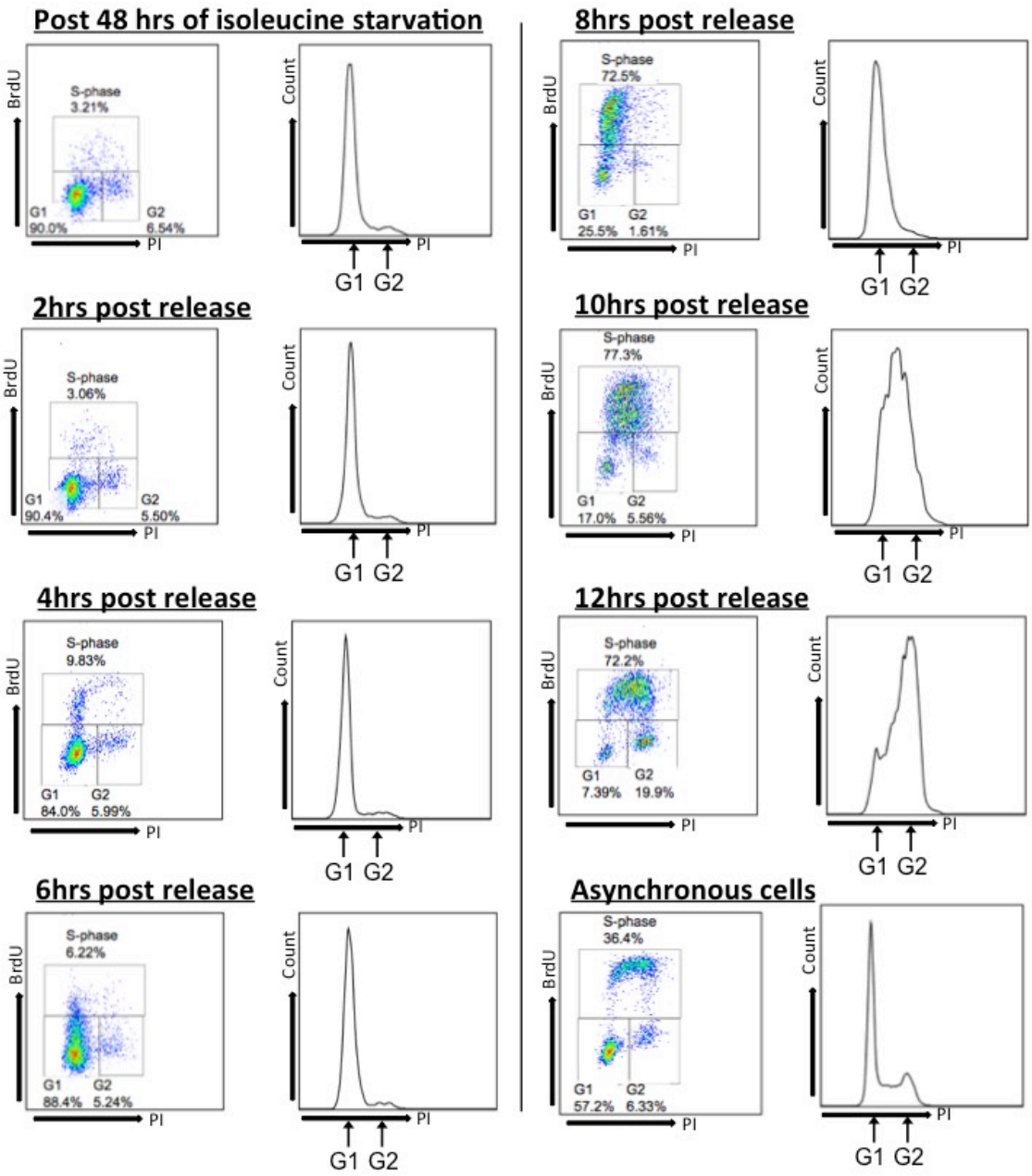



**Figure 3.1: Timing of entry of synchronised WT CHO cells into early S-phase.**

WT CHO cells were synchronised to G1 by isoleucine starvation for 48 hours. Cells were then released to cycle by addition of isoleucine complete media. Samples were collected after pulse labelling with BrdU and cell cycle profile obtained by flow cytometry analysis.

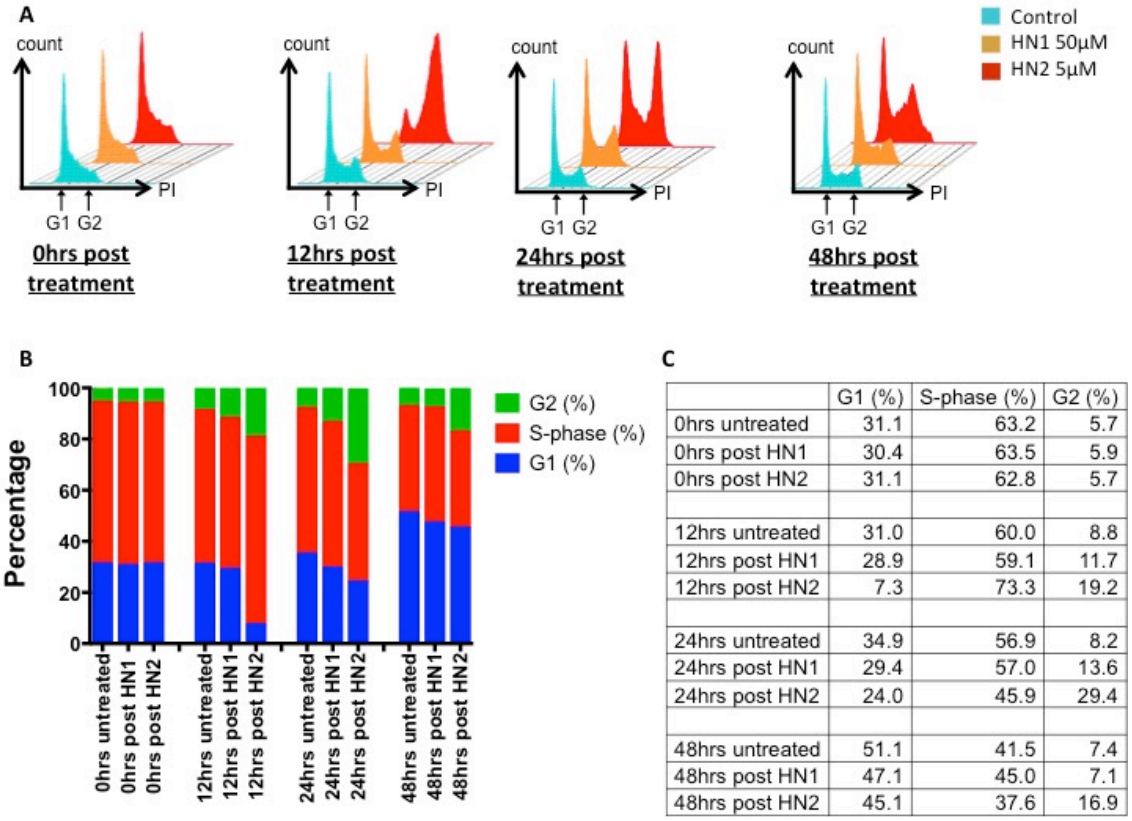
Data presented are representative of 3 independent experiments.

### 3.2.2 Cell cycling is stalled in asynchronous cells to allow repair of ICL

Previous studies have demonstrated that following treatment with HN2, mammalian cells arrest in late S-phase/G2 for up to 48 hours (Osawa et al., 2011). To examine the induction and prolongation of cell cycle arrest asynchronous WT CHO cells were treated with 50μM HN1 and 5μM HN2 for one hour. The cells were pulse labelled with 5-bromo-2-deoxyuridine (BrdU) and then harvested. The changes in cell cycle following drug treatment were analysed by FACS with staining for BrdU and propidium iodide (Figure 3.2).

Both HN1 and HN2 treatment were used to allow comparison of the lesions formed. HN1 forms only monoadducts whereas, as discussed previously, HN2 forms monoadducts and a small minority of ICLs. By using a dose of HN1 ten times that of HN2 the intention was to assess clearly if toxic cell cycle stalling effects were due to ICL. A dose of 5μM HN2 was chosen after careful dose optimisation. The dose of 5μM was selected, as this dose of HN2 was high enough to cause cell cycle stalling without permanent arrest, which might lead to apoptosis.

The cell cycle arrest seen here mirrors the findings of Osawa *et al*, cell cycle arrest is not as marked as previously demonstrated but this is likely to be a consequence of the lower dose of HN2 used (5μM versus 10μM). Treatment with higher doses (10-15μM HN2) did result in a more prolonged arrest in late S-phase as seen by Osawa and colleagues (results not shown). In comparison, treatment with HN1 causes minor prolongation of cell cycling, suggesting that ICLs are a major block to cell cycle progression and that their repair is slow, whilst even large numbers of monoadducts can be repaired quickly with minimal cell cycle delay.




C

| | G1 (%) | S-phase (%) | G2 (%) |
|---|---|---|---|
| 0hrs untreated | 31.1 | 63.2 | 5.7 |
| 0hrs post HN1 | 30.4 | 63.5 | 5.9 |
| 0hrs post HN2 | 31.1 | 62.8 | 5.7 |
| | | | |
| 12hrs untreated | 31.0 | 60.0 | 8.8 |
| 12hrs post HN1 | 28.9 | 59.1 | 11.7 |
| 12hrs post HN2 | 7.3 | 73.3 | 19.2 |
| | | | |
| 24hrs untreated | 34.9 | 56.9 | 8.2 |
| 24hrs post HN1 | 29.4 | 57.0 | 13.6 |
| 24hrs post HN2 | 24.0 | 45.9 | 29.4 |
| | | | |
| 48hrs untreated | 51.1 | 41.5 | 7.4 |
| 48hrs post HN1 | 47.1 | 45.0 | 7.1 |
| 48hrs post HN2 | 45.1 | 37.6 | 16.9 |

**Figure 3.2: Cell cycle dynamics of asynchronous WT CHO cells following treatment with 50µM HN1 and 5µM HN2.**

Asynchronous WT CHO cells were treated with 50µM HN1 and 5µM HN2 for 1 hour. Samples were then collected 0, 12, 24 and 48hrs after treatment following 30 minutes of BrdU pulse labelling.

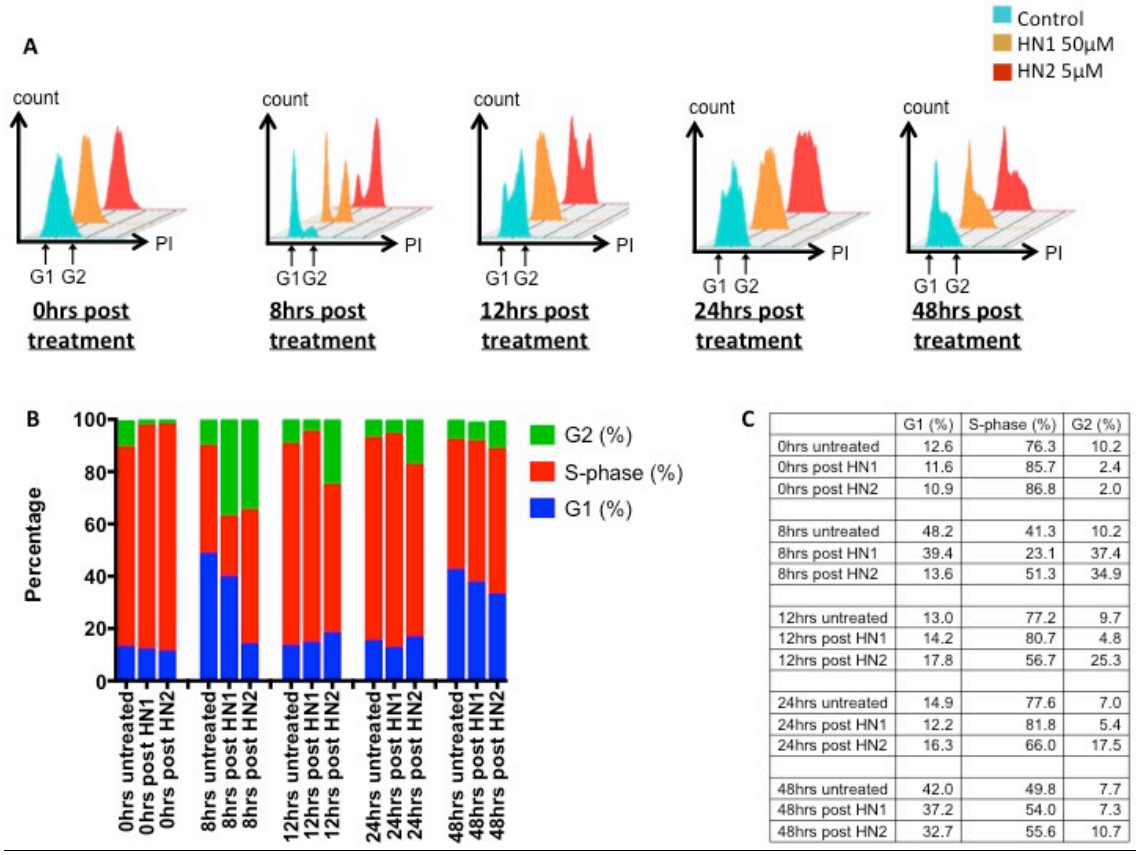
A: PI histograms of cell cycle dynamics.
B: Graphical representation of cell cycle position from BrdU gated plots.
C: Percentage of cells within each phase of the cell cycle at each defined time point.

Data presented are representative of 3 independent experiments.

### 3.2.3 Treatment in early S-phase causes cell cycle stalling

Based on the results from previous experiments (Figure 3.1, Figure 3.2) the effect of ICL treatment in early S-phase was assessed. AA8 cells were synchronised to G1 by isoleucine starvation and then released. Cells were treated with 50μM HN1 and 5μM HN2 for one hour 8 hours after release, at early S-phase, and subsequent cell cycle progression was analysed by FACS. As with asynchronous cells HN2 treatment delays progression through S-phase (Figure 3.3). This occurred at 4 hours in both HN1 and HN2 treated cells compared to untreated synchronised controls. Treatment with HN1 resulted in only minor delay in cell cycle progression with cells remaining in G2 phase 8 hours after treatment. HN2 treated cells showed more marked delayed with cells remaining in G2 phase for up to 12 hours after treatment. After 24 hours the delay in cell cycle was abolished in all treatment groups.

These findings are in keeping with the delay in cell cycle seen in asynchronous cells following ICL treatment. The onset of delay was more rapid for synchronised cells presumably because stalling commences when a replication fork meets an ICL and, since all cells were in early S-phase, the onset of this would be expedited. The delay in progression in synchronised cells was of a similar duration to unsynchronised cells.




| | G1 (%) | S-phase (%) | G2 (%) |
|---|---|---|---|
| 0hrs untreated | 12.6 | 76.3 | 10.2 |
| 0hrs post HN1 | 11.6 | 85.7 | 2.4 |
| 0hrs post HN2 | 10.9 | 86.8 | 2.0 |
| | | | |
| 8hrs untreated | 48.2 | 41.3 | 10.2 |
| 8hrs post HN1 | 39.4 | 23.1 | 37.4 |
| 8hrs post HN2 | 13.6 | 51.3 | 34.9 |
| | | | |
| 12hrs untreated | 13.0 | 77.2 | 9.7 |
| 12hrs post HN1 | 14.2 | 80.7 | 4.8 |
| 12hrs post HN2 | 17.8 | 56.7 | 25.3 |
| | | | |
| 24hrs untreated | 14.9 | 77.6 | 7.0 |
| 24hrs post HN1 | 12.2 | 81.8 | 5.4 |
| 24hrs post HN2 | 16.3 | 66.0 | 17.5 |
| | | | |
| 48hrs untreated | 42.0 | 49.8 | 7.7 |
| 48hrs post HN1 | 37.2 | 54.0 | 7.3 |
| 48hrs post HN2 | 32.7 | 55.6 | 10.7 |

**Figure 3.3: Cell cycle dynamics of S-phase synchronised WT CHO cells following treatment with 50µM HN1 and 5µM HN2.**

S-phase synchronised WT CHO cells were treated with 50µM HN1 and 5µM HN2 for 1 hour and samples collected 0, 8, 12, 24 and 48 hours after treatment following 30 minutes of BrdU pulse labelling.

A: PI histograms of cell cycle dynamics.
B: Graphical representation of cell cycle position from BrdU gated plots.
C: Percentage of cells within each phase of the cell cycle at each defined time point.

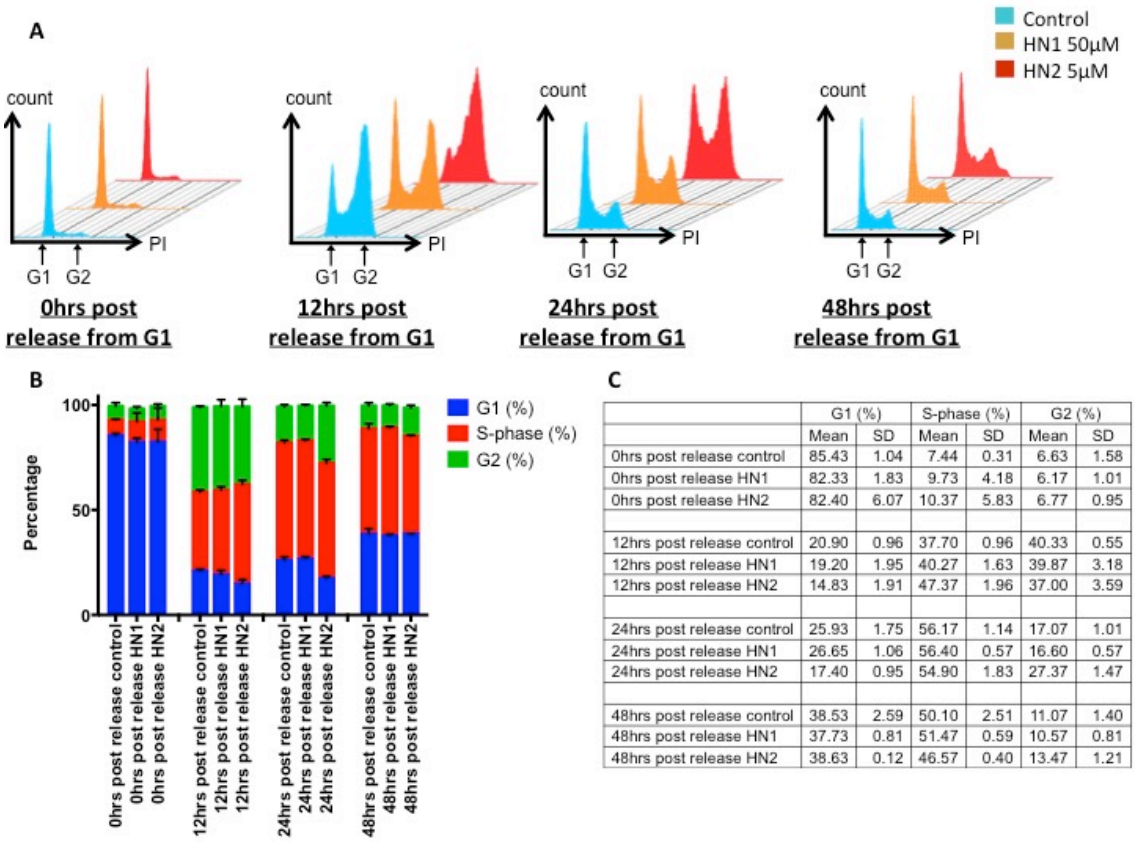
Data presented are representative of 3 independent experiments.

### 3.2.4 ICL repair occurs in G1 and is time dependent

#### 3.2.4.1 Repair of ICL in G1 with immediate release to cell cycle

To assess the repair of ICL in G1 cells, WT CHO cells were synchronised to G1 by isoleucine starvation for 48 hours. Following synchronisation cells were treated for 1 hour with 50μM HN1 and 5μM HN2 and then immediately released to progress through the cell cycle by addition of isoleucine complete media. WT CHO cells were harvested at progressive time points following release from G1 and were pulse labelled with BrdU for 30 minutes prior to collection at 12, 24 and 48 hours post-release. As illustrated in Figure 3.4 after release from G1 untreated cells cycled normally through S-phase and, as seen previously, the majority of untreated cells appear to be in late S-phase/G2 12 hours after release and returned to G1 by 24 hours. Cells treated with HN2 showed significant stalling in late S-phase/G2 resulting in approximately 30% of cells persisting in G2 at 24 hours after release compared to 12% of untreated cells. Cells treated with HN1 showed a similar but much less marked stalling at 24 hours after release; 15% remaining in G2 versus 12% in untreated cells.

Importantly, these findings infer that ICLs are formed in CHO cells in G1 phase of the cell cycle. This is suggested by the persistence of stalling in S-phase in HN2 treated cells. Similar to S-phase treated cells, treatment with HN1 in G1 caused minor stalling with 57.5% of cells in S-phase and 14.8% of cells in G2 24 hours after treatment and release compared with 51.1% in S-phase and 11.8% cells in G2 in the untreated samples.




C

| | G1 (%) | | S-phase (%) | | G2 (%) | |
|---|---|---|---|---|---|---|
| | Mean | SD | Mean | SD | Mean | SD |
| 0hrs post release control | 85.43 | 1.04 | 7.44 | 0.31 | 6.63 | 1.58 |
| 0hrs post release HN1 | 82.33 | 1.83 | 9.73 | 4.18 | 6.17 | 1.01 |
| 0hrs post release HN2 | 82.40 | 6.07 | 10.37 | 5.83 | 6.77 | 0.95 |
| | | | | | | |
| 12hrs post release control | 20.90 | 0.96 | 37.70 | 0.96 | 40.33 | 0.55 |
| 12hrs post release HN1 | 19.20 | 1.95 | 40.27 | 1.63 | 39.87 | 3.18 |
| 12hrs post release HN2 | 14.83 | 1.91 | 47.37 | 1.96 | 37.00 | 3.59 |
| | | | | | | |
| 24hrs post release control | 25.93 | 1.75 | 56.17 | 1.14 | 17.07 | 1.01 |
| 24hrs post release HN1 | 26.65 | 1.06 | 56.40 | 0.57 | 16.60 | 0.57 |
| 24hrs post release HN2 | 17.40 | 0.95 | 54.90 | 1.83 | 27.37 | 1.47 |
| | | | | | | |
| 48hrs post release control | 38.53 | 2.59 | 50.10 | 2.51 | 11.07 | 1.40 |
| 48hrs post release HN1 | 37.73 | 0.81 | 51.47 | 0.59 | 10.57 | 0.81 |
| 48hrs post release HN2 | 38.63 | 0.12 | 46.57 | 0.40 | 13.47 | 1.21 |

**Figure 3.4: Cell cycle dynamics of G1 synchronised WT CHO cells following treatment with 50µM HN1 and 5µM HN2 and immediate release to cell cycle.**

G1 synchronised WT CHO cells were treated with 50µM HN1 and 5µM HN2 for 1 hour and then immediately released to cell cycle. Samples were collected 0, 12, 24 and 48 hours following release from G1 and following 30 minutes of BrdU pulse labelling.

A: PI histograms of cell cycle dynamics.
Histograms presented are representative of 3 independent experiments.

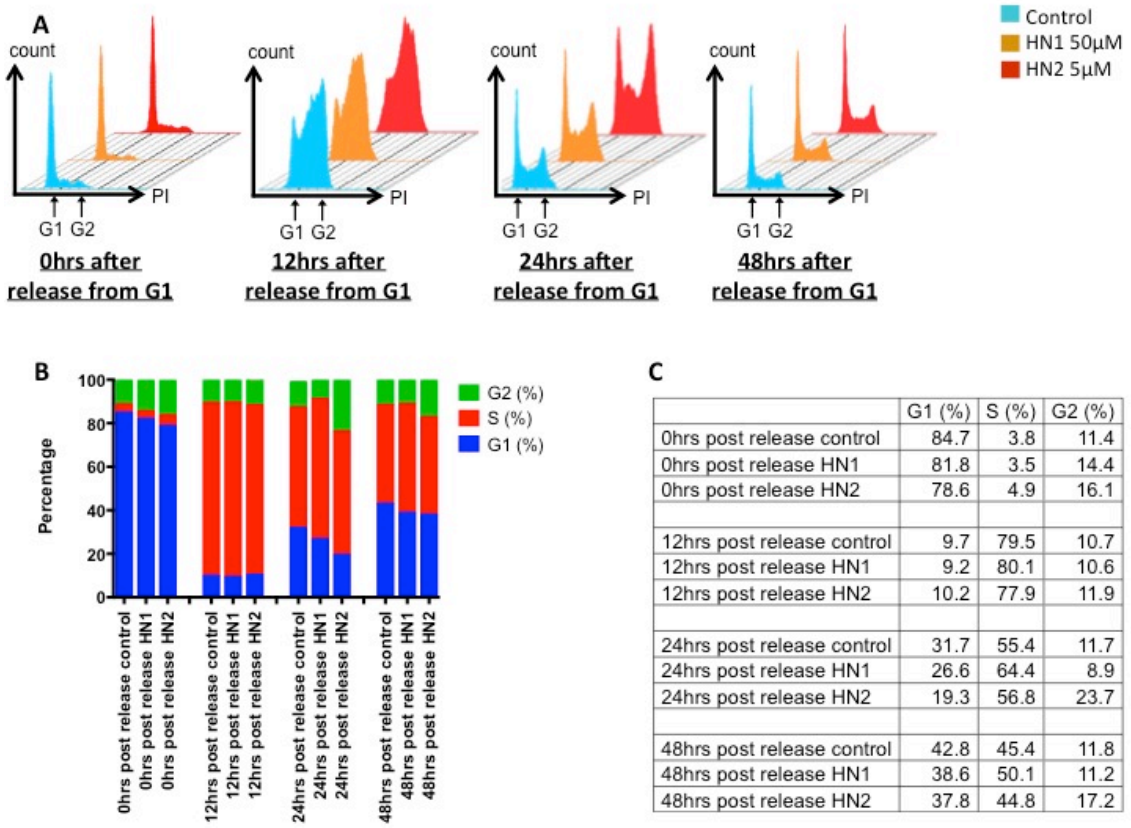
B: Graphical representation of cell cycle position from BrdU gated plots.
C: Table of percentage of cells within each phase of the cell cycle at each defined time point.
Data in B and C represent the mean + SD, n=3.

### 3.2.4.2 Repair of ICL in cells held in G1 for 12 hours

The kinetics of repair of ICL in G1 are unknown and since it appears from previous studies that ICL identification in G1 might proceed through either the GG-NER or TC-NER pathways it is possible that detection may be slower than in replicating cells. To assess for a time-dependent phenomenon cells were treated in G1 and held for a further 12 hours in G1 prior to release to cell cycle. As before, WT CHO cells were seeded and synchronised to G1 for 48 hours in isoleucine-free media. After synchronisation cells were treated for 1 hour with 50μM HN1 and 5μM HN2 before being re-incubated for a further 12 hours in isoleucine free media. After 12 hours of incubation in G1, cells were released to cell cycle by addition of complete media containing isoleucine. WT CHO cells were harvested immediately after release and at 12, 24 and 48 hours after release to cell cycle.

Figure 3.5 demonstrates that WT CHO cells treated with 5μM HN2 remain persistently stalled around 24 hours following release; 23.7% cells in G2 versus 11.7% of untreated cells. This suggests that complete resolution of all ICLs induced has not occurred. This stalling did appear less marked compared to previous experiments when treated WT cells were immediately allowed to enter cell cycling after treatment. At 24 hours, after immediate release into cell cycle 27.3% of HN2 treated cells remained in G2 contrasting to 23.7% when WT CHO cells were held in G1 for 12 hours prior to release.

As before, treatment with HN1 resulted in minor stalling 24 hours after release to cell cycling which was not of the same magnitude as seen following HN2 treatment.




| | G1 (%) | S (%) | G2 (%) |
|---|---|---|---|
| 0hrs post release control | 84.7 | 3.8 | 11.4 |
| 0hrs post release HN1 | 81.8 | 3.5 | 14.4 |
| 0hrs post release HN2 | 78.6 | 4.9 | 16.1 |
| | | | |
| 12hrs post release control | 9.7 | 79.5 | 10.7 |
| 12hrs post release HN1 | 9.2 | 80.1 | 10.6 |
| 12hrs post release HN2 | 10.2 | 77.9 | 11.9 |
| | | | |
| 24hrs post release control | 31.7 | 55.4 | 11.7 |
| 24hrs post release HN1 | 26.6 | 64.4 | 8.9 |
| 24hrs post release HN2 | 19.3 | 56.8 | 23.7 |
| | | | |
| 48hrs post release control | 42.8 | 45.4 | 11.8 |
| 48hrs post release HN1 | 38.6 | 50.1 | 11.2 |
| 48hrs post release HN2 | 37.8 | 44.8 | 17.2 |

**Figure 3.5: Cell cycle dynamics of G1 synchronised WT CHO cells following treatment with 50µM HN1 and 5µM HN2 and holding in G1 for 12 hours prior to release to cell cycle.**

G1 synchronised WT CHO cells were treated with 50µM HN1 and 5µM HN2 for 1 hour and then held in G1 for 12 hours before release to cell cycle. Samples were collected 0, 12, 24 and 48 hours after release to cell cycle following 30 minutes of BrdU pulse labelling.

A: PI histograms of cell cycle dynamics.
B: Graphical representation of cell cycle position from BrdU gated plots.
C: Percentage of cells within each phase of the cell cycle at each defined time point.

Data presented is representative of 3 independent experiments.

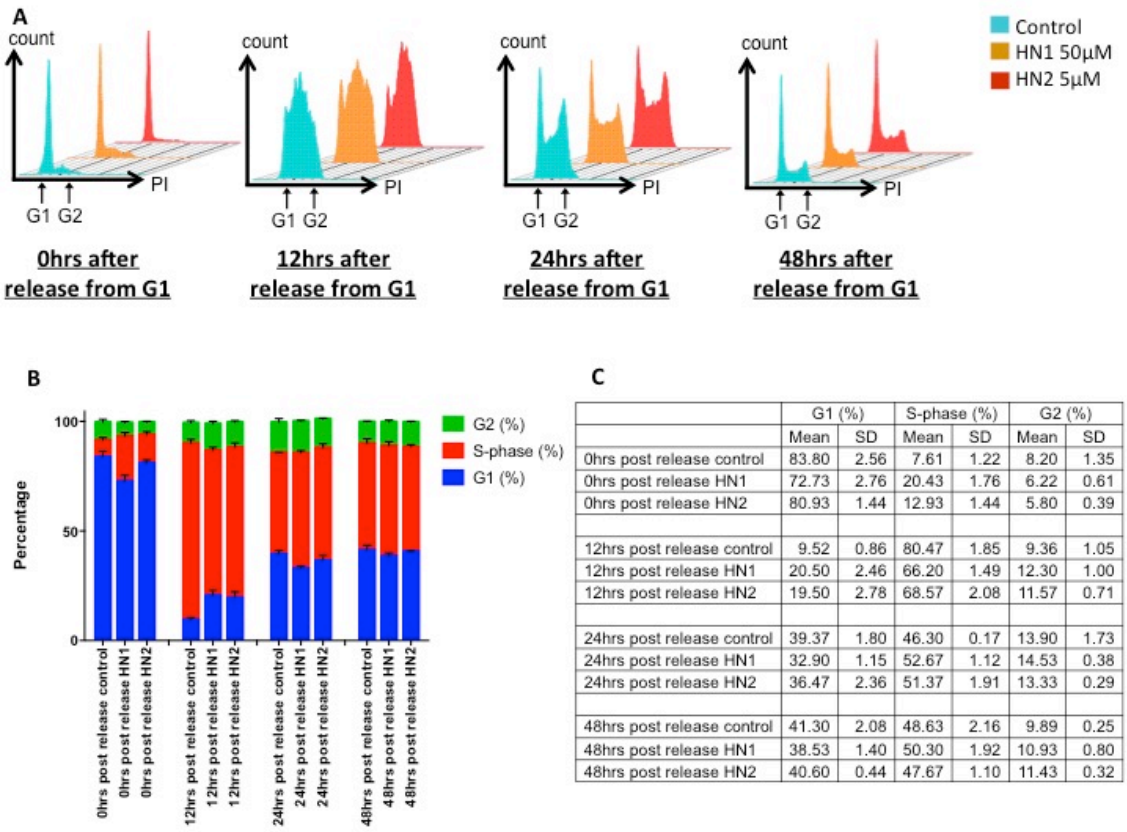
### 3.2.4.3 Repair of ICL in cells held in G1 for 24 hours

It was apparent from previous experiments that some degree of repair of ICL could occur in G1 held cells within 12 hours, but it appeared that this repair was not complete. If recognition of ICL in G1 repair was time dependent, it was hypothesised that holding treated WT CHO cells in G1 for prolonged periods of time would allow complete resolution of ICL to occur. It would be possible to identify this in the experimental model by a complete abolition of stalling in cell cycling after release from G1 in HN2 treated cells.

With this hypothesis in mind, WT CHO cells were again synchronised to G1 by isoleucine starvation for 48 hour and then treated with 50μM HN1 and 5μM HN2 for 1 hour. Following treatment cells were held in G1 for a further 24 hours by continuous isoleucine starvation prior to release to cell cycle by addition of complete isoleucine containing media. Figure 3.6 demonstrates that at release over 80% of cells in each treatment group were in G1. Unlike previous experiments (Figure 3.4, Figure 3.5) no apparent stalling was seen in treated groups after release to cell cycle and all groups showed similar percentages of cells in each cell cycle sub-group at every time point. Since previous experiments have clearly identified that ICLs can be formed in G1 this lack of stalling suggests that any ICL formed have completely resolved in the 24 hours the cells were held in G1.

Unrepaired ICL lead to cell cycle stalling and eventually apoptosis and cell death (Osawa et al., 2011). It is possible that even in G1, cells with ICL may have these lesions detected and undergo apoptosis. These cells may not be detected by FACS analysis since they would not progress to S-phase on addition of isoleucine free media. Treatment doses of HN2 were carefully optimised in asynchronous cells to

allow use of the lowest dose of HN2 to identify cell cycle delay without cell death but in order to exclude the possibility of false negative results due to cell death further experiments were performed using a commercially available live/dead fluorescent stain (LIVE/DEAD® Fixable Blue Stain, Thermo Fisher, UK). Briefly, as previously WT CHO cells were synchronised to G1 by isoleucine starvation for 48 hours and treated cells with 5μM HN2. Following treatment cells were incubated in isoleucine free media and were harvested at intervals after treatment. Harvested populations were incubated with LIVE/DEAD® stain for 30 minutes and analysed by flow cytometry. A control sample of dead cells was created by incubation in formaldehyde prior to staining with LIVE/DEAD® stain. Figure 3.7 illustrates that dead cells could easily be distinguished from live cells and that at each time point after treatment there was no significant population of dead cells. This supports the theory that ICLs can be fully repaired in G1 cells and this occurs after allowing between 12 and 24 hours for detection.




| | G1 (%) | | S-phase (%) | | G2 (%) | |
|---|---|---|---|---|---|---|
| | Mean | SD | Mean | SD | Mean | SD |
| 0hrs post release control | 83.80 | 2.56 | 7.61 | 1.22 | 8.20 | 1.35 |
| 0hrs post release HN1 | 72.73 | 2.76 | 20.43 | 1.76 | 6.22 | 0.61 |
| 0hrs post release HN2 | 80.93 | 1.44 | 12.93 | 1.44 | 5.80 | 0.39 |
| | | | | | | |
| 12hrs post release control | 9.52 | 0.86 | 80.47 | 1.85 | 9.36 | 1.05 |
| 12hrs post release HN1 | 20.50 | 2.46 | 66.20 | 1.49 | 12.30 | 1.00 |
| 12hrs post release HN2 | 19.50 | 2.78 | 68.57 | 2.08 | 11.57 | 0.71 |
| | | | | | | |
| 24hrs post release control | 39.37 | 1.80 | 46.30 | 0.17 | 13.90 | 1.73 |
| 24hrs post release HN1 | 32.90 | 1.15 | 52.67 | 1.12 | 14.53 | 0.38 |
| 24hrs post release HN2 | 36.47 | 2.36 | 51.37 | 1.91 | 13.33 | 0.29 |
| | | | | | | |
| 48hrs post release control | 41.30 | 2.08 | 48.63 | 2.16 | 9.89 | 0.25 |
| 48hrs post release HN1 | 38.53 | 1.40 | 50.30 | 1.92 | 10.93 | 0.80 |
| 48hrs post release HN2 | 40.60 | 0.44 | 47.67 | 1.10 | 11.43 | 0.32 |

**Figure 3.6: Cell cycle dynamics of G1 synchronised WT CHO cells following treatment with 50µM HN1 and 5µM HN2 and holding in G1 for 24 hours prior to release to cell cycle.**

G1 synchronised WT CHO cells were treated with 50µM HN1 and 5µM HN2 for 1 hour and then held in G1 for 24 hours before release to cell cycle. Samples were collected at 0, 12, 24 and 48 hours following release to cell cycle and following 30 minutes of BrdU pulse labelling.

A: PI histograms of cell cycle dynamics.
Histograms presented are representative of 3 individual experiments.

B: Graphical representation of cell cycle position from BrdU gated plots.
C: Percentage of cells within each phase of the cell cycle at each defined time point.
Data presented in B and C represent the mean + SD, n=3.

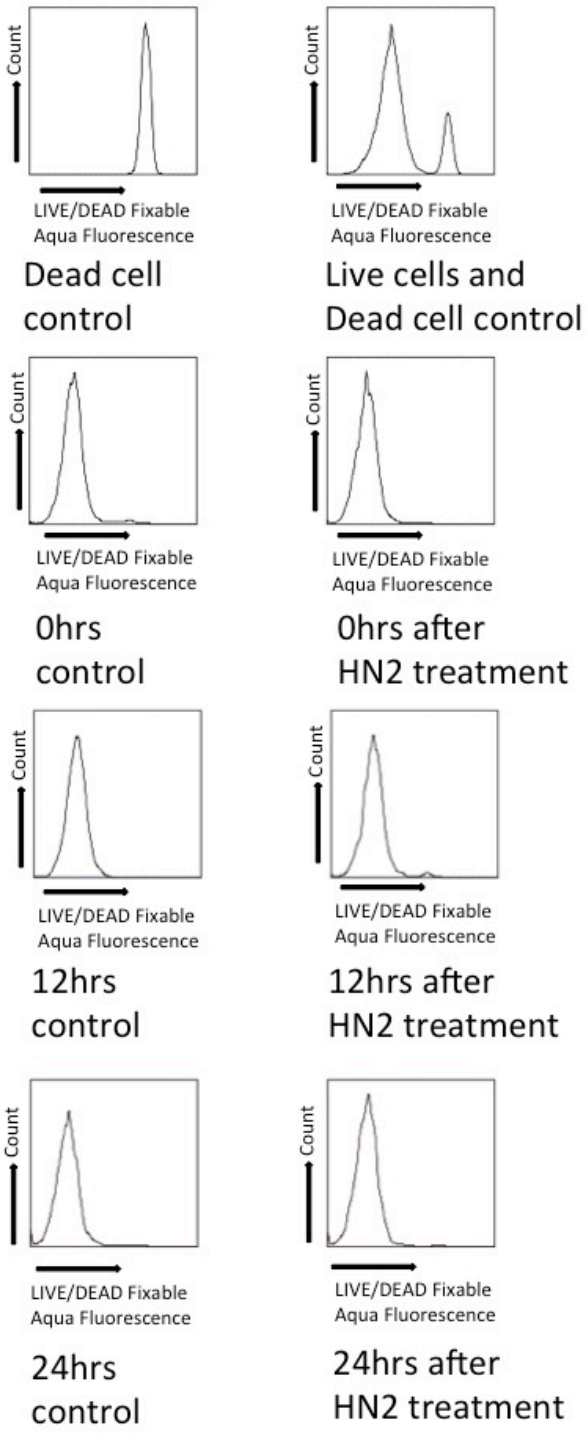



**Figure 3.7: Flow cytometry assessment of Live/Dead Stain**

WT CHO cells were synchronised to G1 and treated with 5μM HN2 for 1 hour. Cells were held in G1 and were harvested at progressive time points and stained with Live/Dead Stain.

Dead control sample was created by incubating sample of cells with formaldehyde prior to staining with Live/Dead stain.

### 3.2.5 Assessment of ICL repair in DNA Damage Repair Mutants

The previous experiments described in this chapter demonstrate that ICL can form in G1 and these lesions are resolved within 24 hours in G1 in WT CHO cells. Having established that ICL can be resolved in G1, further experiments were performed to define which DNA damage repair proteins might play a role in this repair pathway. Previous studies have suggested that G1 repair of ICL may principally occur via the nucleotide excision pathway (NER) (Enoiu et al., 2012) and also involve several polymerases (Sarkar et al., 2006).

Multiple DNA damage CHO stable mutant cell lines have been identified and a panel of these CHO mutant cell lines (Table 2.1) was utilised in the experimental framework established in the previous experiments. Using this model, cells defective for repair proteins essential to G1 repair would be highly likely to arrest following incubation and release to cell cycle since resolution of ICL would not be able to proceed.

For each cell line, experiments were performed as described previously: after G1 synchronisation for 48 hours cells were treated with 5μM HN2 for 1 hour and then held for a further 24 hours in G1 prior to release to cell cycle by addition of isoleucine complete media.

A panel of NER mutant cell lines were examined, these included mutants for XPB, XPD, XPG, XPF and CSB. Experimental findings are illustrated in Figure 3.8. Interestingly, XPF mutant CHO cells showed marked stalling when released to cell cycle. This stalling was persistent and did not resolve by 48 hours after release. This suggests that XPF may play a key role in G1 repair.

The mutant cell lines for XPD and XPB also showed stalling on release to cell cycle (Figure 3.8). This stalling was present at 24 hours and resolved in both mutated cell lines by 48 hours after release to cell cycle. The degree of stalling was not as marked as seen in XPF mutated cells.

Two other NER mutant cell lines were also treated in G1- CSB and XPG mutated cells. Both of these cell lines demonstrated similar cell cycle profiles to wild-type cells without any significant stalling following treatment in G1 with 5μM HN2, holding in G1 for 24 hours and release to cell cycle (Figure 3.8). This suggests that these proteins are unlikely to play a significant role in G1 ICL repair. Further experiments were performed with these cell lines, treating each cell line in G1 with HN2 but then releasing each cell line to cell cycle immediately. Both cell lines showed typical stalling at 24 hours after release (Figure 3.9, Figure 3.10) confirming ICL are formed in these mutated cell lines in G1 excluding this as a possible cofounding factor and suggesting ICLs formed in these mutated cells can be resolved within 24 hours in G1.

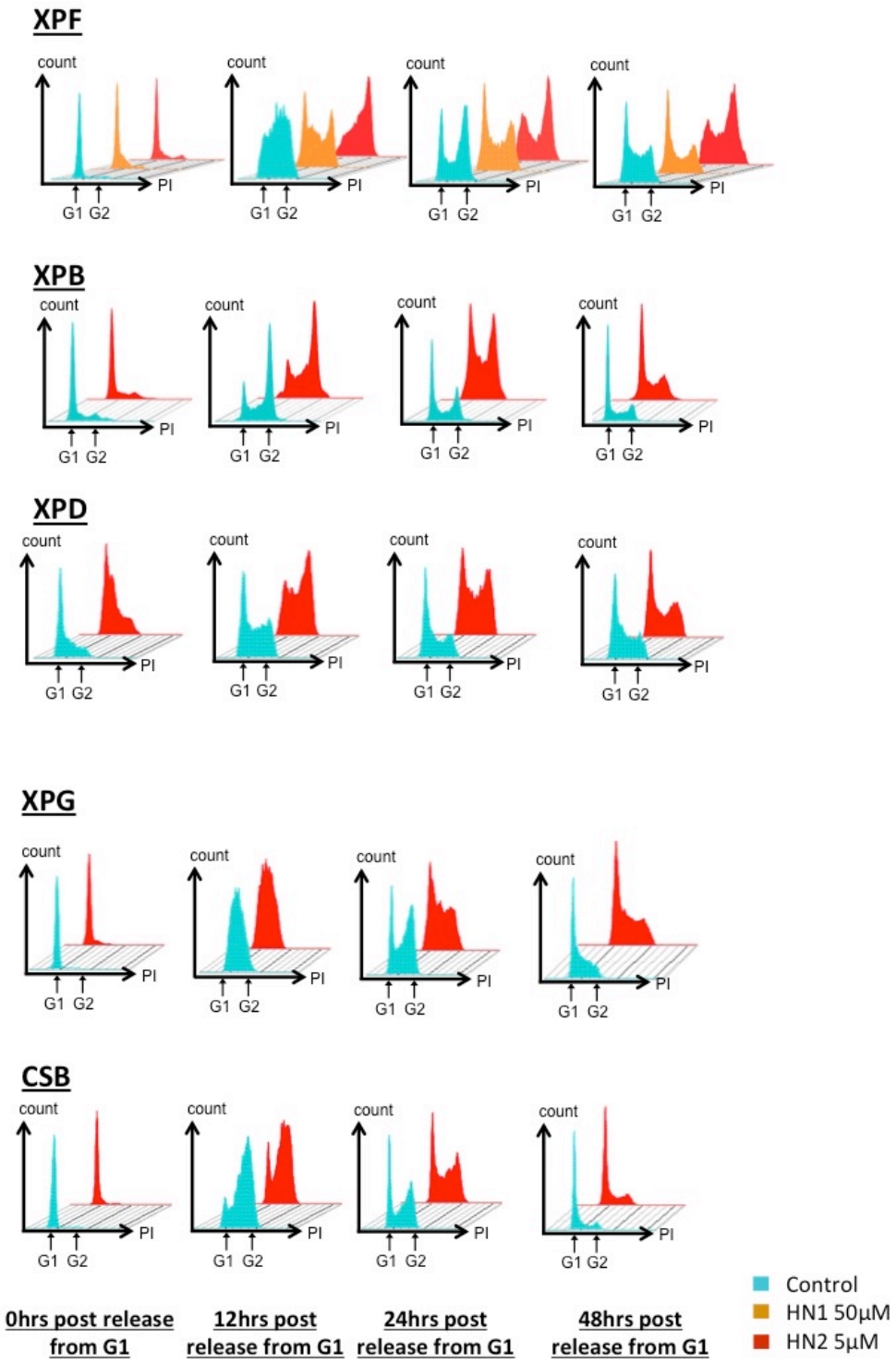



**Figure 3.8: Cell cycle dynamics of G1 synchronised NER mutant CHO cells following treatment and holding in G1 for 24 hours prior to release.**

G1 synchronised mutant CHO cells were treated with 5µM HN2 for 1 hour and then held in G1 for 24 hours before release to cell cycle. Samples were collected 0, 12, 24 and 48 hours post release from G1 and following 30 minutes of BrdU pulse labelling.

Histograms are representative of 3 independent experiments.

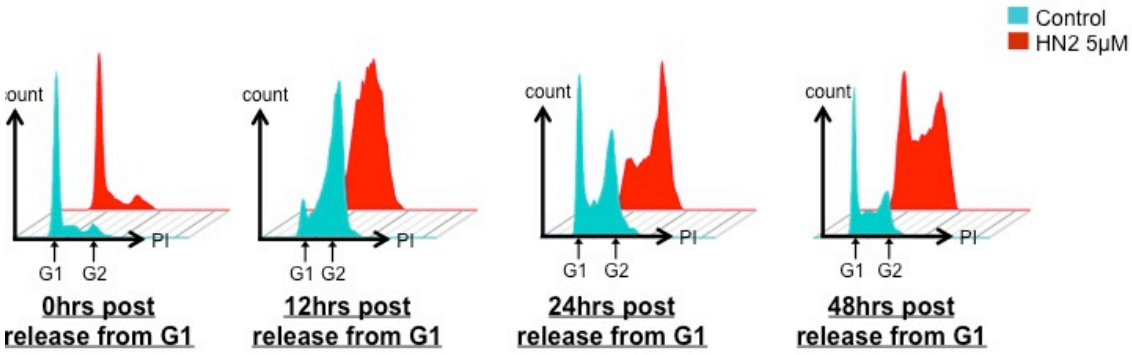



**Figure 3.9: Cell cycle dynamics of G1 synchronised XPG mutant CHO cells following treatment in G1 and release to cell cycle.**

G1 synchronised XPG mutant CHO cells were treated with 5μM HN2 for 1 hour and then released to cell cycle. Samples were collected 0, 12, 24 and 48 hours post release from G1 and following 30 minutes of BrdU pulse labelling.

Histograms are representative of 3 independent experiments.

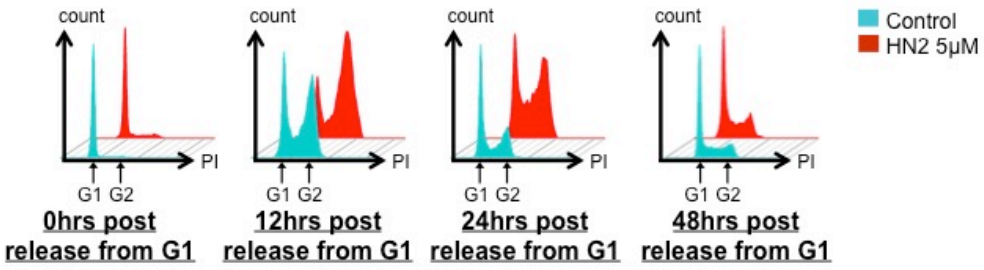



**Figure 3.10: Cell cycle dynamics of G1 synchronised CSB mutant CHO cells following treatment in G1 and release to cell cycle.**

G1 synchronised CSB mutant CHO cells were treated with 5μM HN2 for 1 hour and then released to cell cycle. Samples were collected 0, 12, 24 and 48 hours post release from G1 and following 30 minutes of BrdU pulse labelling.

Histograms are representative of 3 independent experiments.

Two other mutant cell lines were also examined using the experimental model. The XRS5 CHO cell line, which is mutated for Ku80 a protein that is encoded by the XRCC5 gene. This protein along with Ku70 forms a heterodimer that is required for non-homologous end joining (NHEJ) repair of DNA strand breaks(Taccioli et al., 1994; Kemp et al., 1984). This mutated cell line showed quite marked stalling after release to cell cycle (Figure 3.11) showing persistent stalling even up to 48 hours after release. Similarly, the irs1SF cell line, which is mutated in XRCC3, also demonstrated significant stalling (Figure 3.11). XRCC3 is a paralog of RAD51 and is required for repair of DNA double strand breaks (DSB) by homologous recombination (HR) (Brenneman et al., 2000). These results are somewhat surprising, as it would be expected for G1 repair to proceed through NER or even base excision repair (BER). Both of these cell lines showed poor synchronisation to G1 through isoleucine starvation. It is possible, therefore, that these results may be artefact from incomplete synchronisation to G1. Importantly, the XRS5 cell line also has a different parental cell line than all the other cell lines used in these experiments originating from a CHO-K1 line. The effects of HN2 were assessed in the CHO-K1 line and this also showed stalling on release from G1 (Figure 3.12). It is possible that the apparent stalling seen in this cell line reflects previously unidentified abnormality within the parental cell line's DNA damage repair pathway.

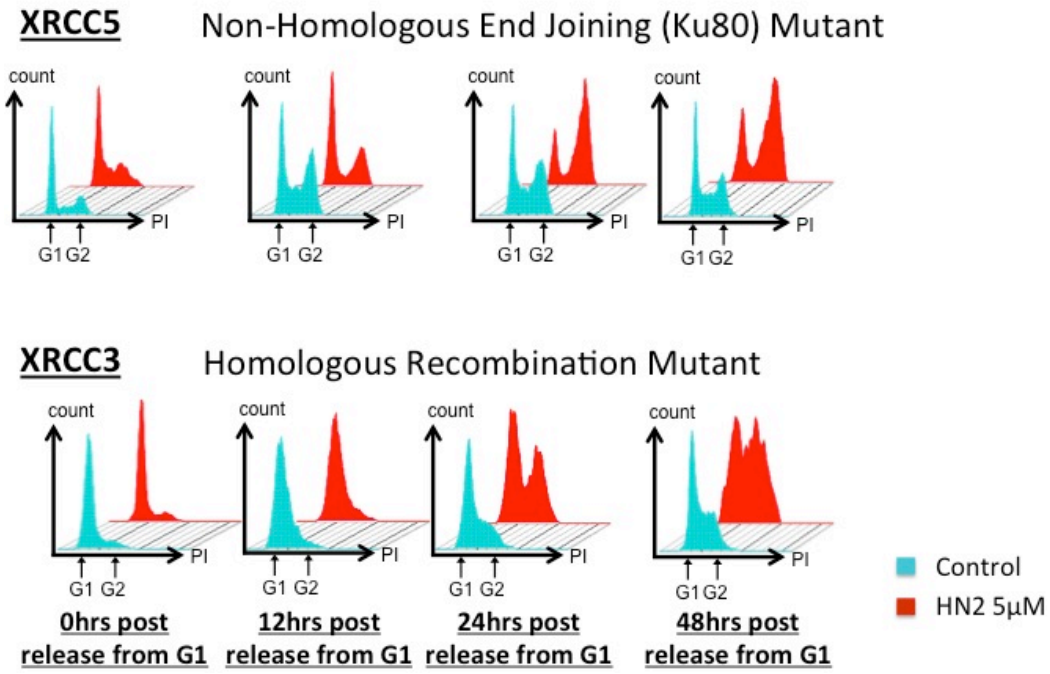



**Figure 3.11: Cell cycle dynamics of G1 synchronised mutant NHEJ and HR CHO cells following treatment and holding in G1 for 24 hours prior to release.**

G1 synchronised mutant CHO cells were treated with 50µM HN1 and 5µM HN2 for 1 hour and then held in G1 for 24 hours before release to cell cycle. Samples were collected 0, 12, 24 and 48 hours after release to cell cycle and following 30 minutes of BrdU pulse labelling.

Histograms are representative of 2 independent experiments.

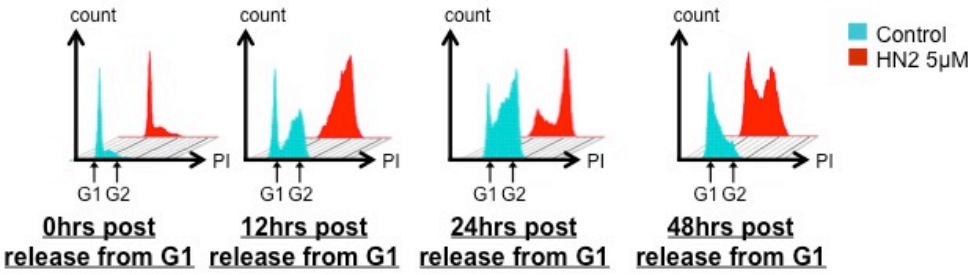



**Figure 3.12: Cell cycle dynamics of G1 synchronised CHO-K1 WT CHO cells following treatment and holding in G1 for 24 hours prior to release.**

G1 synchronised CHOK1 WT CHO cells were treated with 50µM HN1 and 5µM HN2 for 1 hour and then held in G1 for 24 hours before release to cell cycle. Samples were collected 0, 12, 24 and 48 hours after release to cell cycle and following 30 minutes of BrdU pulse labelling.

Histograms are representative of 2 independent experiments.

## 3.3 Determination of exonuclease involvement in G1 ICL repair

It has been proposed the resolution of an ICL is likely to require recognition of the lesion and initial incisions either side of the ICL to enable unhooking to occur. The resulting gap in the single strand would then undergo bypass by the translesion synthesis (TLS) polymerases (Sarkar et al., 2006). Several exonucleases have been implicated in ICL bypass in replicating cells and it is possible they may also play a role in incision in non-replicating cells. The 5' to 3' exonuclease SNM1A is thought to play a role in digestion of the unhooked oligonucleotide in replication based ICL repair (Wang et al., 2011). Since SNM1A has also been shown to interact with CSB (Iyama and Wilson, 2013) it may play a role in G1 repair of ICL. The 5' to 3' exonucleases EXO1 and FAN1 have also been implicated in replication based ICL repair. EXO1 in particular is involved in 5' end resection and resolution of Holliday Junctions in meiosis. FAN1 possesses both exonuclease and endonuclease functions, although it preferentially acts a 5' flap endonuclease. FAN1 could, therefore, play a role in incision on either side of the ICL.

With this in mind further experiments were performed to investigate whether the nucleases FAN1, EXO1 and SNM1A might be involved in repair of ICL in G1.

In previous experiments it was possible to use stable mutant CHO cell lines in the experimental model. As there are no stable CHO mutant cell lines for the nucleases of interest, knockdown using siRNA suppression was initially performed. Using optimised conditions, as described in Section 2.5.2, CHO cells were transfected with siRNA and 24 hours after transfection synchronised to G1 by isoleucine starvation for 48 hours. As described previously, following synchronisation cells were treated with 5μM HN2 for 1 hour before further incubation in isoleucine free

media for a further 24 hours. Cells were released to cell cycle 24 hours after treatment by addition of isoleucine complete media. Prior to release samples were collected and total RNA was extracted from cells in order to measure mRNA levels and assess for adequate siRNA suppression.

Initially to ensure that RNAi could be used within this experimental model the effects of siRNA suppression of XPF in CHO cells were assessed. In previous experiments with stable XPF mutants, widespread stalling was seen in XPF mutated cells treated in G1 once they were released to cell cycle. It would therefore be reasoned that CHO cells that underwent siRNA knockdown for XPF should demonstrate a similar phenotype.

Figure 3.13 illustrates that knockdown of XPF in CHO WT cells resulted in stalling after release to cell cycle with 18.5% of XPF KD treated cells remaining in G2 at 24 hours after release compared with 11.8% of control treated cells. This stalling was not as marked as seen in stably mutated XPF cells, presumably due to the incomplete total suppression of XPF. Using RT-qPCR mRNA expression of XPF was found to be approximately 15-18% (Figure 3.13C) when compared to the house keeping gene glyceraldehyde 3-phosphate dehydrogenase (GAPDH).

It is important to note that siRNA suppression itself did not appear to affect ICL resolution. Control experiments performed using a non-transfecting (NT) siRNA did not cause any significant stalling after release to cell cycle suggesting the effects seen with XPF siRNA suppression are not due to off-target effects.

FAN1 encodes for a structure dependent endonuclease, FANCD2/FANCI-associated nuclease 1, which has been shown to play a role in the unhooking of ICL

by catalysing incisions close to ICL following stalling of the replication fork (MacKay et al., 2010). To assess if FAN1 played a role in G1 repair further experiments were performed following siRNA FAN1 knockdown.

As before CHO WT cells were transfected with FAN1 and NT siRNA and again synchronised to G1. FAN1 and NT siRNA KD cells were treated in G1 with 5μM HN2 and held in G1 for a further 24 hours prior to release to cell cycling. Figure 3.14 demonstrates that following release from G1 no clear stalling was evident in the FAN1 siRNA knockdown cells. This was despite qRT-PCR demonstrating adequate knockdown of FAN1 with mRNA expression levels of 17.5% compared to GAPDH Figure 3.14C. This suggests that in G1 cells it is unlikely that FAN1 plays a role in ICL incision, repair or processing.

DNA cross-link repair 1A (SNM1A) is a 5'-3' exonuclease which has been previously demonstrated to load onto DNA strands at double-strand ends and single-stranded nicks and has the ability to digest past ICL on substrate strands effectively assisting in ICL removal in actively dividing cells (Wang et al., 2011). Since ICL repair in G1 would require digestion of portions of single strand DNA to allow unhooking followed by TLS bypass, it is possible SNM1A may play a role in G1 repair. To investigate this possibility, further experiments were performed utilising SNM1A siRNA suppression. Following SNM1A knockdown cells were again treated in G1 with 5μM HN2 and on release to cell cycle (Figure 3.15) significant stalling was seen at 24 hours. At this time point 24% SNM1A KD cells treated with HN2 remained in G2 compared with only 11.8% of NT cells. Adequate KD of SNM1A was demonstrated with mRNA expression of SNM1A measured at 12.3% and 16% compared to expression of GAPDH (Figure 3.15).

Further experiments were performed to assess the effects of EXO1 suppression on G1 repair. EXO1 encodes for the protein Exonuclease 1 which has 5' to 3' exonuclease activity. Previous studies have implicated this protein in DNA double strand break end resection and mismatch repair (Qiu et al., 1999). As in previous experiments WT CHO cells were transfected with EXO1 siRNA and then synchronised to G1 where they were treated with 5μM HN2. Following holding for a further 24 hours in G1 cells were released to cell cycle and assessed by FACS. Adequate suppression of EXO1 proved difficult to achieve and mRNA levels compared to GAPDH showed expression of 52% and 37% (Figure 3.16). This subsequently makes interpretation of changes in cell cycle difficult but WT KD EXO1 cells treated with HN2 appeared to show mild stalling at 24 hours after release with 16.4% of cells persisting in G2 compared with 11.8% cells treated with NT siRNA (Figure 3.16).

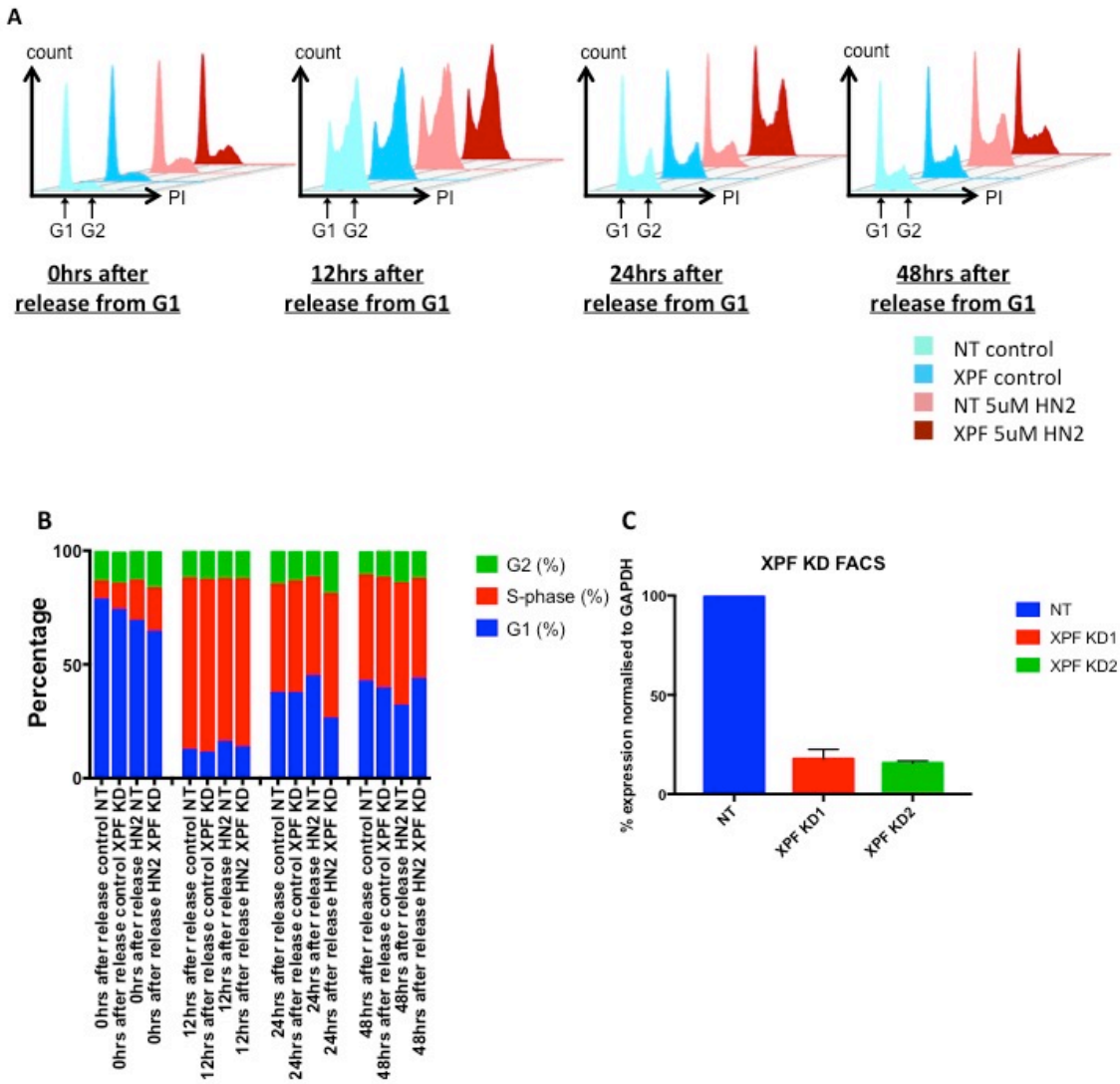



**Figure 3.13: Cell cycle dynamics after siRNA knockdown of XPF, synchronisation to G1 and treatment in G1 with 5μM HN2 for 1 hour followed by further incubation in G1 for 24 hours prior to release to cell cycle.**

WT CHO were transfected with non-targeting (NT) or XPF siRNA and 24 hours later synchronised to G1 by isoleucine starvation for 48 hours. G1 synchronised cells were treated with 5μM HN2 for 1 hour and then held in G1 for 24 hours before release to cell cycle. Samples were collected 0, 12, 24 and 48 hours after release to cell cycle and following 30 minutes of BrdU pulse labelling.

A: PI histograms of cell cycle dynamics.
B: Graphical representation of cell cycle position from BrdU gated plots.
Histograms and bar chart are representative of 2 independent experiments.

C: XPF siRNA knockdown as normalised to GAPDH expression.
Data represent the mean + SD, n=2.

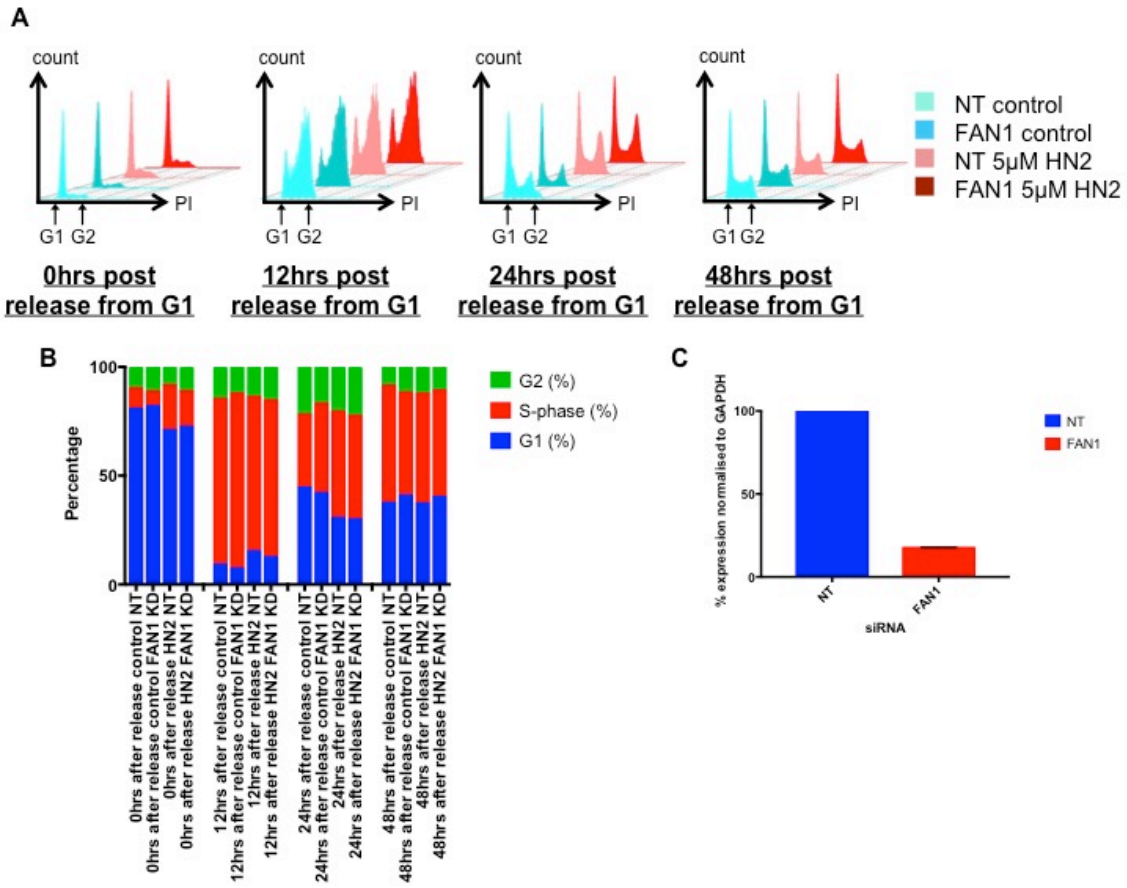



**Figure 3.14: Cell cycle dynamics after siRNA knockdown of FAN1, synchronisation to G1 and treatment in G1 with 5μM HN2 for 1 hour followed by further incubation in G1 for 24 hours prior to release to cell cycle.**

WT CHO were transfected with non-targeting (NT) or FAN1 siRNA and 24 hours later synchronised to G1 by isoleucine starvation for 48 hours. G1 synchronised cells were treated with 5μM HN2 for 1 hour and then held in G1 for 24 hours before release to cell cycle. Samples were collected 0, 12, 24 and 48 hours after release to cell cycle and following 30 minutes of BrdU pulse labelling.

A: PI histograms of cell cycle dynamics.
B: Graphical representation of cell cycle position from BrdU gated plots.
Histograms and bar chart are representative of 2 independent experiments.

C: FAN1 siRNA knockdown as normalised to GAPDH expression.
Data represent mean + SD.

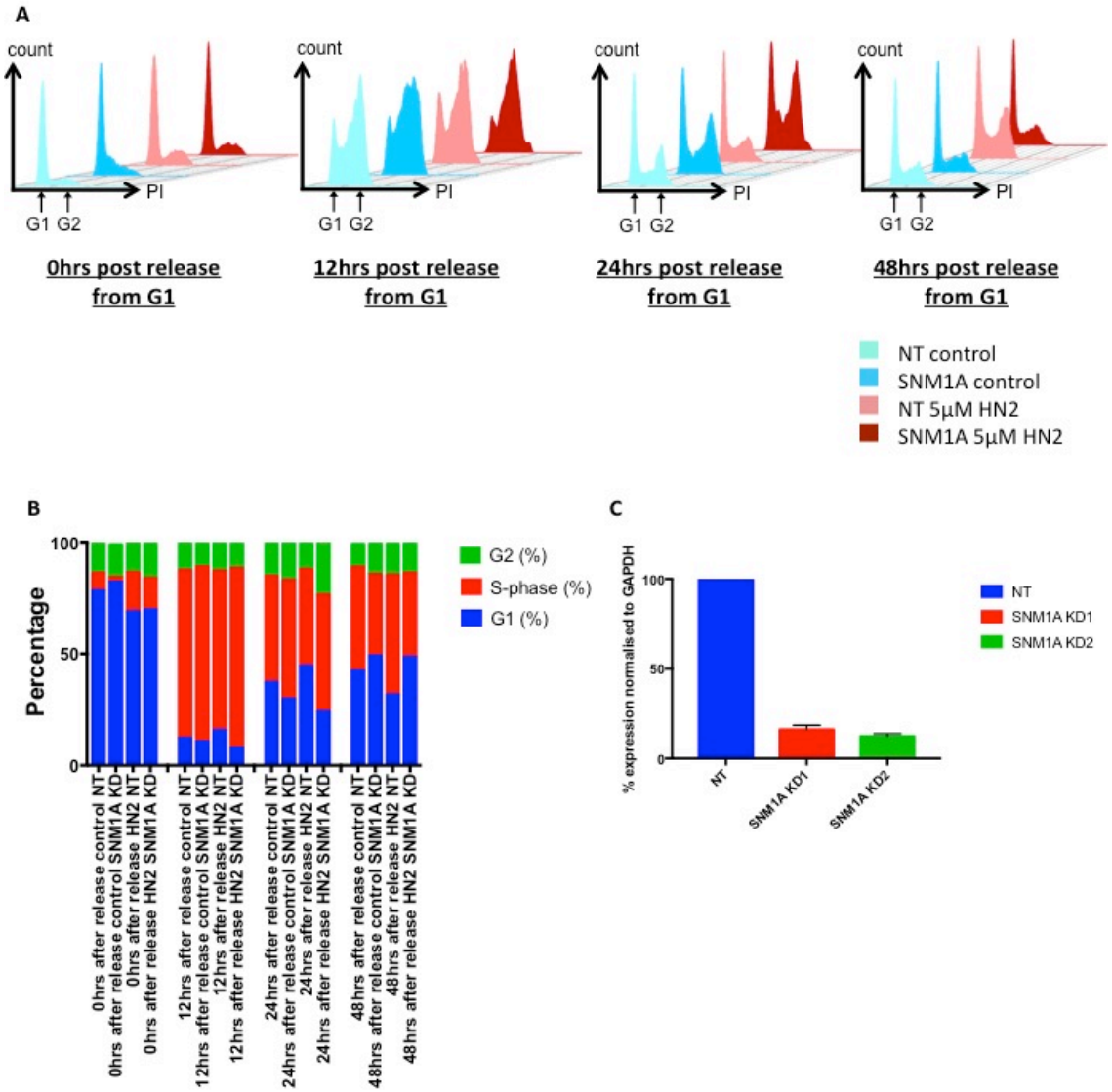



**Figure 3.15: Cell cycle dynamics after siRNA knockdown of SNM1A, synchronisation to G1 and treatment in G1 with 5µM HN2 for 1 hour followed by further incubation in G1 for 24 hours prior to release to cell cycle.**

WT CHO were transfected with non-targeting (NT) or SNM1A siRNA and 24 hours later synchronised to G1 by isoleucine starvation for 48 hours. G1 synchronised cells were treated with 5µM HN2 for 1 hour and then held in G1 for 24 hours before release to cell cycle. Samples were collected 0, 12, 24 and 48 hours after release to cell cycle and following 30 minutes of BrdU pulse labelling.

A: PI histograms of cell cycle dynamics.
B: Graphical representation of cell cycle position from BrdU gated plots.
Histogram and bar chart are representative of 2 independent experiments.

C: SNM1A siRNA knockdown as normalised to GAPDH expression.
Data represent mean + SD, n=2.

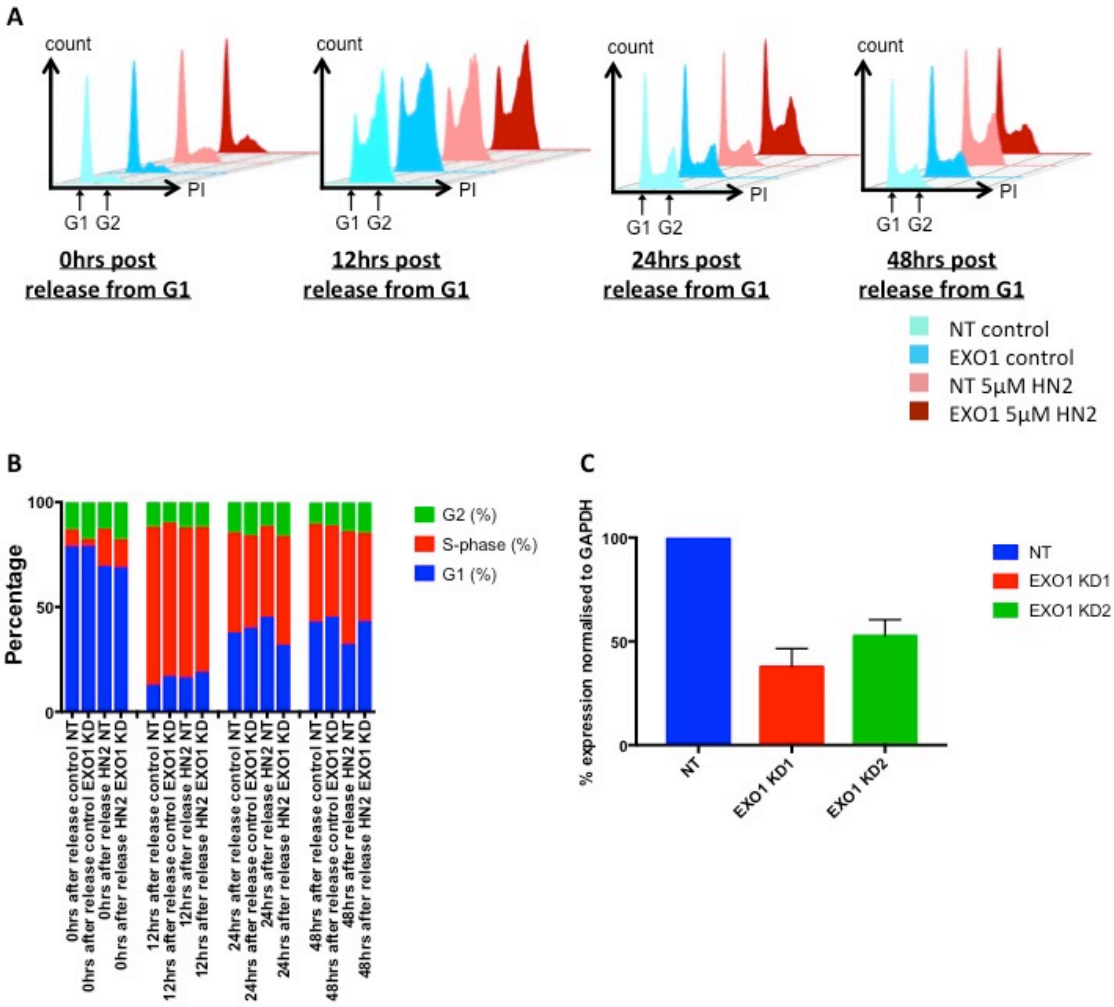



**Figure 3.16: Cell cycle dynamics after siRNA knockdown of EXO1, synchronisation to G1 and treatment in G1 with 5µM HN2 for 1 hour followed by further incubation in G1 for 24 hours prior to release to cell cycle.**

WT CHO were transfected with non-targeting (NT) or EXO1 siRNA and 24 hours later synchronised to G1 by isoleucine starvation for 48 hours. G1 synchronised cells were treated with 5µM HN2 for 1 hour and then held in G1 for 24 hours before release to cell cycle. Samples were collected 0, 12, 24 and 48 hours after release to cell cycle and following 30 minutes of BrdU pulse labelling.

A: PI histograms of cell cycle dynamics.
B: Graphical representation of cell cycle position from BrdU gated plots.
Histograms and bar chart represent 2 independent experiments.

C: EXO1 siRNA knockdown as normalised to GAPDH expression.
Data represent mean + SD, n=2.

## 3.4 Comet assay analysis of ICL induction and unhooking in G1 cells.

### 3.4.1 Comet assay analysis of ICL induction and unhooking in G1 WT cells.

Previous experiments performed using FACS analysis have suggested the formation and repair of ICL can occur in G1. This was inferred from the persistence of stalling of the cells at late S-phase/G2 which assumes that if ICL are still present cells will slow in their transition through the cell cycle, particularly in late S-phase/G2 prior to cell division, to allow time for ICL to be resolved. To further confirm that ICL can be formed in G1 and that these can under go resolution further analysis of G1 repair using alkaline comet assays was performed.

The comet assay or single cell gel electrophoresis assay (SCGE) is a sensitive technique for measuring DNA damage in single eukaryotic cells (Hartley et al., 2011; Spanswick et al., 2010). The technique was initially developed to measure DNA strand breaks in individual cells but has been adapted with the addition of a γ-ray irradiation step to allow for assessment of ICL caused by cross-linking agents (Azqueta et al., 2014). The assay involves initially embedding cells in a thin layer of low melting point agarose on microscope slides. Cells undergo lysis with high salt detergent to allow removal of cell membranes, nucleoplasm and cytoplasm. Electrophoresis is performed in alkaline conditions, which allows for degradation of contaminating RNA and breaks any DNA protein cross-links. Fragments of negatively charged DNA migrate towards the anode under electrophoresis with the extent of migration reflecting the size of the DNA. Small fragments of DNA formed by breaks migrate further and create a “tail” appearance. Undamaged DNA

migrates slowly forming the "head" of the comet shape (Ostling and Johanson, 1984) (Figure 3.17).

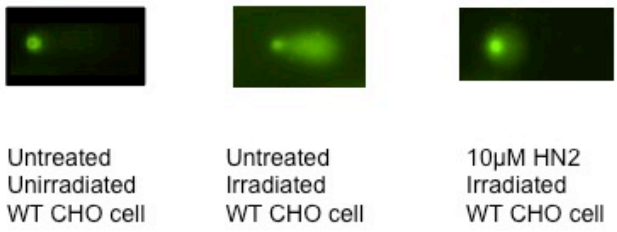



**Figure 3.17: Comet Assay assessment of ICL formation.**

WT CHO cells as assessed by modified Comet Assay.

**Left:** Untreated, unirradiated cells have intact DNA that remains concentrated within the nucleus and only a comet head is formed.
**Centre:** Untreated, irradiated cells have fragmented DNA this results in the formation of a tail as broken DNA migrates with electrophoresis.
**Right:** HN2 treated, irradiated cells have multiple ICLs this impedes DNA migration during electrophoresis and comet tail decreases in size.

The modified-alkaline comet assay used in experiments in this chapter involves the addition of an irradiation step prior to embedding cells in agarose. This causes a fixed level of random DNA double-strand breaks to occur. At electrophoresis in alkaline conditions the presence of ICL prevents denaturation of double strand DNA and therefore a decreased number of DNA fragments, resulting in reduced DNA migration at electrophoresis.

The level of DNA damage in the assay is assessed by calculation of the "tail moment" (or Olive tail moment) for each individual analysed cell. This measurement, proposed by Olive *et al* (Olive et al., 1990), is the product of the percentage of DNA in the comet tail and the distance between the means of the

head and tail DNA distributions. Tail moment is considered a superior measurement of DNA damage than simple tail length as it better reflects the variation in DNA distribution within the comet tail.

To assess that ICL can be formed in G1 cells comet assays were initially performed assessing decrease in tail moment in asynchronous and G1 synchronised cells with increasing doses of HN2. Briefly, WT CHO cells were either treated in G1 or in an asynchronous state with increasing doses of HN2. Following treatment cells were trypsinised and re-suspended in the appropriate media and samples divided into either irradiated or un-irradiated samples. Irradiated samples were exposed to 10Gy and then both irradiated and un-irradiated cell suspensions were mixed with warmed low-melting point agarose and applied to microscope slides. Samples were lysed and underwent electrophoresis under alkaline conditions. All samples were stained with SYBR gold and images of samples taken using a Zeiss Observer Z1 microscope. Images were analysed using OpenComet software (www.cometbio.org Version 3.0) and the percentage decrease in tail moment calculated. Figure 3.18 (A and B) demonstrates that ICL are formed in both asynchronous and G1 synchronised CHO WT cells with decreasing tail moment with increasing doses of ICL. In both asynchronous and G1 synchronised cells tail moment was decreased by 80% with 10μM HN2. These findings are similar to de Silva et al (De Silva et al., 2000) and demonstrate that ICL can be clearly formed in G1 cells in a dose dependent fashion.

To analyse ICL resolution in G1 cells further time course experiments were performed assessing the resolution of ICL over time. WT CHO cells were synchronised to G1 by isoleucine and then treated with 10μM HN2 for 1 hour.

After treatment cells were held in G1 by continued incubation in isoleucine free media and cells were harvested at progressive time points. Following harvesting cells samples were divided and either irradiated or left untreated. Samples were then frozen at -20°C until the completion of the time course when samples were defrosted, suspended in molten agarose, lysed and electrophoresis performed. The percentage ICL unhooking was calculated by comparing the decrease in tail moment at each time point with that immediately after treatment. Figure 3.19 demonstrates that by 4 hours only approximately 10% of ICL had under gone resolution but by 12 hours 76% of ICL lesions had resolved. Almost all ICL, 98%, had been resolved by 24 hours. This confirms previous FACS experimental findings confirming ICL can form in G1 cells and that ICL resolution is time dependent requiring up to 24 hours.

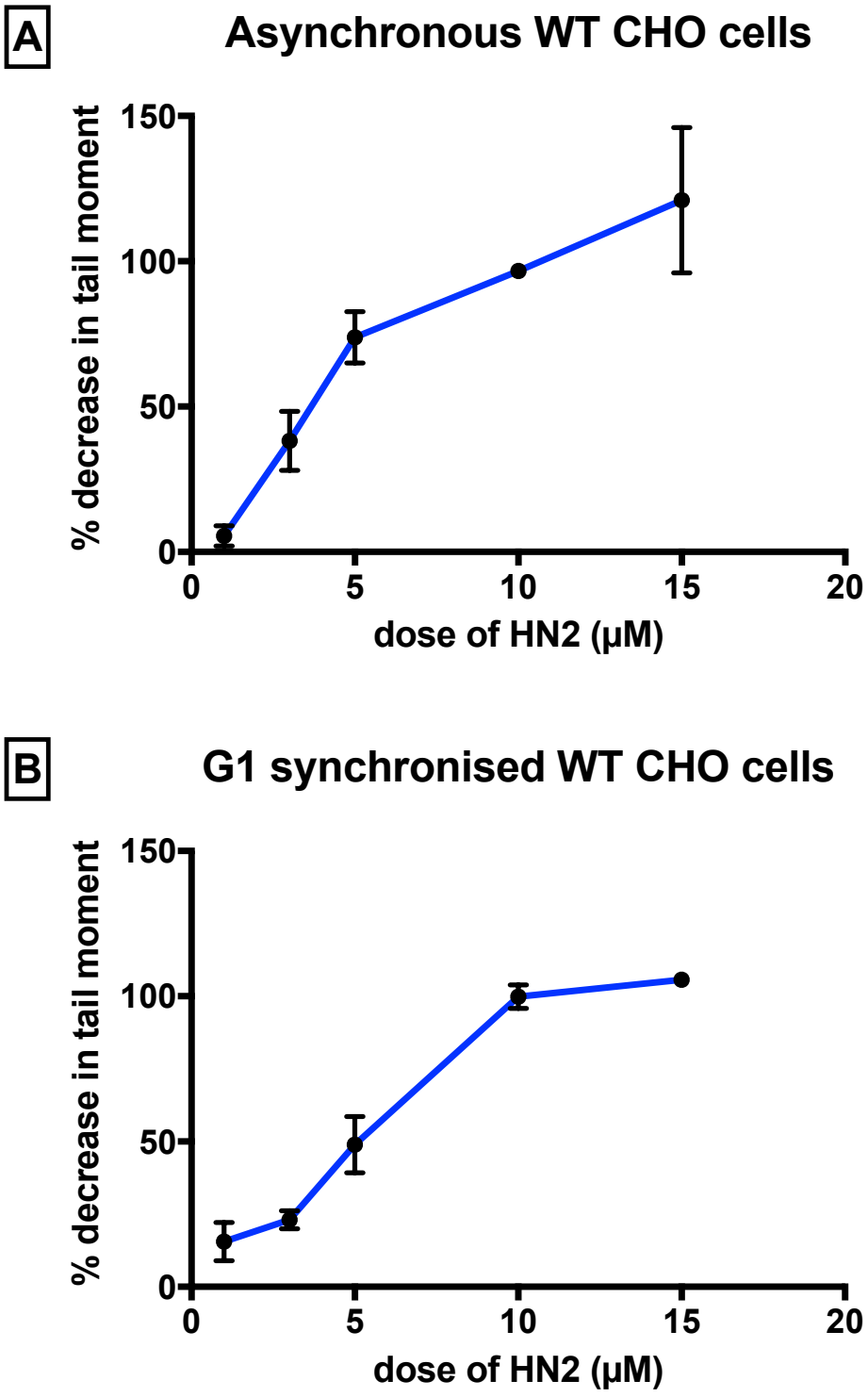



**Figure 3.18: Change in comet tail moment with increasing doses of HN2**

WT CHO cells were treated with increasing doses of HN2 and analysed by modified comet assay.

A: Change in comet tail moment in asynchronous WT CHO cells.
B: Change in comet tail moment in G1 synchronised WT CHO cells.

Data points represent mean ± SEM, n=3.

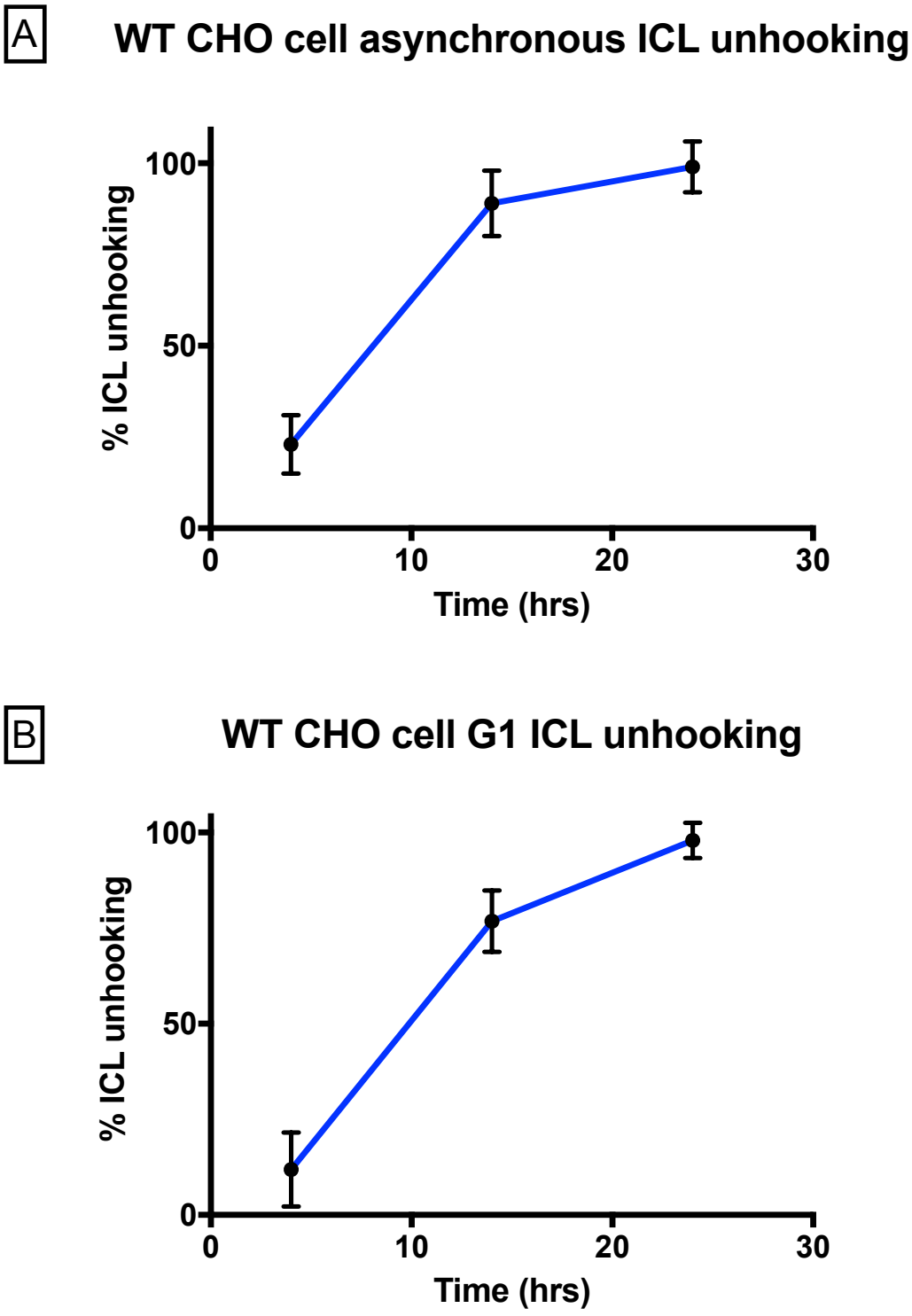



**Figure 3.19: Unhooking of WT CHO cells after treatment with HN2 in G1**

ICL unhooking in WT CHO cells treated with 10μM HN2 for 1 hour. Samples were collected for analysis at 4, 12 and 24 hours after treatment.

A: ICL unhooking in asynchronous WT CHO cells.
B: ICL unhooking in G1 synchronised WT CHO cells.

Data points represent mean ± SEM, n=3.

### 3.4.2 Comet Assay analysis of ICL unhooking in mutant and siRNA KD CHO cells.

Further experiments were performed to assess ICL unhooking in repair mutant CHO cell lines. As described before, each DNA damage mutant was synchronised to G1 by isoleucine starvation and treated with 10μM HN2 for 1 hour, samples were then collected and divided into irradiated and un-irradiated samples. Following lysis, electrophoresis and staining comet tail moment was assessed using OpenComet analysis software.

Cell lines mutated for XPF showed minimal unhooking with approximately 18% of ICLs unhooked by 12 hours and samples showing very little further unhooking 24 hours after treatment (Figure 3.20). This corresponds with the marked stalling seen in FACS experiments assessing repair of ICL in XPF mutated cells.

CHO Cell lines mutated for the proteins XPB and XPD were also examined and both showed significantly slower resolution of ICL than WT CHO cells. XPB mutated cells showed unhooking of 35% ICL 12 hours after treatment and approximately 48% of ICL were unhooked by 24 hours. Similarly unhooking of ICL in XPD mutated cells was also reduced with only 11% ICL resolved by 12 hours and 40% of ICL unhooked by 24 hours (Figure 3.20).

The resolution of ICL in these mutated cells reflects the less striking degree of stalling seen in FACS experiments with these cell lines. Both XPB and XPD mutated cell lines showed initial stalling in late S-phase/G2 24 hours after release to cell cycle but unlike XPF mutated cells this stalling appeared to completely resolve 48 hours after release to cell cycle. This is reflected in the increased levels of ICL

unhooking seen in XPB and XPD cells at 24 hours after treatment, 48% and 40% respectively versus only 28% in XPF mutated cells.

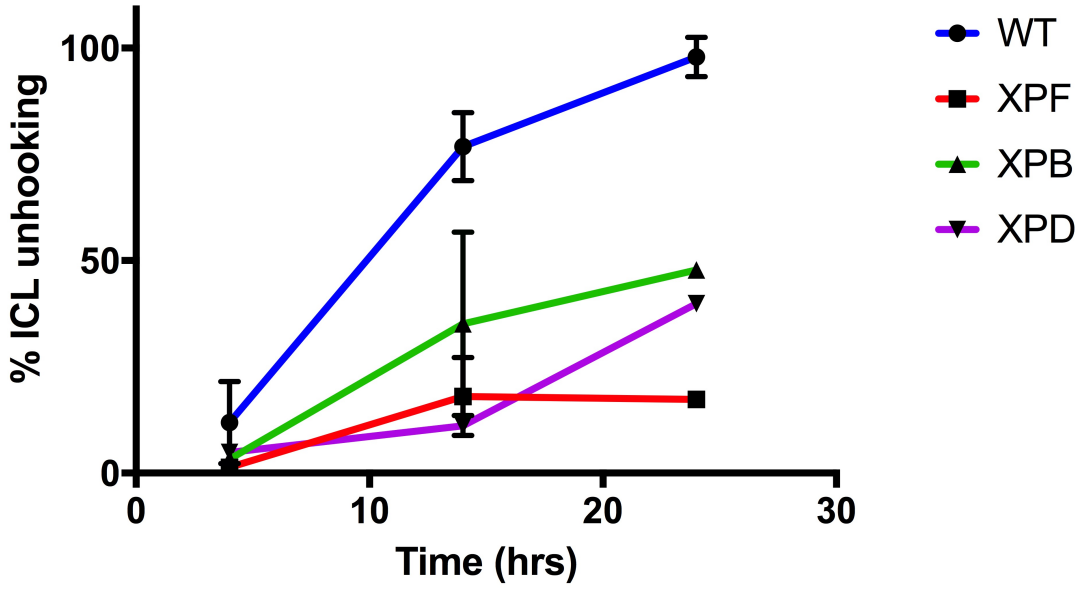



**Figure 3.20: ICL unhooking in WT and DNA damage mutant CHO cells**

WT and DNA damage mutant CHO cells were synchronised to G1 by isoleucine starvation, treated with 10μM HN2 for 1 hour and then incubated in G1 and harvested at the specified time points.

Data points represent mean ± SEM, n=2.

Previous experiments detailed in this chapter using FACS analysis have suggested that SNM1A may play a role in ICL unhooking in G1. To confirm this comet assays were performed in CHO WT cells that had undergone SNM1A siRNA KD. As described earlier in this chapter CHO WT cells were transfected with SNM1A siRNA at a final concentration of 40nM and 24 hours later synchronised to G1 by 48 hours of isoleucine starvation. As described previously SNM1A KD CHO cells were treated with 10μM HN2 and then harvested at progressive time points before

being used in comet assay analysis. Figure 3.21 shows that ICL unhooking in SNM1A siRNA KD cells appeared reduced. In comparison to WT and other mutant cell lines initial unhooking appeared increased with 46% of lesions undergoing unhooking 4 hours after treatment. Following this time-point any further unhooking appeared to stall and at 12 and 24 hours post treatment ICL unhooking was 48 and 57% respectively.

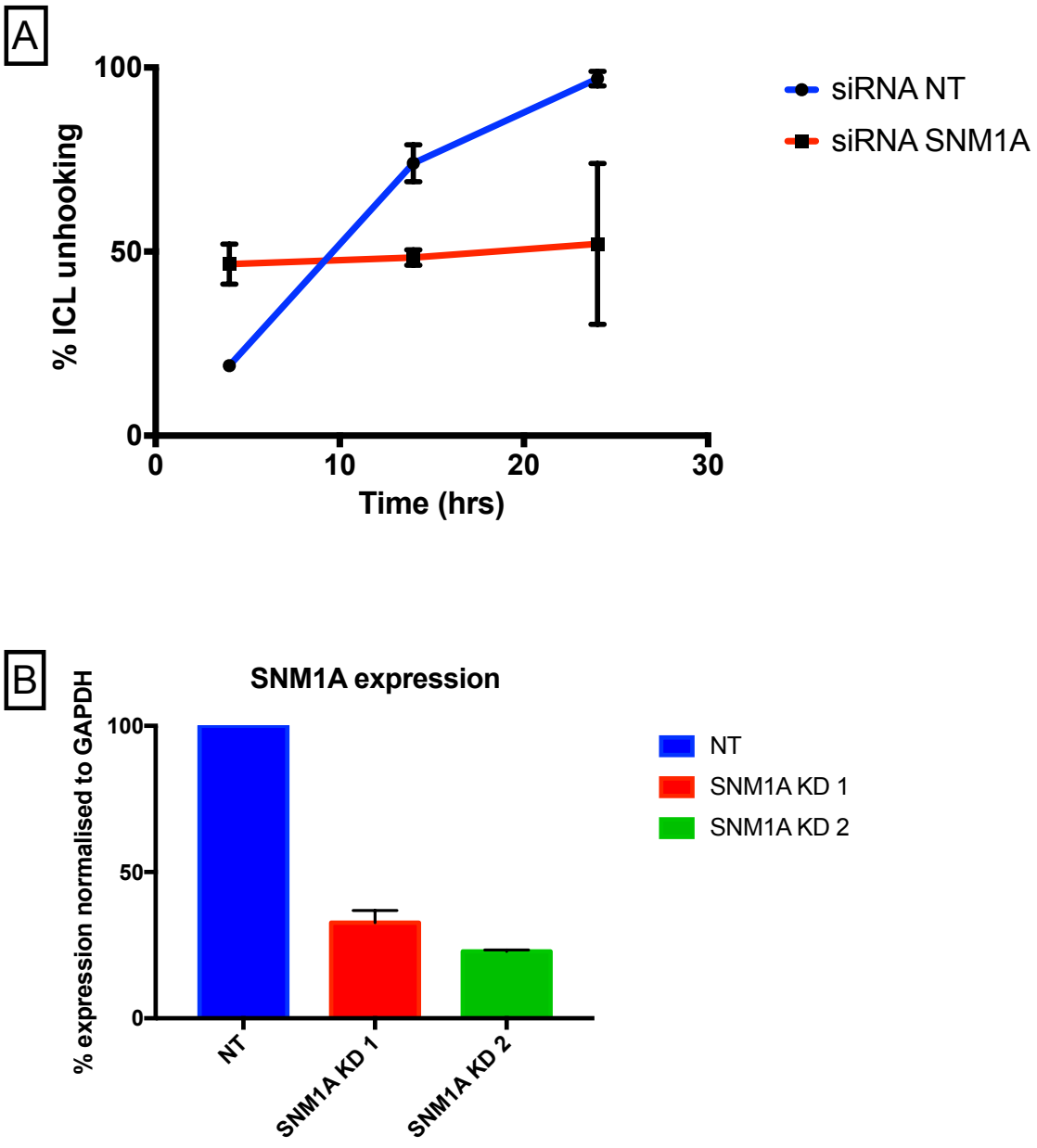



**Figure 3.21: ICL unhooking in SNM1A siRNA and NT KD CHO cells**

CHO cells were transfected with NT and SNM1A siRNA and 24 hours later synchronised to G1 by isoleucine starvation. In G1 cells were treated with 10μM HN2 for 1 hour and samples harvested at 0, 4, 14 and 24 hours after treatment with HN2.

A: % ICL unhooking by time after treatment with 10μM HN2
B: SNM1A expression normalised to GAPDH

Data points represent mean ± SEM, n=2.

## 3.5 Assessment of survival following treatment in G1 or in asynchronous state

Previous experiments have demonstrated that ICL can be formed and repaired in G1. In order to assess the impact of G1 repair on cell survival clonogenic assays were performed with WT and DNA mutant cell lines.

As before cells were synchronised to G1 by isoleucine starvation for 48 hours. Once synchronised to G1 cells were treated in G1 for 1 hour with increasing doses of HN2. Following treatment cells were either left to incubate for a further 24 hours in isoleucine free media and then trypsinised and counted or were immediately lifted and counted. After counting, 4000 cells from each experiment were plated to 10cm petri dishes and allowed to form colonies for 7 days in isoleucine complete media. After 7 days of incubation the plates were stained with crystal violet and the total number of colonies counted.

Figure 3.22 demonstrates survival for each cell line after treatment in G1 and either immediate lifting to isoleucine complete media or following a further 24 hours incubation in G1 and then seeding. In all cell lines, both WT and mutant, cell survival was reduced when cells were treated in G1 and immediately lifted to seed for clonogenic experiments compared to experiments where cells were left in G1 for 24 hours prior to lifting. This can be illustrated in WT cells which showed increased sensitivity when treated and immediately lifted for survival assay, treatment with 15μM HN2 resulted in approximately 3% survival compared to 10% when cells were treated in G1 and held for 24 hours prior to use in cell survival assays. This appears to support findings presented earlier in this chapter. If, as demonstrated previously by FACS and comet assays, repair of ICL can occur

in G1 it would be expected that cells that have been held in G1 would have improved survival since these cells will have undergone a significant degree of ICL resolution prior to lifting for use in cell survival assays. Should repair of ICL occur in G1 this would be limited by the burden of ICL present and this would account for the decreased survival seen at high doses of HN2 in cells held in G1 for 24 hours.

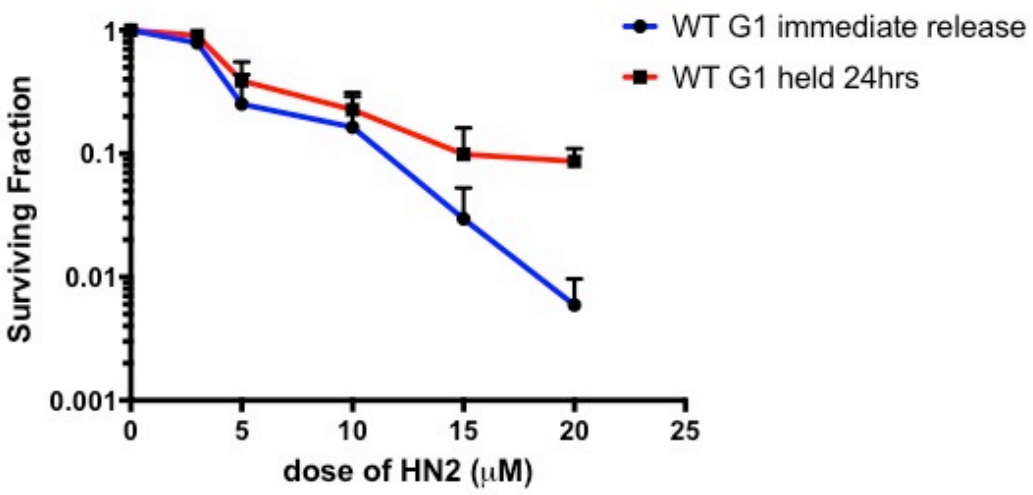



**Figure 3.22: Survival of WT CHO cells following treatment in G1.**

WT CHO cells were synchronised to G1 by isoleucine starvation and then treated with HN2. Following treatment cells were either trypsinised and counted immediately, or left to incubate for a further 24 hours in G1, prior to seeding for clonogenic assays.

Data points represent the mean + SEM, n=3.

Figure 3.23 compares survival assays in WT and XPF mutated cells. XPF mutant cells are exquisitely sensitive to HN2 and the survival assays suggest that XPF mutated cells are much more sensitive than WT cells to HN2 both when treated in G1 and then immediately used in clonogenic assay and when treated and held in G1 for 24 hours (Figure 3.23 A and B). When comparing survival of XPF mutated cells in both states, cells appeared much more sensitive to HN2 treatment when treated with HN2 and immediately used in clonogenic experiments (Figure 3.23 C). Treatment with 2μM HN2 resulted in survival of 7% in cells left in G1 for 24 hours compared to less than 1% in cells treated in G1 and immediately lifted. These results suggest that although XPF is required for G1 repair, the increased sensitivity in cells immediately used in clonogenic experiments may suggest that the role of XPF in ICL repair is more essential to replicating cells or that the absence of XPF in replicating cells leads to the accumulation of more toxic intermediates. It is also possible that an alternative pathway that does not require XPF such as BER is more dominant in G1.

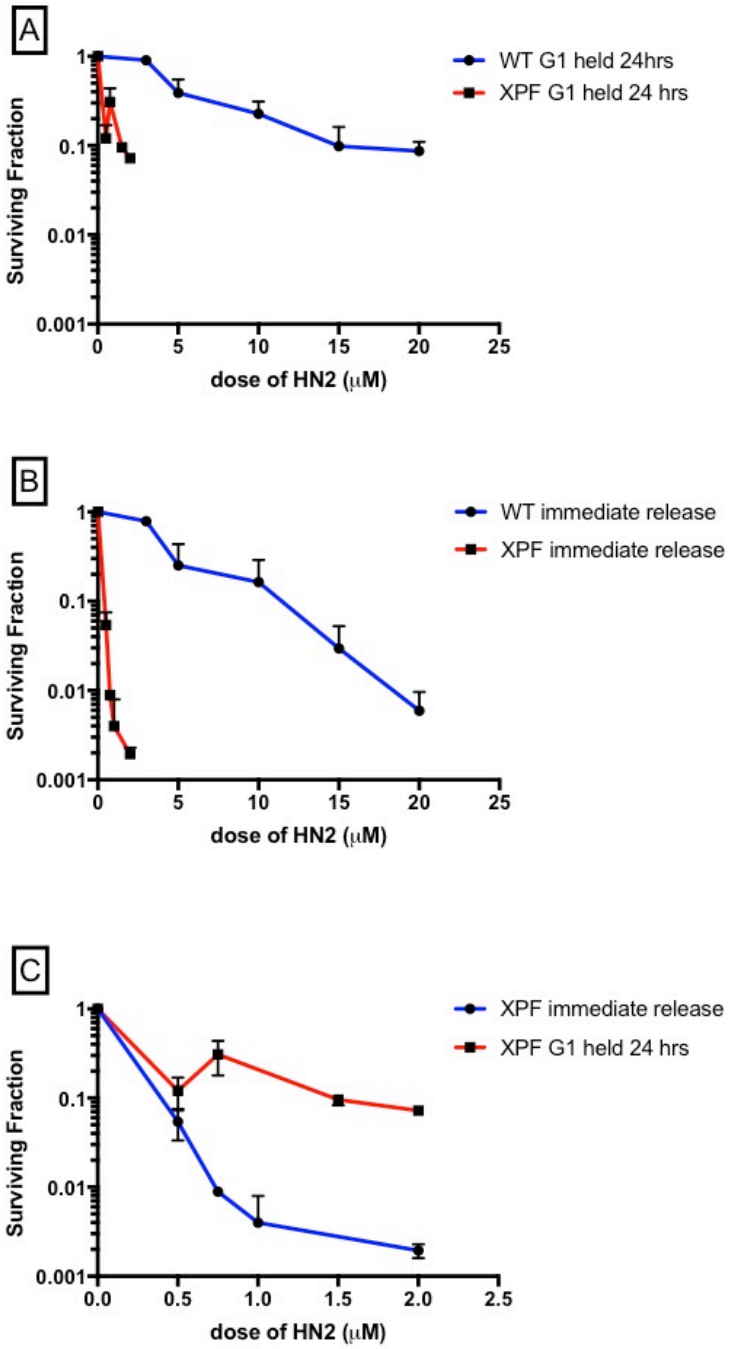



**Figure 3.23: Survival of XPF mutant CHO cells following treatment in G1.**

XPF mutant CHO cells were synchronised to G1 by isoleucine starvation and then treated with HN2. Following treatment cells were either trypsinised and counted immediately, or left to incubate for a further 24 hours in G1, prior to seeding for clonogenic assays.

A: Comparison of survival of WT and XPF mutated CHO cells treated in G1 and held in G1 for 24 hours prior to seeding for CFA.
B: Comparison of survival of WT and XPF mutated CHO cells treated in G1 and immediately seeded for CFA.
C: Comparison of survival of XPF mutated CHO cells treated in G1 and immediately seed for CFA with those treated and held in G1 for 24 hours prior to seeding for CFA.

Data points represent mean + SEM, n=3

Examination of XPB mutants using clonogenic assays demonstrates that XPB mutants are more sensitive than WT cells to HN2 when treated and held in G1 and when treated in G1 and immediately used for colony forming assays (Figure 3.24 A and B). This suggests a role for XPB in G1 repair but when the sensitivity of XPB mutated cells is compared in the two different treatment states, XPB mutated cells treated and immediately seeded for clonogenic assays appear more sensitive to HN2 than those held in G1 after treatment (Figure 3.24 C). This suggests that XPB may not be essential for G1 repair and since the sensitivity of XPB mutants was not as marked that in XPF mutated cells the role XPB plays in ICL repair in G1 and dividing cells may not be critical and perhaps can be bypassed by other pathways.

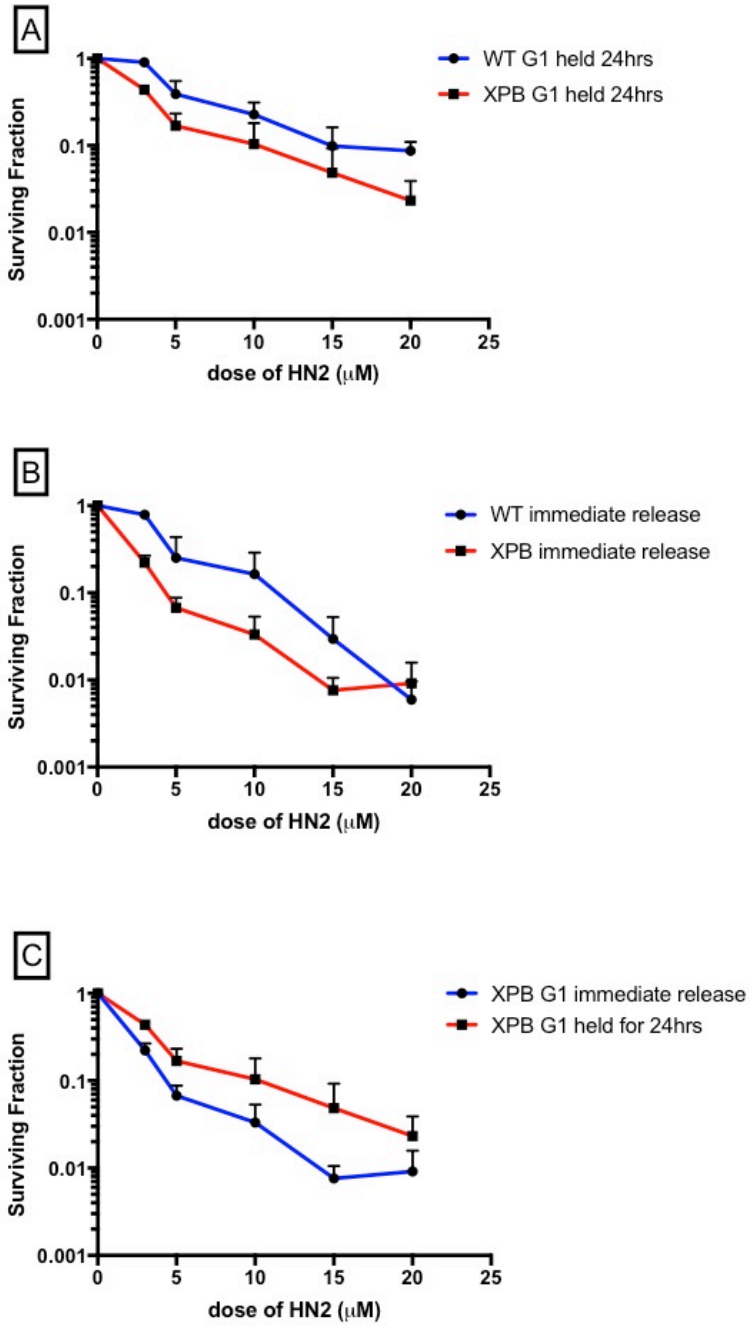



**Figure 3.24: Survival of XPB mutant cells following treatment in G1.**

XPB mutant CHO cells were synchronised to G1 by isoleucine starvation and then treated with HN2. Following treatment cells were either trypsinised and counted immediately, or left to incubate for a further 24 hours in G1, prior to seeding for clonogenic assays.

A: Comparison of survival of WT and XPB mutated CHO cells treated in G1 and held in G1 for 24 hours prior to seeding for CFA.
B: Comparison of survival of WT and XPB mutated CHO cells treated in G1 and immediately seeded for CFA.
C: Comparison of survival of XPB mutated CHO cells treated in G1 and immediately seed for CFA with those treated and held in G1 for 24 hours prior to seeding for CFA.

Data points represent mean + SEM, n=3.

Similarly, assessment of XPD mutant cells with clonogenic assays confirms that XPD mutated cells are more sensitive to HN2 than WT cells when treated in G1 and held for 24 hours or treated and immediately used for clonogenic experiments (Figure 3.25 A and B). The sensitivity of XPD mutated cells compared to WT cells appeared more marked in G1 treated and held cells particularly at higher doses of HN2. Figure 3.25 A demonstrates when treated with 10μM HN2 survival of XPD G1 treated and held cells is approximately 1% compared to 23% in WT cells. This suggests that as illustrated in previous experiments in this thesis chapter XPD may play a role in G1 ICL repair.

Despite this marked difference in survival compared to WT cells when XPD mutated cells are compared in the two experimental states (Figure 3.25) there does not appear to be any significant difference in sensitivity between cells treated and held in G1 compared to cells treated and immediately seeded to clonogenic assay. This apparent lack of variation in sensitivity might imply that whilst XPD plays a role in ICL repair in both G1 and cycling cells this role does not take precedence in a particular part of the cell cycle.

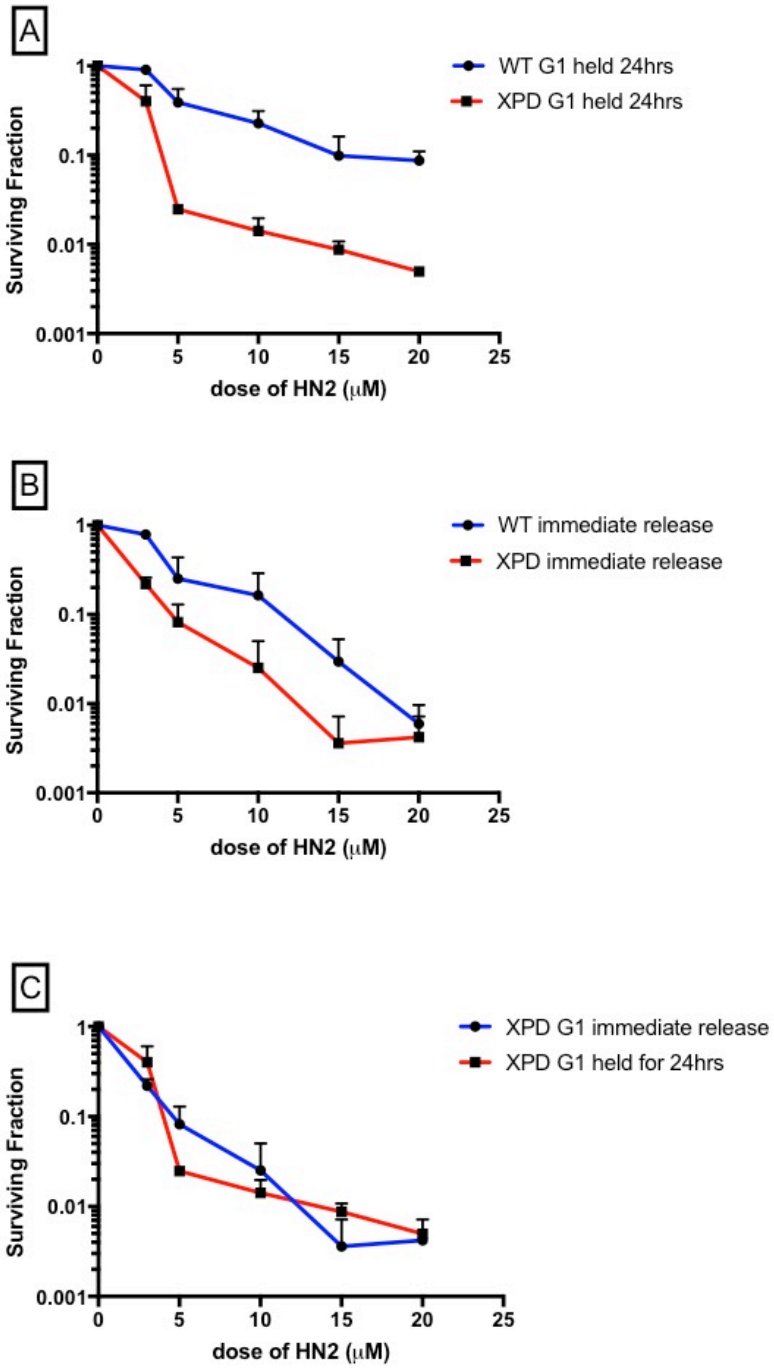



**Figure 3.25: Survival of XPD mutant cells following treatment in G1.**

XPD mutant CHO cells were synchronised to G1 by isoleucine starvation and then treated with HN2. Following treatment cells were either trypsinised and counted immediately, or left to incubate for a further 24 hours in G1, prior to seeding for clonogenic assays.

A: Comparison of survival of WT and XPD mutated CHO cells treated in G1 and held in G1 for 24 hours prior to seeding for CFA.
B: Comparison of survival of WT and XPD mutated CHO cells treated in G1 and immediately seeded for CFA.
C: Comparison of survival of XPD mutated CHO cells treated in G1 and immediately seed for CFA with those treated and held in G1 for 24 hours prior to seeding for CFA

Data points represent mean + SEM, n=3.

## 3.6 Conclusions

In this chapter a successful experimental model was created for the analysis of ICL repair in G1 using CHO cells and isoleucine starvation. The use of isoleucine starvation as a technique for G1 synchronisation is advantageous compared to other methods such as chemical blockade as it more closely mirrors the non-dividing and terminally differentiated cells that may be present physiologically. Chemical blockade with compounds such as thymidine, aphidicolin or hydroxyurea would have been inferior in this model as these techniques result in cell cycle blockage at the G1/S-phase (Rosner et al., 2013) checkpoint making accurate assessment of the role of damage repair factors imprecise. These chemicals also induce DNA damage and genetic instability, which may potentially alter results. Isoleucine starvation offers the advantage that the G1 blockade is easily and quickly reversible by addition of isoleucine containing media and once reversed allows the study of cells as they move in synchrony through the cell cycle. This was clearly illustrated in the initial experiments in this chapter that demonstrated precise synchronisation and achieved accurate estimation of the time to reach early S-phase (Figure 3.1).

Further experiments to assess the effects of ICL on cell cycle dynamics were performed with two different compounds: HN1 and HN2. These drugs were specifically selected, as there has long been debate as to the identity of the major toxic lesion caused by ICL agents. It is well known that ICL-inducing drugs cause a variety of other DNA lesions such as monoadducts, DNA protein crosslinks and intra-strand crosslinks. In particular, ICL comprise only approximately 5% of the

DNA damage caused by cisplatin (Eastman, 1986) and approximately 5-10% of lesions caused by MMC and HN2 (Gargiulo et al., 1995).

Since HN1 forms only monoadducts whereas, HN2 forms monoadducts and a small minority of ICLs, it was possible to easily compare the toxicity of the lesions induced by both drugs. It is clear that even when comparing a dose of HN1 ten times that of HN2 the major toxic effects appear to be due to the small minority of ICL formed by HN2 since this causes major cell cycle stalling (Figure 3.2, Figure 3.3, Figure 3.4, Figure 3.6).

Initial experiments in asynchronous and S-phase synchronised cells demonstrate marked stalling following treatment with HN2, with cells persisting in late S-phase for at least 8 hours. These findings are in keeping with previous studies in CHO cells (Osawa et al., 2011) and are expected as the presence of multiple ICL requires repair, delaying cycling through S-phase. HN1 forms monoadducts, not ICLs, and these should be easily repaired in S-phase, primarily through base excision repair, explaining the absence of any marked cell cycle delay in this population.

Previous studies used higher doses of HN2, which resulted in a more prolonged and marked delay in cell cycle progression, but as it was the intention of this study to use mutant CHO cell lines for further experiments, and these are known to be more sensitive to HN2 (De Silva et al., 2000), the dose of 5μM was selected as suitable for further experiments following careful optimisation (results not shown).

Experiments performed in WT CHO cells synchronised to G1 show that cells treated with HN2 and immediately released to cell cycle still show stalling in late

S/G2 (Figure 3.4) This confirms that HN2 can form ICL in G1 cells and this is corroborated by the modified Comet assays which also show decreased tail moment, and therefore increased numbers of ICL, with increasing dose of H2 in G1 cells. This is not unexpected, as many ICL form through natural endogenous or exogenous sources (Stone et al., 2008; Brooks and Theruvathu, 2005) and G1 repair of these lesions would be necessary in non-dividing cells.

The key finding in this chapter is the examination of CHO cells treated in G1 and held for increasing time periods prior to release. Figure 3.5 demonstrates that WT CHO cells treated in G1 and held for 12 hours in G1 post treatment continue to show cell cycle stalling. When the period of incubation in G1 post treatment is increased to 24 hours it is clear from Figure 3.6 that this stalling is abolished. Since previous experiments have verified that ICL can be formed in G1 it can be inferred that any ICL formed must have resolved. It could be argued that cells that contain ICL have undergone apoptosis and cell death but this is disproven by simple live/dead staining which does not show large population of dead cells after HN2 treatment. The dose of HN2 was also carefully optimised in asynchronous cells, to select a dose that caused stalling but allowed for recovery within 48 hours so that cell dynamics could be accurately followed and avoid large amounts of cell death. This allows the conclusion that ICL are formed in G1 CHO cells and these can be resolved in 24 hours.

With this established model, further experiments were performed using stable DNA damage mutant CHO cells. CSB and XPG mutant CHO cell lines showed similar results to WT CHO cells (Figure 3.8) with complete loss of stalling following

treatment in G1 and incubation in G1 for a further 24 hours suggesting that these DNA damage factors are not essential to G1 repair.

Further analysis of the mutated cell lines XPF, XPB and XPD (Figure 3.8) showed persistent cell cycle stalling following treatment in G1 and continued incubation in G1 for 24 hours. This was most marked in XPF mutated cells in which persistent stalling continued until 48 hours. Cell lines mutated for XPB and XPD also showed stalling after treatment in G1, incubation for a further 24 hours in G1 and release to cell cycle. This suggests that XPF, XPB and XPD may play a role in G1 repair.

To assess the role of the nucleases SNM1A, FAN1 and EXO1, siRNA knockdown was performed and knock down cells treated in G1 and incubated in G1 for 24 hours prior to release. FAN1 siRNA KD CHO cells displayed similar cell cycle dynamics as WT CHO cells suggesting that FAN1 is unlikely to play a role in G1 repair. SNM1A siRNA KD cells, however, exhibited marked stalling in cell cycle. Results with EXO1 KD siRNA were difficult to interpret, as EXO siRNA KD was poor at only approximately 50%. It appeared that EXO siRNA KD cells showed a trend towards delayed cell cycle progression.

These findings were confirmed with comet assays. These verified that ICL can be formed in a dose dependent fashion in G1 cells (Figure 3.18) and that in WT CHO cells these ICL undergo unhooking within 24 hours (Figure 3.19). Further comet assays confirmed that ICL unhooking is reduced in XPF, XPB and XPD mutated cells in G1 and SNM1A siRNA KD CHO cells also have decreased unhooking. The comet assay results appear to support the earlier flow cytometry findings. Further comet assays were attempted with EXO1 siRNA KD CHO cells but effective knock down of EXO1 was difficult to achieve. Increasing EXO1 siRNA concentration to achieve

better knockdown resulted in large amounts of cell death and it was not possible to achieve knockdown in a suitable number of cells that could then be used for G1 synchronisation and drug treatment.

Finally, modified clonogenic experiments were performed to assess CHO cell survival after treatment in G1 (Figure 3.22, Figure 3.23, Figure 3.24, Figure 3.25). Colony formation assays (CFA) are the gold standard method to assess the replicative ability of a single cell (Franken et al., 2006). CFA are usually performed in asynchronous cells but in this experimental work the replicative potential of cells after treatment in G1 was of importance. The standard CFA protocol was adapted so that CHO cells could be seeded and synchronised to G1, as in previous experiments, and treated with HN2 for 1 hour, following which cells were either lifted and counted and used for CFA or left to incubate for a further 24 hours in G1 and then similarly lifted, counted and used for CFA. Previous flow cytometry experiments have shown there is little, if any, cell death in the 24 hours CHO cells are kept incubated in G1 so it would be appropriate to assume that if similar cell numbers are seeded to CFA they should have no difference in replicative potential.

All CFA showed that survival was decreased in CHO cells used immediately for CFA after treatment in G1 compared to those left to repair in G1 for 24 hours and then used for CFA. This decreased survival may reflect that ICL are more toxic in replicating cells and that the stalling of the replication fork associated with detection of ICL is more likely to lead to apoptosis, cell death and therefore decreased colony formation. This finding is important clinically as it corroborates the cancer stem cell theory that a small population of tumour cells are quiescent and it is these cells that are resistant to chemotherapy and potentially responsible

for recurrence and metastatic disease. Targeting of these cells, which potentially do acquire ICL lesions but are able to repair them, would be of clinical importance to improve chemotherapeutic regimes.

The aim of performing the CFA was to try to elucidate which DNA factors were most important to G1 repair and also confirm findings from comet assays and flow cytometry. Survival in mutated XPF, XPD and XPB CHO cells was decreased compared to WT CHO cells in both states suggesting that these DNA Damage factors play a role in both G1 and replication based ICL repair. It is difficult to ascertain from these CFA if any of these factors have a more important role in a particular pathway. It is interesting to note that whilst survival in XPF mutated cells was markedly decreased compared to WT cells in both states, when survival is compared within the cell line, XPF mutated cells treated in G1 and held in G1 for 24 hours seem much less sensitive to HN2 suggesting the role of XPF is more essential to replicative ICL repair. Comparatively, whilst survival of XPD mutated cells compared to WT was decreased in both states, comparison of XPD mutated cells does not show any particular difference between sensitivity after treatment in G1 and further incubation in G1 or immediate use in CFA suggesting that XPD plays an equally important role in both repair in G1 or in replicating cells.

# Chapter 4 - Results: A large-scale siRNA screen to identify cisplatin and radiation sensitising genes.

## 4.1 Introduction

The aim of this chapter was to perform a high-throughput siRNA screen in a lung cancer cell line. Our laboratory recently demonstrated that the gold standard colony formation assay (CFA) can be adapted to a 96-well format for use in a high-throughput screen to identify potential irradiation sensitisers (Tiwana et al., 2015). The CFA is able to assess cellular potential for replication after treatments that cause cell death or permanent cell cycle arrest. This is advantageous in comparison to other assays, such as Resazurin (Anoopkumar-Dukie et al., 2005) or 3-(4,5-Dimethylthiazol-2yl)-2,5-diphenol tetrazolium bromide (MTT) assays (Mosmann, 1983), which are only able to assess cellular viability. Whilst the CFA was initially developed to assess the survival of cells following irradiation, it is commonly used to assess the effects of chemotherapeutic agents, such as cisplatin and etoposide, and anti-angiogenic agents (Munshi et al., 2005).

Lung cancer is currently the leading cause of cancer death in the UK (Statistical Bulletin, 2016). Many patients are diagnosed at an advanced disease stage and cannot receive curative surgery. These patients, with advanced disease, are commonly managed with chemotherapy and radiotherapy treatments. There has been a rapid expansion in the chemotherapy options available for lung cancer patients with recent development of therapies for specific tumour mutations such as epidermal growth factor receptor (EGFR) (Mok et al., 2009) and echinoderm microtubule-associated protein-like 4-anaplastic lymphoma kinase (EML4-ALK) fusion gene mutations (Shaw et al., 2013). Despite these new therapies many

patients develop recurrent disease and the main therapy for these patients with relapsed disease, and for the 70% of patients (El-Telbany and Ma, 2012) who do not have a specific mutation present in their tumour, is cisplatin or carboplatin.

Radiotherapy also has an increasing role in treatment with the advent of stereotactic ablative radiotherapy (SABR), which allows patients with other co-morbid diseases that may preclude them from curative surgery to receive high-dose precise radiotherapy treatment (Lagerwaard et al.).

Identifying potential targets that sensitise lung cancer cells to cisplatin or radiotherapy could dramatically improve treatment outcomes and potentially allow dose reduction of these therapies reducing toxic side effects.

Our laboratory had successfully identified TPK1, as a potential target for radiosensitisation, through a large scale siRNA screen in HeLa cells (Tiwana et al., 2015). It was the goal of this chapter to adapt this screening protocol to perform tandem screens for radiation sensitisation and cisplatin chemosensitisation in a lung cancer line with emphasis on gene targets associated with DNA damage repair.

A commercially available siRNA library (Qiagen) was used, which contained 640 siRNAs directed against genes proposed to play a role in DNA repair. The proposed screening procedure consisted of a transfection step with the library siRNAs followed by a trypsinisation and re-plating procedure for the colony formation assay three days later, at which stage each transfection well was split into 4 wells for each of three treatment arms (untreated, irradiation, and cisplatin) (Figure 4.1). This ensured that cells in the different treatment arms were derived from the

same source well, reducing variability. In addition, optimised cell numbers could be used for both the transfection step, which requires relatively high cell numbers, and the colony formation step, which requires low cell number plating.

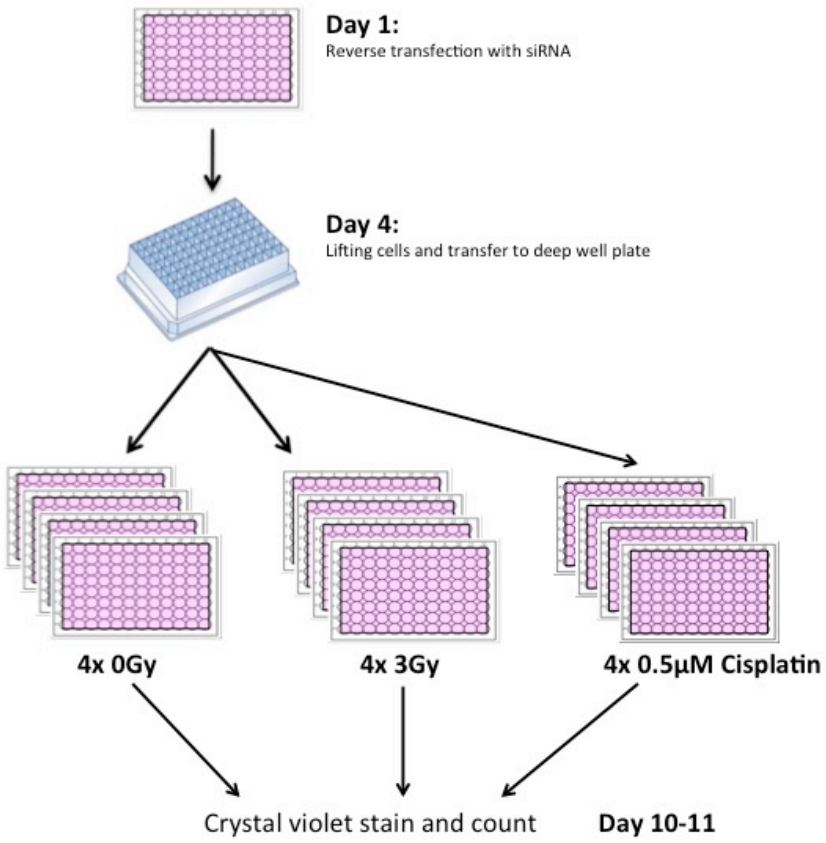



**Figure 4.1: Screening protocol for primary and secondary screens using 96-well colony formation assay**

Day 1: Cells (4000/well) were transfected by reverse transfection with final siRNA concentration 20nM and final concentration INTERFERin 0.05%.

Day 4: Transfected adherent cells were disassociated by trypsinisation and counted before transfer to 96-deep well plate. Cells were then transferred to untreated plates (0Gy, 400 cells/well), irradiated (3Gy, 1500 cells/well) and cisplatin treated (0.5µM cisplatin, 750 cells/well).

Day 10 or 11: Plates were stained with crystal violet and counted.

In order to assess the transfection efficiency of the screen, and allow calculation of Z-factors to assess assay reproducibility, a number of control wells were included. These were placed around the edges of the plates as illustrated in Figure 2.1. The controls included siRNA for PLK-1, suppression of which causes widespread cell death and so this was used as a control for transfection. siRNA for ATR and DNA-PK*cs* were included to allow assessment of chemosensitisation and radiosensitisation respectively. A non-transfecting (NT) was also included.

## 4.2 Results

### 4.2.1 Large scale primary siRNA screen

#### 4.2.1.1 Initial optimisation of siRNA screen conditions

Initial optimisation work was carried out to identify a suitable lung cancer cell line for use in 96-well format. It was essential that the cell line used for the screen be able to form defined, tight, countable colonies to enable automated counting.

Two cell lines were identified as suitable, the H460 and H520 lung cancer cell lines. H460 is a large cell lung cancer line with wild-type p53 and H520 is a p53 mutant squamous cell lung cancer line. Initial plans to use both cell lines in two simultaneous screens were abandoned due to difficulties with transfection efficiency in H520 cells and the cell line's slow doubling time. Further optimisation was performed with H460 cell line only.

The H460 cell line was used for two parallel large-scale siRNA screens in the laboratory. One screen focussed on the suppression of kinases to identify possible druggable targets to increase lung cancer cell sensitivity to radiation and cisplatin and the second screen, as detailed in this thesis, concentrated on the identification

of druggable targets related to the DNA damage repair response. Conditions that had been optimised for the kinome screen were used in the parallel DNA damage response screen.

Following assessment of cell lines for suitability in 96-well colony formation assay (CFA), cell seeding densities and treatment doses of irradiation and cisplatin were optimised to ensure formation of suitably sized and numerous colonies that would allow accurate assessment of colony survival.

#### 4.2.1.2 Optimisation of siRNA transfection conditions

In the initial siRNA transfection step, INTERFERin-HTS (Polyplus, France) was selected for use as a transfection reagent to allow transfection with the lowest possible concentration of siRNA with reduced cell toxicity. Previous studies have shown that increasing concentrations of siRNA are associated with higher incidence of off-target effects (Caffrey et al., 2011).

To achieve optimum transfection, two conditions were compared, a transfection reagent concentration of 0.075% or 0.05% diluted in water or OptiMEM. Transfection induced toxicity was assessed by comparing the viability of untransfected cells with that of cells transfected with non-targeting (NT) siRNA. Transfection efficiency was assessed using PLK1 siRNA, which when transfected successfully causes cell death due to mitosis inhibition. Figure 4.2 A and Figure 4.2 B demonstrates that diluting INTERFERin-HTS in water resulted in increased cell viability. Furthermore, reducing INTERFERin-HTS concentration to 0.05% also improved cell viability (Figure 4.2 C and D), without impairing the transfection efficiency of PLK1 siRNA.

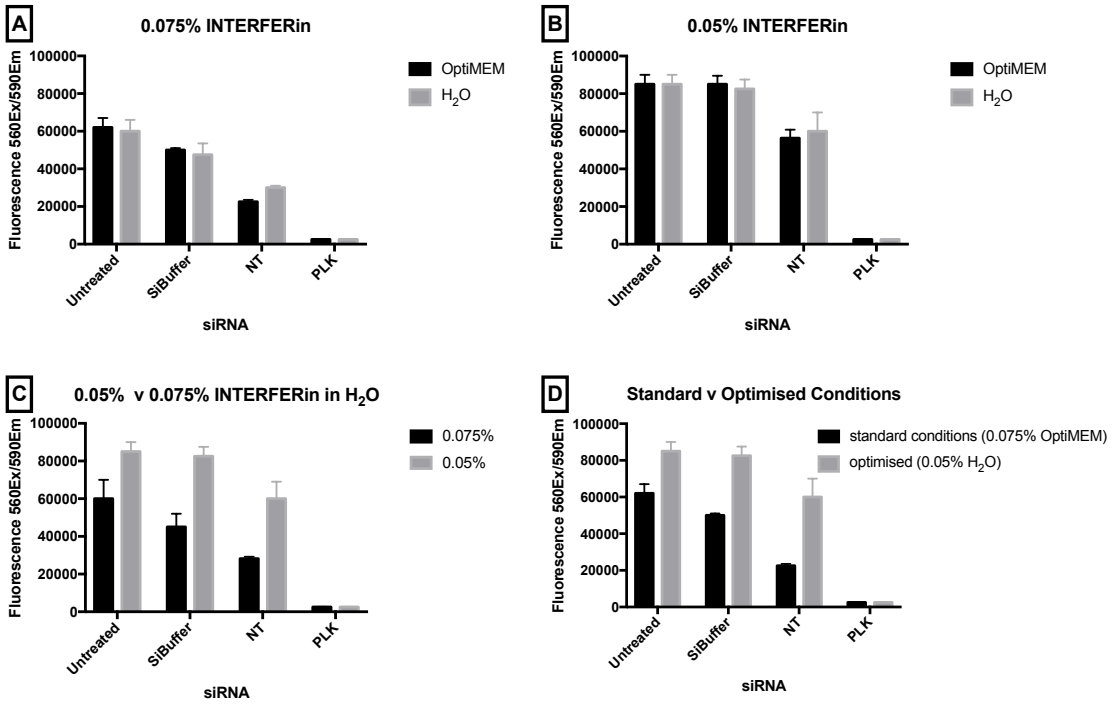



**Figure 4.2: Optimisation of transfection reagent concentrations**

A: Cell viability after transfection with INTERFERin-HTS final concentration per well 0.075% diluted in OptiMEM or water

B: Cell viability after transfection with INTERFERin-HTS final concentration per well 0.05% diluted in OptiMEM or water

C: Cell viability after transfection with INTERFERin-HTS final concentration per well 0.075% or 0.05% diluted in water

D: Cell viability after transfection with initial standard conditions and re-optimised conditions

Data represent the mean + SD, n=3.

To ensure these conditions were also suitable for siRNA transfection with control siRNAs, ATR and DNA-PKcs, qRT-PCR mRNA assessment of these two genes expression was performed after transfection. This demonstrated adequate genetic suppression that was comparable to the use of a higher concentration of transfection reagent (Figure 4.3).

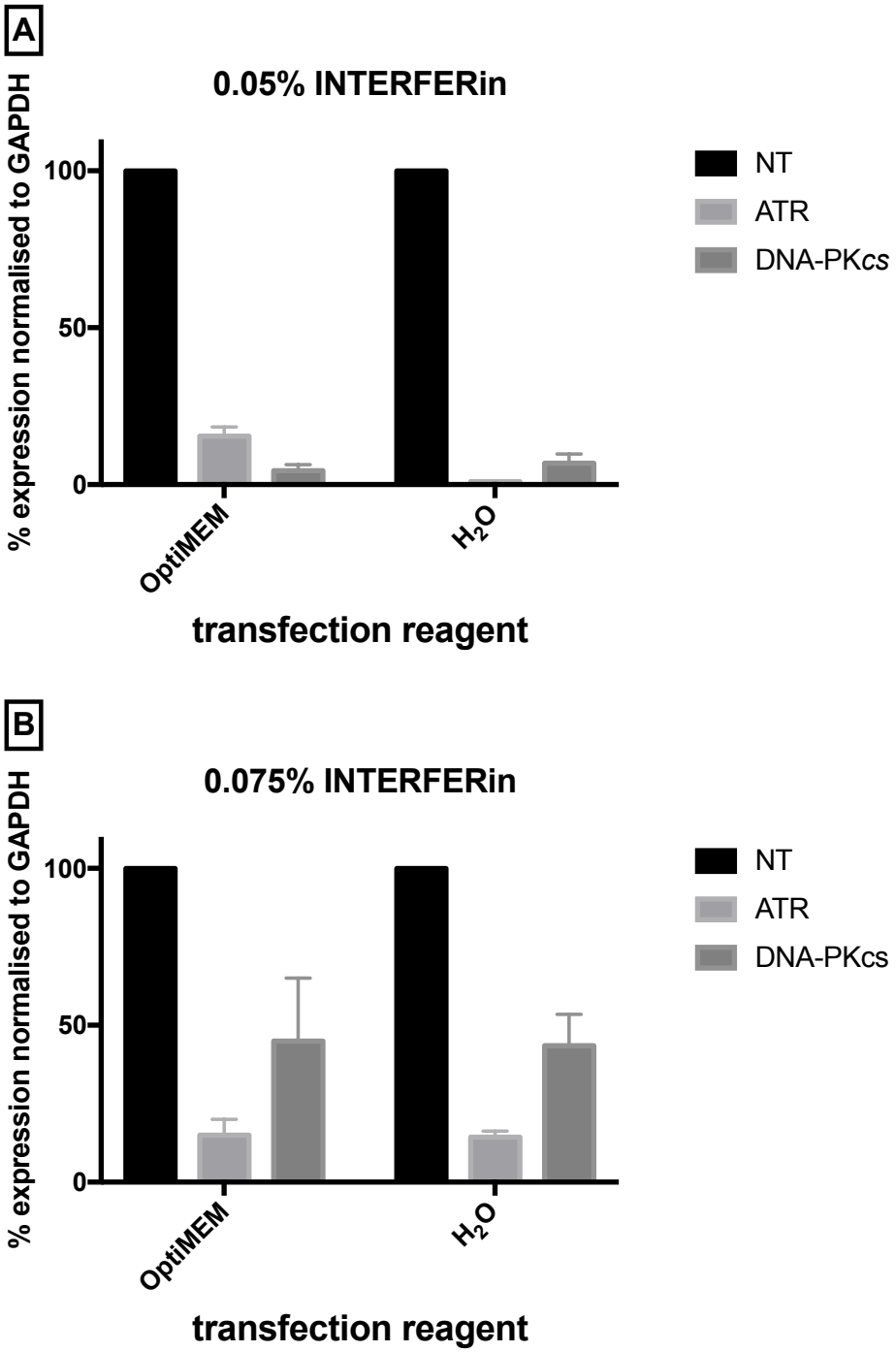



**Figure 4.3: qPCR analysis of optimisation of controls with 0.05% and 0.075% INTERFERin**

A: qPCR analysis of ATR and DNA-PK*cs* knockdown with 0.05% INTERFERin normalised to GAPDH

B: qPCR analysis of ATR and DNA-PK*cs* knockdown with 0.075% INTERFERin normalised to GAPDH

Data represent mean + SD, n=3.

#### 4.2.1.3 Z-factor testing of optimal conditions

High-throughput screens compare the effect of suppression of hundreds of genes to standard positive and negative controls. This is time consuming and expensive, therefore small pilot screens are performed to assess the quality of the assay through the negative and positive controls. This allows assessment of statistical size effect through calculation of a Z-factor (Zhang et al., 1999) (Figure 2.2 D). The positive controls for this screen were siRNAs against DNA-PKcs, known to cause radiosensitisation, and ATR siRNA, which sensitises to cisplatin. PLK-1 was included to assess transfection efficiency after 72h using a resazurin based viability assay.

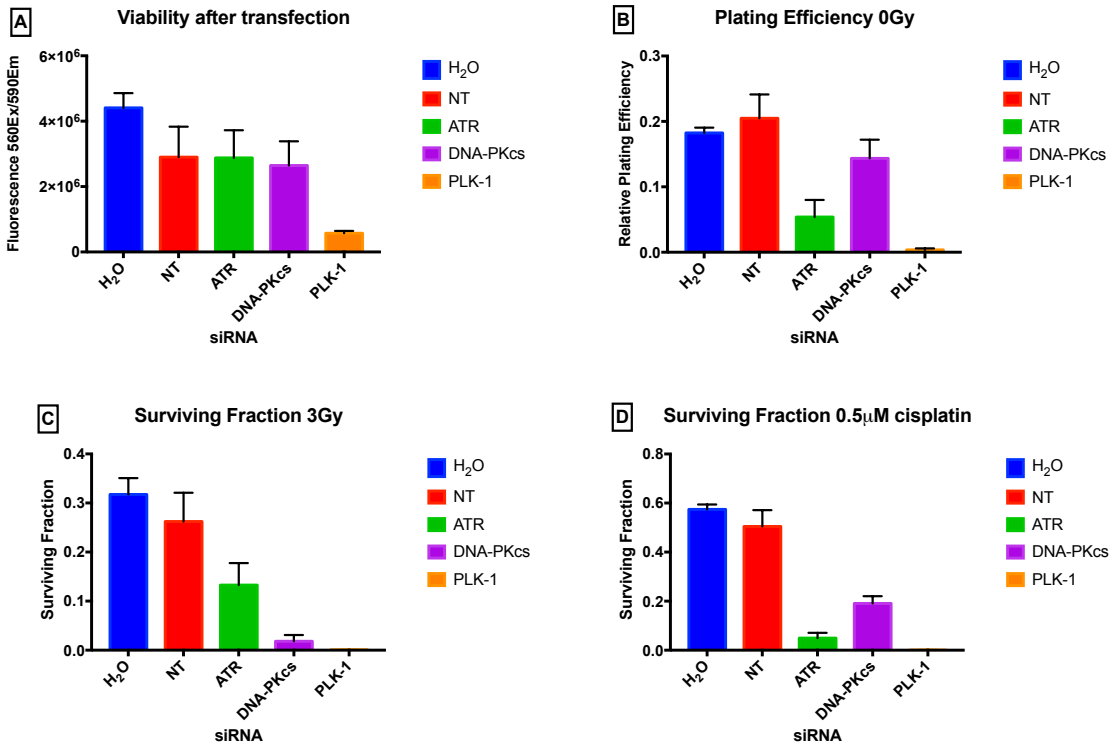
In order to assess the viability of the optimised transfection conditions a small pilot "Z-factor test" was performed using the Janus liquid handling robot and the high-throughput screen protocol (Figure 4.1), to ensure the manually performed experiments were reproducible.

Experiments were performed using the protocol detailed in Sections 2.4.2 to 2.4.6 with the exception that only control siRNAs (PLK-1, ATR, DNA-PK*cs*) were included on the plates. Cells were reverse transfected with INTERFERin-HTS 0.05% and 20nM siRNA in 96 well plates and left to incubate for 72 hours at 37°C. Prior to trypsinisation and splitting, at 72 hours, cell viability was again assessed with Resazurin (Figure 4.4 A). In this assay, cell viability appeared uniform across the control siRNAs. PLK-1 showed significantly decreased viability suggesting adequate transfection had taken place.

At 72 hours following transfection cells were split into triplicate plates for treatment (3Gy radiation, 0.5μM or untreated) and CFA were performed. Figure 4.4 B demonstrates that the PE of NT transfected wells was 20% (± 0.03%) and this was similar to control wells that used water rather than siRNA in transfection reactions suggesting an absence of siRNA toxicity. The mean SF after treatment with 0.5μM cisplatin was 50% (± 0.06%) for NT siRNA and the mean SF for ATR siRNA was 5% (± 2%) (Figure 4.4 D) this resulted in a Z-factor of 0.41. Following irradiation at 3Gy the SF for NT siRNA was 26% (± 5%) and the SF of DNA-PK*cs* was 2% (± 1%) (Figure 4.4 C) resulting in a calculated Z-factor score of 0.12.

Z-factor results range from 0 and 1, with 1 representing an ideal screen that has no standard deviation between replicates. A Z-factor between 0.5 and 1.0 is considered in biochemical assays to represent a screen with good range between positive and negative controls (Poe et al., 2014) but screens performed with cells often have Z-factors between 0 and 0.5 (Iversen et al., 2006).

The Z-factors results from these experiments are variable and sub-standard in the radiation optimisation screen. Whilst these are encouraging, further confirmation of Z-factor scores would be necessary in the primary screens to assess adequate reproducible differentiation between positive and negative controls.




## Figure 4.4: Z-factor test of final conditions for large-scale siRNA screen.

A: H460 cells were reverse transfected in 96-well plates with a final concentration 20nM siRNA and 0.05% INTERFERin. After 72 hours incubation, cell viability was assessed following 1-hour incubation with Resazurin substrate. Data points represent mean ± SD from quadruplicate repeats.

96-well colony formation assays were conducted. 72 hours after transfection cells were lifted by trypsination and seeded to 96-well plates for the appropriate treatment. Following treatment cells were incubated for 6 days prior to staining with crystal violet and colonies counted with GelCount colony counter.

B: Plating efficiencies in untreated plates.

C and D: Surviving fraction of cells following 3Gy irradiation or treatment with 0.5μM cisplatin respectively.

Data points represent mean and ± SD from quadruplicate repeats.

#### 4.2.1.4 Results from primary DNA damage siRNA screen

Having achieved successful optimisation of conditions, the assay was used to perform a primary screen of a 640-gene siRNA DNA damage library. The screen was performed twice (replicate A and replicate B) and within each screen each transfection plate was lifted in quadruplicate for each condition.

The screen was performed as detailed in Sections 2.4.2 to 2.4.5. Briefly, on day 1 the library plates were used to perform reverse transfection with H460 cells to a final siRNA concentration of 20nM and with 0.05% INTERFERin-HTS. Following incubation for 72 hours, on day 4, adherent cells were dissociated with trypsin and control wells were counted and the appropriate number of cells transferred to 96-deep well plates. Cells were transferred from deep well plates to 96-well flat bottom plates in quadruplicate for each treatment condition- untreated (400 cells/well), 0.5μM cisplatin (750 cells/well) and 3Gy irradiation (1500 cells/well). Following treatment plates were left to incubate for 6 to 7 days and on day 10 or 11 they were stained with crystal violet and counted (Figure 4.1).

Prior to trypsination, cell viability was assessed using Resuzarin. The assay suggested adequate transfection, reflected by decreased viability in transfection control PLK-1 wells. Cell viability appeared to be adequate and uniform in all other control wells (Figure 4.5).

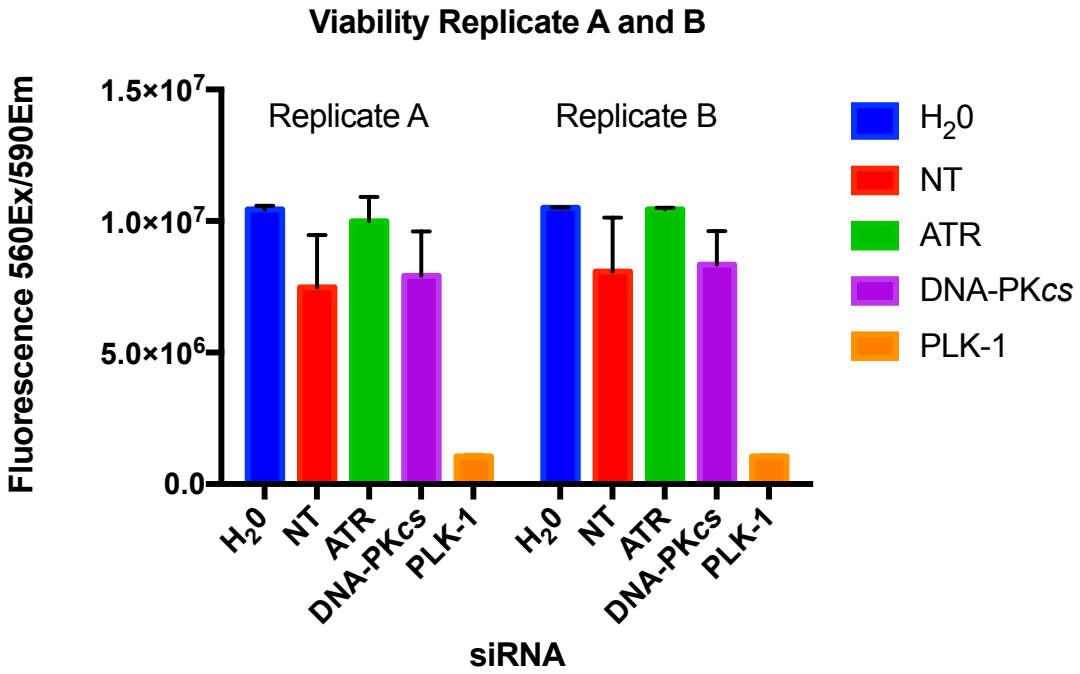



**Figure 4.5: Cell viability of screen control wells 72 hours after transfection.**

H460 cells were transfected with the 640-gene siRNA library in 96-well plates in two repeats (replicate A & B). 72 hours after transfection viability of the control wells was assessed by incubation with Resazurin for 1 hour. Values are the mean ± SD from 4 replicate plates.

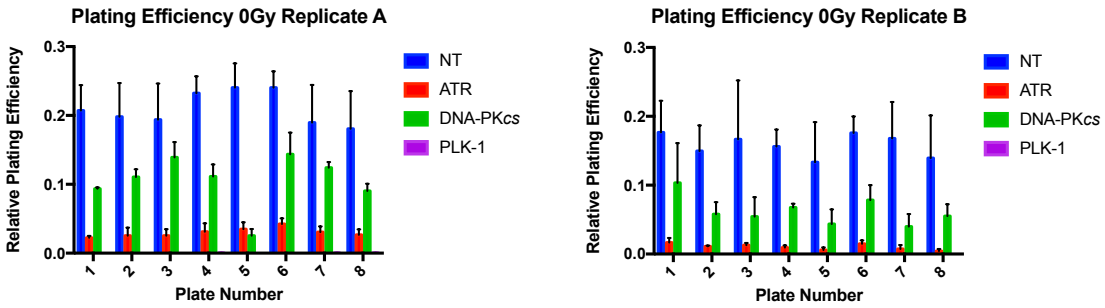
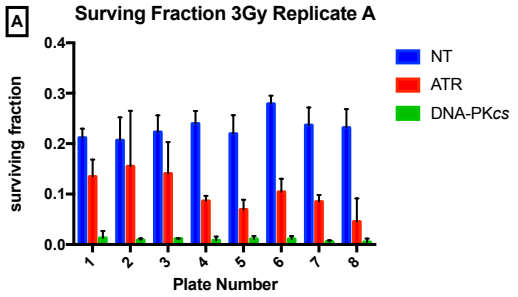



**Figure 4.6: Plating efficiencies for control wells in the siRNA screen.**

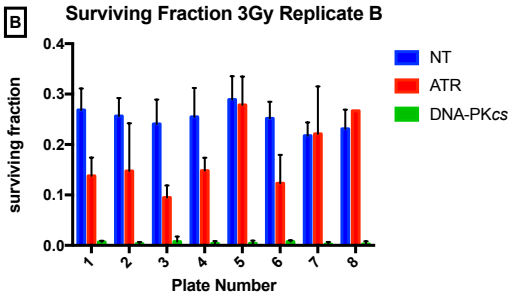
Plating efficiencies in 96-well CFA of H460 cells transfected with the 640-gene (8 plates) siRNA library in 96-well plates in two repeats (replicate A & B) and re-plated 72h later for colony formation. Values for each library plate are mean ± SD from 4 replicate plates.

Following staining and colony counting, the individual plating efficiencies (PE) for each plate were calculated and each replicate is shown in Figure 4.6. The mean PE for NT siRNA treated wells was 21% (± 2.3%) for replicate A and 15.8% (± 1.6%) for replicate B. Following treatment with 3Gy irradiation the SF of NT siRNA wells was on average 23% (± 2.2%) for replicate A and 25% (± 2.2%) for replicate B (Figure 4.7). The mean SF of the positive control DNA-PK*cs* siRNA wells was 0.9% (± 0.28%) in replicate A and 0.4% (± 0.2%) in replicate B (Figure 4.7). Individual Z-Factors were calculated for each plate in each replicate and these are shown in Figure 4.7. These ranged from 0.24 to 0.97 for the irradiated plates in both replicates suggesting clear differentiation between positive and negative controls and a good quality assay.

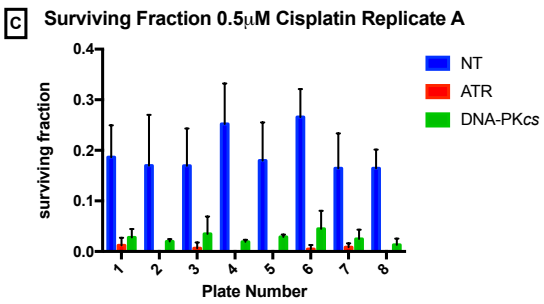
In the cisplatin arm of the screen average SF of NT siRNA in both replicates was lower than those obtained in the optimisation studies and the mean NT siRNA SF was 19.4% (± 4%) in replicate A and 16.3% (± 3%) in replicate B (Figure 4.7). Mean SF for the ATR siRNA positive control wells was 0.4% (± 0.47%) in replicate A and 1.4% (± 3.2%) in replicate B (Figure 4.7). Individual Z-Factors were calculated for each plate and these ranged from -7.18 to 0.26 (Figure 4.7). These suggest that in this assay the differentiation between the positive and negative controls was not consistent. It is likely that this is due to the lower SF of the NT siRNA controls and the higher standard deviations seen in these control wells.



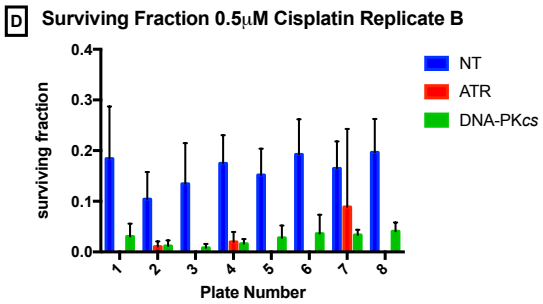

| Plate | Z Factor |
|---|---|
| 1 | 0.51 |
| 2 | 0.26 |
| 3 | 0.52 |
| 4 | 0.58 |
| 5 | 0.39 |
| 6 | 0.75 |
| 7 | 0.50 |
| 8 | 0.42 |




| Plate | Z Factor |
|---|---|
| 1 | 0.48 |
| 2 | 0.53 |
| 3 | 0.24 |
| 4 | 0.26 |
| 5 | 0.45 |
| 6 | 0.97 |
| 7 | 0.57 |
| 8 | 0.42 |




| Plate | Z Factor |
|---|---|
| 1 | -0.34 |
| 2 | -0.77 |
| 3 | -0.56 |
| 4 | 0.049 |
| 5 | -0.25 |
| 6 | 0.26 |
| 7 | -0.46 |
| 8 | 0.32 |




| Plate | Z Factor |
|---|---|
| 1 | -0.67 |
| 2 | -1.04 |
| 3 | -0.79 |
| 4 | -0.45 |
| 5 | -0.03 |
| 6 | -0.07 |
| 7 | -7.18 |
| 8 | -0.006 |

## Figure 4.7: Surviving fractions of control wells and Z-Factor results

H460 cells were transfected with the 640-gene (8 plates) siRNA library in 96-well plates and re-plated 72h later for colony formation after 3Gy or 0.5μM cisplatin treatment. SF values for each library plate and both screens are shown and are the mean and SD of quadruplicate repeat plates.

A and B: SF 3Gy treated control siRNA by plate in replicates A and B respectively.

C and D: SF 0.5μM cisplatin treated control siRNA by plate in replicates A and B respectively.

Standard scores, or simple Z-scores, are used to assess the number of standard deviations an observed data point is above or below the mean value of all data being measured. These are commonly used to analyse screen data and assess if suppression of a particular gene leads to significant difference. However, for large-scale siRNA screens a simple Z-score may be affected by plate-to-plate variation. It is therefore essential that normalisation of raw data to specific plate controls occurs to reduce this plate-to-plate variability and allow comparison between plates (Malo et al., 2006). Since siRNA screens, by their nature, may produce significant outlier data, such as strong positive or negative hits, these adversely affect the mean and standard deviation as used in standard Z-scores. Therefore by normalising the surviving fraction of the library well to the negative control wells on that plate and using more robust statistical methods such as the median and mean absolute deviation, a more accurate detection of outliers can be achieved (Birmingham et al., 2009).

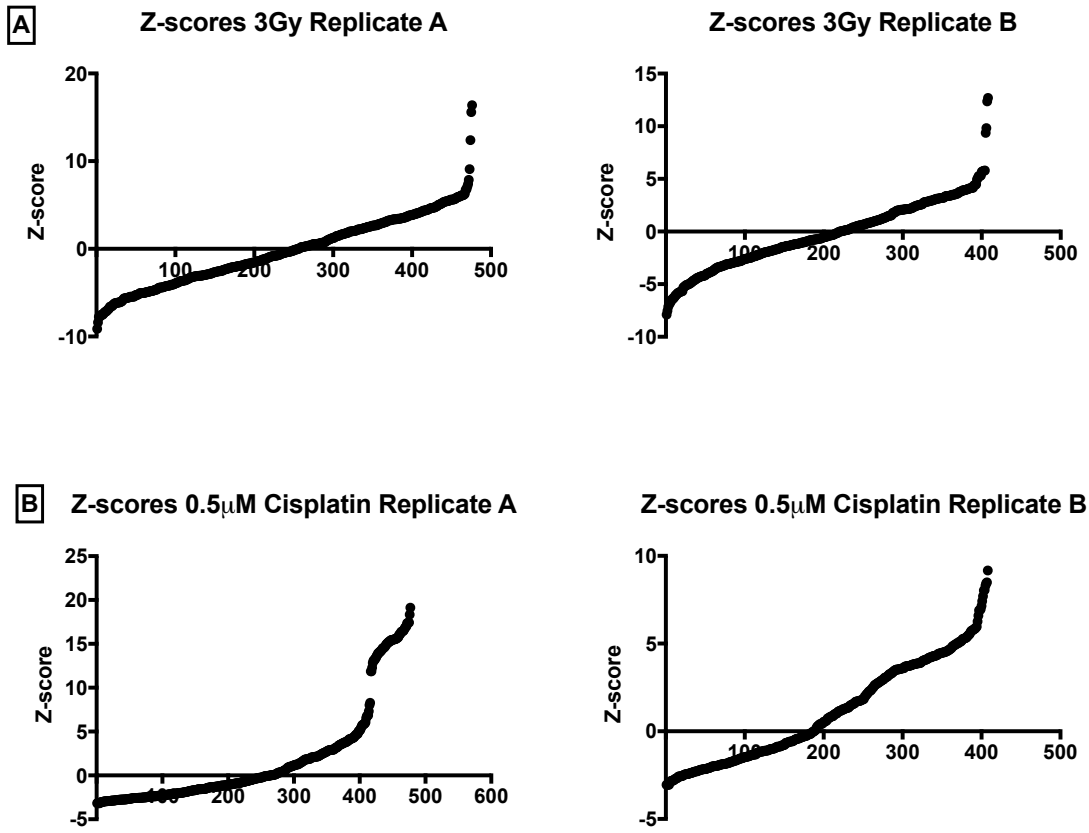
Robust Z-scores were calculated for each gene in each replicate (Figure 2.2) with negative Z-scores representing greater chemo or radiosensitisation compared to NT siRNA controls.

Figure 4.8 shows the Z-score distribution by treatment modality and replicate. Both treatment modalities and replicates showed evenly distributed Z-scores suggesting the siRNA library was not biased towards detection of chemo or radiosensitisers.

For each arm of the screen a co-efficient of determination ($R^2$) was calculated. This assesses inter-assay variability by comparing the Z-scores between the two replicates. Perfect correlation between replicates would result in an $R^2$ score of 1.

For both the radiation and the cisplatin treated arms the $R^2$ was 0.53 suggesting good correlation between replicates.

After calculating Z-scores, targets from the screen were ordered and a rank-product analysis performed by treatment modality to fully identify potential sensitising genes. At this point in the analysis, siRNAs that demonstrated a PE less than 4% were excluded from further analysis as it was deemed their Z-scores might be unreliable due to low colony numbers. Within the radiation arm, in both replicate A and B, DNA-PK*cs* ranked first as the most radiosensitising siRNA. ATM and several Rad51 paralogs that are known potential radiosensitisers also ranked in the 50 lowest Z-scores. In the cisplatin treated arm several Rad51 paralogs and members of the Fanconi anaemia complementation group (FANC), whose suppression is known to sensitise to DNA damaging agents, were ranked in the 50 lowest Z-scores. The presence of these sensitising genes confirms the validity of the screen.




## Figure 4.8: Z-score distributions from primary siRNA screen

Z-score distributions from primary screen replicate A and replicate B. Sensitising siRNA have Z-scores <0. Genes with PE <4% were excluded from the analysis.

A: Z-score distribution for radiation replicates.

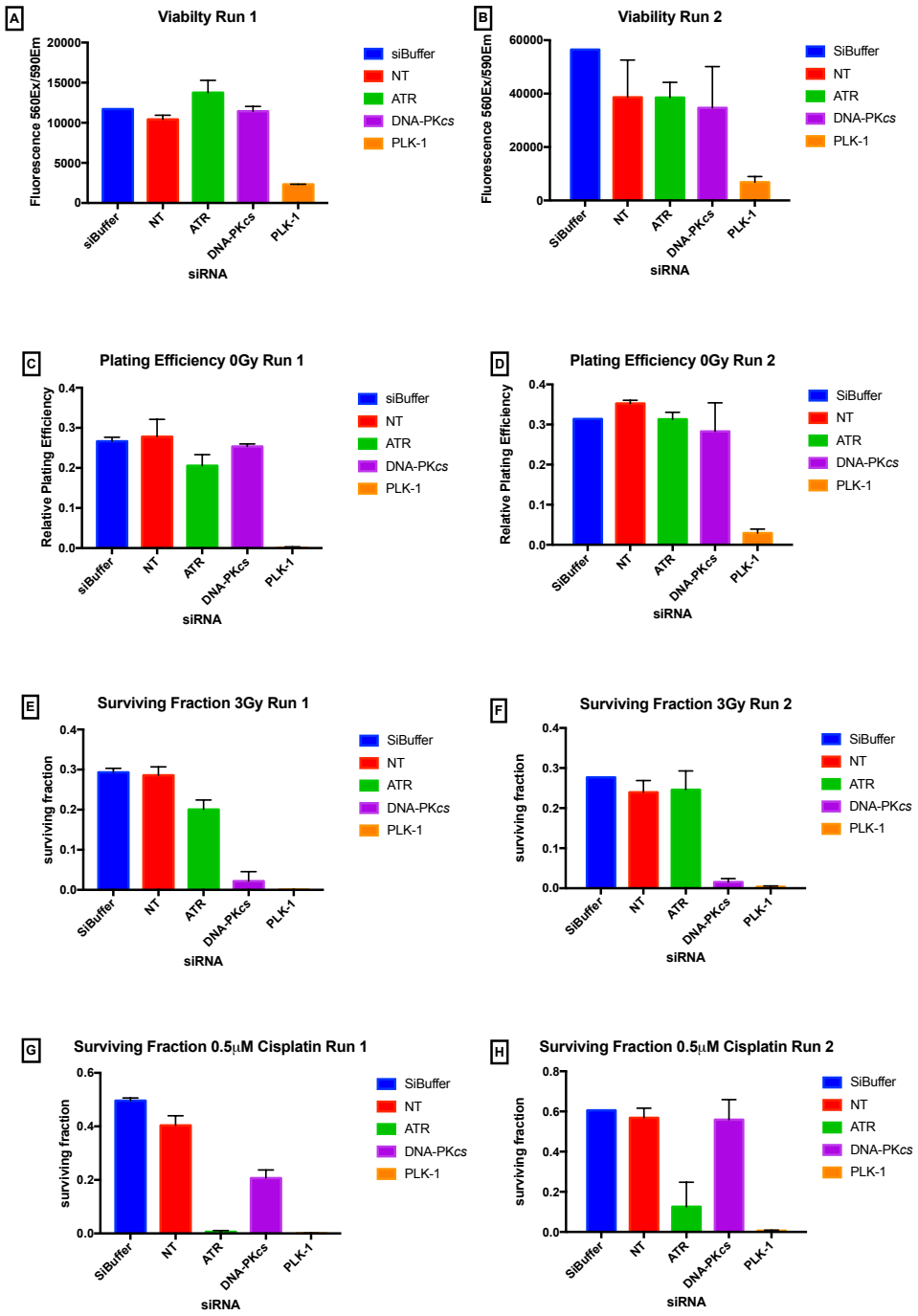
B: Z-score distribution for cisplatin treated replicates.

### 4.2.2 Secondary screen of 40 potential radiation and cisplatin sensitisers.

In order to narrow down the number of genes for further studies, a secondary screen was carried out using the 40 most promising targets. Potential targets for inclusion in a secondary screen were selected from the top 50 radio and chemosensitising siRNAs based on the gene's novelty as a potential radiation or chemotherapy sensitiser, the genes suitability for drug targeting and the availability of good quality antibodies to validate gene suppression in further experimentation. A list of 40 genes chosen to be included in the secondary screen is found in Table 5.1 within the Appendix.

To reduce the potential of false-positive results through off-target effects, the secondary screen siRNAs were obtained from a manufacturer different from that used in the primary screen (Dharmacon rather than Qiagen).

The secondary screen was performed twice (run 1 & 2) using the protocol from the primary screen (Section 2.4.2 to 2.4.6). Assessment of the control siRNA results confirmed that the screen was performed successfully (Figure 4.9). There appeared to be adequate transfection as assessed by viability results (Figure 4.9 A and B). The controls showed good plating efficiencies (Figure 4.9 C and D) and adequate suppression was seen with the controls in the treatment plates (Figure 4.9 E, F, G and H).




## Figure 4.9: Quality control parameters for secondary screen

H460 cells were transfected with the 40-gene secondary screen library using 20nM siRNA and 0.05% INTERFERin and re-plated for 96-well plate colony formation assays with 3Gy radiation or 0.5 μM cisplatin three days after transfection. Data points are the mean and SD of quadruplicate repeat plates.

A and B: Cell viability of control siRNAs wells at 72h after transfection.

C and D: Plating efficiencies of untreated control siRNA.

E and F: Surviving fractions of control siRNA following treatment with 3Gy irradiation.

G and H: Surviving fraction of control siRNA following treatment with 0.5μM cisplatin.

The Z-factors for the two repeats of the radiation arm were 0.74 and 0.49 suggesting good statistical differentiation between positive and negative controls. The Z-factors for the two repeats of the cisplatin arm were both 0.69. These parameters were better than those achieved for the primary screen; most likely this was caused by reduced toxicity in the non-targeting siRNA samples.

Z-scores were calculated as described before and Figure 4.10 demonstrates their distribution. It was expected that the Z-scores would exhibit a more negative distribution, because the genes in the secondary screen were specifically selected as potential radio or chemosensitisers based on the primary screen. However, this was not demonstrated and may be due to some selected targets representing false positive results due to off-target effects in the primary screen or false negative due to inefficient transfection for that particular siRNA. Each gene was also selected for it's potential chemosensitising or radiosensitising ability and therefore would not necessarily produce negative Z-scores in other treatment modalities.

The $R^2$ co-efficient for the radiation arm of the secondary screen was 0.71 suggesting minimal inter-assay variability between the two experimental replicates. The $R^2$ co-efficient comparing the cisplatin treated replicates was 0.12 suggesting the variability between these two replicates was much higher. The cause for this is not clear and may represent variable transfection between the two replicates.

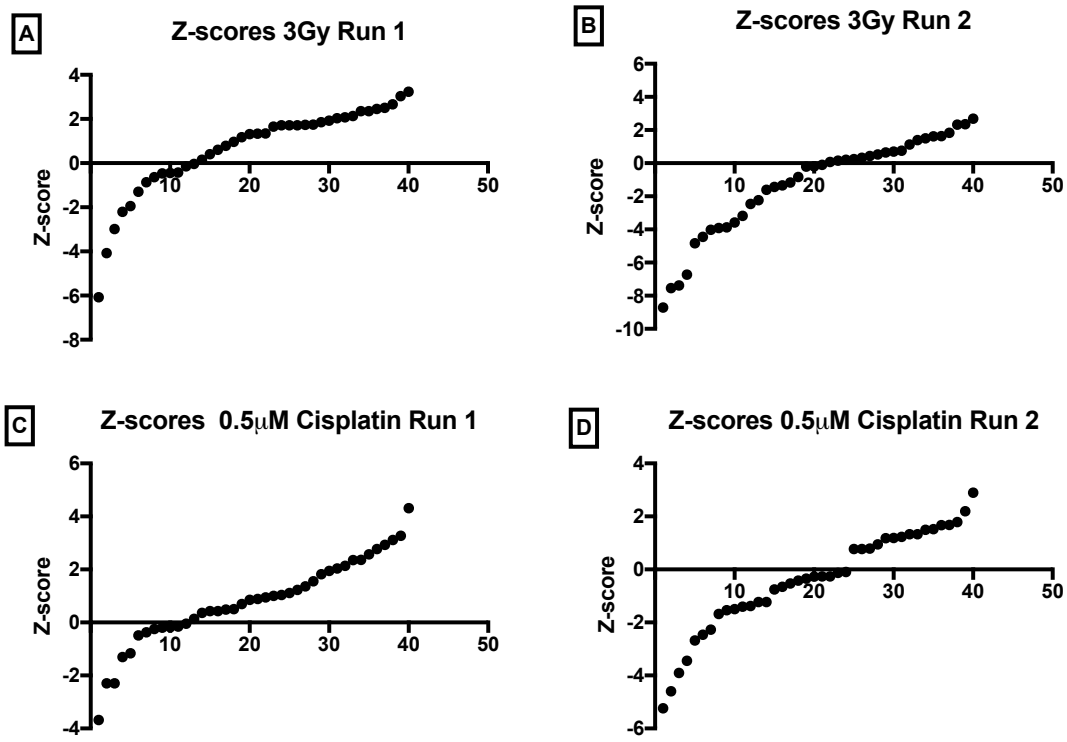



**Figure 4.10: Z-scores for secondary screen genes.**

Following staining and counting Z-scores were calculated for each gene. A Z-score <0 suggests a sensitiser.

A and B: Z-scores for 3Gy irradiated genes.

C and D: Z-scores for 0.5μM cisplatin treated genes.

### 4.2.3 Confirmation of sensitising genes with further colony survival assays.

Z-scores from the secondary screen were ordered by rank-product. Those targets that ranked in the top 20 of all genes were considered for further analysis. Selection for further study was assessed on the basis of the target's novelty as a potential sensitiser, suitability as a drug target, differential expression in tumour cells compared to normal tissue (Rhodes et al., 2007) and the availability of antibodies to enable further studies. Eight genes were selected for further assessment as potential radiation or cisplatin sensitisers (Table 4.1). To validate these targets, siRNA was obtained from a third vendor (Ambion) and CFAs after gene knockdown were performed in 6-well format as detailed in Section 2.5.1 and 2.6.1.

| siRNA | Selected condition | Z-score cisplatin Run 1 | Z –score cisplatin Run 2 | Z-score radiation Run1 | Z-score radiation Run 2 |
|---|---|---|---|---|---|
| **DCLRE1C** | Radiosensitiser | 2.93 | 1.94 | -1.14 | -2.23 |
| **CHD4** | Chemo/Radiosensitiser | -1.81 | -1.41 | -1.86 | -4.8 |
| **CHD5** | Chemo/Radiosensitiser | -1.00 | -1.37 | -0.32 | -3.91 |
| **KDM2B** | Radiosensitiser | 1.22 | 1.18 | -0.63 | -3.88 |
| **LIG1** | Chemosensitiser | -2.30 | -3.44 | 0.34 | -0.20 |
| **LIG3** | Radiosensitiser | 2.35 | -0.34 | -2.98 | -6.72 |
| **PIF1** | Chemosensitiser | -1.15 | -1.22 | 1.18 | 0.16 |
| **TAL1** | Chemo/Radiosensitiser | -0.42 | -1.22 | -2.21 | -7.38 |

**Table 4.1: Genes selected from secondary screen for further analysis.**

Selected genes for further analysis and their Z-scores for each replicate and treatment modality. Sensitising siRNA shown by Z score <0.

#### 4.2.3.1 siRNA suppression of LIG1 causes cisplatin sensitisation.

Included within the genes for further analysis were the genes LIG1 and DCLRE1C. Previous studies have shown mutations in these genes lead to sensitivity to DNA damaging agents and further analysis of the effect of knockdown of these genes

was performed to validate the secondary screen. LIG1 encodes for the DNA ligase I enzyme, an ATP-dependent DNA ligase, involved in DNA replication and base excision repair (Tomkinson and Mackey, 1998). Mutations in LIG1, leading to DNA ligase I deficiency, have been shown to result in immunodeficiency and an increased sensitivity to DNA damaging agents such as UV, radiation and alkylating agents (Barnes et al., 1992). Previous studies have shown that Ligase I is up-regulated in tumour cells and inhibiting Ligase I can decrease tumour cell growth (Sun et al., 2001) suggesting that Ligase I might be a potential target for cancer therapy.

Colony formation assays assessing the effect of LIG1 suppression in H460 cells are shown in Figure 4.11. These demonstrate suppression of LIG1 causes significant sensitisation to cisplatin with *p*-values <0.001 for all doses of cisplatin. Knockdown of LIG1 also caused a trend towards increased sensitisation to radiation that was not significant by 2-way ANOVA analysis. The siRNA suppression of LIG1 was measured by qRT-PCR assessment of mRNA levels. Figure 4.11 demonstrates that adequate knockdown was achieved with LIG1 siRNA causing suppression of LIG1 to 25% (± 10%) of expression seen with NT siRNA.

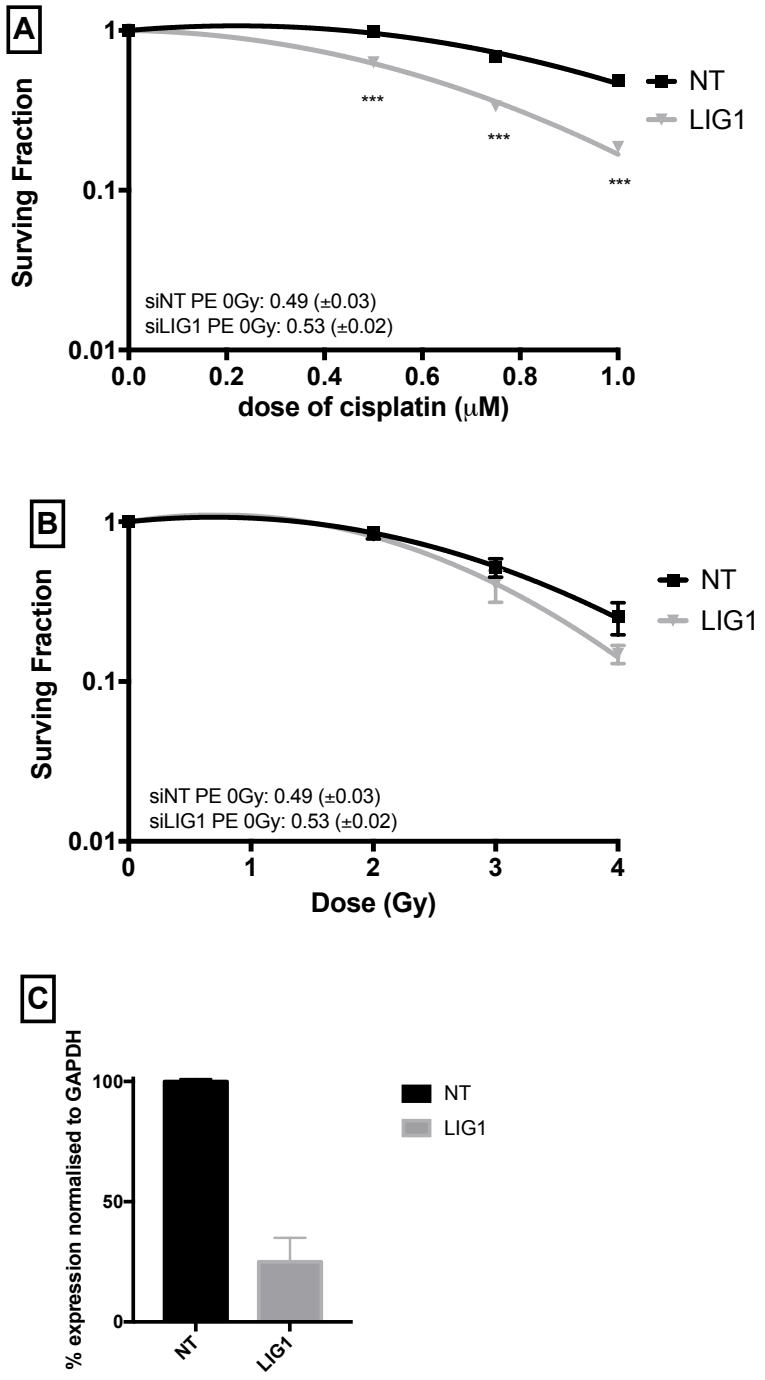



**Figure 4.11: Validation of LIG1 knockdown as potential cisplatin and radiation sensitiser.**

A and B: CFA of LIG1 depleted H460 cells following transfection with 20nM NT or LIG1 siRNA and treatment with cisplatin or irradiation.
C: Confirmation of LIG1 knockdown by qRT-PCR.

CFA are mean of 3 separate experiments. PE are mean ± SD of 3 experiments.
*p*-values calculated by factorial 2-way ANOVA: *** $p<0.0001$, ** $p<0.001$, * $p<0.05$

#### 4.2.3.2 siRNA suppression of DCLRE1C does not appear to sensitise to radiation in H460 cells

DCLRE1C or DNA cross-link repair 1C encodes for the protein Artemis that has an important role in the immune response and DNA repair. Artemis is essential to V(D)J recombination and the assembly of B-cell antibody and T cell receptor genes. Deficiency of Artemis leads to severe combined immune deficiency (SCID) (Moshous et al., 2001). Artemis also assists in repair of double strand breaks (DSB) via non-homologous end joining (NHEJ) and previous research has suggested cells that are deficient in Artemis are also sensitive to irradiation (Nicolas et al., 1998).

Within the secondary screen DCLRE1C ranked in the top 15 most radiosensitising genes. Further confirmatory CFA were performed to assess the effect of suppressing DCLRE1C in H460 cells (Figure 4.12 A). These showed a trend towards DCLRE1C suppression causing sensitisation to radiation. This trend was not significant by statistical analysis but it is important to note that siRNA suppression did not appear to be fully effective. Figure 4.12 B demonstrates that a mean knockdown of DCLRE1C to 66% (±3%) was achieved and it likely that a more significant sensitising effect might be observed if more effective knockdown was achieved.

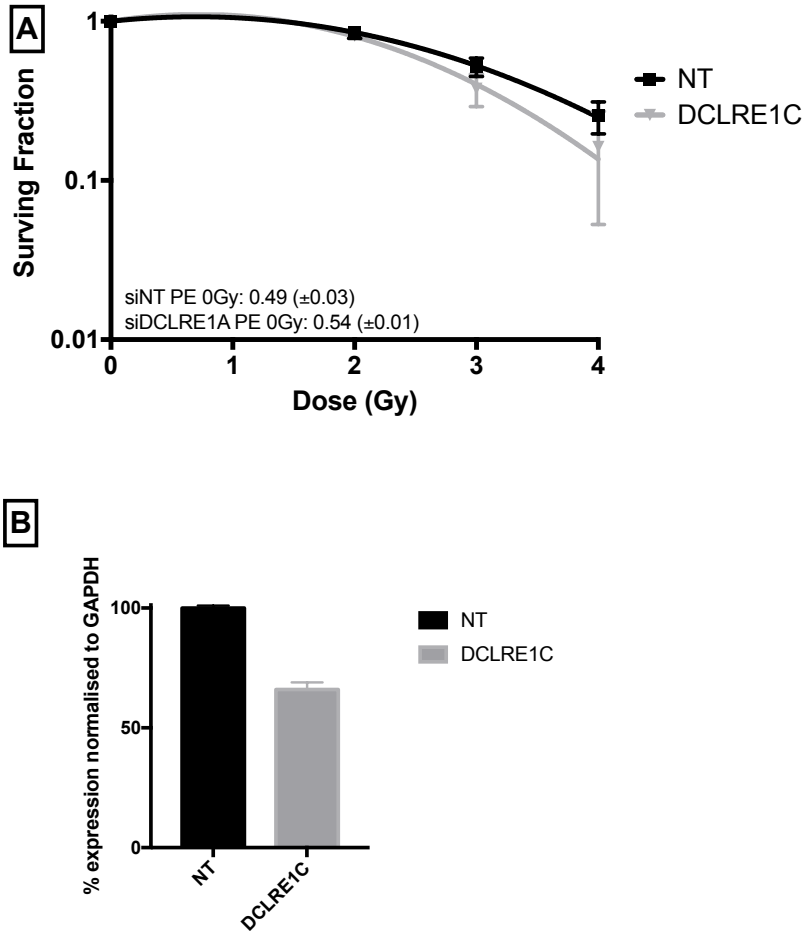



**Figure 4.12: Validation of DCLRE1C knockdown as potential radiation sensitiser.**

A: CFA of H460 cells following transfection with 20nM NT or DCLRE1C siRNA and treatment with irradiation.
B: Confirmation of DCLRE1C knockdown by qRT-PCR.

CFA are mean of 3 separate experiments. PE are mean ± SD of 3 experiments.
*p*-values calculated by factorial 2-way ANOVA: *** $p<0.0001$, ** $p<0.001$, * $p<0.05$

#### 4.2.3.3 siRNA suppression of CHD4 results in sensitisation to cisplatin and radiation.

Other genes that were included for further analysis included CHD4 and CHD5. Both of these genes encode for members of the chromodomain-helicase-DNA binding (CHD) family. CHD family proteins are members of the SNF2 superfamily of ATPases that remodel nucleosome structure (Eisen et al., 1995). CHD4 (chromodomain-helicase-DNA binding 4) is known to be a component of the NuRD (nucleosome remodelling and deacetylation) complex and may play a role in the DNA damage response through recruitment to sites of DNA damage by binding to poly(ADP-ribose) polymerase 1 (Polo et al., 2010). Previous studies have reported that depletion of CHD4 leads to hypersensitivity to ionising radiation and an increase in markers of replication stress (Larsen et al., 2010). There appear to be no previous reports of CHD4 depletion leading to cisplatin sensitivity.

H460 cells were transfected with CHD4 siRNA and colony formation assays were performed to assess for cisplatin and radiation sensitivity. It proved difficult to achieve effective CHD4 siRNA suppression and mRNA expression of CHD4 assessed by qRT-PCR analysis demonstrated expression was only reduced to 78% (±5%) (Figure 4.13 C). Despite poor knockdown mild suppression of CHD4 appeared to cause significant sensitisation to cisplatin ($p<0.0001$ for all doses of cisplatin) and also sensitisation to radiation. Sensitivity to radiation was not as marked as to cisplatin with $p<0.001$ for the majority of doses of radiation (Figure 4.13 A and B).

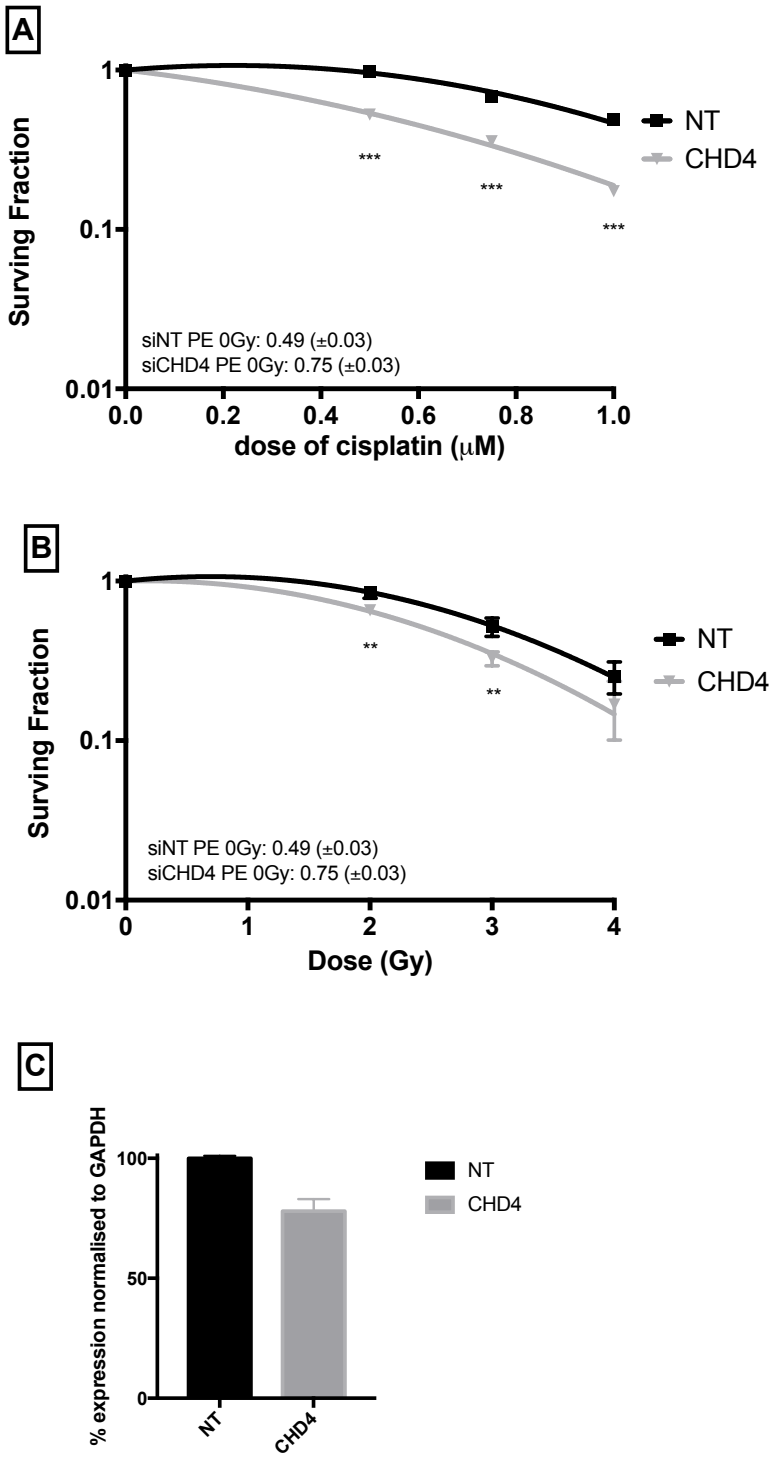



**Figure 4.13: Validation of CHD4 knock down as a potential radiation and cisplatin sensitiser**

A and B: CFA of H460 cells following transfection with 20nM NT or CHD4 siRNA and treatment with cisplatin or irradiation.
C: Confirmation of CHD4 knockdown by qRT-PCR.

CFA are mean of 3 separate experiments. PE are mean ± SD of 3 experiments.
*p*-values calculated by factorial 2-way ANOVA: *** $p<0.0001$, ** $p<0.001$, * $p<0.05$

#### 4.2.3.4 siRNA suppression of CHD5 leads to sensitisation to cisplatin and radiation.

The function of CHD5 is less well defined but a previous study has suggested it plays a role in remodelling of chromatin through an ability to loop out nucleosomal DNA (Quan and Yusufzai, 2014). CHD5 has been identified as a tumour suppressor that is lost via deletions of chromosome 1p36.3 (Bagchi et al., 2007). Loss of expression of CHD5 has been shown to correlate with poor prognosis in neuroblastoma (Garcia et al., 2010). There have been no previous publications to suggest CHD5 is a potential radiation or cisplatin sensitiser but siRNA suppression of CHD5 in H460 appeared to cause significant sensitisation to both cisplatin and radiation with $p<0.0001$ for cisplatin and $p<0.05$ for radiation (Figure 4.14 A and B). This sensitisation correlated with highly effective knockdown of CHD5 to 12% (±3%) expression compared to samples transfected with NT siRNA (Figure 4.14 C).

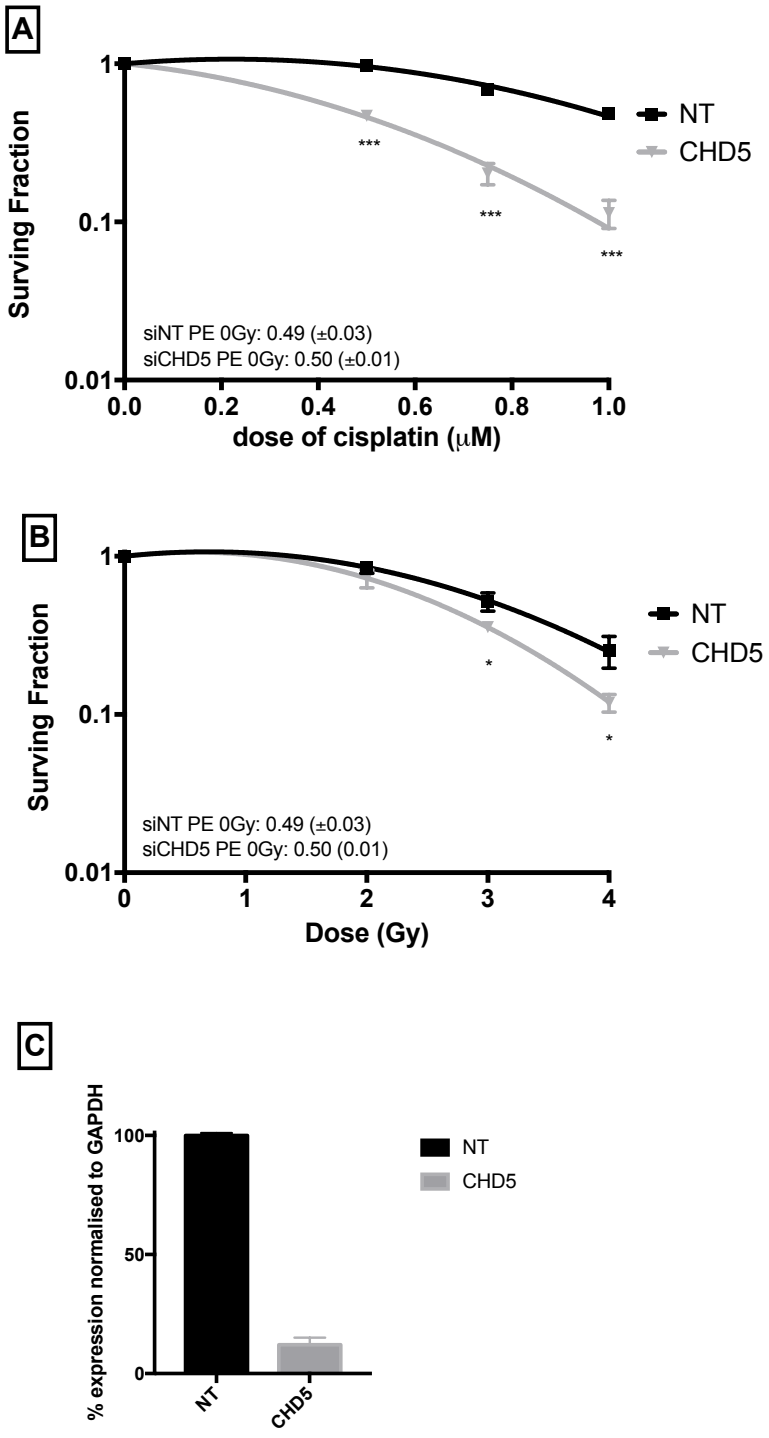



**Figure 4.14: Validation of CHD5 knockdown as potential cisplatin and radiation sensitiser**

A and B: CFA of H460 cells following transfection with 20nM NT or CHD5 siRNA and treatment with cisplatin or irradiation.
C: Confirmation of CHD5 knockdown by qRT-PCR.

CFA are mean of 3 separate experiments. PE are mean ± SD of 3 experiments.
*p*-values calculated by factorial 2-way ANOVA: *** $p<0.0001$, ** $p<0.001$, * $p<0.05$

#### 4.2.3.5 siRNA suppression of LIG3 leads to sensitisation to cisplatin but not radiation.

LIG3 encodes for multiple DNA ligase polypeptides with differing cellular functions. In particular, LIG3 encodes for the only mitochondrial DNA ligase (Arakawa et al., 2012). In the nucleus DNA ligase IIIα is essential for DNA replication in the absence of DNA ligase I (Le Chalony et al., 2012). DNA ligase IIIα also acts in DSB repair when the DNA ligase IV pathway is defective (Wang, 2005). DNA ligase IIIα is overexpressed in a number of cancer cell lines (Sallmyr et al., 2008) and this overexpression has been targeted in pre-clinical studies (Tobin et al., 2013).

It does not seem surprising that the secondary screen identified this gene as a potential cisplatin and radiation sensitiser. Further CFA confirmed that siRNA suppression of LIG3 caused significant sensitisation to cisplatin (*p*-values < 0.001) (Figure 4.15 A). However, despite effective knockdown of LIG3 as demonstrated by qRT-PCR to 21% (±3%) compared to NT siRNA, suppression of LIG3 did not appear to cause significant sensitisation to radiation (Figure 4.15 B and C).

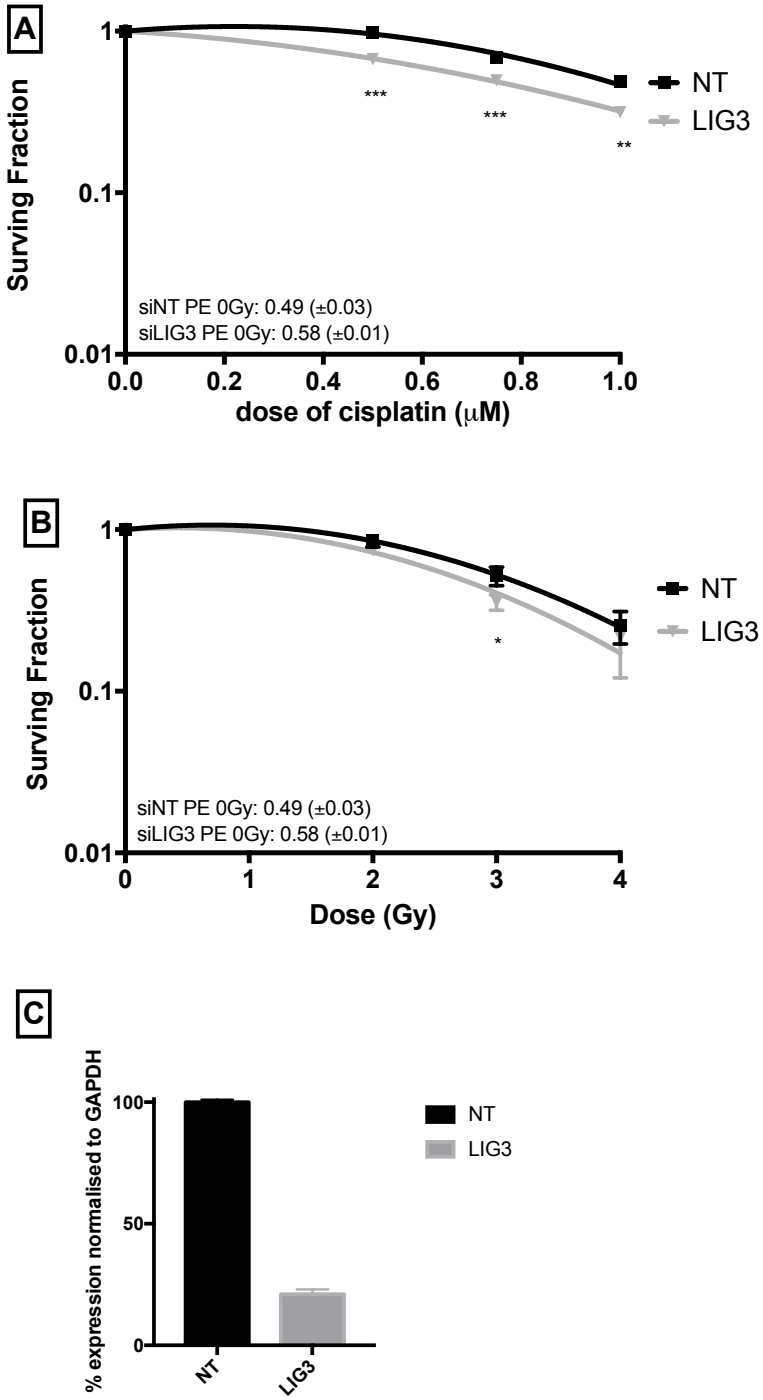



**Figure 4.15: Validation of LIG3 knockdown as potential cisplatin and radiation sensitiser.**

A and B: CFA of H460 cells following transfection with 20nM NT or LIG3 siRNA and treatment with cisplatin or irradiation.
C: Confirmation of LIG3 knockdown by qRT-PCR.

CFA are mean of 3 separate experiments. PE are mean ± SD of 3 experiments.
*p*-values calculated by factorial 2-way ANOVA: *** $p<0.0001$, ** $p<0.001$, * $p<0.05$

#### 4.2.3.6 siRNA suppression of KDM2B induces weak sensitisation to cisplatin but not radiation.

KDM2B encodes for a member of the F-box protein family- Lysine (K)-specific demethylase 2B. Previous studies have shown that KDM2B inhibits replicative senescence and supports immortalisation and proliferation of mouse embryo fibroblasts in culture (Tzatsos et al., 2009). KDM2B is overexpressed in T and B cell acute leukaemias and solid tumours such as pancreatic and breast adenocarcinomas (Tzatsos et al., 2013) (Kottakis et al., 2014) suggesting a role as an oncogene. No previous studies have identified the gene as a potential cisplatin or radiation sensitiser but suppression of the gene inhibited tumour cell growth by inducing senescence or inhibiting G1 progression (Kottakis et al., 2014) in one previous study.

It proved difficult to obtain effective knockdown of KDM2B in further experiments with a mean suppression to 69% (±7%) compared to NT siRNA transfection achieved (Figure 4.16 C). Despite only mild decrease in expression, suppression of KDM2B did appear to sensitise to cisplatin ($p<0.05$) but not to radiation (Figure 4.16 A and B).

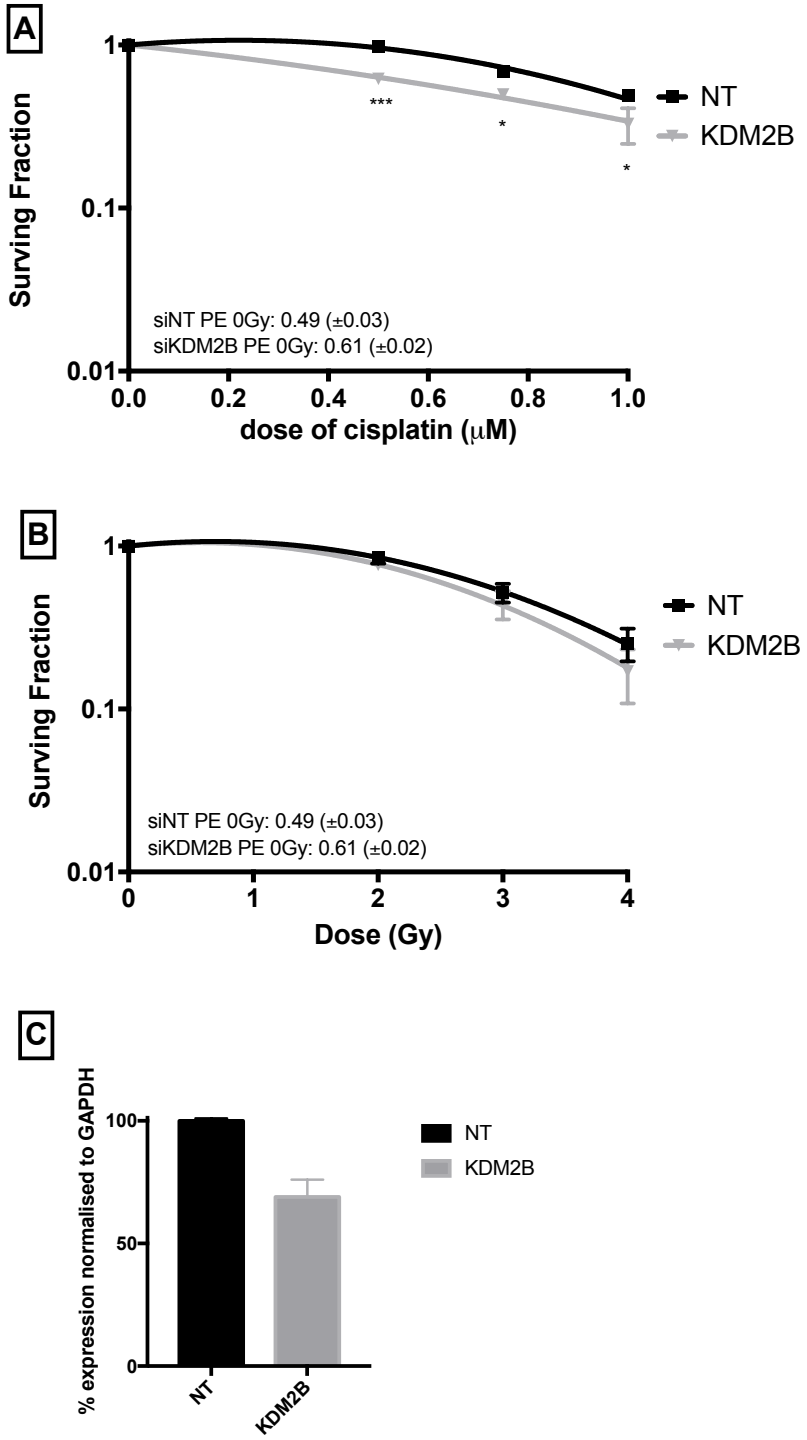



**Figure 4.16: Validation of KDM2B knockdown as potential cisplatin and radiation sensitiser.**

A and B: CFA of H460 cells following transfection with 20nM NT or KDM2B siRNA and treatment with cisplatin or irradiation.
C: Confirmation of KDM2B knockdown by qRT-PCR.

CFA are mean of 3 separate experiments. PE are mean ± SD of 3 experiments.
*p*-values calculated by factorial 2-way ANOVA: *** $p<0.0001$, ** $p<0.001$, * $p<0.05$

#### 4.2.3.7 siRNA suppression of TAL1 induces sensitisation to cisplatin but not radiation.

The screen also identified the gene TAL1 as a potential sensitiser. TAL1 encodes for a b-HLH transcription factor that is normally expressed in haemopoietic stem cells (Hsu et al., 1994) and the TAL1 protein acts as a positive regulator of erythroid differentiation (Aplan et al., 1992). Aberrant expression of TAL1 is common in acute lymphoblastic leukaemias and, in a previous study, expression of wild-type TAL1 in leukaemic cells was able to protect them from apoptosis caused by chemotherapeutic agents (Bernard et al., 1998).

The identification of suppression of TAL1 as a potential cisplatin and radiation sensitiser in a lung cancer cell line was surprising and for this reason this gene was included in further analysis. Further CFA demonstrated that suppression of TAL1 caused sensitivity to cisplatin ($p<0.0001$) (Figure 4.17 A). Sensitivity to radiation was less convincing and it was not possible to assess knockdown of TAL1 using qRT-PCR. This was due to difficulties designing PCR primers that could produce sequences for analysis.

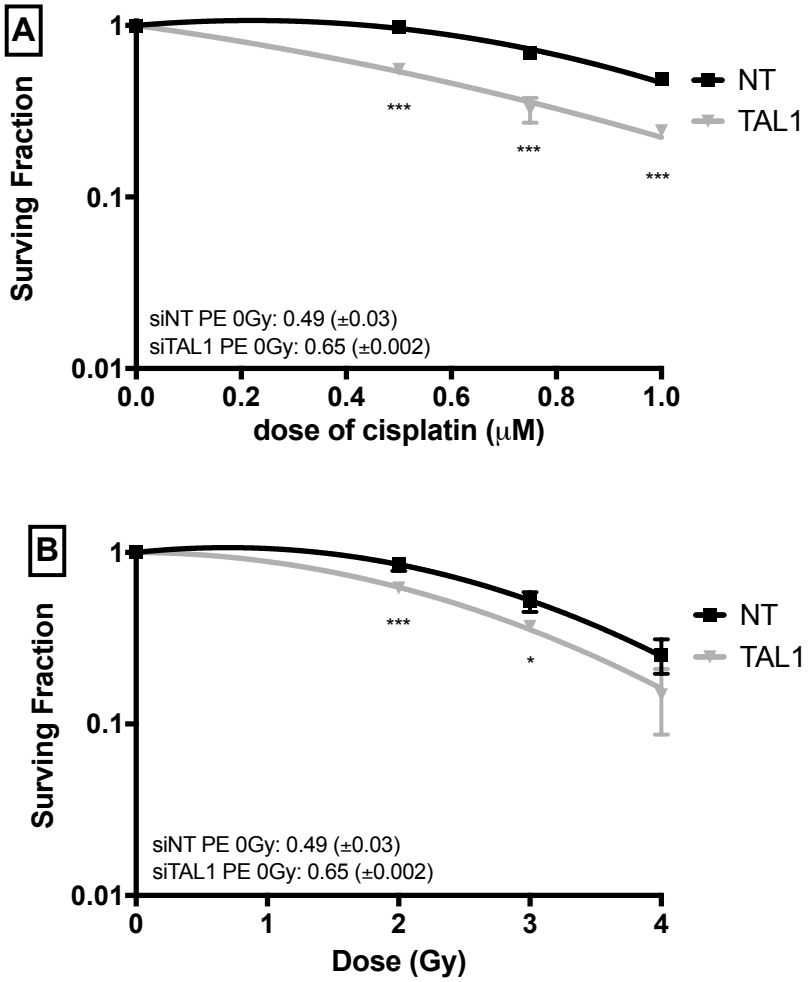



**Figure 4.17: Validation of TAL1 knockdown as potential cisplatin and radiation sensitiser.**

A and B: CFA of H460 cells following transfection with 20nM NT or TAL siRNA and treatment with cisplatin or irradiation.

CFA are mean of 3 separate experiments. PE are mean ± SD of 3 experiments.
*p*-values calculated by factorial 2-way ANOVA: *** $p<0.0001$, ** $p<0.001$, * $p<0.05$

#### 4.2.3.8 siRNA suppression of PIF1 causes sensitisation to cisplatin.

Finally the gene PIF1, a 5' to 3' DNA helicase was identified as a potential cisplatin sensitiser. This gene had previously been identified in yeast as a potential cisplatin sensitiser (Ribeyre et al., 2009) and is discussed in more detail in section 4.2.4. As this gene had not been identified as a cisplatin sensitiser in human cells it was included for further investigation.

Colony formation assays demonstrated that suppression of PIF1 lead to significant sensitisation to cisplatin ($p<0.0001$) at all doses (Figure 4.18 A). Assessment of mRNA expression of PIF1 after siRNA transfection demonstrated that knockdown to 5% (±1%) was achieved (Figure 4.18 B) compared to NT siRNA transfected controls.

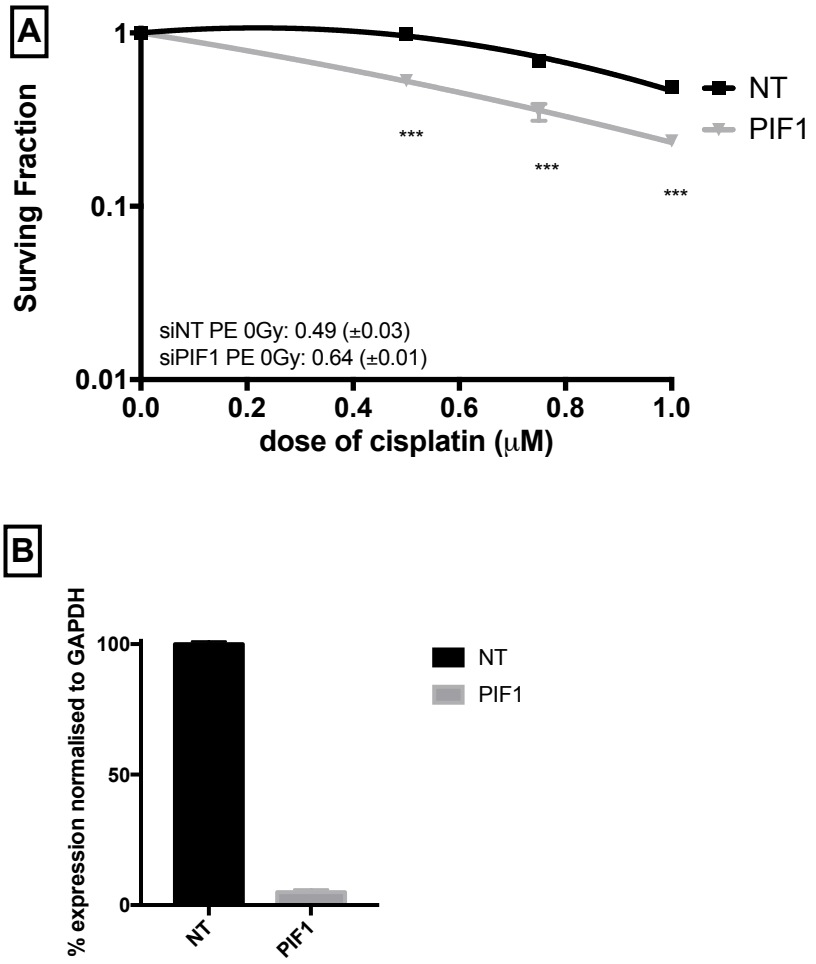



**Figure 4.18: Validation of PIF1 knockdown as potential cisplatin sensitiser.**

A: CFA of H460 cells following transfection with 20nM NT or PIF1 siRNA and treatment with cisplatin.
B: Confirmation of PIF1 knockdown by qRT-PCR.

CFA are mean of 3 separate experiments. PE are mean ± SD of 3 experiments.
*p*-values calculated by factorial 2-way ANOVA: *** $p<0.0001$, ** $p<0.001$, * $p<0.05$

### 4.2.4 Clonogenic assay confirmation of cisplatin sensitisation in a HAP1 knock out cell line

Colony formation assays (CFA) in H460 cell lines confirmed that suppression of PIF1 resulted in significant cisplatin sensitisation. PIF1 has been previously extensively investigated in yeast where it encodes for a 5' to 3' DNA helicase with several roles in genome stability (Lahaye et al., 1991). It was shown that PIF1 plays a role in telomere maintenance specifically by inhibiting telomere elongation and de novo formation (Schulz and Zakian, 1994). PIF1 has also been demonstrated to play a role in the processing of G-quadruplex DNA (G4-DNA) facilitating DNA replication and repair (Ribeyre et al., 2009). Studies have illustrated that human PIF1 expressed in deficient yeast can suppress telomere lengthening and G-quadruplex associated DNA damage (Paeschke et al., 2013).

In humans, PIF1 expression results in two protein isoforms that have different subcellular localisation. The major transcript, hPIF1a, encodes a 70kDa nuclear polypeptide. A second transcript encodes a 75kDa mitochondrial polypeptide, hPIF1b (Futami et al., 2007).

Human PIF1 has been shown to have similar properties to yeast PIF1 proteins. It also appears to have a role in processing G4 structures particularly those that form in single stranded nucleic acid intermediates that are formed during DNA replication (Sanders, 2010). Human PIF1 has been shown to recognise and unwind structures similar to stalled replication forks suggesting a role in restarting replication (George et al., 2009) and, similar to yeast, it inhibits telomerase activity (Zhang et al., 2006). Previous studies in human colorectal tumour cells have shown that siRNA suppression of PIF1 leads to increased sensitivity to

gemcitabine (Gagou et al., 2011) and PIF1 siRNA suppression slows replication fork rates and increases the number of arrested replication forks in human fibroblasts (Gagou et al., 2014). Both these findings suggest a role for PIF1 in DNA damage repair and tumorigenesis. This makes the identification of suppression PIF1 as a potential cisplatin sensitiser in lung cancer cells not entirely unexpected but warrants further confirmation and investigation.

Suppression of PIF1 in the previous experiments was performed using siRNA. It was therefore important to confirm in a stable knockout cell line that loss of PIF1 rendered cells cisplatin sensitive. This would further rule out that siRNA induced off-target effects caused the sensitisation seen.

With the advent of clustered regularly interspaced short palindromic repeats (CRISPR) technology, it is relatively easy to obtain stable genetic knockouts to confirm experimental findings. The CRISPR system is a genome engineering method that utilises the RNA-guided DNase Cas9. This technology was derived from the type II CRISPR-Cas systems that provide bacteria with adaptive immunity to viruses and plasmids (Barrangou et al., 2007). The CRISPR-Cas9 protein is an DNA endonuclease that uses a partially complementary trans-acting RNA (tracrRNA) and mature CRISPR RNA (crRNA) (tracrRNA-crRNA) duplex to guide DNA cleavage (Jinek et al., 2012). By engineering small guide RNAs (sgRNA) that contain a hairpin, mimicking the tracrRNA-crRNA complex, and a short sequence complementary to the target DNA, it is possible to induce sequence-specific double-strand breaks. To achieve cleavage the binding site of a target DNA must contain a protospacer-adjacent motif (PAM) (Marraffini and Sontheimer, 2010).

This technology has been successfully used to edit the genome of human cells with high efficiency (Horii et al., 2013; Kim et al., 2014).

CRISPR PIF1 disrupted HAP1 cells were purchased from Horizon Discovery and used to perform confirmatory CSA. HAP1 cells are derived from a patient with chronic myeloid leukaemia and being a near haploid cell line they are easily amenable to CRISPR knockout.

Figure 4.19 demonstrates that PIF1 KO cells were significantly more sensitive to cisplatin than a HAP1 wild-type cell line ($p<0.05$).

These CSA confirm suppression of PIF1 sensitises cells to cisplatin both through siRNA suppression and stable knockdown.

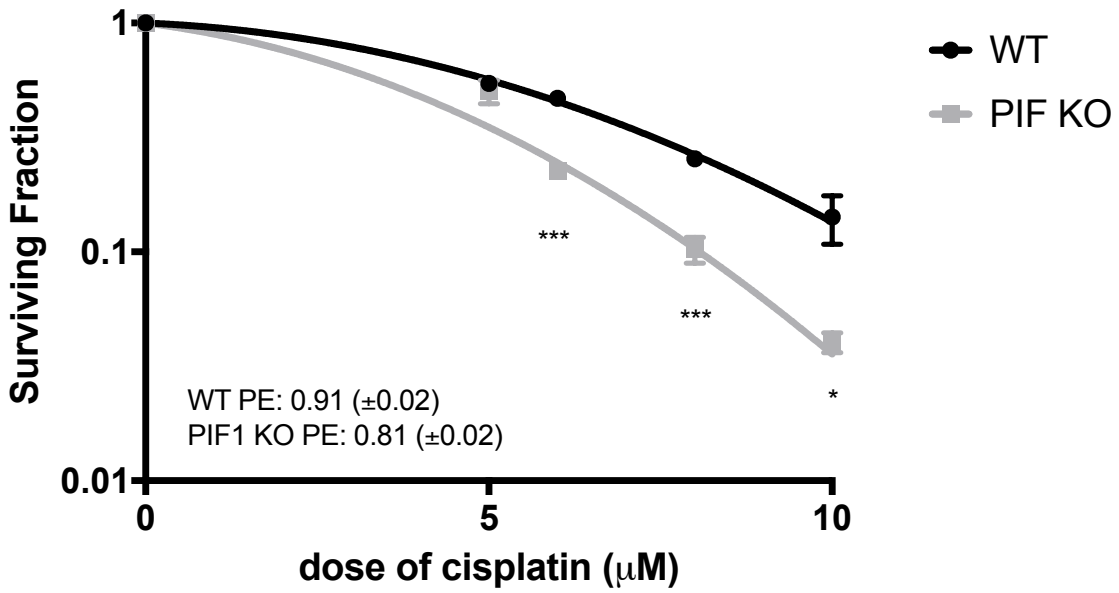



**Figure 4.19: Clonogenic survival assay comparing WT HAP1 and PIF1 KO HAP1 cells**

3000 cells were seeded in 10cm petri dishes and allowed to adhere before treatment for 4 hours with the appropriate dose of cisplatin. Plates were then incubated for 7 days before staining with crystal violet and colony counting with GelCount software.

PE and SF values ± SD are mean of 3 separate experiments using duplicate plates.

*p*-values calculated by factorial 2-way ANOVA: *** $p<0.0001$, ** $p<0.001$, * $p<0.05$

## 4.3 Conclusions

This chapter describes the successful completion of a siRNA screen in a lung cancer cell line. Our laboratory has previously described the successful adaption of the traditional 10cm format CFA to a 96-well form for a radiation screen (Tiwana et al., 2015). This screen builds on this experience by extending the use of the 96-well CFA to include a cisplatin treatment group allowing screening for potential DNA damage repair modulators in both DSB repair and ICL repair.

### 4.3.1 Assessment of primary and secondary siRNA screens

This screen was performed in non-small cell lung cancer (NSCLC) H460 cells in the hope that any sensitisers identified may offer the potential for clinical translation since non-small cell lung cancer (NSCLC) is commonly treated with cisplatin and or radiation in both curative and palliative settings. The use of cell lines as opposed to primary tumour cells does have limitations, as studies have demonstrated that cancer cells in culture can develop highly altered chromosomal copy number and extensive genomic rearrangements over time (Landry et al., 2013) and this may influence results.

The initial optimisation of the primary screen was challenging. In particular, the cell line used in this screen proved to be variable in transfection efficiency and sensitivity to the toxic effects of siRNA. Despite careful optimisation to reduce transfection toxicity and encouraging Z-factor results with trial run experiments with liquid handling robotics, the Z-factor results from the primary screen were variable and poorer than in the pilot experiments. It is likely this was caused by reduced PE for NT siRNA controls causing lower SF in NT siRNA wells in treated plates, particularly those treated with 0.5μM cisplatin (Figure 4.7).

The cause for this decreased PE and SF may be related to a number of factors. It may in part be due to toxicity from either siRNA or transfection reagents, although attempts were made to ameliorate this in optimisation experiments. It is also possible that using the robotic equipment lead to shearing of cells and hence decreased PE.

The control wells in this screen were positioned around the edges of the plate and "edge effect" has been well described in 96-well plates used in absorption assays (Oliver et al., 1981). Uneven distribution of cells in the wells from edge effect may have lead to variable transfection and decreased PE. Efforts were made to avert this by pre-incubating the 96-well plates at room temperature prior to placing in $CO_2$ incubator (Lundholt et al., 2003) and by placing plates on wet filter paper inside large square dishes in an attempt to equalise temperature gradients and reduce evaporation.

The secondary screen had much improved PE in the untreated plates and subsequently Z-factor results for both the radiation and cisplatin treated groups were also improved (Figure 4.9). It is not clear why this occurred, as conditions were identical for the primary and secondary screens. The only difference was the supplier of the control siRNA and it is possible that transfection with siRNA from Dharmacon was more effective and less toxic.

False negative results, incorrectly excluding a gene as non-sensitising, may occur due to inaccurate counting of colonies. In these screens, colony counting was performed using a GelCount plate reader and software. The software allows specific selection criteria for colony size and edge removing some potential inaccuracies that may be associated with manual counting.

Within the primary screen genes with a PE less than 4% were removed from final analysis. This may potentially remove genes that are cisplatin or radiation sensitisers but allows for the exclusion of extremely toxic siRNA that would have been difficult to investigate further.

### 4.3.2 Assessment of potential cisplatin and radiation sensitisers from the siRNA screen.

Eight genes were selected for further assessment as cisplatin or radiation sensitisers. Individual CFA were performed alongside assessment of siRNA knockdown by qRT-PCR analysis.

All CFA were performed in 6-well format but using the same concentration of siRNA and transfection reagent, INTERFERin-HTS, as the primary and secondary screen.

Transfection efficiency for each gene was variable as assessed by mRNA expression. This may be responsible for the lack of sensitisation seen in some experiments, particularly DCLRE1C which has previously been shown to sensitise to radiation when depleted. siRNA suppression was also poor in KDM2B and CHD4 experiments making interpretation of results difficult.

Validation of other genes did not demonstrate radiation sensitisation and it is presumed that the selected genes represent either false positive results from the screen or that transient suppression was not consistent. The advent of CRISPR technology now offers the potential for large-scale screens with stable knockdown cells. Several recent studies have used CRISPR to identify genes that are essential for cancer and stem cell viability (Wang et al., 2014) (Shalem et al., 2014) and to

identify synergistic drug therapies for cancer (Han et al., 2017). The use of CRISPR can lead to complete disruption of gene expression rather than partial suppression as caused by siRNA and CRISPR targeting appears more precise and to cause less off-target effects than the use of siRNA. This would seem an ideal tool for further genetic screens for cisplatin or radiation sensitivity.

### 4.3.3 Further analysis of PIF1 as a cisplatin sensitiser.

The gene PIF1 was selected for further analysis with a knockout cell line. Previous CFA had shown that PIF1 suppression appeared to result in sensitisation to cisplatin (Figure 4.18) and this is in keeping with previous findings in yeast (McMurdie et al., 2010). However, assessment of adequate suppression of PIF1 at protein level was difficult to achieve by western blotting and it was essential to demonstrate sensitivity in a stable knockout cell line. Figure 4.19 demonstrates that HAP1 cells lacking expression of PIF1 are clearly more sensitive to cisplatin than wild-type cells.

Further mechanistic assessment of PIF1 as a potential cisplatin sensitiser was limited by time. In the future, further CFA experiments assessing the effect of PIF1 suppression in normal cell lines could be useful to assess whether suppression of PIF1 would also sensitise normal tissue.

Previous studies have suggested that suppression of PIF1 in human fibroblasts results in slowing of fork DNA replication and increased fork stalling (Gagou et al., 2014). This finding was demonstrated by DNA fibre studies in human fibroblasts. It would be interesting to investigate whether this can be demonstrated in a cancer cell line such as the H460. The authors of this study noted that human

fibroblasts that expressed the Rat Sarcoma (RAS) proto-oncogene appeared, when PIF1 was suppressed, to have slower progression of replication. The H460 cell line is homozygous for mutations to the K-RAS gene. It therefore seems possible that H460 and other cancer cell lines with RAS mutations would demonstrate decreased replication and DNA fibre studies would be a useful way of illustrating this.

If PIF1 depletion results in delayed replication and increased fork stalling it is likely this results in increased cell cycle stalling in S-phase. This could easily be demonstrated by FACS analysis. It would be likely that cisplatin treatment coupled with PIF depletion would result in extremely marked cell cycle delay with increased apoptosis, which could be quantified with Annexin staining. There may also be an increase in DSB intermediates due to replication fork collapse that could be quantified by γH2AX foci analysis.

PIF1 offers an interesting potential target for cisplatin sensitisation that warrants further detailed investigation.

# Chapter 5 - General Discussion and Further Work

The work presented in this thesis sought to identify potential new targets to improve chemotherapeutic treatment with ICL agents. ICL agents are well-established treatment options for solid and haematological malignancies. However, their use is limited by drug toxicity (Travis et al., 1999; Sanderson and Shield, 1996), lack of sensitivity in some tumours (Rosell et al., 2002) and acquired resistance or recurrent disease after treatment (Wynne et al., 2007).

It is possible that long-living tumour stem cells contribute to the clinical issues of tumour recurrence or acquired resistance (Bonnet and Dick, 1997). As this population of cells is believed to divide rarely, selective targeting of this group of cells may need to acknowledge their quiescent state. With this in mind, the specific role of ICL repair in quiescent or G1 phase cells was investigated.

Previous studies in yeast (Sarkar et al., 2006) and *Xenopus* egg extracts (Williams et al., 2012) had suggested that repair of ICL in G1 could occur but evidence in mammalian cells was sparse and potential mechanisms not well defined. A mammalian cell model was created and used to demonstrate that repair of ICL can occur in mammalian cells in G1. This model was also used to define several of the NER proteins and exonucleases involved in this G1 repair. The identification of this pathway of ICL repair offers potential insights into the selective targeting of quiescent cells, such as tumour stem cells.

To address the issues of drug toxicity and poor sensitivity to ICL agents, a large-scale siRNA screen was performed to identify novel, druggable targets of sensitisation to cisplatin and radiation. Increasing tumour sensitivity to ICL agents

by synergistic targeting of repair factors (Hartley and Hochhauser, 2012) might increase the therapeutic index of ICL agents, potentially allowing for lower treatment doses of ICL agents and reducing drug toxicity (Deans and West, 2011). Likewise, increasing sensitivity to ICL agents can lead to increased tumour cell death and decreased disease burden.

The large-scale siRNA screen successfully identified several DNA damage repair targets, with the gene PIF1 confirmed in stable knockout cell line as a cisplatin sensitiser. This screen was performed in a clinically relevant lung cancer cell line and the identified genes may be appropriate for drug targeting to improve ICL agent outcomes.

## 5.1 Investigation of ICL repair in G1 phase of the cell cycle

### 5.1.1 General findings from study of ICL repair in G1 phase

Within Chapter 3 a model for ICL repair in G1 was developed using CHO cells and HN2. Using WT CHO cells synchronised to G1 by isoleucine starvation it was possible to demonstrate, using flow cytometry and modified comet assays, that repair of ICLs occurs in G1 in mammalian cells. This model was utilised to further identify that the NER proteins XPF, XPB and XPD and the exonucleases SNM1A and EXO1 are required for the repair of ICL induced by HN2 in G1.

Within the experiments presented, the TC-NER protein CSB did not appear essential for HN2 induced ICL repair in G1. HN2 induces ICL in the major groove of DNA with significant amounts of DNA helix distortion (Rink and Hopkins, 1995; Rajski and Williams, 1998). It is possible that due to this distortion, these lesions can be recognised by GG-NER and therefore CSB and the proteins of TC-NER are

not required. These findings differ from those of Enoiu *et al* (Enoiu et al., 2012) who identified that CSB was required for cisplatin ICL repair in G1 but match findings by Muniandy *et al* (Muniandy et al., 2009) that identified GG-NER and XPC were required for repair of psoralen ICL in G1. This underlines the possibility that ICL with specific chemical structures might show differential requirements for GG-NER versus TC-NER pathways. It might also reflect the different origins of cell lines used in each of these studies since Enoiu *et al* and Muniandy *et al* both assessed ICL repair in human fibroblast lines but used cisplatin and psoralen ICL respectively.

Following recognition of DNA damage by the NER pathway the TFIIH complex is recruited (as discussed in 1.2.2). This complex contains both XPB and XPD, which unwind the DNA duplex to form a repair "bubble" structure.

Both of these helicases appeared to be required for repair of G1 HN2 ICL in the model created in this thesis and previous studies in recombination-independent host reactivation assays also showed a role for XPD in G1 (Zheng et al., 2003; Wang et al., 2001a).

Following unwinding of the DNA duplex in the NER pathway, further recruitment of XPA, RPA, XPG and XPF-ERCC1 occurs leading ultimately to dual incisions either side of the damaged DNA.

Previous studies assessing repair of MMC and psoralen ICL (Wang et al., 2001a; Zheng et al., 2003) suggested both XPF-ERCC1 and XPG played a role in incising around ICLs in G1. However, studies in this thesis implied that whilst XPF is required for G1 ICL repair, XPG is not. It is therefore possible that whilst HN2 G1

ICL repair appears to proceed via the NER pathway, the key endonucleases may differ from those in classical NER and also those involved in the repair of MMC and psoralen ICL in G1.

Since studies in this thesis suggested that SNM1A is required for G1 ICL repair, it is possible that, similar to the classical NER pathway, an initial incision is made by XPF-ERCC1 on one DNA strand 5' to the ICL and subsequently SNM1A acts from this incision to digest past the ICL allowing unhooking of the ICL and creating a single strand gap.

This process is supported by recent findings by Abdullah *et al* (Abdullah et al., 2017) who identified, using model replication fork structures, that SNM1A can load from XPF-ERCC1-RPA-induced incisions and digest past ICL to complete unhooking.

It is possible that resection by SNM1A occurs in preference to, or obviates the requirement for, additional incision by XPG. Recent work has revealed the crystal structure of XPG (Miętus et al., 2014) confirming and elucidating how *in vitro* XPG cleaves single strand 5' overhangs and splayed arm DNA structures (Evans et al., 1997; Hohl et al., 2003). XPG is unique in its ability to recognise DNA bubbles and cleaves all substrates at the junction of single and double stranded DNA (ss-dsDNA). This cleavage is performed one nucleotide into the double stranded region of DNA (Dunand-Sauthier et al., 2005; Grasby et al., 2012). Previous work using ethylation interference footprinting demonstrated that XPG binds significantly to the double stranded section of DNA (Hohl et al., 2003). The presence of a HN2 ICL causes significant helical distortion and this may inhibit XPG

binding. Similarly the presence of an ICL may inhibit the ability of XPG to perform incisions beyond the ss-dsDNA junction and, hence, SNM1A may be required.

Following SNM1A resection and, therefore, ICL unhooking, recruitment of PCNA may occur leading to the recruitment of the DNA polymerases and translesion bypass of the DNA strand gap created. The studies in this thesis also identified that EXO1 played a potential role in G1 ICL repair, previous studies have suggested that EXO1 has modest 5' flap activity (Keijzers et al., 2015). Therefore, further resection of any flap structures at this stage may be performed by EXO1 allowing completion of ICL bypass on one strand. Alternatively, EXO1 could act in an analogous fashion to SNM1A, resecting past the ICL. However, recent studies have demonstrated that EXO1 is unable to digest past HN2, SJG-136 or Triazole ICLs ((Pizzolato et al., 2015) and unpublished studies from our laboratory).

To complete ICL removal, further incision, DNA strand resection and bypass may occur on the opposing strand by the NER pathway. This potential model of G1 ICL repair is detailed in Figure 5.1 below.

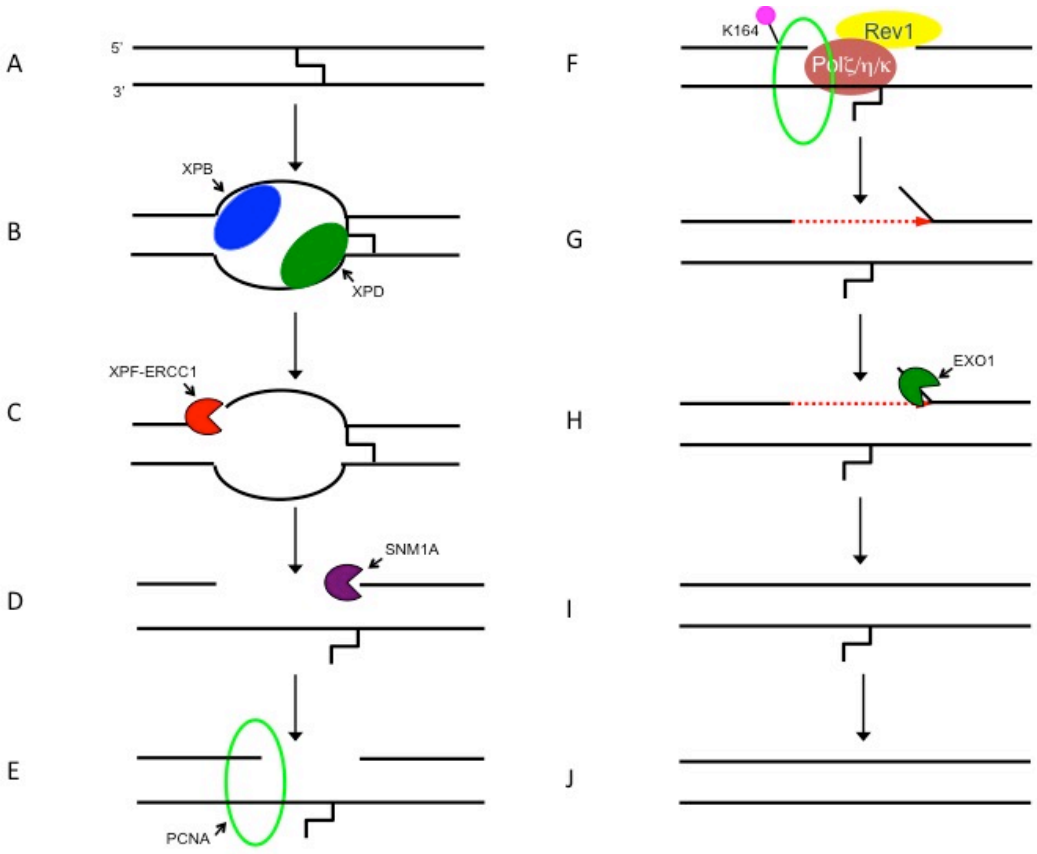



**Figure 5.1: Model of G1 HN2 ICL repair based on experimental findings in this thesis**

A: Helix distorting ICL present in duplex DNA detected by the GG-NER pathway.

B: Recruitment of the GG-NER helicases XPD and XPB leading to unwinding of the DNA.

C: Incision by XPF-ERCC1 5' to the ICL.

D: SNM1A digests from the incision, past the ICL releasing it and allowing unhooking to occur.

E: PCNA is recruited.

F: Following PCNA monoubiquitination recruitment of TLS Polymerases occurs.

G: TLS bypass occurs in the DNA strand gap created.

H: Resection of 5' flap by EXO1 and ligation.

I: Completion of repair of one DNA strand.

J: A further round of NER occurs, removing the ICL, resulting in completion of repair and undamaged DNA.

### 5.1.2 Further areas for study in ICL repair in G1 phase

The experimental model of ICL repair in G1 developed in this thesis is a useful tool that could be adapted to assess the repair of other ICL inducing agents. It is possible that the structure of ICL formed influences ICL repair in G1 phase. In particular, the degree of distortion of the DNA helix inflicted by the ICL may alter the initial recognition pathway (the dependence on TC-NER versus GG-NER, for example) and thereafter the DNA damage repair proteins responsible for repair (Smeaton et al., 2008).

Accordingly, it would be interesting to use the experimental model created to assess ICL repair in G1 phase for other ICL agents, in particular MMC. MMC induces lesions within the minor groove of the DNA helix (Rajski and Williams, 1998) and causes only minor DNA helix distortion (Rink et al., 1996). This may alter the DNA damage repair proteins responsible for recognition and repair of MMC lesions in G1 and this could be easily screened for with the model created. Specifically this may allow for further assessment of the role of CSB and the TC-NER pathway. MMC is also used extensively in clinical practice and further study of this ICL agent and others such as cisplatin would be relevant to allow development of clinical targets for treatment.

The apparent lack of role for XPG in ICL repair in G1 could be considered surprising and further confirmation of the role of XPG may help to define the pathway of G1 ICL repair in more detail. Work is currently being undertaken to confirm with comet assays that unhooking of ICL in G1 in XPG mutants is similar to WT CHO cells.

Our laboratory has extensive experience examining the role of XPF-ERCC1 using biochemical reconstitution analysis with purified protein and model ICL structures (Abdullah et al., 2017). Adaption of this assay to assess the role of XPG could be performed. This would allow assessment of the precise incisions that XPG is capable of performing on a model G1 ICL lesion.

Finally, as discussed previously, several studies have isolated a group of cells that are presumed to be tumour stem cells using FACS (Al-Hajj et al., 2003; Singh et al., 2003; Hemmati et al., 2003). Studying ICL repair in G1 phase in tumour stem cell such as these would provide an insight into mechanisms of tumour recurrence or metastases that may be clinically translatable and potentially improve clinical treatments.

## 5.2 Large-scale siRNA screen of DNA damage response and repair targets

### 5.2.1 General findings from large-scale siRNA screen

The aim of the work described in Chapter 4 was to identify potential novel molecular determinants of tumour cisplatin and radiation sensitivity. This was achieved through the use of a high-throughput siRNA screen of DNA damage response genes, utilising colony formation assays as the end-point for analysis of sensitivity. Our laboratory had previously successfully developed and utilised a high-throughput colony formation assay to assess a HeLa cell line for potential targets of radiosensitivity (Tiwana et al., 2015). This was the first published large-scale screen to use CFA as an end-point for determining radiosensitivity. Like-wise, this large-scale screen is unique in its use of CFA to determine sensitisation to cisplatin.

The initial primary screen demonstrated good internal validation in the radiation treated arm of the study, with excellent Z-factor results and $R^2$ score, suggesting good differentiation between positive and negative controls (Figure 4.7) and good reproducibility between the two replicates of the screen.

The quality metrics in the cisplatin arm in the initial primary screen showed some limitations with weak Z-factor results (Figure 4.7) possibly resulting from decreased survival in the non-targeting (NT) sample wells from siRNA or transfection reagent toxicity. Despite these lower Z-factor scores, reproducibility between the two replicates was good with an $R^2$ score of 0.53. There was good internal validation within the primary screen with several genes that are known to sensitise to either radiation or cisplatin, such as ATM, DNA-PK*cs* and RAD51 paralogs demonstrating high Z-scores suggesting the use of CFA in large-scale siRNA screens is a robust technique to identify potential cisplatin or radiation sensitisers.

Following the primary screen, and a secondary confirmatory screen, eight genes were selected for further study based on their potential as novel druggable targets for cisplatin or radiation sensitisation. These targets were initially investigated with further clonogenic experiments with siRNA knockdown confirmed by qRT-PCR quantification of mRNA expression.

The results from these experiments were variable, in particular, assessment of gene suppression demonstrated that siRNA knockdown in this cell line (Non-small cell lung cancer, H460) was not consistent for all genes. Despite this, adequate suppression was achieved for siRNAs targeting PIF1, LIG3, CHD5 and LIG1 and suppression of these genes individually resulted in cisplatin sensitisation.

Disappointingly, none of the genes selected for further study showed marked radiosensitisation.

This inconsistency in siRNA suppression limited further analysis, as it proved difficult to perform deconvolution studies to assess sensitisation to individual siRNA strands from within each pool. Performing deconvolution studies would have been valuable to exclude off-target effects and prevent further investigation of false positive results.

As consistent siRNA suppression of gene targets was difficult to achieve, CRISPR-Cas9 knockout cells were obtained to assess cisplatin sensitisation in a stable knockout cell line. Clonogenic assays performed with PIF1 knockout cells confirmed that PIF1 suppression sensitises HAP1 cells to cisplatin confirming findings seen with siRNA suppression in H460 NSCLC cells.

The identification of PIF1 as a cisplatin sensitiser is significant and is in keeping with previous studies of the function of PIF1 which have identified that PIF1 depletion in yeast sensitises to cisplatin (Ribeyre et al., 2009) and slows replication fork progression and increases replication fork arrest in human fibroblasts (Gagou et al., 2014).

### 5.2.2 Further area for study related to large-scale screen

Following the identification of PIF1 as a potential cisplatin sensitiser there are several areas that may be of interest for further validation and investigation. Previous studies suggest PIF1 may play a role in DSB repair in yeast ((Kwon et al., 2017; Wilson et al., 2013). Since DSB are formed as intermediates of ICL repair, it might be expected that PIF1 depleted cells would also be sensitive to other ICL

agents and further assessment of PIF1 knockout cells to other ICL agents such as MMC or HN2 is warranted. No sensitisation to ionising radiation was seen in the initial primary and secondary radiation siRNA screens when PIF1 was depleted (Table 4.1) but confirmation of this in a stable knockout cell line would be important. A lack of sensitivity to radiation despite sensitivity to a range of ICL agents might suggest that PIF1 sensitisation operates via a particular pathway of DSB repair. Sensitivity to ICL agents but not radiation might suggest PIF1 plays a more important role in HR rather than NHEJ or rather repair of single-sided DSB rather than double-sided DSB.

Alongside these suggested studies, and in order to consider whether PIF1 might be a potential clinical target, it is essential to assess for PIF1 sensitivity in normal tissue cell lines. High levels of sensitisation in normal tissue cell lines may preclude PIF1 from use as a clinical target. However, should PIF1 depletion sensitise to both irradiation and ICL drug treatment, there may be a significant role for drug targeting of PIF1 in the management of tumours, such as lung cancer, that are targeted with both treatment modalities prior to surgical resection (Feliciano et al., 2013).

In order to consider drug targeting of PIF1, detailed further studies would be needed to assess the structure of the helicase to allow identification of specific sites for small molecule inhibitors targeting. Specific inhibition of DNA helicases is an area of interest for cancer drug targeting (Gupta and Brosh, 2008) and offers, along with the specific inhibition of DNA damage repair proteins (Madhusudan and Hickson, 2005; Belzile et al., 2006), an opportunity to improve clinical outcomes from treatment with DNA damaging agents.

# Appendix

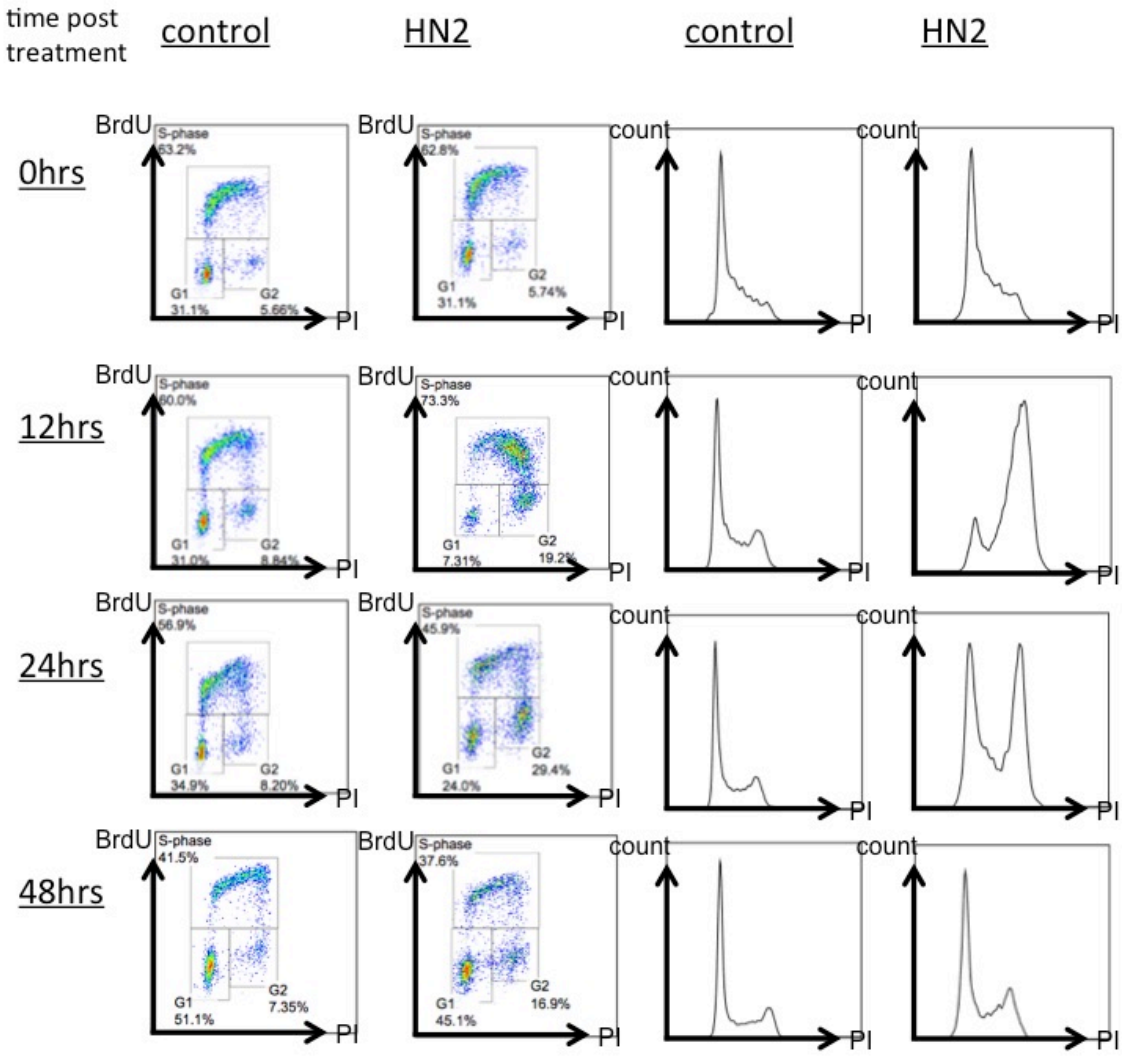



**Figure 5.2: Cell cycle assessment with BrdU and PI staining of asynchronous WT CHO cells following treatment with 5µM HN2.**

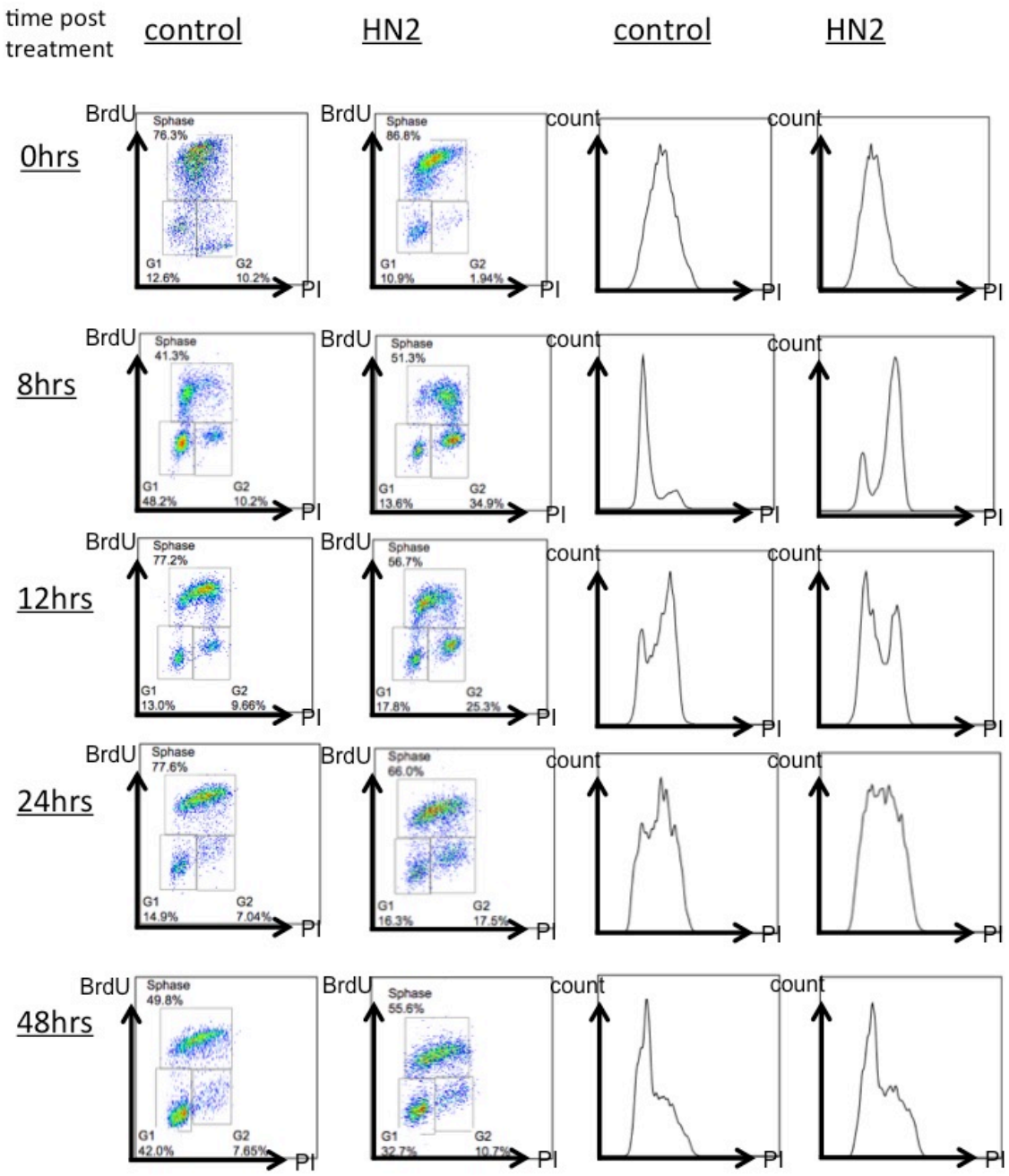



**Figure 5.3: Cell cycle assessment with BrdU and PI staining of S-phase synchronised WT CHO cells following treatment with 5µM HN2.**

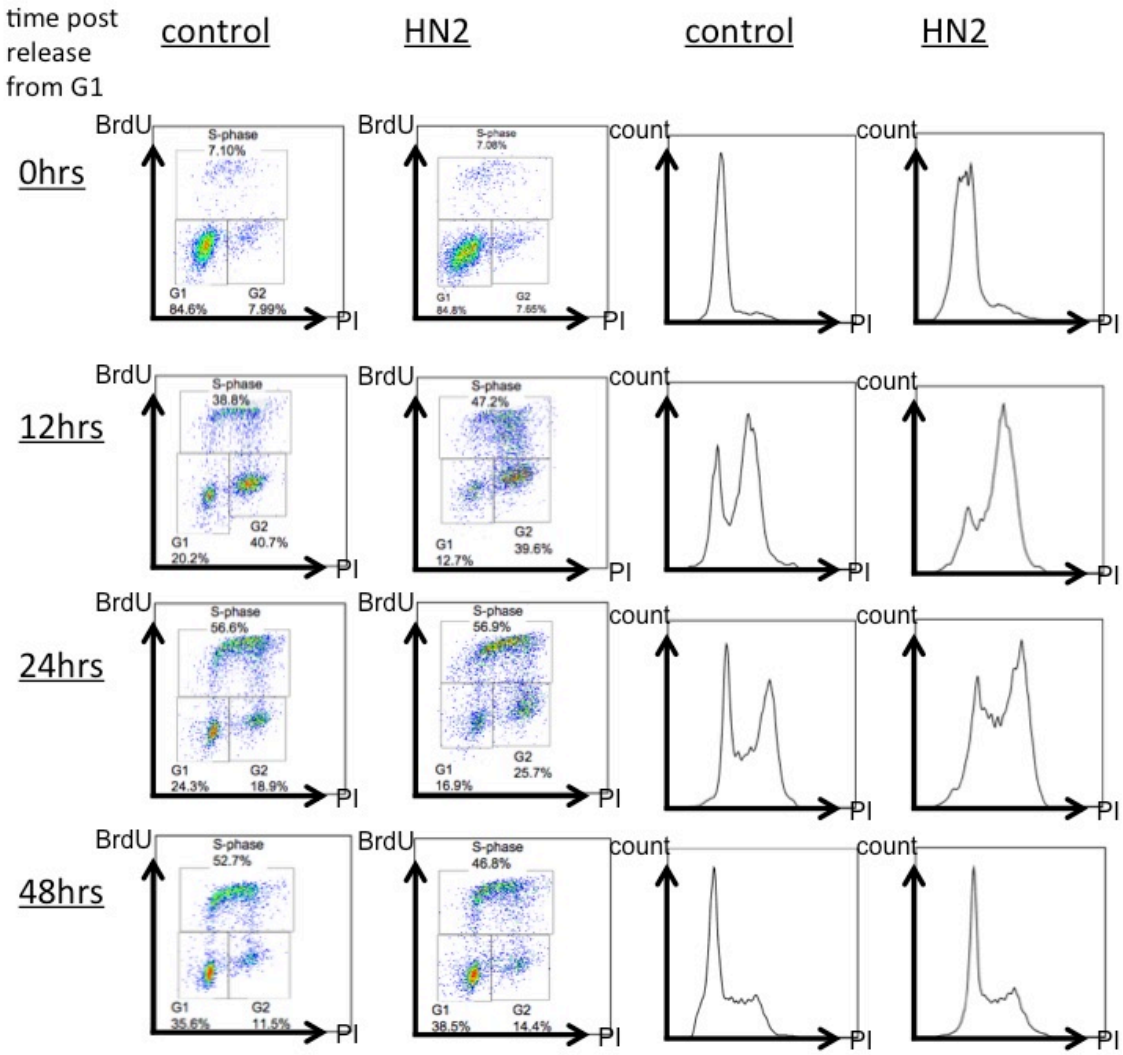



**Figure 5.4: Cell cycle assessment with BrdU and PI staining of G1 synchronised WT CHO cells following treatment with 5µM HN2 and immediate release to cell cycle.**

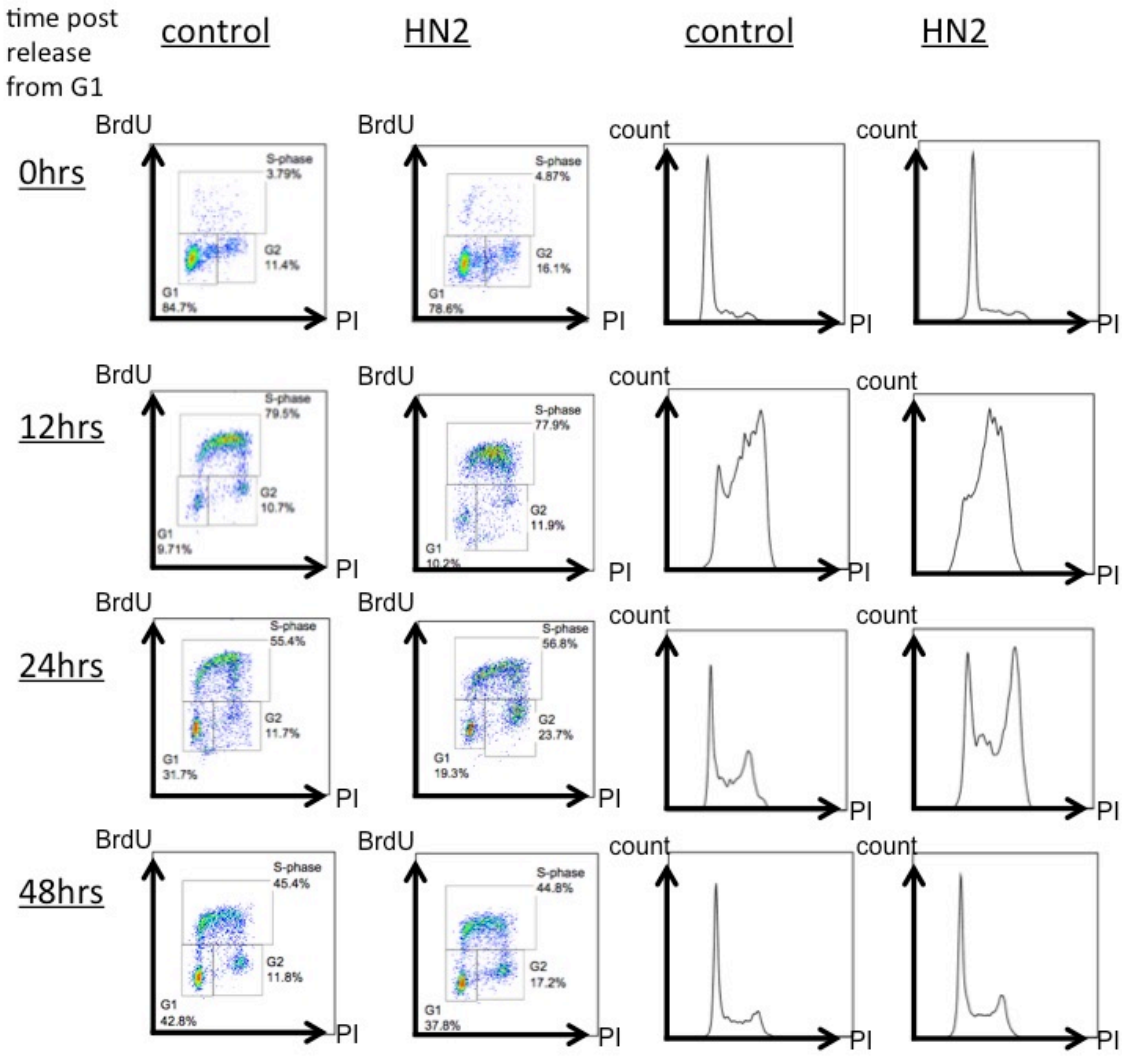



**Figure 5.5: Cell cycle assessment with BrdU and PI staining of G1 synchronised WT CHO cells following treatment with 5µM HN2 and holding in G1 for 12 hours prior to release to cell cycle.**

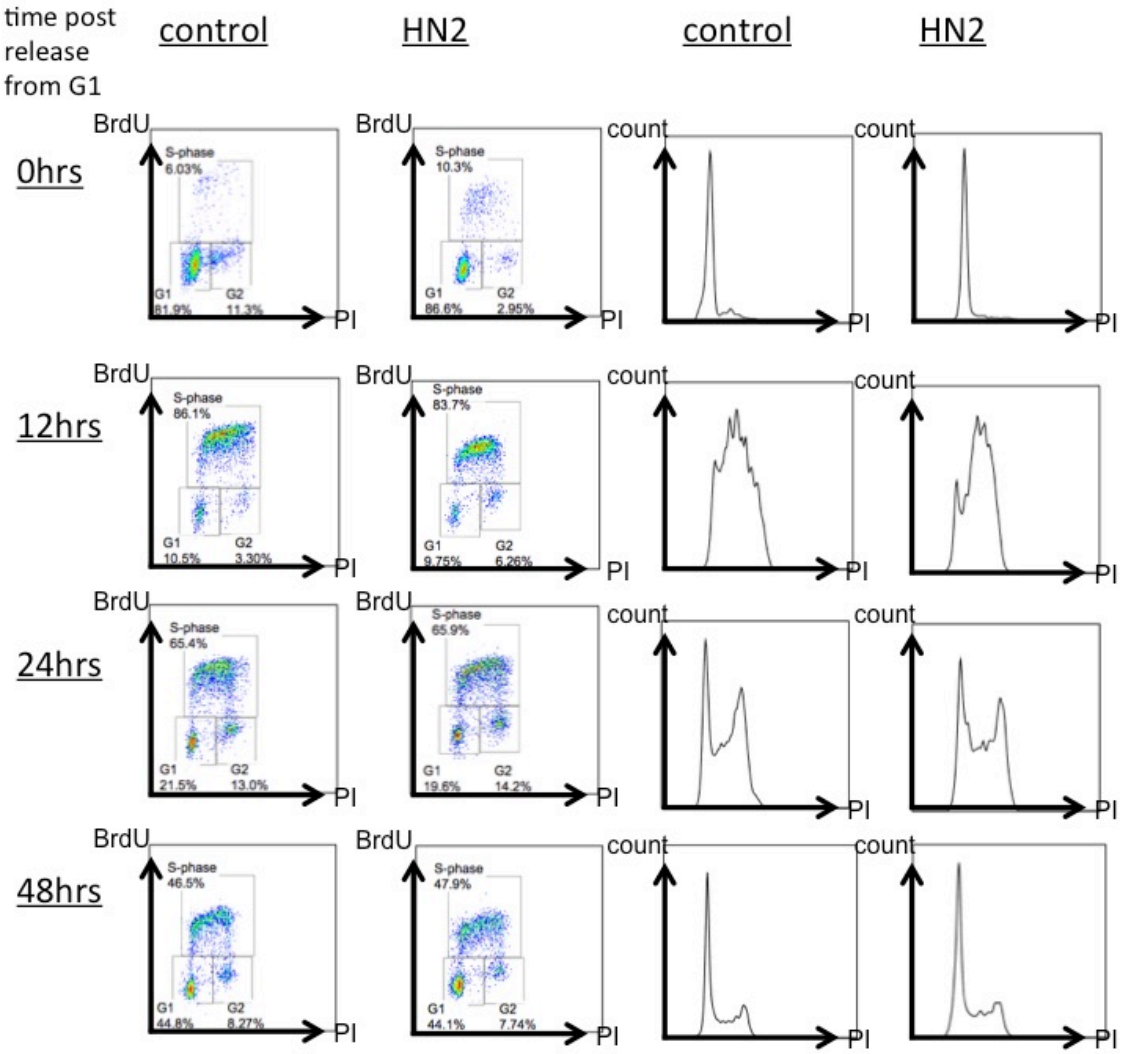



**Figure 5.6: Cell cycle assessment with BrdU and PI staining of G1 synchronised WT CHO cells following treatment with 5µM HN2 and holding in G1 for 24 hours prior to release to cell cycle.**

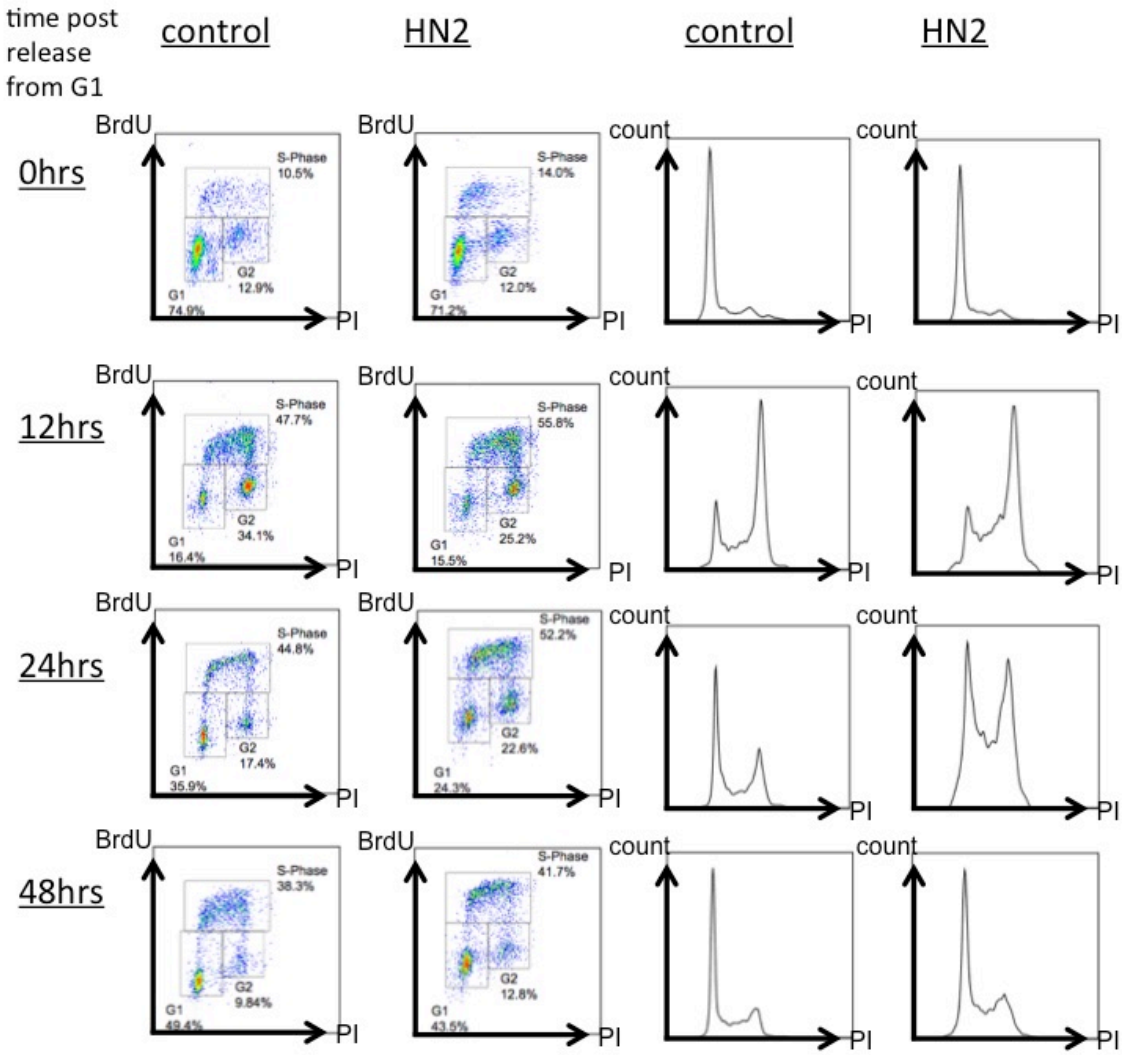



**Figure 5.7: Cell cycle assessment with BrdU and PI staining of G1 synchronised XPB mutated CHO cells following treatment with 5µM HN2 and holding in G1 for 24 hours prior to release to cell cycle.**

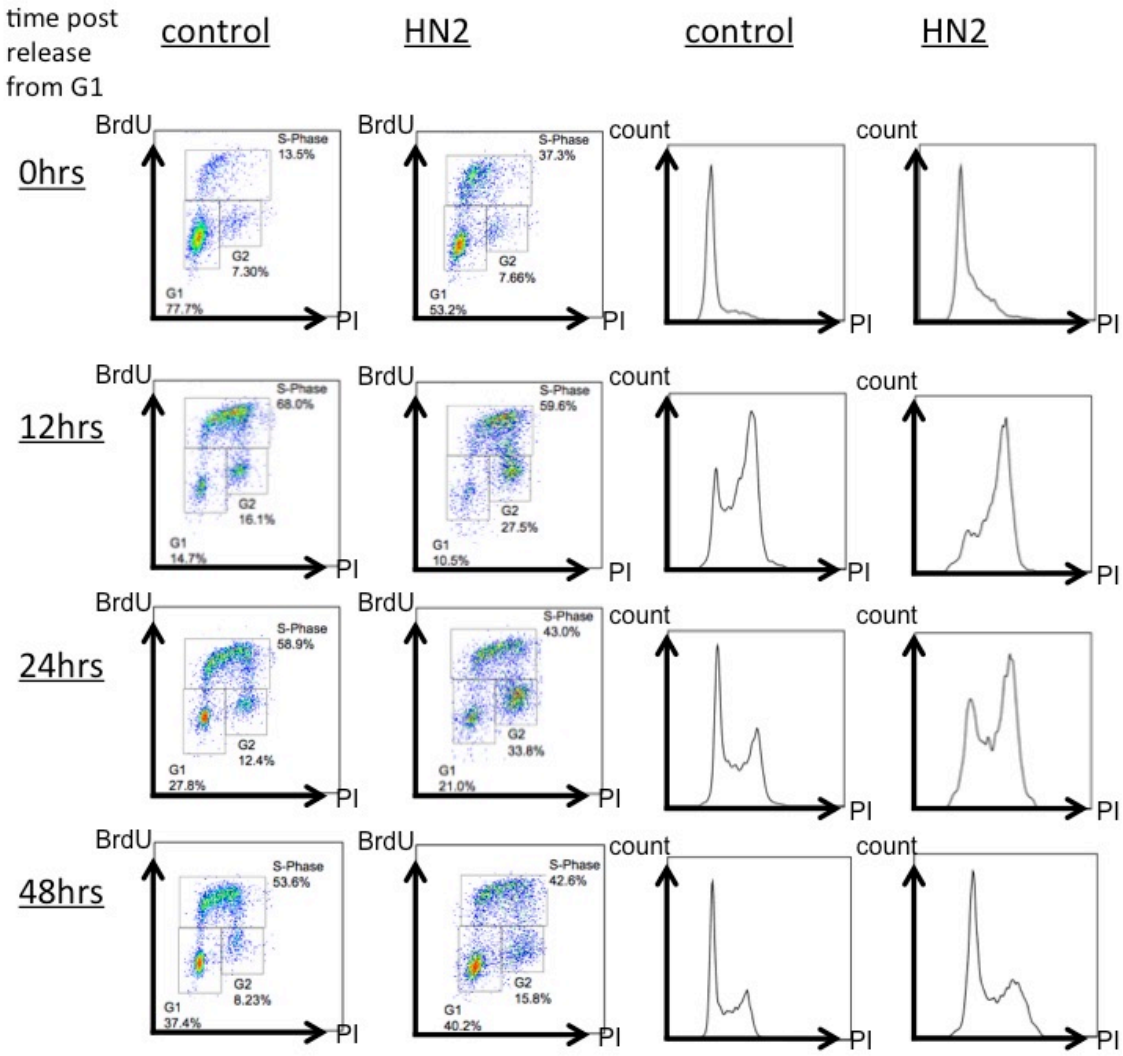



**Figure 5.8: Cell cycle assessment with BrdU and PI staining of G1 synchronised XPD mutated CHO cells following treatment with 5µM HN2 and holding in G1 for 24 hours prior to release to cell cycle.**

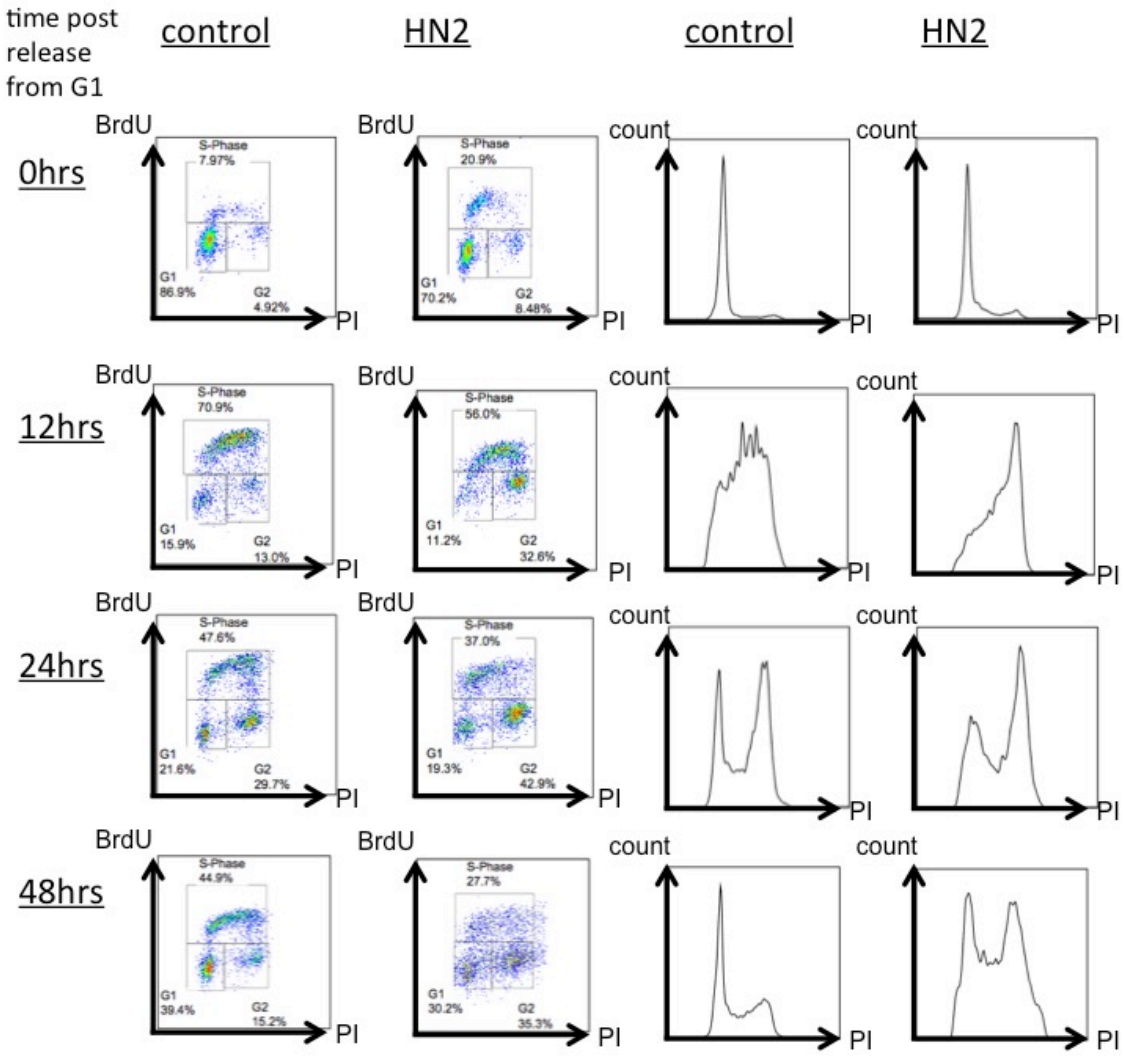



**Figure 5.9: Cell cycle assessment with BrdU and PI staining of G1 synchronised XPF mutated CHO cells following treatment with 5µM HN2 and holding in G1 for 24 hours prior to release to cell cycle.**

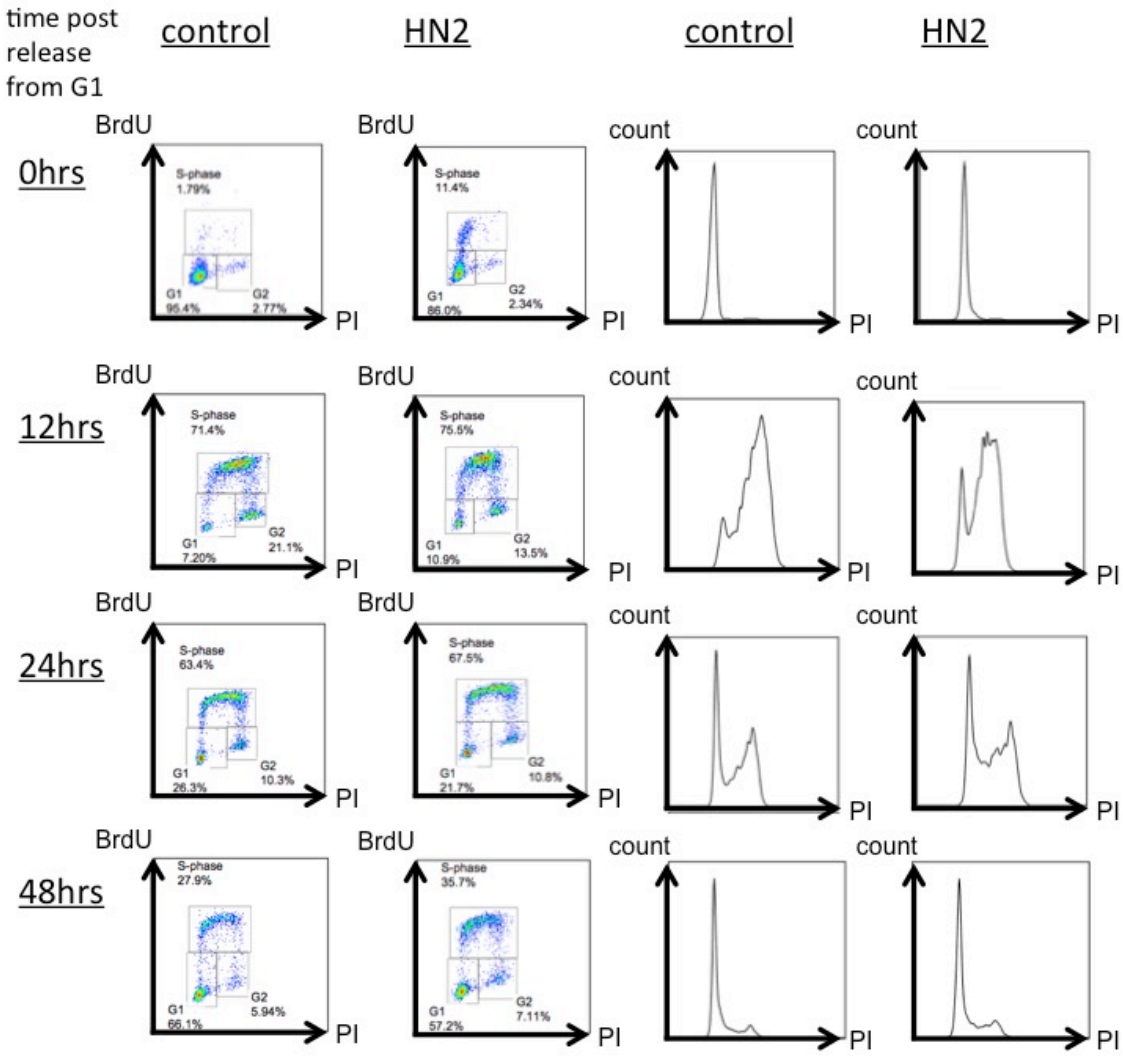



**Figure 5.10: Cell cycle assessment with BrdU and PI staining of G1 synchronised CSB mutated CHO cells following treatment with 5µM HN2 and holding in G1 for 24 hours prior to release to cell cycle.**

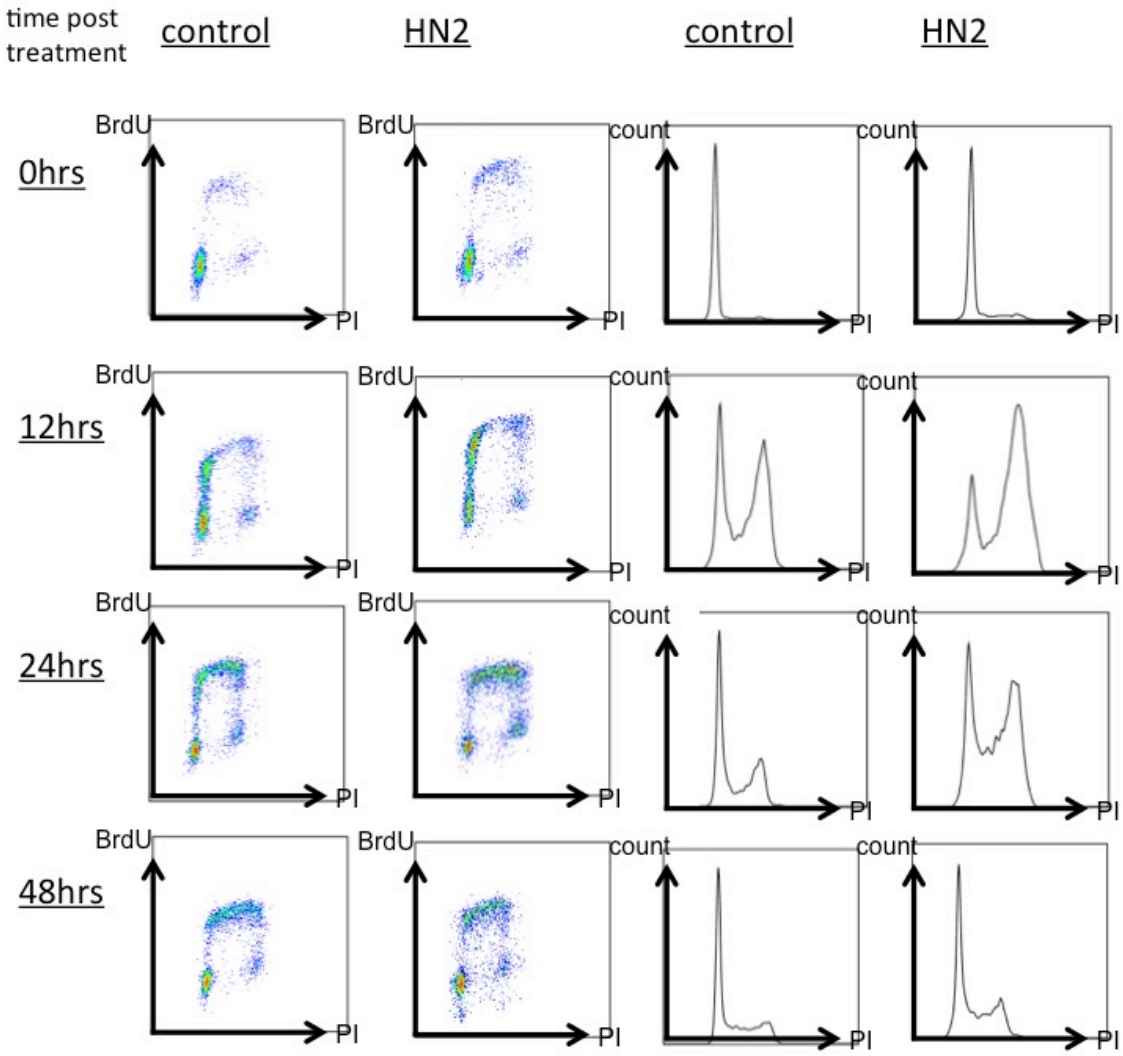



**Figure 5.11: Cell cycle assessment with BrdU and PI staining of G1 synchronised CSB mutated CHO cells following treatment with 5µM HN2 and immediate release to cell cycle.**

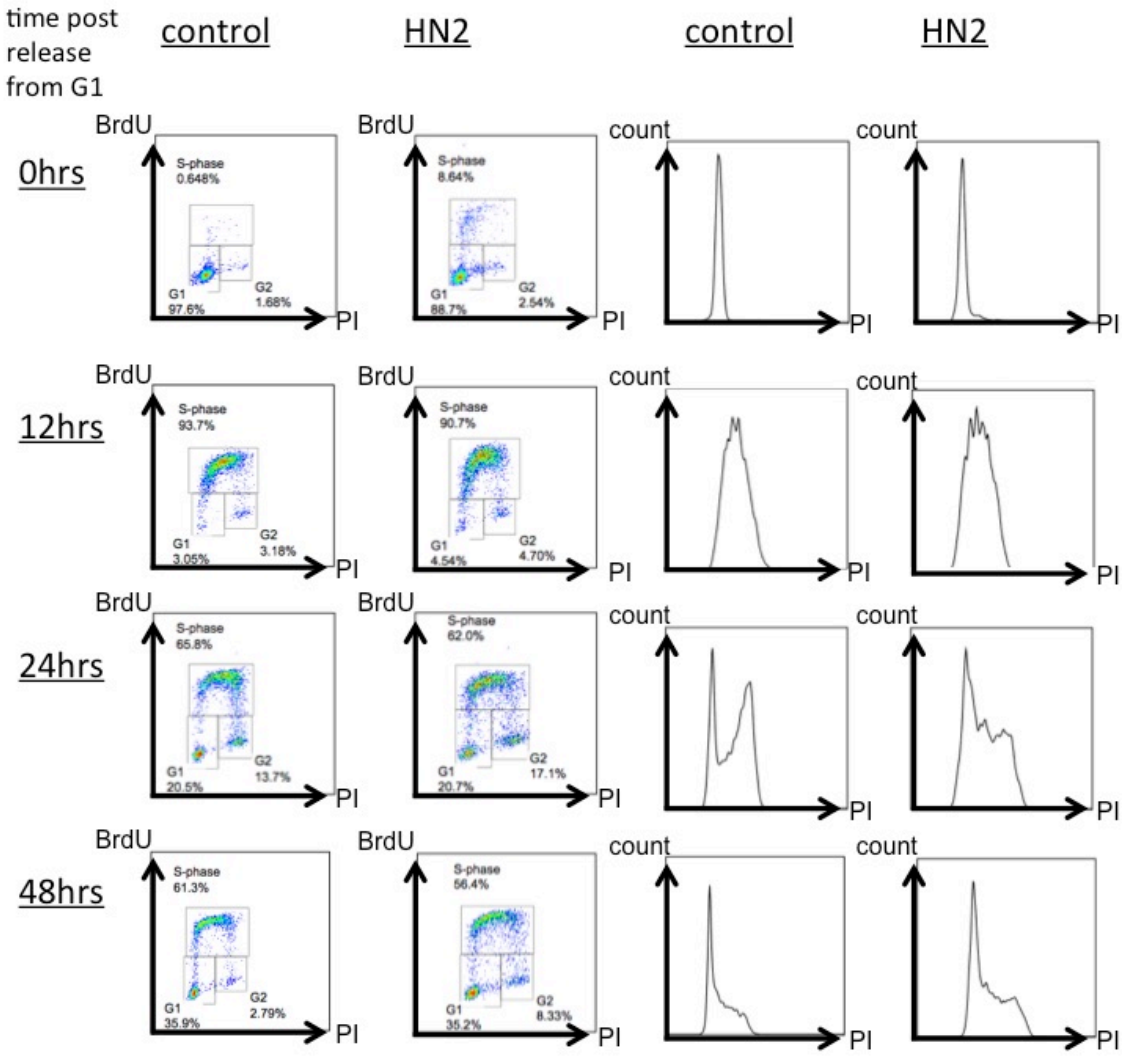



**Figure 5.12: Cell cycle assessment with BrdU and PI staining of G1 synchronised XPG mutated CHO cells following treatment with 5µM HN2 and holding in G1 for 24 hours prior to release to cell cycle.**

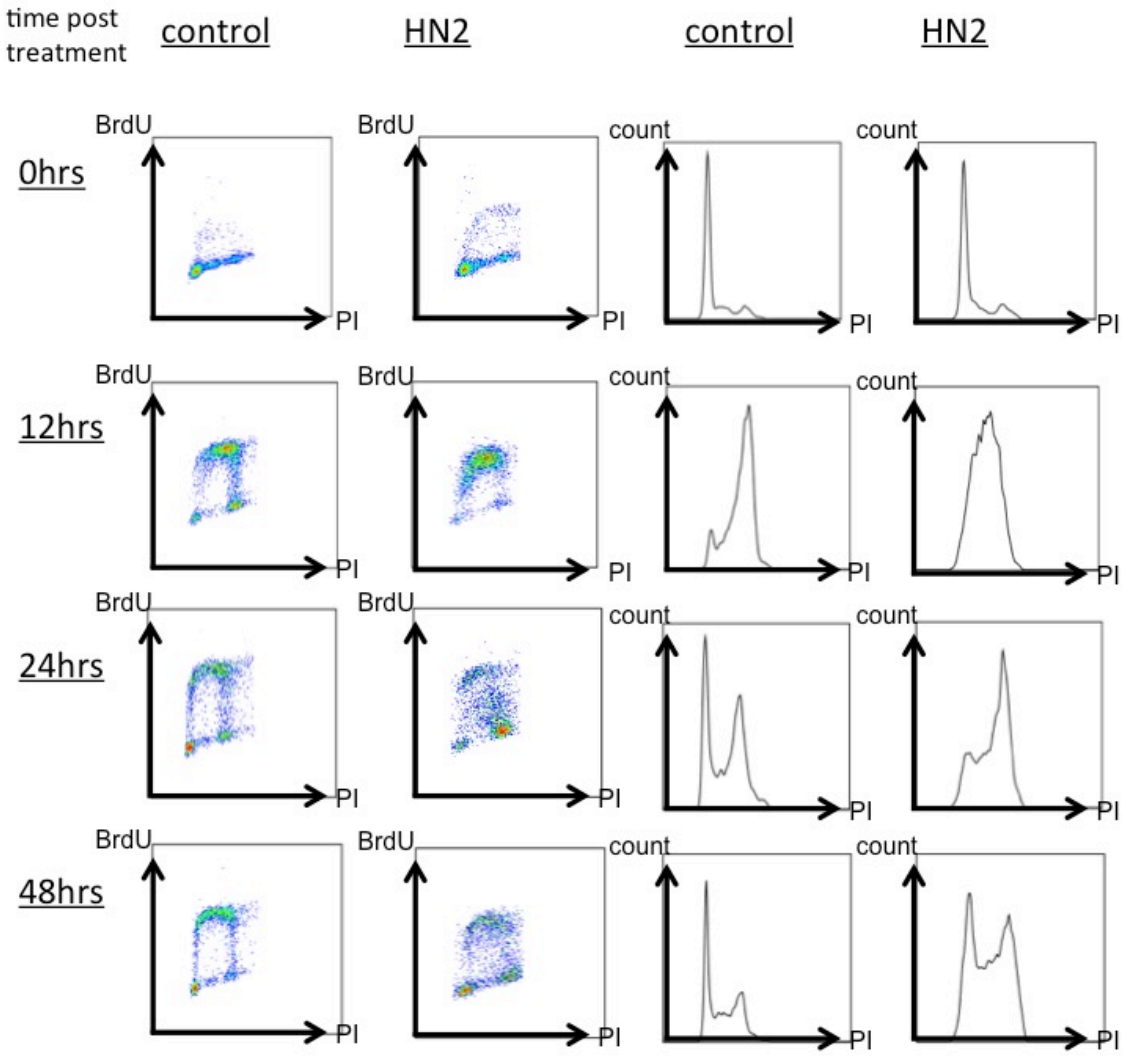



**Figure 5.13: Cell cycle assessment with BrdU and PI staining of G1 synchronised XPG mutated CHO cells following treatment with 5µM HN2 and immediate release to cell cycle.**

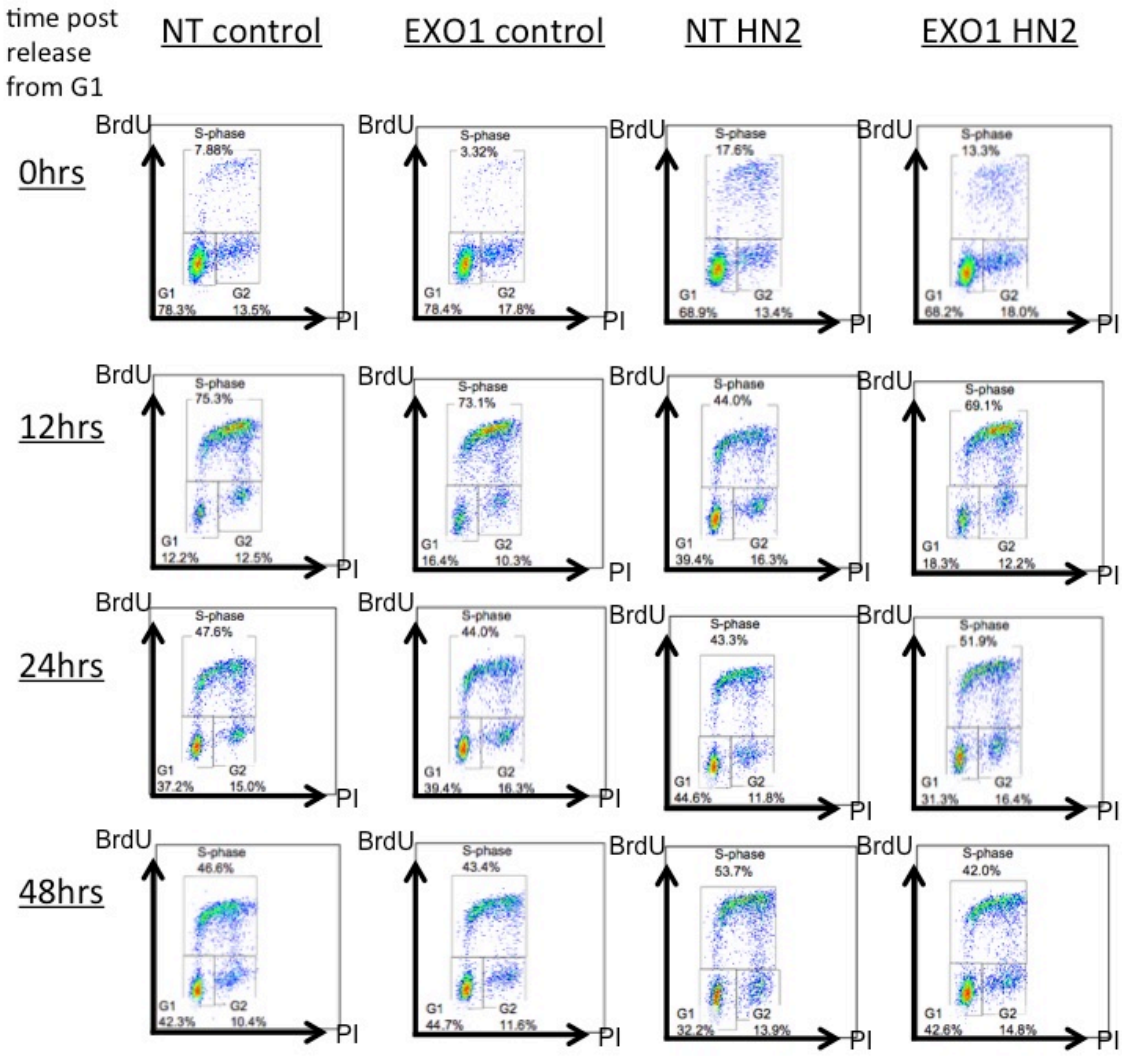



**Figure 5.14: Cell cycle assessment with BrdU and PI staining of G1 synchronised and EXO1 siRNA suppressed CHO cells following treatment with 5µM HN2 and holding in G1 for 24 hours prior to release to cell cycle.**

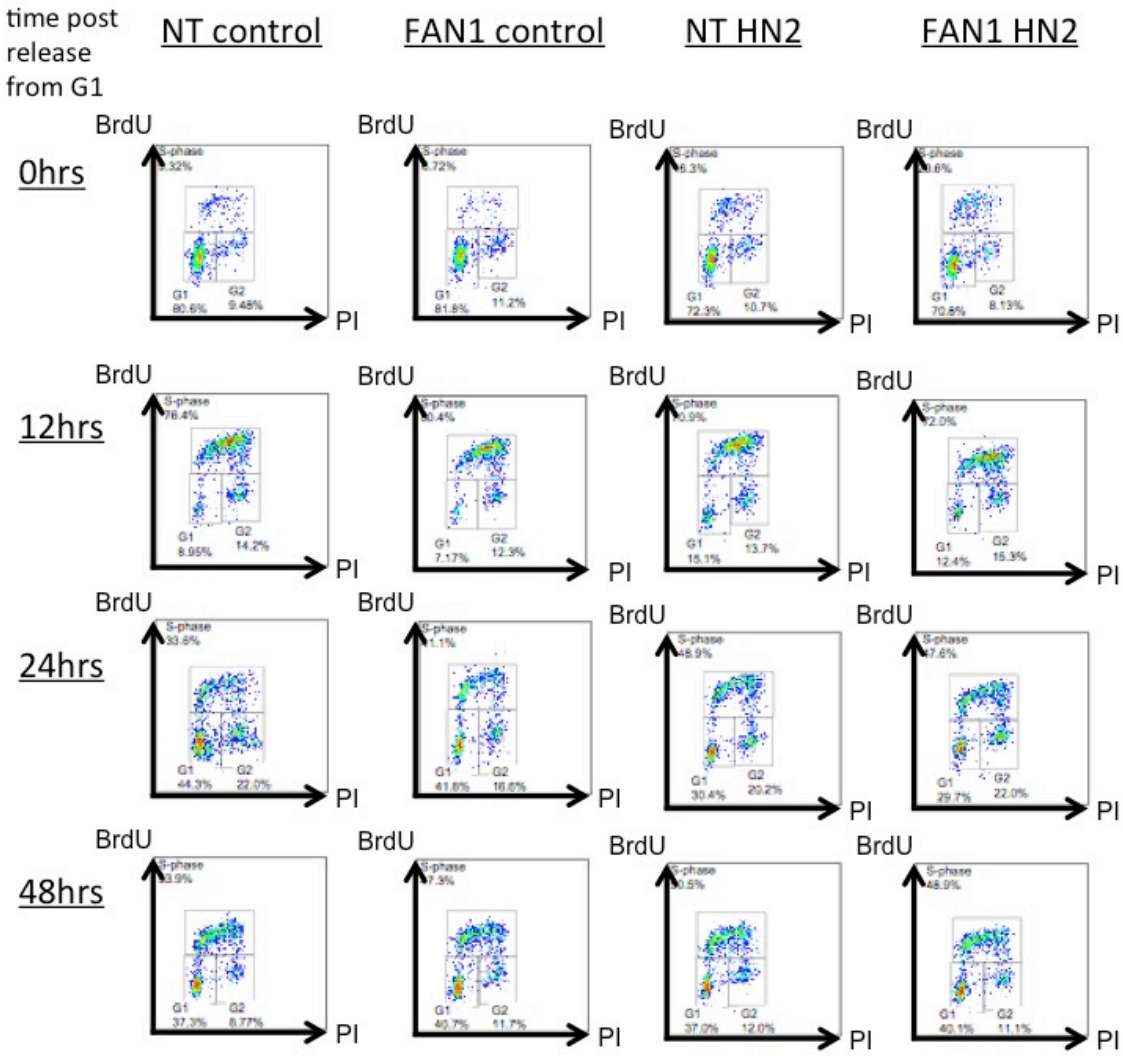



**Figure 5.15: Cell cycle assessment with BrdU and PI staining of G1 synchronised and FAN1 siRNA suppressed CHO cells following treatment with 5μM HN2 and holding in G1 for 24 hours prior to release to cell cycle.**

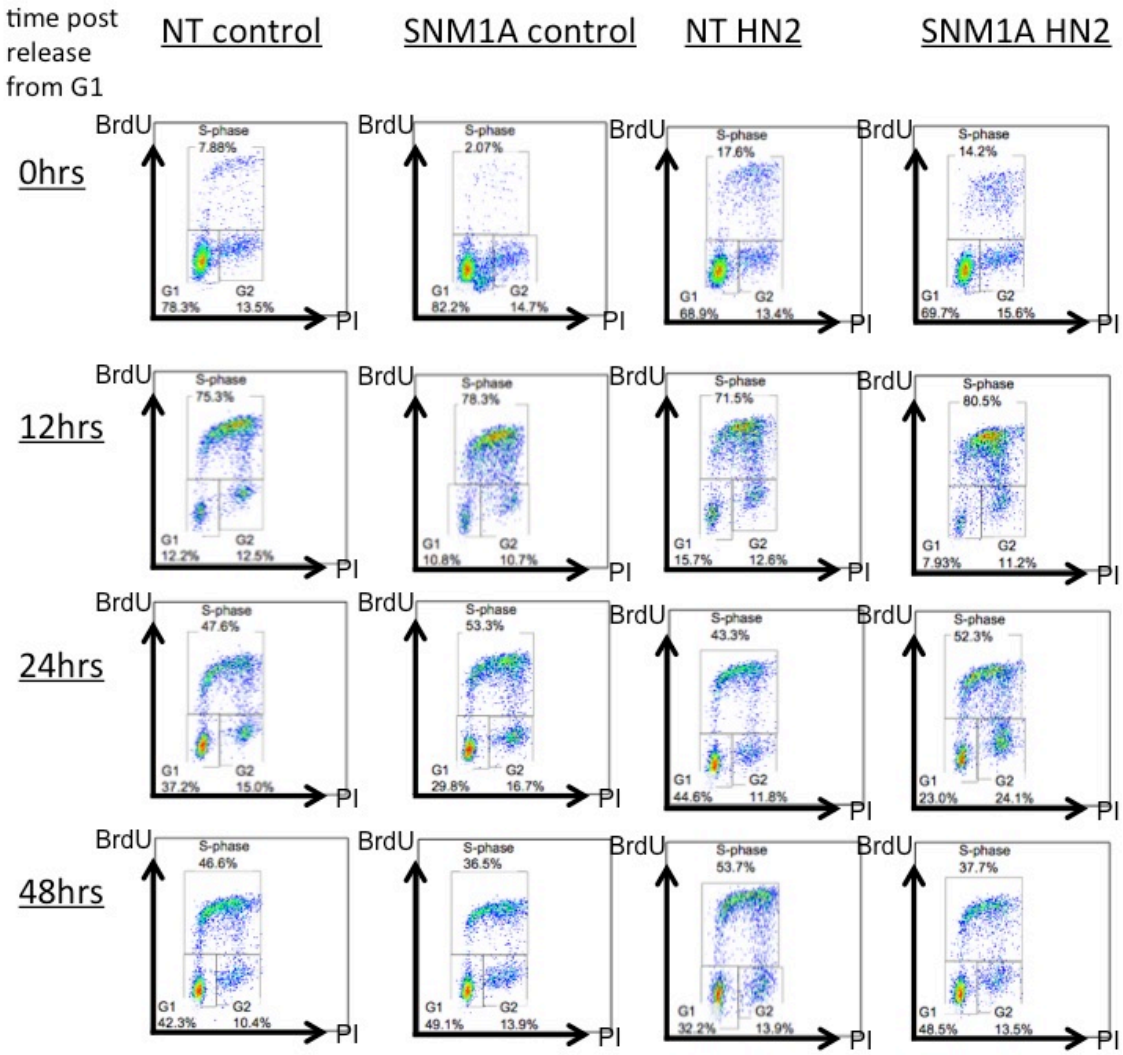



**Figure 5.16: Cell cycle assessment with BrdU and PI staining of G1 synchronised and SNM1A siRNA suppressed CHO cells following treatment with 5μM HN2 and holding in G1 for 24 hours prior to release to cell cycle.**

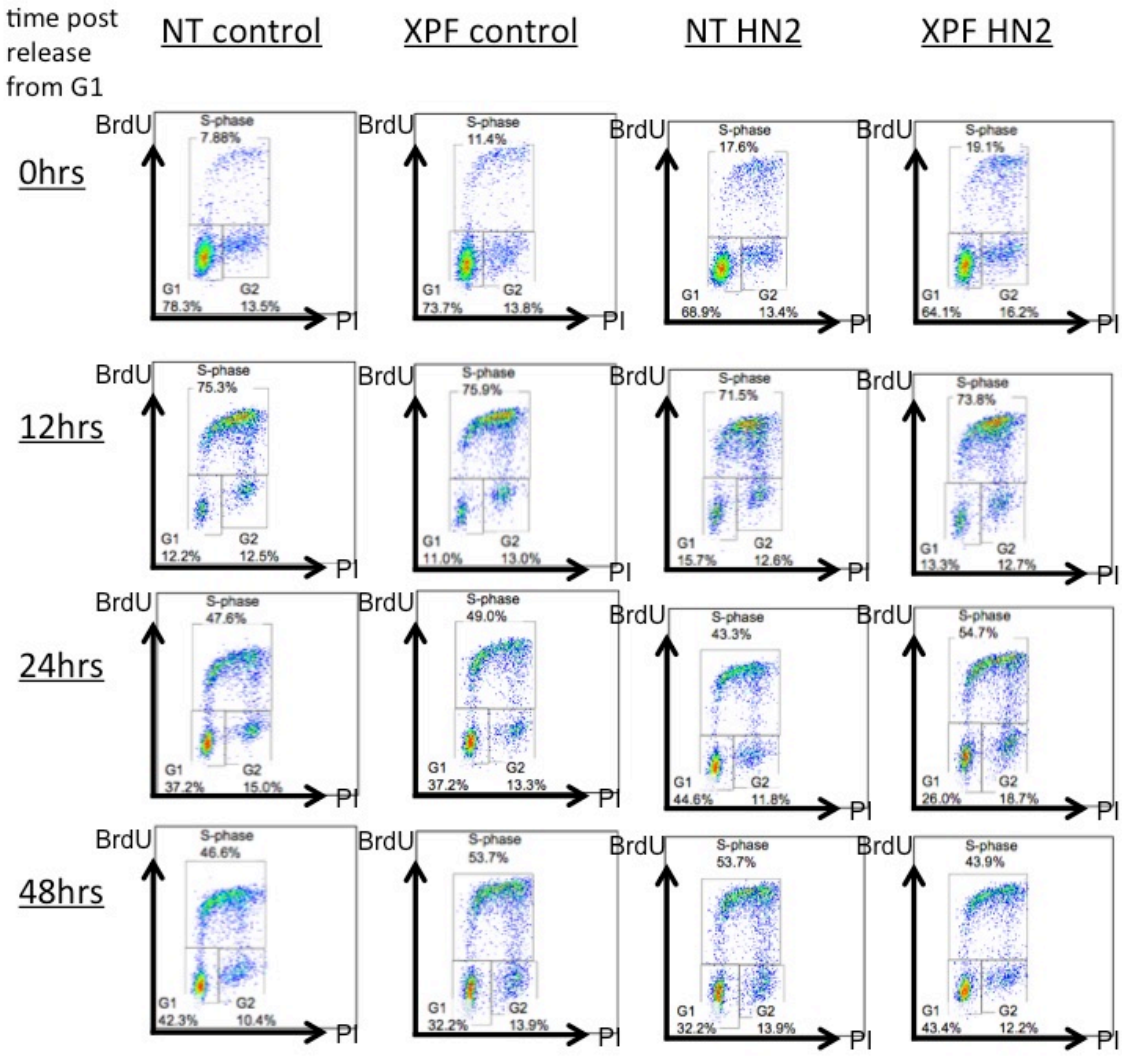



**Figure 5.17: Cell cycle assessment with BrdU and PI staining of G1 synchronised and XPF1 siRNA suppressed CHO cells following treatment with 5μM HN2 and holding in G1 for 24 hours prior to release to cell cycle.**

**Table 5.1: List of genes from primary siRNA screen and their respective Z scores for sensitisation to radiation.**

| Gene | Z Score Rep A | Z Score Rep B | Rank A | Rank B | Ranked product |
|---|---|---|---|---|---|
| **ABL1** | -2.101752388 | 1.068307762 | 172 | 268 | 23265 |
| **ACD** | -2.547558399 | -6.096976251 | 156 | 1000 | 135000 |
| **ACLY** | -2.315848835 | 0.156701426 | 164 | 229 | 110004 |
| **ADI1** | 0.637151086 | 0.829076809 | 284 | 257 | 35112 |
| **ADO** | 1.472052325 | 1.332982541 | 306 | 278 | 102442 |
| **AHCY** | -2.678238899 | 0.129865817 | 149 | 228 | 24167 |
| **AKT1** | -0.349796662 | -0.832921692 | 244 | 183 | 23214 |
| **AKT2** | 3.452340881 | -0.183811008 | 385 | 215 | 88368 |
| **ALKBH1** | -5.13285244 | -5.748852946 | 54 | 1000 | 327000 |
| **ALKBH2** | 5.015313076 | 6.568697104 | 1000 | 1000 | 1000000 |
| **ALKBH3** | 0.40003026 | 0.023314595 | 271 | 222 | 137772 |
| **ALKBH4** | 3.81933807 | 2.518041154 | 398 | 321 | 84084 |
| **ALKBH5** | -5.641 | -3.795 | 36 | 58 | 4440 |
| **ALKBH6** | 0.568010487 | -2.206506123 | 280 | 1000 | 151000 |
| **ALKBH7** | -3.798432055 | UC | 1000 | 1000 | 1000000 |
| **ALKBH8** | -5.468082757 | -5.130262506 | 43 | 25 | 154 |
| **APEX1** | -1.124062865 | -0.748757536 | 216 | 189 | 2294 |
| **APEX2** | -4.118127101 | -6.02121884 | 94 | 1000 | 276000 |
| **APTX** | 5.062968038 | 0.180054308 | 435 | 231 | 108916 |
| **ARID1A** | -7.440457215 | -4.811045619 | 1000 | 1000 | 1000000 |
| **ARID1B** | -5.044634764 | -2.509834054 | 58 | 105 | 43166 |
| **ARID3A** | 6.747679406 | 0.203116135 | 468 | 232 | 122008 |
| **ARID3B** | -0.876846068 | 3.551842124 | 222 | 367 | 47040 |
| **ARID4A** | -2.988 | -6.071 | 137 | 12 | 114 |
| **ARID4B** | -2.62182937 | -2.986527214 | 152 | 1000 | 306000 |
| **ARID5A** | 5.604172584 | 5.766508162 | 449 | 403 | 84091 |
| **ARID5B** | 1.472445087 | 2.936069334 | 307 | 336 | 15600 |
| **ASF1A** | -0.728991431 | 1.937056199 | 230 | 1000 | 247000 |
| **ASF1B** | -0.430377701 | 0.040576139 | 239 | 223 | 126720 |
| **ASPH** | -0.235803108 | -1.036730823 | 249 | 174 | 12905 |
| **ASPHD1** | 16.38699321 | 18.21278572 | 476 | 1000 | 112000 |
| **ASPHD2** | -4.292097126 | -5.957296952 | 87 | 1000 | 160000 |
| **ATAD5** | -4.445 | -4.628 | 79 | 35 | 2508 |
| **ATF4** | 3.524883256 | 1.907437544 | 388 | 291 | 5609 |
| **ATM** | -6.092271001 | -4.517774395 | 30 | 38 | 6380 |
| **ATR** | -5.414453183 | -1.718177265 | 1000 | 138 | 15000 |
| **ATRIP** | -6.385953562 | -2.94115976 | 1000 | 1000 | 1000000 |
| **BAZ1A** | 0.68842591 | -2.354109112 | 285 | 112 | 84735 |
| **BAZ1B** | -10.26723582 | UC | 1000 | 1000 | 1000000 |
| **BAZ2A** | -2.144755521 | -1.886361162 | 170 | 131 | 54080 |
| **BAZ2B** | -0.388 | -1.257 | 241 | 161 | 455 |
| **BBOX1** | -2.603524934 | UC | 1000 | 1000 | 1000000 |
| **BLM** | -1.733031871 | -4.255044883 | 189 | 45 | 87216 |
| **BRCA1** | 9.271599538 | -4.142457675 | 1000 | 1000 | 1000000 |

| | | | | | |
|---|---|---|---|---|---|
| **BRCA2** | 0.686353698 | -2.829146447 | 1000 | 93 | 20000 |
| **BRD1** | 4.083692348 | -0.890318036 | 408 | 181 | 65932 |
| **BRD2** | -2.075252983 | -4.961614596 | 175 | 1000 | 8000 |
| **BRD3** | 0.092140814 | -0.720213915 | 258 | 192 | 102808 |
| **BRD4** | 2.403522061 | -5.108247529 | 1000 | 1000 | 342000 |
| **BRD7** | 2.026501393 | -1.291523088 | 325 | 158 | 63109 |
| **BRD8** | -1.665032312 | -5.052221619 | 195 | 27 | 3454 |
| **BRD9** | 3.369701848 | 2.088768807 | 378 | 301 | 145635 |
| **BRDT** | -5.520022489 | -2.91938297 | 42 | 87 | 72158 |
| **BRIP1** | 1.053860407 | 3.507466607 | 295 | 365 | 7476 |
| **BTAF1** | 1.967001438 | 2.136726833 | 321 | 307 | 133221 |
| **BTBD12** | -0.07886989 | -0.649040413 | 1000 | 197 | 84000 |
| **BUB3** | -3.174226809 | -7.336287225 | 1000 | 1000 | 1000000 |
| **C14orf169** | -5.658213138 | -2.092226668 | 1000 | 1000 | 1000000 |
| **C17orf101** | -2.276360581 | -2.362341743 | 1000 | 1000 | 1000000 |
| **C19orf40** | 4.881069697 | 3.816540587 | 432 | 374 | 62604 |
| **C2orf60** | -4.842261754 | -2.283921237 | 68 | 1000 | 106000 |
| **C9orf102** | -0.095313102 | -2.960947348 | 253 | 86 | 20940 |
| **CANX** | -5.020696697 | -2.911005224 | 60 | 89 | 42846 |
| **CARM1** | 0.746022684 | 0.916762427 | 289 | 1000 | 309000 |
| **CBX3** | 4.184866086 | -0.018415639 | 411 | 220 | 10209 |
| **CCNA1** | -0.946506364 | -4.123320245 | 219 | 1000 | 55000 |
| **CCNA2** | -2.874162983 | 2.127311174 | 1000 | 305 | 273000 |
| **CCNB1** | -1.124840808 | -2.759049618 | 215 | 96 | 59860 |
| **CCNB2** | 1.814838996 | 3.406863236 | 318 | 360 | 163618 |
| **CCNB3** | 2.650156699 | 4.403098612 | 350 | 1000 | 348000 |
| **CCND1** | -2.658 | -3.617 | 151 | 62 | 3564 |
| **CCND2** | 5.989485462 | 2.467677636 | 461 | 318 | 71677 |
| **CCND3** | -3.444150458 | -2.323230205 | 1000 | 1000 | 1000000 |
| **CCNE1** | 0.768587854 | 0.01057123 | 290 | 221 | 67626 |
| **CCNE2** | 2.242645186 | 2.956566861 | 335 | 338 | 74888 |
| **CCNH** | -0.436375263 | -0.931830014 | 1000 | 178 | 55000 |
| **CCRN4L** | -2.240632841 | UC | 1000 | 1000 | 1000000 |
| **CCT4** | -5.787636628 | UC | 1000 | 1000 | 1000000 |
| **CCT5** | -4.891716789 | UC | 1000 | 1000 | 1000000 |
| **CDC2** | -0.497818142 | -0.515541176 | 1000 | 1000 | 1000000 |
| **CDK2** | -7.010763261 | -2.810008168 | 1000 | 95 | 39000 |
| **CDK4** | 3.564379588 | -0.324485537 | 391 | 211 | 38016 |
| **CDK6** | -2.101752388 | -1.137856684 | 173 | 168 | 68136 |
| **CDK7** | 0.551403327 | 0.117564765 | 276 | 227 | 145668 |
| **CDKN3** | 3.790816878 | -0.511118107 | 396 | 202 | 63960 |
| **CDO1** | 4.437060443 | 0.082874028 | 419 | 225 | 110490 |
| **CDYL** | 5.258150309 | 4.156360407 | 439 | 389 | 106353 |
| **CENPA** | -8.406394358 | -4.205164474 | 1000 | 48 | 80000 |
| **CETN2** | 2.510804498 | 1.029660817 | 345 | 267 | 131596 |
| **CFDP1** | -2.912 | -0.733 | 141 | 191 | 1872 |
| **CHAF1A** | -3.368653063 | UC | 1000 | 1000 | 1000000 |
| **CHAF1B** | -0.83156866 | -2.979843875 | 223 | 85 | 51684 |

| | | | | | |
|---|---|---|---|---|---|
| **CHD1** | -3.048067737 | -1.455234682 | 133 | 149 | 24563 |
| **CHD2** | 5.463365847 | 0.898594938 | 446 | 261 | 128478 |
| **CHD3** | -4.918045786 | 0.59022605 | 65 | 247 | 57750 |
| **CHD4** | -3.120 | -1.448 | 127 | 150 | 1914 |
| **CHD5** | -1.887 | -5.774 | 185 | 17 | 19928 |
| **CHD6** | 3.4817132 | 1.98598132 | 387 | 293 | 52452 |
| **CHD7** | -6.158723009 | -4.149635773 | 26 | 50 | 68580 |
| **CHD8** | -3.696838026 | -3.846596215 | 106 | 57 | 1089 |
| **CHD9** | -4.234154589 | -1.977947214 | 89 | 125 | 116382 |
| **CHEK1** | 1.467057707 | 1.023433603 | 305 | 266 | 107450 |
| **CHEK2** | 4.171973329 | 4.134629358 | 410 | 387 | 167280 |
| **CHRAC1** | -7.088 | -3.635 | 13 | 61 | 1404 |
| **CHTF18** | -1.984929094 | -0.298005673 | 179 | 1000 | 246000 |
| **CITED1** | -2.077143262 | -1.117665521 | 174 | 170 | 34040 |
| **CITED2** | -0.493564853 | -1.816665954 | 237 | 135 | 31850 |
| **CITED4** | -7.605785129 | -2.549344487 | 1000 | 1000 | 1000000 |
| **CKS2** | 3.03978874 | -0.914981319 | 366 | 180 | 1872 |
| **CLK2** | 0.325246351 | 1.177862346 | 268 | 273 | 18156 |
| **CLSPN** | -6.192191231 | -2.524018712 | 1000 | 1000 | 175000 |
| **COL1A2** | -2.16223745 | 0.041045963 | 1000 | 224 | 36000 |
| **COPB2** | -10.26723582 | UC | 1000 | 1000 | 1000000 |
| **CRIP2** | 0.198393233 | -0.035049518 | 260 | 219 | 25704 |
| **CSNK2A1** | 2.124844323 | -0.3815644 | 330 | 208 | 96815 |
| **CUL1** | -3.684304675 | -3.699420553 | 107 | 1000 | 47000 |
| **CUL3** | -9.44612394 | -8.034758308 | 1000 | 1000 | 1000000 |
| **CUL4A** | 2.229686462 | -0.834156419 | 334 | 182 | 40851 |
| **CUL4B** | 2.806153339 | 3.335339205 | 358 | 354 | 42770 |
| **DCLRE1A** | 5.411361356 | -0.774326773 | 443 | 187 | 96380 |
| **DCLRE1B** | -5.016089235 | -6.549125398 | 61 | 1000 | 38000 |
| **DCLRE1C** | -5.220 | -6.498 | 53 | 7 | 24684 |
| **DDB1** | 0.459967905 | -6.044377302 | 1000 | 1000 | 1000000 |
| **DDB2** | 3.371324102 | 3.916051841 | 379 | 377 | 94794 |
| **DHX58** | 1.627691212 | 0.531183641 | 311 | 242 | 103617 |
| **DMC1** | -2.017557843 | -0.845892235 | 177 | 1000 | 120000 |
| **DNMT1** | 1.241941171 | 2.331252835 | 300 | 314 | 24310 |
| **DNMT3A** | -0.306260932 | -2.593716765 | 1000 | 100 | 99000 |
| **DNMT3B** | -5.606596194 | -3.395524385 | 38 | 67 | 19712 |
| **DOT1L** | 5.031630126 | 2.876959272 | 434 | 334 | 26730 |
| **DSCC1** | -5.999857421 | -5.569239862 | 32 | 1000 | 34000 |
| **DUT** | -2.09412822 | 1.786629933 | 1000 | 288 | 199000 |
| **DVL3** | -3.582897409 | 0.832089516 | 113 | 258 | 6096 |
| **E2F5** | -3.008533627 | -2.654034122 | 135 | 98 | 45248 |
| **ECT2** | -4.074599478 | -0.769867638 | 1000 | 188 | 31000 |
| **EGFR** | -1.972141539 | -0.1412815 | 181 | 217 | 35638 |
| **EGLN1** | 2.201532883 | 3.414362052 | 332 | 361 | 155540 |
| **EGLN2** | -7.637980097 | -1.795100086 | 1000 | 1000 | 1000000 |
| **EGLN3** | 3.264802327 | 1.008694387 | 372 | 265 | 88298 |
| **EHMT1** | 7.867436183 | 3.192680746 | 472 | 351 | 120765 |

| | | | | | |
|---|---|---|---|---|---|
| **EIF4A3** | -1.308037434 | UC | 1000 | 1000 | 1000000 |
| **EME1** | -5.457820847 | -4.038918067 | 46 | 51 | 12876 |
| **EME2** | -8.15017277 | 18.70663407 | 1000 | 1000 | 1000000 |
| **EP400** | -4.947830296 | -5.541804681 | 1000 | 1000 | 1000000 |
| **ERCC1** | -5.645145736 | -1.279525804 | 1000 | 160 | 29000 |
| **ERCC2** | -1.583308995 | -0.121780164 | 1000 | 218 | 69000 |
| **ERCC3** | -3.665072275 | -0.547762208 | 108 | 200 | 15200 |
| **ERCC4** | -3.874 | -2.249 | 102 | 115 | 2703 |
| **ERCC5** | -3.154414177 | -1.928927855 | 124 | 129 | 18745 |
| **ERCC6** | -10.26723582 | -5.049186799 | 1000 | 1000 | 1000000 |
| **ERCC8** | -4.400966103 | -3.396977324 | 83 | 66 | 16560 |
| **EXO1** | 3.845718107 | 2.442307932 | 400 | 317 | 128432 |
| **EZH2** | 3.361958808 | 2.117237932 | 376 | 303 | 59280 |
| **FANCA** | -3.957820236 | -1.182302309 | 100 | 165 | 2200 |
| **FANCB** | 3.266981842 | 0.91900313 | 373 | 262 | 40725 |
| **FANCC** | -2.805803548 | 0.094376746 | 146 | 226 | 13965 |
| **FANCD2** | -9.083063981 | -5.699377928 | 1000 | 19 | 12000 |
| **FANCE** | 3.390979187 | 1.809558557 | 381 | 290 | 45353 |
| **FANCF** | -2.200065162 | -1.851872631 | 169 | 132 | 70613 |
| **FANCG** | -5.547052599 | -3.252989307 | 41 | 72 | 37901 |
| **FANCI** | 0.173493101 | -0.378882969 | 259 | 209 | 750 |
| **FANCL** | -0.513389161 | -1.365710389 | 236 | 153 | 29890 |
| **FANCM** | -4.559429257 | -4.117259752 | 1000 | 1000 | 1000000 |
| **FAP** | -0.754690023 | -1.124756326 | 229 | 169 | 125164 |
| **FBXO18** | -4.937936719 | -2.587437638 | 63 | 101 | 21543 |
| **FEN1** | -6.648932977 | -6.213053659 | 1000 | 11 | 89000 |
| **FLJ35220** | 0.558127274 | -3.777220176 | 279 | 1000 | 11815 |
| **FOXO1** | -3.1999975 | -0.824321458 | 123 | 184 | 9464 |
| **FOXO3** | 2.198802402 | 1.950505061 | 331 | 292 | 92953 |
| **FTO** | -3.280927754 | -8.034758308 | 1000 | 1000 | 1000000 |
| **G3BP1** | -4.719424512 | -1.345119046 | 1000 | 157 | 64000 |
| **GADD45A** | 4.803416258 | 0.674421524 | 430 | 250 | 54784 |
| **GEN1** | 1.383058094 | 2.608339509 | 303 | 325 | 113553 |
| **GINS2** | -4.863678626 | -3.09679247 | 67 | 79 | 75348 |
| **GIYD2** | -0.373147438 | 0.261740158 | 242 | 234 | 83486 |
| **GTF2H1** | 0.357233313 | -1.206645692 | 269 | 163 | 91800 |
| **GTF2H2** | -6.093892346 | -4.876835372 | 29 | 32 | 28210 |
| **GTF2H3** | -2.947163763 | -5.259536838 | 139 | 23 | 13289 |
| **GTF2H4** | -3.436309908 | -2.385200316 | 1000 | 1000 | 1000000 |
| **GTF2H5** | -1.701 | 0.598 | 192 | 248 | 25 |
| **H2AFX** | -8.47192837 | -6.845377678 | 1000 | 1000 | 1000000 |
| **H2AFZ** | -0.529 | -3.231 | 235 | 73 | 1776 |
| **HAAO** | -0.792194083 | -0.968118106 | 226 | 177 | 44232 |
| **HAT1** | 2.372800609 | 5.752812886 | 340 | 402 | 100166 |
| **HDAC1** | -1.6101643 | -1.222851064 | 1000 | 1000 | 1000000 |
| **HDAC10** | 7.400284167 | 1.436151493 | 471 | 281 | 285000 |
| **HDAC11** | -1.363117696 | -2.357814675 | 208 | 111 | 4554 |
| **HDAC2** | -1.574168161 | -2.199677269 | 198 | 118 | 81840 |

| | | | | | |
|---|---|---|---|---|---|
| **HDAC3** | -6.730138489 | -8.034758308 | 1000 | 1000 | 1000000 |
| **HDAC4** | -4.075182252 | -4.971210368 | 97 | 1000 | 74000 |
| **HDAC5** | -4.194890248 | 0.739152888 | 92 | 1000 | 46000 |
| **HDAC6** | 6.085 | 5.335 | 462 | 399 | 46872 |
| **HDAC7** | -0.031884836 | -2.441150447 | 254 | 109 | 60230 |
| **HDAC8** | -6.140 | -4.366 | 27 | 41 | 784 |
| **HDAC9** | -0.420490678 | -4.16456189 | 240 | 1000 | 54000 |
| **HELLS** | -5.266022206 | -2.650496295 | 50 | 99 | 21942 |
| **HELQ** | 0.294660593 | -0.177751269 | 266 | 216 | 27140 |
| **HFM1** | -5.047580369 | -6.549125398 | 57 | 1000 | 22000 |
| **HGD** | -1.972540069 | 6.766422864 | 180 | 1000 | 1000 |
| **HIF1AN** | -3.352008638 | UC | 1000 | 1000 | 1000000 |
| **HIST1H2BD** | -3.598951001 | -5.953342206 | 1000 | 1000 | 1000000 |
| **HIST2H2AA3** | 2.24809849 | 1.544273683 | 336 | 1000 | 91000 |
| **HIST2H3C** | -1.210910549 | 1.312683352 | 212 | 277 | 124532 |
| **HIST2H4A** | -3.996926914 | -3.843931812 | 99 | 1000 | 17000 |
| **HIST3H2A** | -6.126118766 | -5.729465861 | 28 | 18 | 35145 |
| **HLTF** | -3.282 | -2.056 | 120 | 123 | 189 |
| **HMGA1** | -2.833737989 | -2.64756369 | 1000 | 1000 | 1000000 |
| **HMGB1** | 1.037590788 | -1.390632031 | 294 | 152 | 37347 |
| **HMGB2** | -2.646338884 | -5.259536838 | 1000 | 1000 | 1000000 |
| **HMGN1** | -1.42911229 | -4.964300512 | 204 | 30 | 11218 |
| **HMGXB4** | -2.223433791 | 1.200937688 | 167 | 1000 | 67000 |
| **HNRNPA2B1** | 5.687253045 | 0.394760543 | 454 | 237 | 102648 |
| **HNRNPK** | -10.26723582 | -8.034758308 | 1000 | 1000 | 1000000 |
| **HP1BP3** | 0.204764604 | -1.955881238 | 261 | 127 | 117810 |
| **HPRT1** | -8.716471909 | -6.702652002 | 1000 | 1000 | 1000000 |
| **HR** | -1.023411729 | -1.53995807 | 217 | 146 | 50481 |
| **HRAS** | 2.033046313 | 12.36311949 | 327 | 407 | 13158 |
| **HSP90B1** | -4.646 | -4.740 | 75 | 34 | 72240 |
| **HSPBAP1** | -6.019608042 | -3.858363694 | 31 | 56 | 114918 |
| **HSPD1** | -10.26723582 | UC | 1000 | 1000 | 1000000 |
| **HSPE1** | -9.378131178 | -1.979729647 | 1000 | 1000 | 1000000 |
| **HUS1** | -5.597191233 | -5.214775202 | 39 | 24 | 104 |
| **IARS** | -2.422194856 | 0.537592454 | 1000 | 243 | 94000 |
| **IFNGR2** | -2.718234138 | 0.939659172 | 148 | 263 | 851 |
| **IGF1** | 0.105651677 | -0.042120475 | 1000 | 1000 | 1000000 |
| **IGF1R** | 0.402019891 | 1.791025815 | 272 | 289 | 65184 |
| **IGF2** | -4.205158712 | -2.751163587 | 91 | 1000 | 275000 |
| **ILF2** | -8.933578857 | -8.034758308 | 1000 | 1000 | 1000000 |
| **ILK** | -8.489026536 | -7.34095294 | 1000 | 1000 | 1000000 |
| **INCENP** | 16.40590346 | -5.953342206 | 1000 | 1000 | 1000000 |
| **INO80** | -0.987060814 | -0.555897428 | 1000 | 1000 | 1000000 |
| **INO80C** | -1.232119741 | -0.775067594 | 210 | 186 | 73548 |
| **INSR** | -2.299381116 | -0.660598403 | 165 | 196 | 112176 |
| **IRS1** | 9.083865226 | -2.736608229 | 473 | 1000 | 141000 |
| **JARID2** | -7.155 | -2.503 | 12 | 106 | 8687 |
| **JHDM1D** | -3.881900491 | -5.558703458 | 1000 | 1000 | 1000000 |

| | | | | | |
|---|---|---|---|---|---|
| **JMJD1C** | -4.627247538 | -2.214333483 | 77 | 116 | 42120 |
| **JMJD4** | 2.674491968 | 1.511631229 | 353 | 285 | 100232 |
| **JMJD5** | -4.422659033 | 4.051746722 | 80 | 383 | 29610 |
| **JMJD6** | 0.379625518 | 0.092654169 | 270 | 1000 | 110000 |
| **JMJD7** | 0.573785948 | 0.289462799 | 281 | 1000 | 90000 |
| **JMJD7-PLA2G4B** | -3.050288349 | -2.876818005 | 132 | 90 | 69012 |
| **JMJD8** | -0.703417178 | -8.034758308 | 1000 | 1000 | 1000000 |
| **KAT2B** | 1.74305736 | -0.770659048 | 315 | 1000 | 64000 |
| **KDELR2** | 0.956648825 | -1.605021859 | 293 | 144 | 84812 |
| **KDM2A** | -1.38417793 | -0.921893929 | 207 | 179 | 64698 |
| **KDM2B** | -4.215 | -1.617 | 90 | 143 | 7719 |
| **KDM3A** | -1.893695423 | -3.415461882 | 184 | 65 | 3430 |
| **KDM3B** | 0.308447488 | 2.15244006 | 267 | 308 | 111910 |
| **KDM4A** | -6.613970459 | 0.409306603 | 17 | 1000 | 122000 |
| **KDM4B** | -3.099877111 | -4.557790403 | 1000 | 1000 | 1000000 |
| **KDM4C** | 2.457422758 | 0.78384174 | 343 | 255 | 19780 |
| **KDM4D** | -6.523654188 | -6.066637024 | 20 | 1000 | 318000 |
| **KDM5A** | -6.146420211 | -6.766476776 | 1000 | 1000 | 1000000 |
| **KDM5B** | 6.099690013 | 0.967803615 | 464 | 264 | 131625 |
| **KDM5C** | -1.944280987 | -0.74340164 | 183 | 190 | 42768 |
| **KDM5D** | -1.13718314 | 0.255291919 | 214 | 233 | 156016 |
| **KDM6A** | 1.185032708 | 1.241456256 | 298 | 274 | 135408 |
| **KDM6B** | -0.30495015 | 3.180015402 | 246 | 348 | 54237 |
| **KIAA0101** | -2.049488335 | -1.825595554 | 176 | 134 | 55600 |
| **KIF11** | -10.26723582 | UC | 1000 | 1000 | 1000000 |
| **KIF2C** | 2.367643469 | -0.509881275 | 339 | 203 | 24192 |
| **KIN** | -3.086198946 | -2.201687152 | 129 | 1000 | 261000 |
| **KPNA2** | -1.806401318 | -1.355928617 | 188 | 155 | 8 |
| **LDHA** | 1.437325297 | -0.394924492 | 304 | 207 | 119187 |
| **LEPRE1** | -7.196768153 | -4.887545358 | 11 | 31 | 1920 |
| **LEPREL1** | -1.555138583 | -3.097732498 | 199 | 78 | 30710 |
| **LEPREL2** | 1.992719867 | 2.047879242 | 324 | 297 | 67872 |
| **LIG1** | -4.644 | -4.186 | 76 | 49 | 6630 |
| **LIG3** | -2.531 | -5.805 | 158 | 16 | 11745 |
| **LIG4** | -5.316 | -5.678 | 49 | 20 | 8265 |
| **LOC642846** | -2.092755697 | -8.034758308 | 1000 | 1000 | 1000000 |
| **LOC730323** | 5.328938772 | 1.214376255 | 440 | 1000 | 305000 |
| **MAD1L1** | 3.298271714 | 3.38729822 | 374 | 358 | 41796 |
| **MAD2L2** | -3.878102387 | -3.97908311 | 101 | 53 | 55062 |
| **MANF** | -6.29604018 | -6.837379309 | 22 | 5 | 12648 |
| **MAP2K2** | 1.580109057 | -8.034758308 | 1000 | 1000 | 1000000 |
| **MAPK1** | -2.387079655 | 1.351846156 | 162 | 279 | 142259 |
| **MBD1** | 0.87832595 | -2.502573404 | 291 | 107 | 28220 |
| **MBD2** | -3.212017 | -3.199189274 | 122 | 75 | 6468 |
| **MBD3** | 0.487837181 | -1.70296198 | 273 | 140 | 61920 |
| **MBD4** | -3.494172416 | -2.578776643 | 115 | 102 | 10414 |
| **MCM10** | 3.433422831 | -1.023326233 | 382 | 175 | 37200 |
| **MCM2** | -4.932607965 | -8.034758308 | 1000 | 1000 | 1000000 |

| | | | | | |
|---|---|---|---|---|---|
| **MCM3** | -6.266264929 | -7.656319016 | 1000 | 1000 | 1000000 |
| **MCM4** | -1.903624352 | -5.606439522 | 1000 | 1000 | 1000000 |
| **MCM5** | -6.173 | -4.427 | 25 | 40 | 11360 |
| **MCM6** | -7.373451843 | -5.633124344 | 9 | 1000 | 12000 |
| **MCM7** | -6.331854616 | -5.655997048 | 1000 | 1000 | 1000000 |
| **MCM8** | -2.698735415 | -5.806308943 | 1000 | 1000 | 1000000 |
| **MCM9** | 2.679819567 | 3.989116624 | 354 | 1000 | 220000 |
| **MDC1** | -3.197613821 | -1.569771111 | 1000 | 1000 | 1000000 |
| **MECP2** | -5.015223883 | -4.347135259 | 62 | 42 | 18000 |
| **MEN1** | 16.40590346 | -1.36388434 | 1000 | 154 | 148000 |
| **MGMT** | -0.245536091 | -0.440637633 | 248 | 204 | 1044 |
| **MINA** | 5.819657755 | 2.828932346 | 456 | 1000 | 219000 |
| **MLH1** | -10.26723582 | UC | 1000 | 1000 | 1000000 |
| **MLH3** | -5.464994722 | -5.209410864 | 44 | 1000 | 32000 |
| **MLL** | -7.513 | -6.851 | 8 | 4 | 26134 |
| **MLLT1** | -1.217420708 | -3.911572124 | 211 | 55 | 11523 |
| **MLLT3** | 2.689645004 | 1.26306452 | 355 | 276 | 98325 |
| **MMP9** | -4.178801855 | -2.382472379 | 93 | 110 | 8175 |
| **MMS19** | -0.862590346 | 2.661798643 | 1000 | 1000 | 1000000 |
| **MNAT1** | -0.918344811 | -2.539819798 | 220 | 104 | 55160 |
| **MPG** | -1.844139206 | -5.041260992 | 187 | 28 | 16275 |
| **MRC1** | 0.506434315 | -1.242073377 | 274 | 162 | 155588 |
| **MRE11A** | -4.07525706 | -6.994050257 | 1000 | 1000 | 1000000 |
| **MRPL3** | -3.834990825 | -3.310926913 | 103 | 71 | 43674 |
| **MRPS12** | -4.086012407 | -4.705519286 | 96 | 1000 | 180000 |
| **MSH2** | 1.735676855 | 4.453738306 | 1000 | 1000 | 1000000 |
| **MSH3** | 0.211497468 | -4.912634154 | 1000 | 1000 | 1000000 |
| **MSH4** | -7.292 | -6.342 | 10 | 9 | 17898 |
| **MSH5** | -4.551563118 | -5.953342206 | 1000 | 1000 | 1000000 |
| **MSH6** | -2.200440851 | -0.400013257 | 168 | 206 | 84800 |
| **MTHFD2** | -5.555697989 | -8.034758308 | 40 | 1000 | 45000 |
| **MUC1** | -10.26723582 | -5.953342206 | 1000 | 1000 | 1000000 |
| **MUS81** | -6.2562449 | -4.31097869 | 23 | 43 | 114450 |
| **MUTYH** | 3.069333819 | UC | 1000 | 1000 | 1000000 |
| **MYL4** | -6.163675932 | -4.967408262 | 1000 | 1000 | 1000000 |
| **MYST1** | 1.376610958 | UC | 1000 | 1000 | 1000000 |
| **NAPRT1** | 13.02045774 | -8.034758308 | 1000 | 1000 | 1000000 |
| **NBN** | -7.52926457 | -3.951470668 | 7 | 54 | 27404 |
| **NCBP2** | -0.860077515 | UC | 1000 | 1000 | 1000000 |
| **NDC80** | 2.275641921 | UC | 1000 | 1000 | 1000000 |
| **NEIL1** | 12.15795057 | 27.62043153 | 1000 | 1000 | 1000000 |
| **NEIL2** | -0.564030172 | 9.361523831 | 234 | 405 | 16851 |
| **NEIL3** | -7.882674724 | -1.303783516 | 1000 | 1000 | 1000000 |
| **NEK2** | 4.728578399 | 2.121781376 | 429 | 304 | 163212 |
| **NHEJ1** | -1.385417813 | -3.577859578 | 206 | 1000 | 153000 |
| **NME1** | -0.307444683 | -0.793044667 | 245 | 185 | 43433 |
| **NONO** | -1.780327868 | -6.369625426 | 1000 | 1000 | 1000000 |
| **NRAS** | 3.9391101 | 1.245821016 | 402 | 275 | 2914 |

| | | | | | |
|---|---|---|---|---|---|
| **NTHL1** | UC | 0.290906101 | 1000 | 1000 | 1000000 |
| **NUDT1** | 4.997 | 3.943 | 433 | 379 | 408 |
| **NUDT10** | -1.170480525 | -2.150486782 | 213 | 120 | 14212 |
| **NUDT11** | -7.536887687 | -6.322729914 | 6 | 10 | 20710 |
| **NUDT12** | 0.034029044 | 0.412231803 | 257 | 239 | 29875 |
| **NUDT14** | 1.622917087 | 0.419528753 | 310 | 240 | 62160 |
| **NUDT15** | -2.54556815 | -1.054488153 | 157 | 172 | 57330 |
| **NUDT17** | -7.938466465 | 0.879039152 | 1000 | 1000 | 1000000 |
| **NUDT18** | 0.625395036 | 2.429264797 | 283 | 1000 | 1000000 |
| **NUDT19** | 6.552980488 | -3.410191026 | 1000 | 1000 | 1000000 |
| **NUDT2** | -1.019417643 | -1.178098844 | 218 | 166 | 18954 |
| **NUDT22** | -6.051360263 | -3.577859578 | 1000 | 1000 | 1000000 |
| **NUDT3** | -5.877228611 | -5.725834309 | 33 | 1000 | 60000 |
| **NUDT4** | -4.053333087 | 0.731326027 | 98 | 253 | 7668 |
| **NUDT5** | 1.234966475 | 0.400510702 | 299 | 238 | 45066 |
| **NUDT7** | -1.774269458 | -1.868668599 | 1000 | 1000 | 1000000 |
| **NUDT8** | 1.783594829 | -2.872450645 | 316 | 1000 | 132000 |
| **NUDT9** | 0.229091153 | 0.358783399 | 263 | 236 | 106733 |
| **NUP205** | -10.26723582 | UC | 1000 | 1000 | 1000000 |
| **OBFC2B** | -2.664176052 | -3.357765814 | 150 | 68 | 95931 |
| **OGFOD1** | -3.075980662 | -3.09993617 | 130 | 77 | 90592 |
| **OGFOD2** | -3.314435227 | -1.762086022 | 118 | 137 | 50861 |
| **OGG1** | 6.188370267 | 1.48772036 | 466 | 282 | 12096 |
| **OGT** | -6.435380378 | -4.442621311 | 1000 | 1000 | 1000000 |
| **ORC1L** | -0.820498993 | -2.94685228 | 1000 | 1000 | 1000000 |
| **ORC2L** | -2.586046978 | -1.954216885 | 153 | 128 | 41989 |
| **ORC3L** | -1.908169995 | -5.363736565 | 1000 | 1000 | 1000000 |
| **ORC4L** | -3.3211058 | 2.561541849 | 1000 | 1000 | 1000000 |
| **ORC5L** | -2.573061029 | -3.723253525 | 154 | 60 | 133472 |
| **ORC6L** | -5.463735943 | -5.877394592 | 45 | 1000 | 7000 |
| **P4HA1** | -2.265294037 | 0.545773379 | 166 | 244 | 46240 |
| **P4HA2** | -7.727517678 | -5.93934506 | 4 | 14 | 92953 |
| **P4HA3** | -0.010065287 | -2.202501482 | 256 | 117 | 86580 |
| **P4HTM** | -6.03342326 | -0.555897428 | 1000 | 1000 | 1000000 |
| **PAFAH1B3** | -3.404729113 | -4.586755876 | 117 | 37 | 10578 |
| **PAICS** | -3.820617093 | 3.965096348 | 104 | 380 | 155115 |
| **PALB2** | -2.977998407 | -4.246394388 | 138 | 1000 | 42000 |
| **PARP1** | 2.534070104 | 0.59022605 | 346 | 246 | 158592 |
| **PARP2** | 0.554070466 | -1.835164674 | 278 | 133 | 45426 |
| **PCNA** | -4.551563118 | 4.453738306 | 1000 | 1000 | 1000000 |
| **PDS5A** | -6.822 | -4.995 | 16 | 29 | 18209 |
| **PDS5B** | -8.475396144 | -1.877627644 | 1000 | 1000 | 1000000 |
| **PER1** | -4.314946607 | -2.116111158 | 86 | 1000 | 50000 |
| **PES1** | -0.763487794 | -7.099900698 | 228 | 1000 | 147000 |
| **PHB** | -2.774843804 | -5.815265627 | 1000 | 1000 | 1000000 |
| **PHF1** | -3.699685943 | -7.146961235 | 1000 | 1000 | 1000000 |
| **PHF2** | -2.140071702 | -4.483570018 | 171 | 1000 | 143000 |
| **PHF8** | -9.126974208 | -4.340479909 | 1000 | 1000 | 1000000 |

| | | | | | |
|---|---|---|---|---|---|
| **PHYH** | 1.676145014 | 3.112027157 | 312 | 343 | 16368 |
| **PHYHD1** | -8.437981528 | UC | 1000 | 1000 | 1000000 |
| **PIF1** | -3.221 | -2.852 | 121 | 91 | 2714 |
| **PIR** | -4.809744735 | -3.048205262 | 70 | 81 | 40309 |
| **PLK1** | -10.26723582 | UC | 1000 | 1000 | 1000000 |
| **PLK2** | 4.215002536 | -0.430477225 | 412 | 205 | 159594 |
| **PLK3** | -2.992137549 | -1.287704052 | 136 | 159 | 44704 |
| **PLK4** | -4.779726809 | -5.571906042 | 1000 | 1000 | 1000000 |
| **PLOD1** | 3.01581875 | 1.500839878 | 364 | 1000 | 310000 |
| **PLOD2** | 0.260783414 | 2.718840034 | 264 | 326 | 31428 |
| **PLOD3** | -2.828928195 | -4.011564872 | 145 | 1000 | 134000 |
| **PMS1** | -0.482490671 | -2.088193011 | 238 | 121 | 10422 |
| **PMS2** | 6.096334878 | 3.141659383 | 463 | 346 | 168498 |
| **PMS2L3** | 5.223790918 | 5.707853909 | 438 | 401 | 5824 |
| **PNKP** | -2.830747041 | -3.046305948 | 144 | 82 | 44528 |
| **POLB** | 1.132403622 | -4.002841472 | 297 | 52 | 95106 |
| **POLD1** | -4.772815008 | -8.034758308 | 1000 | 1000 | 1000000 |
| **POLE** | -10.26723582 | UC | 1000 | 1000 | 1000000 |
| **POLE3** | -5.62797528 | -3.92871704 | 37 | 1000 | 98000 |
| **POLE4** | -0.666618605 | 0.679143819 | 232 | 252 | 59202 |
| **POLG** | 4.650755572 | 2.407772831 | 424 | 316 | 152800 |
| **POLH** | -0.656853127 | -0.565311785 | 233 | 199 | 11968 |
| **POLI** | -3.068714682 | 3.294362114 | 131 | 353 | 107257 |
| **POLK** | -5.707745371 | -8.034758308 | 1000 | 1000 | 1000000 |
| **POLL** | -6.690394175 | -0.555897428 | 1000 | 1000 | 1000000 |
| **POLM** | -2.880 | -5.859 | 143 | 15 | 35632 |
| **POLN** | 2.843781001 | 3.913062732 | 359 | 376 | 106912 |
| **POLQ** | -0.145868099 | -0.525077629 | 250 | 201 | 109836 |
| **POLS** | -1.5029656 | 2.130104679 | 202 | 306 | 44863 |
| **POT1** | -3.724070954 | -4.231947691 | 105 | 46 | 59784 |
| **PPARG** | -4.416306788 | -5.423590448 | 81 | 1000 | 103000 |
| **PPP1R14C** | 2.965358453 | 4.108402214 | 363 | 385 | 119498 |
| **PPP1R1B** | -5.034046258 | -4.214559397 | 59 | 47 | 3936 |
| **PPP2R1B** | -3.31335948 | -6.851028878 | 1000 | 1000 | 1000000 |
| **PPP2R5C** | -3.655479433 | -2.918170819 | 109 | 88 | 9617 |
| **PPP3CA** | -6.958 | -5.075 | 14 | 26 | 70 |
| **PRDX2** | -2.785994241 | -6.039126643 | 1000 | 1000 | 1000000 |
| **PRDX4** | 2.547002257 | 0.299533759 | 347 | 235 | 137317 |
| **PRKDC** | -9.120204672 | -7.89921677 | 1 | 1 | 14074 |
| **PRMT1** | -10.26723582 | -8.034758308 | 1000 | 1000 | 1000000 |
| **PSMA1** | -10.26723582 | UC | 1000 | 1000 | 1000000 |
| **PSMC4** | -10.26723582 | UC | 1000 | 1000 | 1000000 |
| **PSME2** | -5.49083591 | -5.075434733 | 1000 | 1000 | 1000000 |
| **PTCH1** | -3.519 | -4.615 | 114 | 36 | 1281 |
| **PTEN** | 3.05286534 | -2.565294201 | 367 | 103 | 15477 |
| **PTMA** | -2.737381843 | -3.51110565 | 147 | 63 | 24180 |
| **PTTG1** | -6.435380378 | UC | 1000 | 1000 | 1000000 |
| **RAD1** | -3.04529622 | -4.439180164 | 134 | 39 | 8120 |

| | | | | | |
|---|---|---|---|---|---|
| **RAD17** | -6.403971187 | -3.595772946 | 1000 | 1000 | 1000000 |
| **RAD18** | -3.421334224 | -1.477948769 | 116 | 147 | 6048 |
| **RAD21** | -5.771800611 | 0.843212417 | 1000 | 1000 | 1000000 |
| **RAD23A** | -2.690252281 | 9.721183141 | 1000 | 1000 | 1000000 |
| **RAD23B** | -6.604288613 | -6.901400343 | 18 | 1000 | 107000 |
| **RAD50** | -5.787636628 | -4.758093989 | 34 | 33 | 46848 |
| **RAD51** | 6.216026618 | -5.075434733 | 1000 | 1000 | 1000000 |
| **RAD51AP1** | 0.288651388 | -0.446510787 | 265 | 1000 | 6000 |
| **RAD51C** | -5.438155029 | -6.473796422 | 48 | 8 | 3465 |
| **RAD51L1** | -4.772815008 | -5.66324558 | 72 | 21 | 9379 |
| **RAD51L3** | -6.913083581 | -7.534590943 | 15 | 2 | 20 |
| **RAD52** | -0.129173889 | 2.474634387 | 251 | 319 | 99443 |
| **RAD54B** | 1.711522101 | 2.17026799 | 314 | 309 | 77000 |
| **RAD54L** | -4.248614706 | -6.062604663 | 88 | 1000 | 43000 |
| **RAD54L2** | -1.612650179 | 0.888034327 | 197 | 260 | 144750 |
| **RAD9A** | -6.363305244 | 9.721183141 | 1000 | 1000 | 1000000 |
| **RARA** | -0.017643541 | -1.767955444 | 255 | 136 | 39932 |
| **RBBP8** | -6.415858155 | -5.016248262 | 21 | 1000 | 215000 |
| **RBM4** | -2.566039436 | -3.328364189 | 155 | 69 | 1824 |
| **RDM1** | 12.38763998 | 12.68379795 | 474 | 408 | 8686 |
| **RECQL** | 5.387126926 | 3.748136661 | 442 | 372 | 67662 |
| **RECQL4** | 1.544988849 | 6.95966578 | 308 | 1000 | 28000 |
| **RECQL5** | 0.707782203 | 0.995699999 | 287 | 1000 | 253000 |
| **REV1** | 1.835801838 | -0.694762219 | 319 | 194 | 9604 |
| **REV3L** | -4.997996189 | -6.13233601 | 1000 | 1000 | 1000000 |
| **RFC1** | -3.524083005 | UC | 1000 | 1000 | 1000000 |
| **RFC4** | -2.921434082 | -6.668916658 | 140 | 1000 | 25000 |
| **RFX1** | -0.701056727 | -7.146961235 | 231 | 1000 | 241000 |
| **RFX2** | -6.257793606 | -6.55509652 | 1000 | 1000 | 1000000 |
| **RFX3** | -5.049 | -3.218 | 56 | 74 | 531 |
| **RFX4** | -1.73126063 | -1.460993726 | 190 | 148 | 22042 |
| **RFX5** | -7.672648215 | -7.693297895 | 5 | 1000 | 21000 |
| **RFX6** | 15.59737465 | 2.943286984 | 475 | 337 | 9506 |
| **RFX7** | -1.690295114 | -2.472012525 | 193 | 108 | 40250 |
| **RIF1** | 0.948408455 | -1.668259647 | 292 | 141 | 73950 |
| **RMI1** | 2.917708325 | -1.579939458 | 361 | 145 | 47180 |
| **RNF40** | -8.233255647 | 0.831509848 | 1000 | 1000 | 1000000 |
| **RPA1** | UC | UC | 1000 | 1000 | 1000000 |
| **RPA2** | -2.849767724 | -8.034758308 | 1000 | 1000 | 1000000 |
| **RPA3** | 3.844613861 | 0.537075495 | 399 | 1000 | 161000 |
| **RPA4** | 1.687660034 | -3.009898654 | 313 | 83 | 117478 |
| **RPL13** | -2.417682204 | -1.170097884 | 160 | 167 | 133170 |
| **RPL27** | UC | UC | 1000 | 1000 | 1000000 |
| **RPL35** | -10.26723582 | UC | 1000 | 1000 | 1000000 |
| **RPN1** | -7.756113809 | -6.061875925 | 3 | 1000 | 3000 |
| **RPS27A** | UC | UC | 1000 | 1000 | 1000000 |
| **RRM2B** | 2.347354425 | 1.08010339 | 338 | 269 | 25935 |
| **RTEL1** | -3.594648188 | -5.230185478 | 112 | 1000 | 16000 |

| | | | | | |
|---|---|---|---|---|---|
| **RUVBL2** | UC | UC | 1000 | 1000 | 1000000 |
| **SDHC** | -10.26723582 | -8.034758308 | 1000 | 1000 | 1000000 |
| **SETD7** | 5.631837355 | 3.171158498 | 453 | 347 | 164400 |
| **SETD8** | -4.322159367 | -3.924031835 | 1000 | 1000 | 1000000 |
| **SHFM1** | 5.060185953 | UC | 1000 | 1000 | 1000000 |
| **SHPRH** | 1.95381188 | 0.159105869 | 320 | 230 | 21716 |
| **SIRT1** | -1.667762824 | -0.312883159 | 194 | 212 | 32706 |
| **SIRT5** | -4.350784056 | 0.831509848 | 1000 | 1000 | 1000000 |
| **SMARCA1** | -4.374854622 | -5.075434733 | 85 | 1000 | 73000 |
| **SMARCA2** | -4.823 | -4.271 | 69 | 44 | 5208 |
| **SMARCA4** | 2.030823264 | 2.539302346 | 326 | 322 | 42744 |
| **SMARCA5** | -0.79040309 | -6.025457933 | 227 | 13 | 96996 |
| **SMARCAD1** | 0.531238238 | 1.491162054 | 275 | 283 | 135965 |
| **SMARCAL1** | 1.303878447 | -3.136631112 | 302 | 76 | 7880 |
| **SMARCB1** | -4.731811868 | -5.815265627 | 73 | 1000 | 63000 |
| **SMARCC1** | -4.523068608 | -4.229913712 | 78 | 1000 | 39000 |
| **SMARCC2** | 2.625030158 | 0.575085784 | 349 | 245 | 11895 |
| **SMARCD1** | -0.268667714 | -1.658120605 | 247 | 142 | 90342 |
| **SMARCD2** | -5.512448579 | -5.075434733 | 1000 | 1000 | 1000000 |
| **SMARCD3** | 1.255044718 | 2.980501665 | 301 | 1000 | 26000 |
| **SMARCE1** | 5.45073229 | 3.496158962 | 445 | 364 | 138242 |
| **SMC5** | -0.824844712 | 0.732524398 | 224 | 254 | 15162 |
| **SMC6** | -4.907 | -0.683 | 66 | 195 | 1230 |
| **SMUG1** | 0.218743148 | -1.962178961 | 262 | 126 | 18774 |
| **SND1** | 0.61523054 | -1.898257073 | 282 | 130 | 21984 |
| **SNRPE** | -10.26723582 | UC | 1000 | 1000 | 1000000 |
| **SNRPF** | UC | UC | 1000 | 1000 | 1000000 |
| **SOD1** | -4.086012407 | -6.686205793 | 95 | 6 | 108 |
| **SOX4** | -1.436916658 | 1.12776276 | 203 | 271 | 13029 |
| **SPO11** | 0.693 | -2.712 | 286 | 97 | 3570 |
| **SRCAP** | 0.955339001 | 0.277368089 | 1000 | 1000 | 1000000 |
| **SSBP1** | -1.731 | -3.501 | 191 | 64 | 72 |
| **SSR1** | -1.954581674 | -5.318481875 | 182 | 22 | 138744 |
| **SSX1** | 0.735663381 | -1.1925926 | 288 | 164 | 56168 |
| **STK11** | 2.665276301 | -3.005766513 | 352 | 1000 | 11000 |
| **SUPV3L1** | 4.740864666 | -5.240873977 | 1000 | 1000 | 1000000 |
| **SUV39H1** | -7.530196219 | -5.240873977 | 1000 | 1000 | 1000000 |
| **SUV39H2** | 1.119761396 | -0.695955136 | 296 | 193 | 129744 |
| **SUZ12** | 1.587 | -0.591 | 309 | 198 | 1292 |
| **TAL1** | 4.658 | -1.354 | 425 | 156 | 920 |
| **TAPBP** | -4.334040296 | UC | 1000 | 1000 | 1000000 |
| **TARS** | -1.288946789 | -2.347208063 | 209 | 113 | 1040 |
| **TDG** | -1.855845823 | -8.034758308 | 1000 | 1000 | 1000000 |
| **TDP1** | -3.136112236 | -1.090101776 | 126 | 171 | 85935 |
| **TERF2** | -1.025702104 | -2.446989647 | 1000 | 1000 | 1000000 |
| **TERF2IP** | -6.17327893 | -0.283112228 | 24 | 213 | 29928 |
| **TET1** | 3.023789282 | 0.674906385 | 365 | 251 | 121968 |
| **TET2** | -2.884060934 | -0.349584024 | 142 | 210 | 18900 |

| | | | | | |
|---|---|---|---|---|---|
| **TET3** | -7.620907008 | -5.182343121 | 1000 | 1000 | 1000000 |
| **TGIF1** | 2.692733864 | 1.504720623 | 356 | 284 | 150480 |
| **TIMELESS** | -2.339 | -2.811 | 163 | 94 | 3705 |
| **TINF2** | -4.928950418 | -6.580535359 | 64 | 1000 | 269000 |
| **TIPIN** | -7.080495184 | -3.879835597 | 1000 | 1000 | 1000000 |
| **TLK1** | -1.654459772 | 1.094780263 | 196 | 270 | 18088 |
| **TLK2** | 5.929704504 | 2.932389672 | 459 | 335 | 101376 |
| **TMEM30A** | -8.390245586 | -3.087204187 | 2 | 80 | 9936 |
| **TMLHE** | -2.034822508 | 4.786146058 | 1000 | 1000 | 1000000 |
| **TNKS2** | -8.637097272 | -2.463634896 | 1000 | 1000 | 1000000 |
| **TOP1** | -5.248866763 | -7.147289167 | 51 | 3 | 19323 |
| **TOP2A** | -0.824449192 | -3.3200785 | 1000 | 1000 | 1000000 |
| **TOP2B** | 4.071648777 | 3.219638653 | 407 | 352 | 64900 |
| **TOP3A** | 3.527443776 | -1.70743203 | 389 | 139 | 14832 |
| **TOP3B** | -3.59570179 | -3.76997605 | 111 | 59 | 76440 |
| **TOPBP1** | -4.460347978 | -6.187619109 | 1000 | 1000 | 1000000 |
| **TOX2** | -5.232058836 | -0.394360486 | 52 | 1000 | 94000 |
| **TP53** | 5.610048617 | 9.825212553 | 450 | 406 | 74418 |
| **TP53BP1** | -2.416605156 | -4.986884493 | 161 | 1000 | 262000 |
| **TP73** | 4.126171189 | 2.188603189 | 409 | 310 | 98560 |
| **TPX2** | -5.054611305 | -3.60162423 | 55 | 1000 | 82000 |
| **TRAF4** | 0.552719154 | 2.850672698 | 277 | 332 | 86403 |
| **TRDMT1** | -6.532 | -2.196 | 19 | 119 | 17864 |
| **TREX1** | -7.006087608 | -5.079335589 | 1000 | 1000 | 1000000 |
| **TREX2** | -4.413892875 | -0.003718311 | 82 | 1000 | 158000 |
| **TRIM28** | -5.450043645 | -6.898057262 | 47 | 1000 | 177000 |
| **TSC1** | -3.628951039 | 0.83704983 | 110 | 259 | 46230 |
| **TSTA3** | -1.865160762 | -1.012292288 | 186 | 176 | 3784 |
| **TTF2** | -1.575466157 | -5.240873977 | 1000 | 1000 | 1000000 |
| **TTRAP** | 3.379287148 | -1.443219905 | 380 | 151 | 26800 |
| **TUBB** | -6.774081788 | 0.879039152 | 1000 | 1000 | 1000000 |
| **UBA52** | 139.1751265 | UC | 1000 | 1000 | 1000000 |
| **UBE2A** | -4.805254029 | -3.314057198 | 71 | 70 | 60192 |
| **UBE2B** | -2.525323803 | -0.994169795 | 159 | 1000 | 111000 |
| **UBE2I** | -1.932950231 | 42.25515964 | 1000 | 1000 | 1000000 |
| **UBE2N** | -5.644018927 | -7.456713274 | 35 | 1000 | 75000 |
| **UBE2S** | 2.05872613 | -0.240333677 | 328 | 214 | 57088 |
| **UBE2V2** | -0.10501104 | -2.835029137 | 252 | 92 | 34880 |
| **UNG** | -3.119992407 | -2.995482276 | 128 | 84 | 52907 |
| **VHL** | -2.000761156 | -5.748852946 | 178 | 1000 | 78000 |
| **WDHD1** | -1.548406171 | -3.85861751 | 201 | 1000 | 136000 |
| **WRN** | -3.289225382 | -1.224665252 | 119 | 1000 | 76000 |
| **XAB2** | -6.974270496 | UC | 1000 | 1000 | 1000000 |
| **XPA** | -1.399227509 | -2.446989647 | 205 | 1000 | 9000 |
| **XPC** | 2.077607178 | -1.053584044 | 329 | 173 | 69300 |
| **XRCC1** | -0.367268603 | -4.682097111 | 243 | 1000 | 205000 |
| **XRCC2** | 2.501329465 | 0.807619795 | 344 | 256 | 77024 |
| **XRCC3** | -0.800298843 | 0.429067752 | 225 | 241 | 5300 |

| | | | | | |
|---|---|---|---|---|---|
| **XRCC4** | 2.438390123 | 0.635917201 | 342 | 249 | 124413 |
| **XRCC5** | -6.818565922 | -3.843931812 | 1000 | 1000 | 1000000 |
| **XRCC6** | -4.398428131 | -2.063615291 | 84 | 122 | 47025 |
| **ZBTB16** | -1.551643048 | -0.211882182 | 200 | 1000 | 265000 |
| **ZDHHC17** | -3.137207105 | -2.038809075 | 125 | 124 | 111800 |
| **ZSWIM7** | -4.714016588 | -2.332142542 | 74 | 114 | 39162 |

UC= unable to calculate.

All genes with plating efficiencies less than 4% were given a ranking of 1000.

**Table 5.2: List of genes from primary siRNA screen and their respective Z-scores for cisplatin treatment.**

| Gene | Z Score Rep A | Z Score Rep B | Rank A | Rank B | Ranked Product |
|---|---|---|---|---|---|
| **ABL1** | -1.525556103 | -0.881039329 | 165 | 141 | 23265 |
| **ACD** | -1.902547317 | -1.060558505 | 135 | 1000 | 135000 |
| **ACLY** | 6.825381797 | 2.69018904 | 412 | 267 | 110004 |
| **ADI1** | 0.029662928 | -1.01870536 | 266 | 132 | 35112 |
| **ADO** | 4.336849719 | 2.48064884 | 391 | 262 | 102442 |
| **AHCY** | -1.414331492 | -0.876118936 | 169 | 143 | 24167 |
| **AKT1** | -1.708017172 | -0.579205142 | 146 | 159 | 23214 |
| **AKT2** | 2.155249672 | 2.508860896 | 336 | 263 | 88368 |
| **ALKBH1** | 2.036857427 | 3.749820985 | 327 | 1000 | 327000 |
| **ALKBH2** | -1.651609026 | 0.650316298 | 1000 | 1000 | 1000000 |
| **ALKBH3** | 4.174294943 | 4.566627297 | 387 | 356 | 137772 |
| **ALKBH4** | 0.988632167 | 3.293011754 | 294 | 286 | 84084 |
| **ALKBH5** | -2.752 | -1.332 | 40 | 111 | 4440 |
| **ALKBH6** | -1.651609026 | -0.938073942 | 151 | 1000 | 151000 |
| **ALKBH7** | -3.15842805 | UC | 1000 | 1000 | 1000000 |
| **ALKBH8** | -2.948986024 | -2.742312844 | 14 | 11 | 154 |
| **APEX1** | -2.807779267 | -1.858587232 | 31 | 74 | 2294 |
| **APEX2** | 0.301888668 | 0.566878574 | 276 | 1000 | 276000 |
| **APTX** | 3.587988638 | 3.515972037 | 373 | 292 | 108916 |
| **ARID1A** | -2.053419874 | -0.395017033 | 1000 | 1000 | 1000000 |
| **ARID1B** | -1.161499691 | 1.256761496 | 191 | 226 | 43166 |
| **ARID3A** | 5.751630457 | 3.601812837 | 404 | 302 | 122008 |
| **ARID3B** | -0.428429203 | 0.415519698 | 240 | 196 | 47040 |
| **ARID4A** | -2.924 | -2.852 | 19 | 6 | 114 |
| **ARID4B** | 1.264759406 | 2.632045818 | 306 | 1000 | 306000 |
| **ARID5A** | 0.635363947 | 3.517980337 | 287 | 293 | 84091 |
| **ARID5B** | -1.67021173 | -1.44113554 | 150 | 104 | 15600 |
| **ASF1A** | -0.290214974 | 3.48122651 | 247 | 1000 | 247000 |
| **ASF1B** | 2.940397529 | 4.499121251 | 360 | 352 | 126720 |
| **ASPH** | -2.372491121 | -0.858004368 | 89 | 145 | 12905 |
| **ASPHD1** | -2.143412663 | -0.973698315 | 112 | 1000 | 112000 |
| **ASPHD2** | -1.558847681 | -0.873546268 | 160 | 1000 | 160000 |
| **ATAD5** | -2.546 | -2.293 | 66 | 38 | 2508 |
| **ATF4** | -2.468916997 | -1.891304027 | 79 | 71 | 5609 |
| **ATM** | -2.574013411 | -1.339830151 | 58 | 110 | 6380 |
| **ATR** | -2.622141675 | -2.644451262 | 1000 | 15 | 15000 |
| **ATRIP** | -2.912416781 | -1.7429725 | 1000 | 1000 | 1000000 |
| **BAZ1A** | 1.656050369 | 2.747441655 | 315 | 269 | 84735 |
| **BAZ1B** | -3.15842805 | UC | 1000 | 1000 | 1000000 |
| **BAZ2A** | -0.055721333 | 0.805669285 | 260 | 208 | 54080 |
| **BAZ2B** | -2.775 | -2.683 | 35 | 13 | 455 |
| **BBOX1** | -3.15842805 | UC | 1000 | 1000 | 1000000 |
| **BLM** | 1.766776704 | 2.952195349 | 316 | 276 | 87216 |
| **BRCA1** | -2.246741213 | -2.686604888 | 1000 | 1000 | 1000000 |

| | | | | | |
|---|---|---|---|---|---|
| **BRCA2** | -2.951226496 | -2.555486927 | 1000 | 20 | 20000 |
| **BRD1** | 1.472582125 | 0.868362843 | 311 | 212 | 65932 |
| **BRD2** | -3.037454499 | -2.619010613 | 8 | 1000 | 8000 |
| **BRD3** | 3.07266166 | 3.263014901 | 362 | 284 | 102808 |
| **BRD4** | 2.405329757 | 3.424425126 | 342 | 1000 | 342000 |
| **BRD7** | 0.453068962 | 1.189616573 | 283 | 223 | 63109 |
| **BRD8** | -1.564669677 | -2.503379752 | 157 | 22 | 3454 |
| **BRD9** | 3.171375418 | 6.954962544 | 365 | 399 | 145635 |
| **BRDT** | 2.1090959 | 1.107156007 | 331 | 218 | 72158 |
| **BRIP1** | -1.307835816 | -2.229265378 | 178 | 42 | 7476 |
| **BTAF1** | 3.121923641 | 4.951396448 | 363 | 367 | 133221 |
| **BTBD12** | -3.15842805 | -1.7429725 | 1000 | 84 | 84000 |
| **BUB3** | -2.011100412 | -3.050932656 | 1000 | 1000 | 1000000 |
| **C14orf169** | -2.727908329 | -2.542281484 | 1000 | 1000 | 1000000 |
| **C17orf101** | -2.348037987 | -3.050932656 | 1000 | 1000 | 1000000 |
| **C19orf40** | 0.419483419 | 1.180120275 | 282 | 222 | 62604 |
| **C2orf60** | -2.219112295 | -1.278857605 | 106 | 1000 | 106000 |
| **C9orf102** | 2.670332035 | -1.996884602 | 349 | 60 | 20940 |
| **CANX** | -0.752587785 | 0.3172956 | 222 | 193 | 42846 |
| **CARM1** | 1.407106607 | -0.946714923 | 309 | 1000 | 309000 |
| **CBX3** | -0.262151175 | -2.249087753 | 249 | 41 | 10209 |
| **CCNA1** | -2.611896979 | 1.552654424 | 55 | 1000 | 55000 |
| **CCNA2** | -2.172820658 | 2.88070811 | 1000 | 273 | 273000 |
| **CCNB1** | 0.918680788 | 0.726773197 | 292 | 205 | 59860 |
| **CCNB2** | 5.576774339 | 8.43063274 | 403 | 406 | 163618 |
| **CCNB3** | 2.653588186 | 10.15033962 | 348 | 1000 | 348000 |
| **CCND1** | -2.436 | -2.198 | 81 | 44 | 3564 |
| **CCND2** | 1.615365233 | 1.326814308 | 313 | 229 | 71677 |
| **CCND3** | -3.15842805 | -2.338117457 | 1000 | 1000 | 1000000 |
| **CCNE1** | 0.735234485 | 1.45762348 | 289 | 234 | 67626 |
| **CCNE2** | 1.004852755 | 2.007954245 | 296 | 253 | 74888 |
| **CCNH** | -2.814395282 | -2.086535622 | 1000 | 55 | 55000 |
| **CCRN4L** | -1.358900135 | UC | 1000 | 1000 | 1000000 |
| **CCT4** | -3.15842805 | UC | 1000 | 1000 | 1000000 |
| **CCT5** | -3.15842805 | UC | 1000 | 1000 | 1000000 |
| **CDC2** | -3.15842805 | -1.229293813 | 1000 | 1000 | 1000000 |
| **CDK2** | -3.15842805 | -2.28242877 | 1000 | 39 | 39000 |
| **CDK4** | -1.161175958 | 0.425271644 | 192 | 198 | 38016 |
| **CDK6** | 2.14840578 | 0.618822338 | 334 | 204 | 68136 |
| **CDK7** | 5.001060353 | 4.932131685 | 398 | 366 | 145668 |
| **CDKN3** | 4.282439166 | -0.468759597 | 390 | 164 | 63960 |
| **CDO1** | 3.864369718 | 3.470228244 | 381 | 290 | 110490 |
| **CDYL** | 2.784893725 | 3.686042137 | 351 | 303 | 106353 |
| **CENPA** | -2.897946097 | -1.805761802 | 1000 | 80 | 80000 |
| **CETN2** | 4.609220904 | 4.206050656 | 394 | 334 | 131596 |
| **CFDP1** | -2.101 | -2.583 | 117 | 16 | 1872 |
| **CHAF1A** | 0.623125908 | UC | 1000 | 1000 | 1000000 |
| **CHAF1B** | -0.508963359 | 1.131449936 | 236 | 219 | 51684 |

| | | | | | |
|---|---|---|---|---|---|
| **CHD1** | -2.060010174 | 0.599219138 | 121 | 203 | 24563 |
| **CHD2** | 5.049782348 | 3.889254766 | 399 | 322 | 128478 |
| **CHD3** | -0.929225125 | 2.937220561 | 210 | 275 | 57750 |
| **CHD4** | -2.836 | -1.958 | 29 | 66 | 1914 |
| **CHD5** | -1.217 | -1.410 | 188 | 106 | 19928 |
| **CHD6** | 0.344105275 | 0.000974376 | 279 | 188 | 52452 |
| **CHD7** | 0.070631387 | 2.089961441 | 270 | 254 | 68580 |
| **CHD8** | -2.79625891 | -2.371588103 | 33 | 33 | 1089 |
| **CHD9** | 2.03457667 | 4.578834925 | 326 | 357 | 116382 |
| **CHEK1** | 1.265368841 | 4.471881778 | 307 | 350 | 107450 |
| **CHEK2** | 6.540481941 | 9.167959876 | 410 | 408 | 167280 |
| **CHRAC1** | -2.644 | -2.436 | 52 | 27 | 1404 |
| **CHTF18** | -0.314729616 | 1.544103447 | 246 | 1000 | 246000 |
| **CITED1** | -1.246174754 | -0.077700279 | 184 | 185 | 34040 |
| **CITED2** | -1.275836253 | -0.293289974 | 182 | 175 | 31850 |
| **CITED4** | -3.15842805 | -2.346646418 | 1000 | 1000 | 1000000 |
| **CKS2** | -2.502538239 | -2.437032342 | 72 | 26 | 1872 |
| **CLK2** | -2.25675975 | -0.263825227 | 102 | 178 | 18156 |
| **CLSPN** | -1.318910625 | -0.36930942 | 175 | 1000 | 175000 |
| **COL1A2** | -2.145442675 | -2.305716766 | 1000 | 36 | 36000 |
| **COPB2** | -3.15842805 | UC | 1000 | 1000 | 1000000 |
| **CRIP2** | -1.177866989 | -0.986845478 | 189 | 136 | 25704 |
| **CSNK2A1** | 2.149547329 | 3.42306597 | 335 | 289 | 96815 |
| **CUL1** | -2.697535751 | -2.455641224 | 47 | 1000 | 47000 |
| **CUL3** | -2.676960202 | -3.050932656 | 1000 | 1000 | 1000000 |
| **CUL4A** | 0.035700114 | -0.65759051 | 267 | 153 | 40851 |
| **CUL4B** | -0.531596114 | -0.16567613 | 235 | 182 | 42770 |
| **DCLRE1A** | 4.69907716 | 1.72142874 | 395 | 244 | 96380 |
| **DCLRE1B** | -2.753233019 | 0.000974376 | 38 | 1000 | 38000 |
| **DCLRE1C** | -1.021 | -1.157 | 204 | 121 | 24684 |
| **DDB1** | -1.817712113 | -1.001588958 | 1000 | 1000 | 1000000 |
| **DDB2** | 3.236430544 | 2.320366459 | 366 | 259 | 94794 |
| **DHX58** | 4.751066342 | 2.397837948 | 397 | 261 | 103617 |
| **DMC1** | -2.079796888 | -2.244402026 | 120 | 1000 | 120000 |
| **DNMT1** | -1.971986275 | -0.025056055 | 130 | 187 | 24310 |
| **DNMT3A** | -1.281425738 | -1.485604806 | 1000 | 99 | 99000 |
| **DNMT3B** | -1.987454131 | -0.647191176 | 128 | 154 | 19712 |
| **DOT1L** | 1.057962403 | -1.630217314 | 297 | 90 | 26730 |
| **DSCC1** | -2.779751018 | -2.076919774 | 34 | 1000 | 34000 |
| **DUT** | -1.907093175 | 0.476626169 | 1000 | 199 | 199000 |
| **DVL3** | -2.678592873 | -1.104398843 | 48 | 127 | 6096 |
| **E2F5** | -0.722623523 | 0.558920464 | 224 | 202 | 45248 |
| **ECT2** | -3.15842805 | -2.384895954 | 1000 | 31 | 31000 |
| **EGFR** | -1.344125886 | 0.755825438 | 173 | 206 | 35638 |
| **EGLN1** | 4.139116987 | 8.045673532 | 385 | 404 | 155540 |
| **EGLN2** | -2.82512246 | -1.219788437 | 1000 | 1000 | 1000000 |
| **EGLN3** | 3.515791195 | 1.57686819 | 371 | 238 | 88298 |
| **EHMT1** | 8.009436717 | 3.488868128 | 415 | 291 | 120765 |

| | | | | | |
|---|---|---|---|---|---|
| **EIF4A3** | -3.15842805 | UC | 1000 | 1000 | 1000000 |
| **EME1** | -1.698404648 | -1.6828364 | 148 | 87 | 12876 |
| **EME2** | -2.219112295 | 15.26050954 | 1000 | 1000 | 1000000 |
| **EP400** | -0.697535174 | -1.744500823 | 1000 | 1000 | 1000000 |
| **ERCC1** | -2.570242994 | -2.429919415 | 1000 | 29 | 29000 |
| **ERCC2** | -2.550636825 | -1.901300826 | 1000 | 69 | 69000 |
| **ERCC3** | -2.284207795 | -0.662293644 | 100 | 152 | 15200 |
| **ERCC4** | -2.655 | -2.109 | 51 | 53 | 2703 |
| **ERCC5** | -2.108788599 | -0.503377583 | 115 | 163 | 18745 |
| **ERCC6** | -3.15842805 | -1.001588958 | 1000 | 1000 | 1000000 |
| **ERCC8** | -1.865255231 | -1.160761284 | 138 | 120 | 16560 |
| **EXO1** | 3.410231664 | 4.467574517 | 368 | 349 | 128432 |
| **EZH2** | 1.236862177 | 0.397169439 | 304 | 195 | 59280 |
| **FANCA** | -2.731074845 | -2.153707555 | 44 | 50 | 2200 |
| **FANCB** | -1.290581847 | 1.254513452 | 181 | 225 | 40725 |
| **FANCC** | -2.317551841 | -0.807440608 | 95 | 147 | 13965 |
| **FANCD2** | -3.15842805 | -2.723037665 | 1000 | 12 | 12000 |
| **FANCE** | -0.94559592 | 1.020060906 | 209 | 217 | 45353 |
| **FANCF** | 0.985603029 | 1.687266249 | 293 | 241 | 70613 |
| **FANCG** | -0.235947595 | -0.751668995 | 251 | 151 | 37901 |
| **FANCI** | -2.824866267 | -2.447964118 | 30 | 25 | 750 |
| **FANCL** | -0.323728661 | -1.153694071 | 245 | 122 | 29890 |
| **FANCM** | -1.594393911 | -0.43806899 | 1000 | 1000 | 1000000 |
| **FAP** | 3.754617181 | 4.141103719 | 377 | 332 | 125164 |
| **FBXO18** | -1.489336208 | -1.088992421 | 167 | 129 | 21543 |
| **FEN1** | -2.989597155 | -1.661547098 | 1000 | 89 | 89000 |
| **FLJ35220** | -1.826535969 | -1.708973328 | 139 | 85 | 11815 |
| **FOXO1** | -2.237042417 | -1.620258754 | 104 | 91 | 9464 |
| **FOXO3** | 2.484103666 | 2.810877252 | 343 | 271 | 92953 |
| **FTO** | -2.12518072 | -3.050932656 | 1000 | 1000 | 1000000 |
| **G3BP1** | -2.249400657 | -1.975558483 | 1000 | 64 | 64000 |
| **GADD45A** | -0.084135226 | 0.985338181 | 256 | 214 | 54784 |
| **GEN1** | 5.893832136 | 3.069505065 | 407 | 279 | 113553 |
| **GINS2** | 1.135747438 | 1.973805164 | 299 | 252 | 75348 |
| **GIYD2** | 2.233655015 | 1.767867922 | 338 | 247 | 83486 |
| **GTF2H1** | 2.34225231 | 2.784004262 | 340 | 270 | 91800 |
| **GTF2H2** | -0.857082635 | -1.08173089 | 217 | 130 | 28210 |
| **GTF2H3** | -1.877862219 | -1.527496253 | 137 | 97 | 13289 |
| **GTF2H4** | -2.914073308 | -3.050932656 | 1000 | 1000 | 1000000 |
| **GTF2H5** | -3.158 | -2.948 | 5 | 5 | 25 |
| **H2AFX** | -3.15842805 | -1.500292031 | 1000 | 1000 | 1000000 |
| **H2AFZ** | -2.761 | -2.160 | 37 | 48 | 1776 |
| **HAAO** | -0.643364576 | 0.343732737 | 228 | 194 | 44232 |
| **HAT1** | 1.837333472 | 3.818695253 | 319 | 314 | 100166 |
| **HDAC1** | -3.15842805 | -1.735237581 | 1000 | 1000 | 1000000 |
| **HDAC10** | 0.550009152 | -3.050932656 | 285 | 1000 | 285000 |
| **HDAC11** | -2.300367983 | -2.181394899 | 99 | 46 | 4554 |
| **HDAC2** | 2.07392917 | 1.773282622 | 330 | 248 | 81840 |

| | | | | | |
|---|---|---|---|---|---|
| **HDAC3** | -2.639924214 | 2.128102809 | 1000 | 1000 | 1000000 |
| **HDAC4** | -2.500246191 | -2.565702847 | 74 | 1000 | 74000 |
| **HDAC5** | -2.708243055 | -2.429231962 | 46 | 1000 | 46000 |
| **HDAC6** | -0.217 | -0.037 | 252 | 186 | 46872 |
| **HDAC7** | 1.82170877 | 0.075818324 | 317 | 190 | 60230 |
| **HDAC8** | -2.589 | -2.681 | 56 | 14 | 784 |
| **HDAC9** | -2.628303664 | -2.577255937 | 54 | 1000 | 54000 |
| **HELLS** | -1.56172253 | -0.971031459 | 159 | 138 | 21942 |
| **HELQ** | -0.621028632 | -1.210349549 | 230 | 118 | 27140 |
| **HFM1** | -2.891208913 | -2.669444277 | 22 | 1000 | 22000 |
| **HGD** | -3.15842805 | -3.050932656 | 1 | 1000 | 1000 |
| **HIF1AN** | -3.15842805 | UC | 1000 | 1000 | 1000000 |
| **HIST1H2BD** | -2.557315384 | 1.290861094 | 1000 | 1000 | 1000000 |
| **HIST2H2AA3** | -2.343038953 | -1.817828974 | 91 | 1000 | 91000 |
| **HIST2H3C** | 3.971582771 | 4.0261923 | 382 | 326 | 124532 |
| **HIST2H4A** | -2.928636577 | -2.619346368 | 17 | 1000 | 17000 |
| **HIST3H2A** | -0.910358544 | -0.446287861 | 213 | 165 | 35145 |
| **HLTF** | -2.860 | -2.822 | 27 | 7 | 189 |
| **HMGA1** | -3.15842805 | -2.767155287 | 1000 | 1000 | 1000000 |
| **HMGB1** | -0.927736514 | -0.270473604 | 211 | 177 | 37347 |
| **HMGB2** | -3.15842805 | -3.050932656 | 1000 | 1000 | 1000000 |
| **HMGN1** | -1.766963544 | -1.819218117 | 142 | 79 | 11218 |
| **HMGXB4** | -2.54187034 | 1.922672896 | 67 | 1000 | 67000 |
| **HNRNPA2B1** | 2.073478493 | 3.779193341 | 329 | 312 | 102648 |
| **HNRNPK** | -0.653791939 | -3.050932656 | 1000 | 1000 | 1000000 |
| **HP1BP3** | 2.91577583 | 4.092610865 | 357 | 330 | 117810 |
| **HPRT1** | -3.15842805 | -3.050932656 | 1000 | 1000 | 1000000 |
| **HR** | -0.46199257 | 0.937122413 | 237 | 213 | 50481 |
| **HRAS** | -0.078402562 | -2.146392292 | 258 | 51 | 13158 |
| **HSP90B1** | 1.147 | 1.664 | 301 | 240 | 72240 |
| **HSPBAP1** | 1.849658502 | 4.632189943 | 321 | 358 | 114918 |
| **HSPD1** | -3.15842805 | UC | 1000 | 1000 | 1000000 |
| **HSPE1** | -3.15842805 | -3.050932656 | 1000 | 1000 | 1000000 |
| **HUS1** | -2.956033213 | -2.817502885 | 13 | 8 | 104 |
| **IARS** | -2.569101907 | -1.550065681 | 1000 | 94 | 94000 |
| **IFNGR2** | -2.87488434 | -2.299106899 | 23 | 37 | 851 |
| **IGF1** | -2.601842248 | -3.050932656 | 1000 | 1000 | 1000000 |
| **IGF1R** | 0.907922342 | 1.251745835 | 291 | 224 | 65184 |
| **IGF2** | 0.256984828 | 1.958829364 | 275 | 1000 | 275000 |
| **ILF2** | -3.15842805 | -3.050932656 | 1000 | 1000 | 1000000 |
| **ILK** | -3.15842805 | -3.050932656 | 1000 | 1000 | 1000000 |
| **INCENP** | -3.15842805 | 0.567228802 | 1000 | 1000 | 1000000 |
| **INO80** | -2.382873932 | -1.483214457 | 1000 | 1000 | 1000000 |
| **INO80C** | 1.894885398 | 1.290955699 | 324 | 227 | 73548 |
| **INSR** | 2.058897012 | 4.309441511 | 328 | 342 | 112176 |
| **IRS1** | -1.783333715 | -1.735237581 | 141 | 1000 | 141000 |
| **JARID2** | -2.090 | -1.861 | 119 | 73 | 8687 |
| **JHDM1D** | -2.82512246 | -1.52497914 | 1000 | 1000 | 1000000 |

| | | | | | |
|---|---|---|---|---|---|
| **JMJD1C** | -0.534948499 | -0.208060352 | 234 | 180 | 42120 |
| **JMJD4** | 3.653106902 | 2.737845844 | 374 | 268 | 100232 |
| **JMJD5** | -1.992506938 | 1.511409721 | 126 | 235 | 29610 |
| **JMJD6** | -2.169068003 | -1.061490436 | 110 | 1000 | 110000 |
| **JMJD7** | -2.371044791 | -1.513779244 | 90 | 1000 | 90000 |
| **JMJD7-PLA2G4B** | 0.499000357 | 1.707582835 | 284 | 243 | 69012 |
| **JMJD8** | -0.442526371 | -0.489010302 | 1000 | 1000 | 1000000 |
| **KAT2B** | -2.554796718 | -2.091852015 | 64 | 1000 | 64000 |
| **KDELR2** | 3.162919589 | 1.454419956 | 364 | 233 | 84812 |
| **KDM2A** | -0.024987447 | 1.737090599 | 263 | 246 | 64698 |
| **KDM2B** | -2.411 | -1.586 | 83 | 93 | 7719 |
| **KDM3A** | -2.67093689 | -1.898198686 | 49 | 70 | 3430 |
| **KDM3B** | 2.959089351 | 3.75019777 | 361 | 310 | 111910 |
| **KDM4A** | -2.057004567 | -0.91938742 | 122 | 1000 | 122000 |
| **KDM4B** | -1.807873065 | -1.880672527 | 1000 | 1000 | 1000000 |
| **KDM4C** | -1.377261331 | -1.23262525 | 172 | 115 | 19780 |
| **KDM4D** | 1.825527628 | 2.931149948 | 318 | 1000 | 318000 |
| **KDM5A** | -1.724027374 | -3.050932656 | 1000 | 1000 | 1000000 |
| **KDM5B** | 5.757430876 | 3.999032495 | 405 | 325 | 131625 |
| **KDM5C** | -1.104855508 | 1.019312018 | 198 | 216 | 42768 |
| **KDM5D** | 4.409481738 | 6.90149433 | 392 | 398 | 156016 |
| **KDM6A** | 3.582121825 | 4.859813704 | 372 | 364 | 135408 |
| **KDM6B** | 1.229260155 | -0.208872341 | 303 | 179 | 54237 |
| **KIAA0101** | 0.338620281 | 0.545007508 | 278 | 200 | 55600 |
| **KIF11** | -3.15842805 | UC | 1000 | 1000 | 1000000 |
| **KIF2C** | -0.870079384 | -1.325770583 | 216 | 112 | 24192 |
| **KIN** | -0.055244458 | 0.352060616 | 261 | 1000 | 261000 |
| **KPNA2** | -3.15842805 | -3.050932656 | 2 | 4 | 8 |
| **LDHA** | 3.450363218 | 3.90813651 | 369 | 323 | 119187 |
| **LEPRE1** | -2.942268541 | -1.100152091 | 15 | 128 | 1920 |
| **LEPREL1** | -1.243969655 | -0.43806899 | 185 | 166 | 30710 |
| **LEPREL2** | -1.025972811 | 4.224865859 | 202 | 336 | 67872 |
| **LIG1** | -2.400 | -1.822 | 85 | 78 | 6630 |
| **LIG3** | -1.719 | -1.759 | 145 | 81 | 11745 |
| **LIG4** | -2.379 | -1.549 | 87 | 95 | 8265 |
| **LOC642846** | -3.15842805 | -3.050932656 | 1000 | 1000 | 1000000 |
| **LOC730323** | 1.245464468 | 0.89048635 | 305 | 1000 | 305000 |
| **MAD1L1** | -0.340834855 | -0.342940256 | 243 | 172 | 41796 |
| **MAD2L2** | 1.885333597 | -0.347886161 | 322 | 171 | 55062 |
| **MANF** | -2.024790117 | -1.44789787 | 124 | 102 | 12648 |
| **MAP2K2** | -1.06659373 | -3.050932656 | 1000 | 1000 | 1000000 |
| **MAPK1** | 2.860182977 | 8.032816864 | 353 | 403 | 142259 |
| **MBD1** | -1.51252432 | -0.38491895 | 166 | 170 | 28220 |
| **MBD2** | -2.406263687 | -1.833637996 | 84 | 77 | 6468 |
| **MBD3** | 0.686239623 | 0.988586632 | 288 | 215 | 61920 |
| **MBD4** | -1.992495099 | -1.748030653 | 127 | 82 | 10414 |
| **MCM10** | -0.262837308 | -0.785089946 | 248 | 150 | 37200 |
| **MCM2** | -3.15842805 | -3.050932656 | 1000 | 1000 | 1000000 |

| | | | | | |
|---|---|---|---|---|---|
| **MCM3** | -2.156573606 | -3.050932656 | 1000 | 1000 | 1000000 |
| **MCM4** | -2.139593022 | -2.146392292 | 1000 | 1000 | 1000000 |
| **MCM5** | -2.455 | -0.880 | 80 | 142 | 11360 |
| **MCM6** | -2.96939891 | -2.772612544 | 12 | 1000 | 12000 |
| **MCM7** | -2.994189617 | -3.050932656 | 1000 | 1000 | 1000000 |
| **MCM8** | 1.491184939 | 1.526927893 | 1000 | 1000 | 1000000 |
| **MCM9** | -0.778780865 | -0.489010302 | 220 | 1000 | 220000 |
| **MDC1** | -1.267651071 | -3.050932656 | 1000 | 1000 | 1000000 |
| **MECP2** | -2.005852141 | -0.87012301 | 125 | 144 | 18000 |
| **MEN1** | -3.15842805 | -0.803627403 | 1000 | 148 | 148000 |
| **MGMT** | -2.926785404 | -2.021497597 | 18 | 58 | 1044 |
| **MINA** | -0.847216916 | -0.189769813 | 219 | 1000 | 219000 |
| **MLH1** | -3.15842805 | UC | 1000 | 1000 | 1000000 |
| **MLH3** | -2.802965746 | -3.050932656 | 32 | 1000 | 32000 |
| **MLL** | -1.307 | -0.847 | 179 | 146 | 26134 |
| **MLLT1** | -2.532269023 | -0.432072934 | 69 | 167 | 11523 |
| **MLLT3** | 2.546081242 | 3.275433487 | 345 | 285 | 98325 |
| **MMP9** | -2.17835305 | -1.855943551 | 109 | 75 | 8175 |
| **MMS19** | -0.774011133 | 6.104788442 | 1000 | 1000 | 1000000 |
| **MNAT1** | 0.369697236 | 0.422502344 | 280 | 197 | 55160 |
| **MPG** | -1.576552612 | -1.424792675 | 155 | 105 | 16275 |
| **MRC1** | 4.221780846 | 7.424506234 | 388 | 401 | 155588 |
| **MRE11A** | -1.727207415 | 0.567228802 | 1000 | 1000 | 1000000 |
| **MRPL3** | -1.340373263 | 1.841138378 | 174 | 251 | 43674 |
| **MRPS12** | -1.29370717 | -0.243439374 | 180 | 1000 | 180000 |
| **MSH2** | -2.156573606 | -3.050932656 | 1000 | 1000 | 1000000 |
| **MSH3** | -1.011597098 | -3.050932656 | 1000 | 1000 | 1000000 |
| **MSH4** | -2.121 | -0.591 | 114 | 157 | 17898 |
| **MSH5** | -3.15842805 | -3.050932656 | 1000 | 1000 | 1000000 |
| **MSH6** | 1.839652074 | 2.638290148 | 320 | 265 | 84800 |
| **MTHFD2** | -2.726524679 | -3.050932656 | 45 | 1000 | 45000 |
| **MUC1** | -3.15842805 | 0.567228802 | 1000 | 1000 | 1000000 |
| **MUS81** | 2.711691747 | 4.048934618 | 350 | 327 | 114450 |
| **MUTYH** | -3.15842805 | UC | 1000 | 1000 | 1000000 |
| **MYL4** | -3.15842805 | -0.765778051 | 1000 | 1000 | 1000000 |
| **MYST1** | 7.174045258 | UC | 1000 | 1000 | 1000000 |
| **NAPRT1** | -0.575309723 | -1.219788437 | 1000 | 1000 | 1000000 |
| **NBN** | -0.769900898 | -1.115101048 | 221 | 124 | 27404 |
| **NCBP2** | -3.15842805 | UC | 1000 | 1000 | 1000000 |
| **NDC80** | -3.15842805 | UC | 1000 | 1000 | 1000000 |
| **NEIL1** | -2.775743854 | 0.000974376 | 1000 | 1000 | 1000000 |
| **NEIL2** | -2.051377339 | -0.983511763 | 123 | 137 | 16851 |
| **NEIL3** | -1.172742074 | 1.652221943 | 1000 | 1000 | 1000000 |
| **NEK2** | 5.801819446 | 7.703047235 | 406 | 402 | 163212 |
| **NHEJ1** | -1.620571558 | -1.7429725 | 153 | 1000 | 153000 |
| **NME1** | -0.083682952 | -0.404964166 | 257 | 169 | 43433 |
| **NONO** | -2.247651283 | -3.050932656 | 1000 | 1000 | 1000000 |
| **NRAS** | -2.559493328 | -2.169086853 | 62 | 47 | 2914 |

| | | | | | |
|---|---|---|---|---|---|
| **NTHL1** | UC | -3.050932656 | 1000 | 1000 | 1000000 |
| **NUDT1** | -2.869 | -2.573 | 24 | 17 | 408 |
| **NUDT10** | -1.221089305 | -1.854106369 | 187 | 76 | 14212 |
| **NUDT11** | -1.164981158 | -1.350997259 | 190 | 109 | 20710 |
| **NUDT12** | -0.429095478 | -1.11019377 | 239 | 125 | 29875 |
| **NUDT14** | 3.486863292 | -0.408950229 | 370 | 168 | 62160 |
| **NUDT15** | 0.132137281 | 0.846588979 | 273 | 210 | 57330 |
| **NUDT17** | -3.15842805 | -3.050932656 | 1000 | 1000 | 1000000 |
| **NUDT18** | -2.325164074 | -0.264408844 | 1000 | 1000 | 1000000 |
| **NUDT19** | -1.417222793 | -3.050932656 | 1000 | 1000 | 1000000 |
| **NUDT2** | -1.540282581 | -1.210705662 | 162 | 117 | 18954 |
| **NUDT22** | -3.15842805 | -2.135360547 | 1000 | 1000 | 1000000 |
| **NUDT3** | -2.567560244 | -1.807531268 | 60 | 1000 | 60000 |
| **NUDT4** | -2.507931383 | -1.364964673 | 71 | 108 | 7668 |
| **NUDT5** | -0.062177538 | -0.315449603 | 259 | 174 | 45066 |
| **NUDT7** | -0.608806066 | -3.050932656 | 1000 | 1000 | 1000000 |
| **NUDT8** | -1.952525761 | -1.978500043 | 132 | 1000 | 132000 |
| **NUDT9** | 2.382975373 | 3.810184166 | 341 | 313 | 106733 |
| **NUP205** | -3.15842805 | UC | 1000 | 1000 | 1000000 |
| **OBFC2B** | 1.889857995 | 3.561532581 | 323 | 297 | 95931 |
| **OGFOD1** | 1.075755281 | 3.695395663 | 298 | 304 | 90592 |
| **OGFOD2** | 0.409620286 | -0.168576014 | 281 | 181 | 50861 |
| **OGG1** | -1.421341715 | -1.875030182 | 168 | 72 | 12096 |
| **OGT** | -1.621109658 | 1.059412951 | 1000 | 1000 | 1000000 |
| **ORC1L** | -2.323549347 | 0.969246742 | 1000 | 1000 | 1000000 |
| **ORC2L** | -1.065947249 | 0.851803299 | 199 | 211 | 41989 |
| **ORC3L** | -2.420160188 | -2.491033299 | 1000 | 1000 | 1000000 |
| **ORC4L** | -2.114829671 | -1.077390043 | 1000 | 1000 | 1000000 |
| **ORC5L** | 2.493058559 | 5.736030886 | 344 | 388 | 133472 |
| **ORC6L** | -3.041027656 | -2.749448387 | 7 | 1000 | 7000 |
| **P4HA1** | -1.390449619 | 2.856269725 | 170 | 272 | 46240 |
| **P4HA2** | 0.094279157 | 4.338347742 | 271 | 343 | 92953 |
| **P4HA3** | 2.12683984 | 2.33399968 | 333 | 260 | 86580 |
| **P4HTM** | -2.5490641 | -1.091284907 | 1000 | 1000 | 1000000 |
| **PAFAH1B3** | -2.380288676 | -1.150484213 | 86 | 123 | 10578 |
| **PAICS** | 3.971596872 | 8.307230377 | 383 | 405 | 155115 |
| **PALB2** | -2.73840881 | -1.677574492 | 42 | 1000 | 42000 |
| **PARP1** | 6.849168845 | 5.512991416 | 413 | 384 | 158592 |
| **PARP2** | -0.711540195 | 0.550643778 | 226 | 201 | 45426 |
| **PCNA** | -3.15842805 | -3.050932656 | 1000 | 1000 | 1000000 |
| **PDS5A** | -1.962 | -0.948 | 131 | 139 | 18209 |
| **PDS5B** | -2.708243055 | -3.050932656 | 1000 | 1000 | 1000000 |
| **PER1** | -2.662585841 | -3.050932656 | 50 | 1000 | 50000 |
| **PES1** | -1.70058265 | -0.111461032 | 147 | 1000 | 147000 |
| **PHB** | -2.85416124 | -3.050932656 | 1000 | 1000 | 1000000 |
| **PHF1** | -2.530877754 | -3.050932656 | 1000 | 1000 | 1000000 |
| **PHF2** | -1.763871837 | -1.927935344 | 143 | 1000 | 143000 |
| **PHF8** | -2.298983969 | -3.050932656 | 1000 | 1000 | 1000000 |

| | | | | | |
|---|---|---|---|---|---|
| **PHYH** | -1.229685897 | -1.678380385 | 186 | 88 | 16368 |
| **PHYHD1** | -3.15842805 | UC | 1000 | 1000 | 1000000 |
| **PIF1** | -2.094 | -2.483 | 118 | 23 | 2714 |
| **PIR** | -0.537103099 | -0.319373867 | 233 | 173 | 40309 |
| **PLK1** | -3.15842805 | UC | 1000 | 1000 | 1000000 |
| **PLK2** | 5.384239025 | 6.896278448 | 402 | 397 | 159594 |
| **PLK3** | -0.151801246 | -0.27216154 | 254 | 176 | 44704 |
| **PLK4** | -3.15842805 | -3.050932656 | 1000 | 1000 | 1000000 |
| **PLOD1** | 1.434706032 | -1.803157864 | 310 | 1000 | 310000 |
| **PLOD2** | -1.150267103 | -0.520234486 | 194 | 162 | 31428 |
| **PLOD3** | -1.902835427 | 2.818640871 | 134 | 1000 | 134000 |
| **PMS1** | -1.150267103 | -2.097444372 | 193 | 54 | 10422 |
| **PMS2** | 7.319839135 | 8.489751192 | 414 | 407 | 168498 |
| **PMS2L3** | -0.96277296 | -2.435591663 | 208 | 28 | 5824 |
| **PNKP** | -0.355893002 | -0.136463161 | 242 | 184 | 44528 |
| **POLB** | 4.536394272 | 1.705868189 | 393 | 242 | 95106 |
| **POLD1** | -3.15842805 | -3.050932656 | 1000 | 1000 | 1000000 |
| **POLE** | -1.150267103 | UC | 1000 | 1000 | 1000000 |
| **POLE3** | -2.310031832 | -2.436141206 | 98 | 1000 | 98000 |
| **POLE4** | 0.596455446 | 0.760492325 | 286 | 207 | 59202 |
| **POLG** | 5.169991383 | 5.417571671 | 400 | 382 | 152800 |
| **POLH** | -1.31347453 | -1.917137292 | 176 | 68 | 11968 |
| **POLI** | 3.788122156 | 3.248967709 | 379 | 283 | 107257 |
| **POLK** | -3.15842805 | -3.050932656 | 1000 | 1000 | 1000000 |
| **POLL** | -3.048112163 | -3.050932656 | 1000 | 1000 | 1000000 |
| **POLM** | 0.127 | -1.056 | 272 | 131 | 35632 |
| **POLN** | 8.275033036 | 2.249596352 | 416 | 257 | 106912 |
| **POLQ** | 2.276017714 | 3.961035827 | 339 | 324 | 109836 |
| **POLS** | -1.022403848 | 1.169096297 | 203 | 221 | 44863 |
| **POT1** | -0.914860779 | 3.193368648 | 212 | 282 | 59784 |
| **PPARG** | -2.238659677 | -2.390346002 | 103 | 1000 | 103000 |
| **PPP1R14C** | 5.170621349 | 3.563687883 | 401 | 298 | 119498 |
| **PPP1R1B** | -1.53309517 | -2.469617031 | 164 | 24 | 3936 |
| **PPP2R1B** | -2.949244618 | -2.302267781 | 1000 | 1000 | 1000000 |
| **PPP2R5C** | -1.534914846 | -2.001402457 | 163 | 59 | 9617 |
| **PPP3CA** | -2.526 | -3.051 | 70 | 1 | 70 |
| **PRDX2** | -2.837449485 | -2.228863535 | 1000 | 1000 | 1000000 |
| **PRDX4** | 4.272870895 | 4.508947783 | 389 | 353 | 137317 |
| **PRKDC** | -0.674105229 | -1.979370335 | 227 | 62 | 14074 |
| **PRMT1** | -3.15842805 | -3.050932656 | 1000 | 1000 | 1000000 |
| **PSMA1** | -3.15842805 | UC | 1000 | 1000 | 1000000 |
| **PSMC4** | -3.15842805 | UC | 1000 | 1000 | 1000000 |
| **PSME2** | -2.702027835 | -2.219082795 | 1000 | 1000 | 1000000 |
| **PTCH1** | -2.560 | -2.552 | 61 | 21 | 1281 |
| **PTEN** | -0.61287192 | -1.947988867 | 231 | 67 | 15477 |
| **PTMA** | -1.576240637 | -0.633581492 | 156 | 155 | 24180 |
| **PTTG1** | -3.15842805 | UC | 1000 | 1000 | 1000000 |
| **RAD1** | -0.571383972 | -2.320984403 | 232 | 35 | 8120 |

| | | | | | |
|---|---|---|---|---|---|
| **RAD17** | -2.844652902 | -3.050932656 | 1000 | 1000 | 1000000 |
| **RAD18** | -2.316543645 | -1.977153067 | 96 | 63 | 6048 |
| **RAD21** | -1.332827189 | -3.050932656 | 1000 | 1000 | 1000000 |
| **RAD23A** | -2.834531123 | 8.179040473 | 1000 | 1000 | 1000000 |
| **RAD23B** | -2.202160932 | -2.334125861 | 107 | 1000 | 107000 |
| **RAD50** | -0.328693796 | 0.279220626 | 244 | 192 | 46848 |
| **RAD51** | -3.15842805 | -3.050932656 | 1000 | 1000 | 1000000 |
| **RAD51AP1** | -3.06482523 | -2.244402026 | 6 | 1000 | 6000 |
| **RAD51C** | -2.478581896 | -2.18708857 | 77 | 45 | 3465 |
| **RAD51L1** | -2.128601923 | -1.743333046 | 113 | 83 | 9379 |
| **RAD51L3** | -3.002756659 | -3.050932656 | 10 | 2 | 20 |
| **RAD52** | 2.921644023 | 3.04396729 | 359 | 277 | 99443 |
| **RAD54B** | 1.354397727 | 1.829222385 | 308 | 250 | 77000 |
| **RAD54L** | -2.734938006 | -1.866185981 | 43 | 1000 | 43000 |
| **RAD54L2** | 3.679882025 | 5.646082516 | 375 | 386 | 144750 |
| **RAD9A** | -2.629964643 | -3.050932656 | 1000 | 1000 | 1000000 |
| **RARA** | 0.054629466 | -0.786064126 | 268 | 149 | 39932 |
| **RBBP8** | -0.879937744 | -2.601733731 | 215 | 1000 | 215000 |
| **RBM4** | -2.582316303 | -2.374428251 | 57 | 32 | 1824 |
| **RDM1** | -2.25995211 | -1.689947088 | 101 | 86 | 8686 |
| **RECQL** | 2.919913515 | 0.045567287 | 358 | 189 | 67662 |
| **RECQL4** | -2.837179534 | -2.465802592 | 28 | 1000 | 28000 |
| **RECQL5** | -0.20408902 | -1.393064139 | 253 | 1000 | 253000 |
| **REV1** | -1.117687616 | -2.156875858 | 196 | 49 | 9604 |
| **REV3L** | -2.829221338 | -3.050932656 | 1000 | 1000 | 1000000 |
| **RFC1** | -3.15842805 | UC | 1000 | 1000 | 1000000 |
| **RFC4** | -2.867390232 | -1.323244483 | 25 | 1000 | 25000 |
| **RFX1** | -0.409160086 | -3.050932656 | 241 | 1000 | 241000 |
| **RFX2** | -3.15842805 | -3.050932656 | 1000 | 1000 | 1000000 |
| **RFX3** | -2.572 | -2.812 | 59 | 9 | 531 |
| **RFX4** | -1.006827035 | -1.379295435 | 206 | 107 | 22042 |
| **RFX5** | -2.910506946 | -3.050932656 | 21 | 1000 | 21000 |
| **RFX6** | -2.311504009 | -1.508916472 | 97 | 98 | 9506 |
| **RFX7** | -0.252419932 | -0.572692359 | 250 | 161 | 40250 |
| **RIF1** | 0.832604159 | 2.133451897 | 290 | 255 | 73950 |
| **RMI1** | 2.197743775 | -0.904073916 | 337 | 140 | 47180 |
| **RNF40** | -1.880876037 | 6.896278448 | 1000 | 1000 | 1000000 |
| **RPA1** | UC | UC | 1000 | 1000 | 1000000 |
| **RPA2** | -1.150267103 | 8.179040473 | 1000 | 1000 | 1000000 |
| **RPA3** | -1.548110309 | -1.114730393 | 161 | 1000 | 161000 |
| **RPA4** | 1.199848899 | 5.767482218 | 302 | 389 | 117478 |
| **RPL13** | 4.152837536 | 4.40503311 | 386 | 345 | 133170 |
| **RPL27** | UC | UC | 1000 | 1000 | 1000000 |
| **RPL35** | 6.295456846 | UC | 1000 | 1000 | 1000000 |
| **RPN1** | -3.15842805 | -2.42704526 | 3 | 1000 | 3000 |
| **RPS27A** | UC | UC | 1000 | 1000 | 1000000 |
| **RRM2B** | -1.124089939 | -1.009632917 | 195 | 133 | 25935 |
| **RTEL1** | -2.933925542 | -2.805976688 | 16 | 1000 | 16000 |

| | | | | | |
|---|---|---|---|---|---|
| **RUVBL2** | UC | UC | 1000 | 1000 | 1000000 |
| **SDHC** | -3.15842805 | -3.050932656 | 1000 | 1000 | 1000000 |
| **SETD7** | 6.762119412 | 7.151156567 | 411 | 400 | 164400 |
| **SETD8** | -2.633505877 | -1.34298442 | 1000 | 1000 | 1000000 |
| **SHFM1** | -0.911578092 | UC | 1000 | 1000 | 1000000 |
| **SHPRH** | 2.901063159 | -1.993494906 | 356 | 61 | 21716 |
| **SIRT1** | -0.974007677 | -0.582827646 | 207 | 158 | 32706 |
| **SIRT5** | -1.909801743 | 6.896278448 | 1000 | 1000 | 1000000 |
| **SMARCA1** | -2.501552974 | -3.050932656 | 73 | 1000 | 73000 |
| **SMARCA2** | -2.329 | -2.074 | 93 | 56 | 5208 |
| **SMARCA4** | 0.188506862 | -0.603804184 | 274 | 156 | 42744 |
| **SMARCA5** | 2.875186106 | 2.920329695 | 354 | 274 | 96996 |
| **SMARCAD1** | 2.899557179 | 5.446184958 | 355 | 383 | 135965 |
| **SMARCAL1** | -1.1145198 | -2.278113826 | 197 | 40 | 7880 |
| **SMARCB1** | -2.558977021 | -3.050932656 | 63 | 1000 | 63000 |
| **SMARCC1** | -2.75273897 | -3.050932656 | 39 | 1000 | 39000 |
| **SMARCC2** | -1.265019157 | -1.958082922 | 183 | 65 | 11895 |
| **SMARCD1** | 3.768948862 | 1.583659429 | 378 | 239 | 90342 |
| **SMARCD2** | -3.15842805 | -3.050932656 | 1000 | 1000 | 1000000 |
| **SMARCD3** | -2.865977427 | -2.01112033 | 26 | 1000 | 26000 |
| **SMARCE1** | 6.069549637 | 4.268367477 | 409 | 338 | 138242 |
| **SMC5** | -1.919154749 | -1.289943131 | 133 | 114 | 15162 |
| **SMC6** | -2.748 | -2.390 | 41 | 30 | 1230 |
| **SMUG1** | -1.692890729 | -1.108034033 | 149 | 126 | 18774 |
| **SND1** | -0.639723722 | -1.54351131 | 229 | 96 | 21984 |
| **SNRPE** | -3.15842805 | UC | 1000 | 1000 | 1000000 |
| **SNRPF** | UC | UC | 1000 | 1000 | 1000000 |
| **SOD1** | -2.772243253 | -3.050932656 | 36 | 3 | 108 |
| **SOX4** | -1.977156905 | -1.467218497 | 129 | 101 | 13029 |
| **SPO11** | -2.224 | -2.345 | 105 | 34 | 3570 |
| **SRCAP** | -2.909641606 | -3.050932656 | 1000 | 1000 | 1000000 |
| **SSBP1** | -3.158 | -2.573 | 4 | 18 | 72 |
| **SSR1** | 3.745199645 | 5.021329411 | 376 | 369 | 138744 |
| **SSX1** | -0.438134708 | 1.529166734 | 238 | 236 | 56168 |
| **STK11** | -2.971190554 | -2.475484271 | 11 | 1000 | 11000 |
| **SUPV3L1** | -2.971190554 | -3.050932656 | 1000 | 1000 | 1000000 |
| **SUV39H1** | -2.837449485 | -0.173690731 | 1000 | 1000 | 1000000 |
| **SUV39H2** | 5.933135474 | 3.867488173 | 408 | 318 | 129744 |
| **SUZ12** | -2.538 | -2.570 | 68 | 19 | 1292 |
| **TAL1** | -2.343 | -2.801 | 92 | 10 | 920 |
| **TAPBP** | -3.15842805 | UC | 1000 | 1000 | 1000000 |
| **TARS** | -2.91242258 | -2.126104895 | 20 | 52 | 1040 |
| **TDG** | -2.500813428 | -3.050932656 | 1000 | 1000 | 1000000 |
| **TDP1** | -0.107572776 | 4.227758986 | 255 | 337 | 85935 |
| **TERF2** | -2.761925117 | -3.050932656 | 1000 | 1000 | 1000000 |
| **TERF2IP** | -2.101648227 | 2.285980364 | 116 | 258 | 29928 |
| **TET1** | 4.704332126 | 3.728494416 | 396 | 308 | 121968 |
| **TET2** | -1.811413002 | -0.996681222 | 140 | 135 | 18900 |

| | | | | | |
|---|---|---|---|---|---|
| **TET3** | -1.749454417 | -0.487330749 | 1000 | 1000 | 1000000 |
| **TGIF1** | 3.861189177 | 6.591715957 | 380 | 396 | 150480 |
| **TIMELESS** | -2.554 | -2.050 | 65 | 57 | 3705 |
| **TINF2** | 0.060603252 | 1.086101482 | 269 | 1000 | 269000 |
| **TIPIN** | -1.920043248 | -2.179978101 | 1000 | 1000 | 1000000 |
| **TLK1** | -1.645806467 | -1.164392619 | 152 | 119 | 18088 |
| **TLK2** | 4.129263907 | 2.597588054 | 384 | 264 | 101376 |
| **TMEM30A** | -2.198679829 | -1.603808164 | 108 | 92 | 9936 |
| **TMLHE** | -2.358637866 | -0.811335228 | 1000 | 1000 | 1000000 |
| **TNKS2** | -2.951778584 | -2.478700088 | 1000 | 1000 | 1000000 |
| **TOP1** | -1.379196611 | -1.324587501 | 171 | 113 | 19323 |
| **TOP2A** | -2.676960202 | 2.883378814 | 1000 | 1000 | 1000000 |
| **TOP2B** | 1.000634639 | 1.160514194 | 295 | 220 | 64900 |
| **TOP3A** | -1.758467692 | -1.443062169 | 144 | 103 | 14832 |
| **TOP3B** | 1.50579173 | 1.721903949 | 312 | 245 | 76440 |
| **TOPBP1** | -2.107996395 | -3.050932656 | 1000 | 1000 | 1000000 |
| **TOX2** | -2.320659944 | -3.050932656 | 94 | 1000 | 94000 |
| **TP53** | 1.647614237 | 1.547276401 | 314 | 237 | 74418 |
| **TP53BP1** | -0.034758596 | 3.619037261 | 262 | 1000 | 262000 |
| **TP73** | 2.823809964 | 3.103526529 | 352 | 280 | 98560 |
| **TPX2** | -2.421761695 | -0.56412988 | 82 | 1000 | 82000 |
| **TRAF4** | 2.607402848 | 1.808773532 | 347 | 249 | 86403 |
| **TRDMT1** | -1.590 | -1.229 | 154 | 116 | 17864 |
| **TREX1** | -2.780272655 | -1.061490436 | 1000 | 1000 | 1000000 |
| **TREX2** | -1.561771935 | -0.88849546 | 158 | 1000 | 158000 |
| **TRIM28** | -1.308754918 | -1.903177529 | 177 | 1000 | 177000 |
| **TSC1** | -1.038161188 | 1.340647124 | 201 | 230 | 46230 |
| **TSTA3** | -2.374643181 | -2.211089068 | 88 | 43 | 3784 |
| **TTF2** | -2.665217084 | -3.050932656 | 1000 | 1000 | 1000000 |
| **TTRAP** | -1.044868403 | -1.004927548 | 200 | 134 | 26800 |
| **TUBB** | -3.15842805 | -3.050932656 | 1000 | 1000 | 1000000 |
| **UBA52** | -3.15842805 | UC | 1000 | 1000 | 1000000 |
| **UBE2A** | 0.007023549 | 1.314537851 | 264 | 228 | 60192 |
| **UBE2B** | -2.161101793 | -2.360394594 | 111 | 1000 | 111000 |
| **UBE2I** | -1.810318075 | 14.21251889 | 1000 | 1000 | 1000000 |
| **UBE2N** | -2.499026432 | -3.050932656 | 75 | 1000 | 75000 |
| **UBE2S** | -0.751719971 | 2.174794677 | 223 | 256 | 57088 |
| **UBE2V2** | -0.855230758 | -0.573307665 | 218 | 160 | 34880 |
| **UNG** | 0.314420472 | 0.205822774 | 277 | 191 | 52907 |
| **UTY** | 2.568928524 | 4.669793037 | 346 | 360 | 124560 |
| **VHL** | -2.476799411 | -2.580111251 | 78 | 1000 | 78000 |
| **WDHD1** | -1.890223979 | 1.273941737 | 136 | 1000 | 136000 |
| **WRN** | -2.496198589 | -2.331622175 | 76 | 1000 | 76000 |
| **XAB2** | -2.092041137 | UC | 1000 | 1000 | 1000000 |
| **XPA** | -3.030036624 | -1.900035886 | 9 | 1000 | 9000 |
| **XPC** | 1.145564218 | 1.341413877 | 300 | 231 | 69300 |
| **XRCC1** | -1.010808059 | -3.050932656 | 205 | 1000 | 205000 |
| **XRCC2** | 2.111867658 | 1.365299136 | 332 | 232 | 77024 |

| | | | | | |
|---|---|---|---|---|---|
| **XRCC3** | -2.629757472 | -1.471270423 | 53 | 100 | 5300 |
| **XRCC4** | 3.286483673 | 4.290995014 | 367 | 339 | 124413 |
| **XRCC5** | -3.15842805 | -3.050932656 | 1000 | 1000 | 1000000 |
| **XRCC6** | -0.720584126 | 0.84570677 | 225 | 209 | 47025 |
| **ZBTB16** | 0.01359542 | 5.293068926 | 265 | 1000 | 265000 |
| **ZDHHC17** | 1.906153144 | 4.344376122 | 325 | 344 | 111800 |
| **ZSWIM7** | -0.879985218 | -0.150673178 | 214 | 183 | 39162 |

UC= unable to calculate.

All genes with plating efficiencies less than 4% were given a ranking of 1000.

## Table 5.3: List of genes included in secondary screen and their respective Z-scores

| Gene | Role | Z-score Cisplatin Run1 | Z-score Cisplatin Run 2 | Z-score Radiation Run1 | Z-score Radiation Run 2 |
|---|---|---|---|---|---|
| **ALKBH5** | demethylation modifies mRNA | -2.752 | -1.332 | -5.641 | -3.795 |
| **ARID4A** | nuclear protein binds to pRB which regulates cell proliferation and represses transcription | -2.924 | -2.852 | -2.988 | -6.071 |
| **ATAD5** | involved in Rad9a related damage checkpoint determines need for apoptosis | -2.546 | -2.293 | -4.445 | -4.628 |
| **BAZ2B** | may play role in transcription regulating interacting with ISWI | -2.775 | -2.683 | -0.388 | -1.257 |
| **CCND1** | cyclin family protein complexes with CDK4/6 for G1-S transition | -2.436 | -2.198 | -2.658 | -3.617 |
| **CFDP1** | may play role in embryogenesis | -2.101 | -2.583 | -2.912 | -0.733 |
| **CHD4** | helicase family gene main component of nucleosome remodelling and deacetylase complex has role in epigenetic transcriptional repression | -2.836 | -1.958 | -3.120 | -1.448 |
| **CHD5** | member of chromodomain helicase DNA-binding protein family may have role in chromatin remodelling and gene transcription | -1.217 | -1.410 | -1.887 | -5.774 |
| **CHRAC1** | histone fold protein that binds DNA combines with larger enzymes for DNA rep, transcription + packaging | -2.644 | -2.436 | -7.088 | -3.635 |
| **DCLRE1C** | involved in V(D)J recombination and DNA repair. Ss 5'-3' exonuclease ARTEMIS. Mutations in ARTEMIS- SCID and radiation sensitivity | -1.021 | -1.157 | -5.220 | -6.498 |
| **ERCC4** | structure specific endonuclease interacts with EME1 | -2.655 | -2.109 | -3.874 | -2.249 |
| **GTF2H5** | (TTA-D) encodes subunit of transcription/repair factor TFIIH which functions in transcription and DNA repair | -3.158 | -2.948 | -1.701 | 0.598 |
| **H2AFZ** | encodes replication independent member of histone H2A family. Mutations are associated with Alzheimer's and expression may correlate with tumourigenesis and cell survival. Encourages metastasis of cancer cells | -2.761 | -2.160 | -0.529 | -3.231 |
| **HDAC6** | Encodes for class II histone deacetylase enzyme. | -0.217 | -0.037 | 6.085 | 5.335 |
| **HDAC8** | class I histone deacetylase represses transcription, possible role in suppressing mutant p53 transcription | -2.589 | -2.681 | -6.140 | -4.366 |
| **HLTF** | regulates transcription by altering chromatin structure, potential tumour suppressor Rad5 homolog | -2.860 | -2.822 | -3.282 | -2.056 |
| **HSP90B1** | member of ATP metabolising molecular chaperones has role in stabilising and folding other proteins. Expression is associated with tumour formation | 1.147 | 1.664 | -4.646 | -4.740 |
| **JARID2** | DNA binding protein acts as transcriptional repressor | -2.090 | -1.861 | -7.155 | -2.503 |
| **KDM2B** | encodes member of F-box protein family. Fbls class involved in ubiquitination | -2.411 | -1.586 | -4.215 | -1.617 |
| **LIG1** | ATP dependant DNA ligase family protein, involved in DNA replication, recombination and BER | -2.400 | -1.822 | -4.644 | -4.186 |
| **LIG3** | DNA ligase involved in excision repair deletion is synthetically lethal | -1.719 | -1.759 | -2.531 | -5.805 |
| **LIG4** | DNA ligase essential for DSB repair through NHEJ forms complex with XRCC4 | -2.379 | -1.549 | -5.316 | -5.678 |
| **MCM5** | member of MCM family of chromatin binding proteins may act in cell cycle regulation | -2.455 | -0.880 | -6.173 | -4.427 |
| **MLL** | transcriptional co-activator regulating gene expression in early development and haematopoiesis | -1.307 | -0.847 | -7.513 | -6.851 |
| **MSH4** | DNA mismatch repair protein meiosis specific needed for HR in meiosis 1 | -2.121 | -0.591 | -7.292 | -6.342 |
| **NUDT1** | enzyme hydrolysing/oxidising purine nucleoside triphosphates to monophosphates. Prevents mis-incorporation aka MTH1 | -2.869 | -2.573 | 4.997 | 3.943 |
| **PDS5A** | may regulate sister chromatid cohesion during mitosis | -1.962 | -0.948 | -6.822 | -4.995 |
| **PIF1** | encodes DNA-dependent ATP metabolising enzyme that is 5' to 3' helicase, inhibits actions of telomerase | -2.094 | -2.483 | -3.221 | -2.852 |
| **POLM** | gap filling polymerase in repair of DSB by NHEJ | 0.127 | -1.056 | -2.880 | -5.859 |
| **PPP3CA** | may have role in calmodulin activation of calcineurin | -2.526 | -3.051 | -6.958 | -5.075 |

| | | | | | |
|---|---|---|---|---|---|
| **PTCH1** | patched gene family, possibly tumour suppressor | -2.560 | -2.552 | -3.519 | -4.615 |
| **RFX3** | regulatory factor X encodes transcription factors | -2.572 | -2.812 | -5.049 | -3.218 |
| **SMARCA2** | has helicase and ATPase activities may regulate transcription of certain genes | -2.329 | -2.074 | -4.823 | -4.271 |
| **SMC6** | may promote sister chromatid HR | -2.748 | -2.390 | -4.907 | -0.683 |
| **SPO11** | causes DSB in paired chromosome homologs in meiosis | -2.224 | -2.345 | 0.693 | -2.712 |
| **SSBP1** | housekeeping gene involved in mitochondrial biogenesis, subunit of ssDNA binding complex involved in maintenance of genome stability | -3.158 | -2.573 | -1.731 | -3.501 |
| **SUZ12** | zinc finger gene identified at breakpoints of recurrent chromosomal translocation | -2.538 | -2.570 | 1.587 | -0.591 |
| **TAL1** | may have role in haemopoietic differentiation | -2.343 | -2.801 | 4.658 | -1.354 |
| **TIMELESS** | cell survival, increases DNA poly epsilon, maintains telomere length | -2.554 | -2.050 | -2.339 | -2.811 |
| **TRDMT1** | encodes protein responsible for methylation of aspartic acid t RNA | -1.590 | -1.229 | -6.532 | -2.196 |

# References


Abdullah, U.B., J.F. McGouran, S. Brolih, D. Ptchelkine, A.H. El-Sagheer, T. Brown, and P.J. McHugh. 2017. RPA activates the XPF-ERCC1 endonuclease to initiate processing of DNA interstrand crosslinks. *EMBO J.* 36:2047–2060. doi:10.15252/embj.201796664.

Ahnesorg, P., P. Smith, and S.P. Jackson. XLF Interacts with the XRCC4-DNA Ligase IV Complex to Promote DNA Nonhomologous End-Joining. *Cell*. 124:301–313.

Akkari, Y.M., R.L. Bateman, C.A. Reifsteck, S.B. Olson, and M. Grompe. 2000. DNA replication is required To elicit cellular responses to psoralen-induced DNA interstrand cross-links. *Mol. Cell. Biol.* 20:8283–8289.

Al-Hajj, M., M.S. Wicha, A. Benito-Hernandez, S.J. Morrison, and M.F. Clarke. 2003. Prospective identification of tumorigenic breast cancer cells. *Proc. Natl. Acad. Sci. U.S.A.* 100:3983–3988.

Albertella, M.R., C.M. Green, A.R. Lehmann, and M.J. O'Connor. 2005. A role for polymerase eta in the cellular tolerance to cisplatin-induced damage. *Cancer Res*. 65:9799–9806. doi:10.1158/0008-5472.CAN-05-1095.

Andersson, B.S., T. Sadeghi, M.J. Siciliano, R. Legerski, and D. Murray. 1996. Nucleotide excision repair genes as determinants of cellular sensitivity to cyclophosphamide analogs. *Cancer Chemother Pharmacol*. 38:406–416. doi:10.1007/s002800050504.

Angelov, T., A. Guainazzi, and O.D. Schärer. 2009. Generation of DNA Interstrand Crosslinks by Post-Synthetic Reductive Amination. *Organic letters*. 11:661–664.

Anoopkumar-Dukie, S., J.B. Carey, T. Conere, E. O'Sullivan, F.N. van Pelt, and A. Allshire. 2005. Resazurin assay of radiation response in cultured cells. *BJR*. 78:945–947. doi:10.1259/bjr/54004230.

Aplan, P.D., K. Nakahara, S.H. Orkin, and I.R. Kirsch. 1992. The SCL gene product: a positive regulator of erythroid differentiation. *EMBO J.* 11:4073–4081.

Arakawa, H., T. Bednar, M. Wang, K. Paul, E. Mladenov, A.A. Bencsik-Theilen, and G. Iliakis. 2012. Functional redundancy between DNA ligases I and III in DNA replication in vertebrate cells. *Nucleic Acids Res.* 40:2599–2610. doi:10.1093/nar/gkr1024.

Arora, S., K.M. Bisanz, L.A. Peralta, G.D. Basu, A. Choudhary, R. Tibes, and D.O. Azorsa. 2010. RNAi screening of the kinome identifies modulators of cisplatin response in ovarian cancer cells. *Gynecol Oncol*. 118:220–227.

doi:10.1016/j.ygyno.2010.05.006.

Audebert, M., B. Salles, and P. Calsou. 2004. Involvement of poly(ADP-ribose) polymerase-1 and XRCC1/DNA ligase III in an alternative route for DNA double-strand breaks rejoining. *J Biol Chem*. 279:55117–55126. doi:10.1074/jbc.M404524200.

Audebert, M., B. Salles, M. Weinfeld, and P. Calsou. 2006. Involvement of polynucleotide kinase in a poly(ADP-ribose) polymerase-1-dependent DNA double-strand breaks rejoining pathway. *J Mol Biol*. 356:257–265. doi:10.1016/j.jmb.2005.11.028.

Auerbach, A.D. 1988. A test for Fanconi's anemia. *Blood*. 72:366–367.

Azqueta, A., J. Slyskova, S.A.S. Langie, I. O'Neill Gaivão, and A. Collins. 2014. Comet assay to measure DNA repair: approach and applications. *Frontiers in Genetics*. 5:288.

Bagchi, A., C. Papazoglu, Y. Wu, D. Capurso, M. Brodt, D. Francis, M. Bredel, H. Vogel, and A.A. Mills. 2007. CHD5 is a tumor suppressor at human 1p36. *Cell*. 128:459–475.

Balmus, G., N.A. Karp, B.L. Ng, S.P. Jackson, D.J. Adams, and R.E. McIntyre. 2015. A high-throughput in vivo micronucleus assay for genome instability screening in mice. *Nat Protoc*. 10:205–215. doi:10.1038/nprot.2015.010.

Banath, J.P., S.H. Macphail, and P.L. Olive. 2004. Radiation sensitivity, H2AX phosphorylation, and kinetics of repair of DNA strand breaks in irradiated cervical cancer cell lines. *Cancer Res*. 64:7144–7149. doi:10.1158/0008-5472.CAN-04-1433.

Barnes, D.E., A.E. Tomkinson, A.R. Lehmann, A.D. Webster, and T. Lindahl. 1992. Mutations in the DNA ligase I gene of an individual with immunodeficiencies and cellular hypersensitivity to DNA-damaging agents. *Cell*. 69:495–503.

Barrangou, R., C. Fremaux, H. Deveau, M. Richards, P. Boyaval, S. Moineau, D.A. Romero, and P. Horvath. 2007. CRISPR Provides Acquired Resistance Against Viruses in Prokaryotes. *Science*. 315:1709–1712. doi:10.1126/science.1138140.

Bartz, S.R., Z. Zhang, J. Burchard, M. Imakura, M. Martin, A. Palmieri, R. Needham, J. Guo, M. Gordon, N. Chung, P. Warrener, A.L. Jackson, M. Carleton, M. Oatley, L. Locco, F. Santini, T. Smith, P. Kunapuli, M. Ferrer, B. Strulovici, S.H. Friend, and P.S. Linsley. 2006. Small interfering RNA screens reveal enhanced cisplatin cytotoxicity in tumor cells having both BRCA network and TP53 disruptions. *Mol. Cell. Biol.* 26:9377–9386. doi:10.1128/MCB.01229-06.

Bauer, G.B., and L.F. Povirk. 1997. Specificity and kinetics of interstrand and intrastrand bifunctional alkylation by nitrogen mustards at a G-G-C sequence. *Nucleic Acids Res.* 25:1211–1218.

Baumann, P., F.E. Benson, and S.C. West. 1996. Human Rad51 protein promotes ATP-dependent homologous pairing and strand transfer reactions in vitro. *Cell*. 87:757–766.

Belzile, J.-P., S.A. Choudhury, D. Cournoyer, and T.Y.-K. Chow. 2006. Targeting DNA repair proteins: a promising avenue for cancer gene therapy. *Curr Gene Ther*. 6:111–123.

Ben-Yehoyada, M., L.C. Wang, I.D. Kozekov, C.J. Rizzo, M.E. Gottesman, and J. Gautier. 2009. Checkpoint signaling from a single DNA interstrand crosslink. *Mol. Cell*. 35:704–715. doi:10.1016/j.molcel.2009.08.014.

Berardini, M., P.L. Foster, and E.L. Loechler. 1999. DNA polymerase II (polB) is involved in a new DNA repair pathway for DNA interstrand cross-links in Escherichia coli. *J Bacteriol*. 181:2878–2882.

Berardini, M., W. Mackay, and E.L. Loechler. 1997. Evidence for a recombination-independent pathway for the repair of DNA interstrand cross-links based on a site-specific study with nitrogen mustard. *Biochemistry*. 36:3506–3513. doi:10.1021/bi962778w.

Bergqvist, A.S., D. Brattstrom, M. Bergqvist, O. Brodin, G. Wagenius, and L.A. Zetterberg. 2001. The frequency of micronuclei in lung cancer cell lines and their correlation to intrinsic radiation sensitivity. *Anticancer Res*. 21:3853–3856.

Bergsagel, D.E., and F.A. Valeriote. 1968. Growth characteristics of a mouse plasma cell tumor. *Cancer Res*. 28:2187–2196.

Bernard, M., E. Delabesse, S. Novault, O. Hermine, and E.A. Macintyre. 1998. Antiapoptotic effect of ectopic TAL1/SCL expression in a human leukemic T-cell line. *Cancer Res*. 58:2680–2687.

Bernstein, E., A.A. Caudy, S.M. Hammond, and G.J. Hannon. 2001. Role for a bidentate ribonuclease in the initiation step of RNA interference. *Nature*. 409:363–366. doi:10.1038/35053110.

Bhattacharyya, A., U.S. Ear, B.H. Koller, R.R. Weichselbaum, and D.K. Bishop. 2000. The breast cancer susceptibility gene BRCA1 is required for subnuclear assembly of Rad51 and survival following treatment with the DNA cross-linking agent cisplatin. *J Biol Chem*. 275:23899–23903.

Bienko, M., C.M. Green, N. Crosetto, F. Rudolf, G. Zapart, B. Coull, P. Kannouche, G. Wider, M. Peter, A.R. Lehmann, K. Hofmann, and I. Dikic. 2005. Ubiquitin-binding domains in Y-family polymerases regulate translesion synthesis. *Science*. 310:1821–1824. doi:10.1126/science.1120615.

Birmingham, A., E.M. Anderson, A. Reynolds, D. Ilsley-Tyree, D. Leake, Y. Fedorov, S. Baskerville, E. Maksimova, K. Robinson, J. Karpilow, W.S. Marshall, and A. Khvorova. 2006. 3' UTR seed matches, but not overall identity, are associated with RNAi off-targets. *Nat Methods*. 3:199–204. doi:10.1038/nmeth854.

Birmingham, A., L.M. Selfors, T. Forster, D. Wrobel, C.J. Kennedy, E. Shanks, J. Santoyo-Lopez, D.J. Dunican, A. Long, D. Kelleher, Q. Smith, R.L. Beijersbergen, P. Ghazal, and C.E. Shamu. 2009. Statistical Methods for Analysis of High-Throughput RNA Interference Screens. *Nat Methods*. 6:569–575.

Bonnet, D., and J.E. Dick. 1997. Human acute myeloid leukemia is organized as a hierarchy that originates from a primitive hematopoietic cell. *Nat Med*. 3:730–737. doi:10.1038/nm0797-730.

Brennecke, J., A. Stark, R.B. Russell, and S.M. Cohen. 2005. Principles of microRNA-target recognition. *PLoS Biol*. 3:e85. doi:10.1371/journal.pbio.0030085.

Brenneman, M.A., A.E. Weiss, J.A. Nickoloff, and D.J. Chen. 2000. XRCC3 is required for efficient repair of chromosome breaks by homologous recombination. *Mutation Research/DNA Repair*. 459:89–97.

Broderick, R., J. Nieminuszczy, H.T. Baddock, R. Deshpande, O. Gileadi, T.T. Paull, P.J. McHugh, and W. Niedzwiedz. 2016. EXD2 promotes homologous recombination by facilitating DNA end resection. *Nat Cell Biol*. 18:271–280. doi:10.1038/ncb3303.

Brooks, P.J., and J.A. Theruvathu. 2005. DNA adducts from acetaldehyde: implications for alcohol-related carcinogenesis. *Alcohol*. 35:187–193. doi:10.1016/j.alcohol.2005.03.009.

Brooks, P.J., and S. Zakhari. 2014. Acetaldehyde and the genome: beyond nuclear DNA adducts and carcinogenesis. *Environ Mol Mutagen*. 55:77–91. doi:10.1002/em.21824.

BRUCE, W.R., and H. van der GAAG. 1963. A QUANTITATIVE ASSAY FOR THE NUMBER OF MURINE LYMPHOMA CELLS CAPABLE OF PROLIFERATION IN VIVO. *Nature*. 199:79–80.

Budzowska, M., T.G. Graham, A. Sobeck, S. Waga, and J.C. Walter. 2015. Regulation of the Rev1–pol ζ complex during bypass of a DNA interstrand cross-link. *EMBO J.* 34:1971–1985.

Buis, J., Y. Wu, Y. Deng, J. Leddon, G. Westfield, M. Eckersdorff, J.M. Sekiguchi, S. Chang, and D.O. Ferguson. 2008. Mre11 nuclease activity has essential roles in DNA repair and genomic stability distinct from ATM activation. *Cell*. 135:85–96. doi:10.1016/j.cell.2008.08.015.

Caffrey, D.R., J. Zhao, Z. Song, M.E. Schaffer, S.A. Haney, R.R. Subramanian, A.B. Seymour, and J.D. Hughes. 2011. siRNA Off-Target Effects Can Be Reduced at Concentrations That Match Their Individual Potency. *PLOS ONE*. 6:e21503. doi:10.1371/journal.pone.0021503.

Cannavo, E., G. Marra, J. Sabates-Bellver, M. Menigatti, S.M. Lipkin, F. Fischer, P. Cejka, and J. Jiricny. 2005. Expression of the MutL homologue hMLH3 in human cells and its role in DNA mismatch repair. *Cancer Res*. 65:10759–10766. doi:10.1158/0008-5472.CAN-05-2528.

Carthew, R.W., and E.J. Sontheimer. 2009. Origins and Mechanisms of miRNAs and siRNAs. *Cell*. 136:642–655. doi:10.1016/j.cell.2009.01.035.

Cary, R.B., S.R. Peterson, J. Wang, D.G. Bear, E.M. Bradbury, and D.J. Chen. 1997. DNA looping by Ku and the DNA-dependent protein kinase. *Proceedings of the National Academy of Sciences*. 94:4267–4272.

Cattell, E., B. Sengerová, and P.J. McHugh. 2010. The SNM1/Pso2 family of ICL repair nucleases: from yeast to man. *Environ Mol Mutagen*. 51:635–645. doi:10.1002/em.20556.

Chen, X.B., R. Melchionna, C.M. Denis, P.H. Gaillard, A. Blasina, I. Van de Weyer, M.N. Boddy, P. Russell, J. Vialard, and C.H. McGowan. 2001. Human Mus81-associated endonuclease cleaves Holliday junctions in vitro. *Mol. Cell*. 8:1117–1127.

Cho, Y.-J., H. Wang, I.D. Kozekov, A.J. Kurtz, J. Jacob, M. Voehler, J. Smith, T.M. Harris, R.S. Lloyd, C.J. Rizzo, and M.P. Stone. 2006. Stereospecific formation of interstrand carbinolamine DNA cross-links by crotonaldehyde- and acetaldehyde-derived alpha-CH3-gamma-OH-1,N2-propano-2'-deoxyguanosine adducts in the 5‘-CpG-3’ sequence. *Chem. Res. Toxicol.* 19:195–208. doi:10.1021/tx050239z.

Chu, G., and E. Chang. 1988. Xeroderma pigmentosum group E cells lack a nuclear factor that binds to damaged DNA. *Science*. 242:564–567.

Chung, F.L., H.J. Chen, and R.G. Nath. 1996. Lipid peroxidation as a potential endogenous source for the formation of exocyclic DNA adducts. *Carcinogenesis*. 17:2105–2111.

Ciccia, A., C. Ling, R. Coulthard, Z. Yan, Y. Xue, A.R. Meetei, E.H. Laghmani, H. Joenje, N. McDonald, J.P. de Winter, W. Wang, and S.C. West. 2007. Identification of FAAP24, a Fanconi anemia core complex protein that interacts with FANCM. *Mol. Cell*. 25:331–343. doi:10.1016/j.molcel.2007.01.003.

Ciccia, A., N. McDonald, and S.C. West. 2008. Structural and functional relationships of the XPF/MUS81 family of proteins. *Annu. Rev. Biochem.* 77:259–287. doi:10.1146/annurev.biochem.77.070306.102408.

Coin, F., V. Oksenych, V. Mocquet, S. Groh, C. Blattner, and J.-M. Egly. 2008. Nucleotide excision repair driven by the dissociation of CAK from TFIIH. *Mol. Cell*. 31:9–20. doi:10.1016/j.molcel.2008.04.024.

Cole, R.S. 1973. Repair of DNA containing interstrand crosslinks in Escherichia coli: sequential excision and recombination. *Proc. Natl. Acad. Sci. U.S.A.* 70:1064–1068.

Cole, R.S., D. Levitan, and R.R. Sinden. 1976. Removal of psoralen interstrand cross-links from DNA of Escherichia coli: mechanism and genetic control. *J Mol Biol*. 103:39–59.

Collins, A.R. 1993. Mutant rodent cell lines sensitive to ultraviolet light, ionizing radiation and cross-linking agents: a comprehensive survey of genetic and biochemical characteristics. *Mutation Research/DNA Repair*. 293:99–118.

Compe, E., and J.-M. Egly. 2012. TFIIH: when transcription met DNA repair. *Nat Rev Mol Cell Biol*. 13:343–354. doi:10.1038/nrm3350.

Coquelle, N., Z. Havali-Shahriari, N. Bernstein, R. Green, and J.N.M. Glover. 2011. Structural basis for the phosphatase activity of polynucleotide kinase/phosphatase on single- and double-stranded DNA substrates. *Proc. Natl. Acad. Sci. U.S.A.* 108:21022–21027. doi:10.1073/pnas.1112036108.

Costantini, S., L. Woodbine, L. Andreoli, P.A. Jeggo, and A. Vindigni. 2007. Interaction of the Ku heterodimer with the DNA ligase IV/Xrcc4 complex and its regulation by DNA-PK. *DNA Repair (Amst)*. 6:712–722. doi:10.1016/j.dnarep.2006.12.007.

Coste, F., J.M. Malinge, L. Serre, W. Shepard, M. Roth, M. Leng, and C. Zelwer. 1999. Crystal structure of a double-stranded DNA containing a cisplatin interstrand cross-link at 1.63 A resolution: hydration at the platinated site. *Nucleic Acids Res.* 27:1837–1846.

Couvé, S., G. Macé-Aimé, F. Rosselli, and M.K. Saparbaev. 2009. The human oxidative DNA glycosylase NEIL1 excises psoralen-induced interstrand DNA cross-links in a three-stranded DNA structure. *Journal of Biological Chemistry*. 284:11963–11970.

Couvé-Privat, S., G. Macé, F. Rosselli, and M.K. Saparbaev. 2007. Psoralen-induced DNA adducts are substrates for the base excision repair pathway in human cells. *Nucleic Acids Res.* 35:5672–5682.

Cummings, J., V.J. Spanswick, M. Tomasz, and J.F. Smyth. 1998. Enzymology of mitomycin C metabolic activation in tumour tissue: implications for enzyme-directed bioreductive drug development. *Biochem Pharmacol*. 56:405–414.

Davies, A.A., D. Huttner, Y. Daigaku, S. Chen, and H.D. Ulrich. 2008. Activation of ubiquitin-dependent DNA damage bypass is mediated by replication protein a. *Mol. Cell*. 29:625–636. doi:10.1016/j.molcel.2007.12.016.

De Silva, I.U., P.J. McHugh, P.H. Clingen, and J.A. Hartley. 2000. Defining the roles of nucleotide excision repair and recombination in the repair of DNA interstrand cross-links in mammalian cells. *Mol. Cell. Biol.* 20:7980–7990.

Deans, A.J., and S.C. West. 2011. DNA interstrand crosslink repair and cancer. *Nat. Rev. Cancer*. 11:467–480. doi:10.1038/nrc3088.

Dizdaroglu, M. 2005. Base-excision repair of oxidative DNA damage by DNA glycosylases. *Mutation Research - Fundamental and Molecular Mechanisms of Mutagenesis*. 591:45–59.

Dizdaroglu, M., and P. Jaruga. 2012. Mechanisms of free radical-induced damage to

DNA. *Free Radic Res*. 46:382–419. doi:10.3109/10715762.2011.653969.

Dudley, D.D., J. Chaudhuri, C.H. Bassing, and F.W. Alt. 2005. Mechanism and control of V(D)J recombination versus class switch recombination: Similarities and differences. 86. 70 pp.

Dunand-Sauthier, I., M. Hohl, F. Thorel, P. Jaquier-Gubler, S.G. Clarkson, and O.D. Schärer. 2005. The spacer region of XPG mediates recruitment to nucleotide excision repair complexes and determines substrate specificity. *J Biol Chem*. 280:7030–7037. doi:10.1074/jbc.M412228200.

Eastman, A. 1986. Reevaluation of interaction of cis-dichloro(ethylenediamine)platinum(II) with DNA. *Biochemistry*. 25:3912–3915.

Echeverri, C.J., and N. Perrimon. 2006. High-throughput RNAi screening in cultured cells: a user's guide. *Nat. Rev. Genet.* 7:373–384. doi:10.1038/nrg1836.

Eisen, J.A., K.S. Sweder, and P.C. Hanawalt. 1995. Evolution of the SNF2 family of proteins: subfamilies with distinct sequences and functions. *Nucleic Acids Res.* 23:2715–2723.

El-Telbany, A., and P.C. Ma. 2012. Cancer Genes in Lung Cancer: Racial Disparities: Are There Any? *Genes & Cancer*. 3:467–480.

Elbashir, S.M., W. Lendeckel, and T. Tuschl. 2001. RNA interference is mediated by 21- and 22-nucleotide RNAs. *Genes Dev.* 15:188–200.

Enoiu, M., J. Jiricny, and O.D. Schärer. 2012. Repair of cisplatin-induced DNA interstrand crosslinks by a replication-independent pathway involving transcription-coupled repair and translesion synthesis. *Nucleic Acids Res.* 40:8953–8964. doi:10.1093/nar/gks670.

Evans, E., J. Fellows, A. Coffer, and R.D. Wood. 1997. Open complex formation around a lesion during nucleotide excision repair provides a structure for cleavage by human XPG protein. *EMBO J.* 16:625–638. doi:10.1093/emboj/16.3.625.

Fan, L., J.O. Fuss, Q.J. Cheng, A.S. Arvai, M. Hammel, V.A. Roberts, P.K. Cooper, and J.A. Tainer. 2008. XPD helicase structures and activities: insights into the cancer and aging phenotypes from XPD mutations. *Cell*. 133:789–800. doi:10.1016/j.cell.2008.04.030.

Farh, K.K.-H., A. Grimson, C. Jan, B.P. Lewis, W.K. Johnston, L.P. Lim, C.B. Burge, and D.P. Bartel. 2005. The widespread impact of mammalian MicroRNAs on mRNA repression and evolution. *Science*. 310:1817–1821. doi:10.1126/science.1121158.

Fekairi, S., S. Scaglione, C. Chahwan, E.R. Taylor, A. Tissier, S. Coulon, M.-Q. Dong, C. Ruse, J.R. Yates, P. Russell, R.P. Fuchs, C.H. McGowan, and P.-H.L. Gaillard. 2009. Human SLX4 is a Holliday Junction Resolvase Subunit that Binds Multiple DNA

Repair/Recombination Endonucleases. *Cell*. 138:78–89.

Feliciano, J., S. Feigenberg, and M. Mehta. 2013. Chemoradiation for Definitive, Pre-operative, or Post-Operative Therapy of Locally Advanced Non-Small Cell Lung Cancer. *Cancer journal (Sudbury, Mass.)*. 19:222–230.

Ferguson, D.O., and W.K. Holloman. 1996. Recombinational repair of gaps in DNA is asymmetric in Ustilago maydis and can be explained by a migrating D-loop model. *Proc. Natl. Acad. Sci. U.S.A.* 93:5419–5424.

Fiala, S. 1968. The cancer cell as a stem cell unable to differentiate. A theory of carcinogenesis. *Neoplasma*. 15:607–622.

Fire, A., S. Xu, M.K. Montgomery, S.A. Kostas, S.E. Driver, and C.C. Mello. 1998. Potent and specific genetic interference by double-stranded RNA in Caenorhabditis elegans. *Nature*. 391:806–811. doi:10.1038/35888.

Fisher, L.A., M. Bessho, and T. Bessho. 2008. Processing of a Psoralen DNA Interstrand Cross-link by XPF-ERCC1 Complex in Vitro. *Journal of Biological Chemistry*. 283:1275–1281.

Fiumicino, S., S. Martinelli, C. Colussi, G. Aquilina, C. Leonetti, M. Crescenzi, and M. Bignami. 2000. Sensitivity to DNA cross-linking chemotherapeutic agents in mismatch repair-defective cells in vitro and in xenografts. *Int. J. Cancer*. 85:590–596. doi:10.1002/(SICI)1097-0215(20000215)85:4<590::AID-IJC23>3.0.CO;2-O.

Franken, N.A.P., H.M. Rodermond, J. Stap, J. Haveman, and C. van Bree. 2006. Clonogenic assay of cells in vitro. *Nat Protoc*. 1:2315–2319. doi:10.1038/nprot.2006.339.

Friedberg, E.C., A.R. Lehmann, and R.P.P. Fuchs. 2005. Trading places: how do DNA polymerases switch during translesion DNA synthesis? *Mol. Cell*. 18:499–505. doi:10.1016/j.molcel.2005.03.032.

Friedberg, E.C., P.L. Fischhaber, and C. Kisker. 2001. Error-Prone DNA Polymerases. *Cell*. 107:9–12.

Fu, Y.V., H. Yardimci, D.T. Long, T.V. Ho, A. Guainazzi, V.P. Bermudez, J. Hurwitz, A. van Oijen, O.D. Schärer, and J.C. Walter. 2011. Selective bypass of a lagging strand roadblock by the eukaryotic replicative DNA helicase. *Cell*. 146:931–941.

Fulawka, L., P. Donizy, and A. Halon. 2014. Cancer stem cells – the current status of an old concept: literature review and clinical approaches. *Biological Research*. 47:66.

Fuller, L.F., and R.B. Painter. 1988. A Chinese hamster ovary cell line hypersensitive to ionizing radiation and deficient in repair replication. *Mutat. Res.* 193:109–121. doi:10.1016/0167-8817(88)90041-7.

Futami, K., A. Shimamoto, and Y. Furuichi. 2007. Mitochondrial and nuclear localization of human Pif1 helicase. *Biol Pharm Bull*. 30:1685–1692.

Gagou, M.E., A. Ganesh, G. Phear, D. Robinson, E. Petermann, A. Cox, and M. Meuth. 2014. Human PIF1 helicase supports DNA replication and cell growth under oncogenic-stress. *Oncotarget*. 5:11381–11398. doi:10.18632/oncotarget.2501.

Gagou, M.E., A. Ganesh, R. Thompson, G. Phear, C. Sanders, and M. Meuth. 2011. Suppression of apoptosis by PIF1 helicase in human tumor cells. *Cancer Res*. 71:4998–5008. doi:10.1158/0008-5472.CAN-10-4404.

Gan, G.N., J.P. Wittschieben, B.O. Wittschieben, and R.D. Wood. 2008. DNA polymerase zeta (pol zeta) in higher eukaryotes. *Cell Res*. 18:174–183. doi:10.1038/cr.2007.117.

Garaycoechea, J.I., G.P. Crossan, F. Langevin, M. Daly, M.J. Arends, and K.J. Patel. 2012. Genotoxic consequences of endogenous aldehydes on mouse haematopoietic stem cell function. *Nature*. 489:571–575. doi:10.1038/nature11368.

Garcia, C.C.M., J.P.F. Angeli, F.P. Freitas, O.F. Gomes, T.F. de Oliveira, A.P.M. Loureiro, P. Di Mascio, and M.H.G. Medeiros. 2011. [13C2]-Acetaldehyde promotes unequivocal formation of 1,N2-propano-2'-deoxyguanosine in human cells. *J Am Chem Soc*. 133:9140–9143. doi:10.1021/ja2004686.

Garcia, I., G. Mayol, E. Rodríguez, M. Suñol, T.R. Gershon, J. Ríos, N.-K.V. Cheung, M.W. Kieran, R.E. George, and A.R. Perez-Atayde. 2010. Expression of the neuron-specific protein CHD5 is an independent marker of outcome in neuroblastoma. *Molecular cancer*. 9:277.

Gargiulo, D., G.S. Kumar, S.S. Musser, and M. Tomasz. 1995. Structural and function modification of DNA by mitomycin C. Mechanism of the DNA sequence specificity of mitomycins. *Nucleic Acids Symp. Ser.* 169–170.

Gari, K., C. Decaillet, M. Delannoy, L. Wu, and A. Constantinou. 2008. Remodeling of DNA replication structures by the branch point translocase FANCM. *Proc. Natl. Acad. Sci. U.S.A.* 105:16107–16112. doi:10.1073/pnas.0804777105.

Gary, R., K. Kim, H.L. Cornelius, M.S. Park, and Y. Matsumoto. 1999. Proliferating cell nuclear antigen facilitates excision in long-patch base excision repair. *J Biol Chem*. 274:4354–4363.

Gelasco, A., and S.J. Lippard. 1998. NMR Solution Structure of a DNA Dodecamer Duplex Containing a cis-Diammineplatinum(II) d(GpG) Intrastrand Cross-Link, the Major Adduct of the Anticancer Drug Cisplatin †. *Biochemistry*. 37:9230–9239. doi:10.1021/bi973176v.

Genschel, J., S.J. Littman, J.T. Drummond, and P. Modrich. 1998. Isolation of MutSbeta from human cells and comparison of the mismatch repair specificities of MutSbeta and MutSalpha. *J Biol Chem*. 273:19895–19901.

George, T., Q. Wen, R. Griffiths, A. Ganesh, M. Meuth, and C.M. Sanders. 2009. Human Pif1 helicase unwinds synthetic DNA structures resembling stalled DNA replication forks. *Nucleic Acids Res.* 37:6491–6502. doi:10.1093/nar/gkp671.

Ghodgaonkar, M.M., F. Lazzaro, M. Olivera-Pimentel, M. Artola-Boran, P. Cejka, M.A. Reijns, A.P. Jackson, P. Plevani, M. Muzi-Falconi, and J. Jiricny. 2013. Ribonucleotides misincorporated into DNA act as strand-discrimination signals in eukaryotic mismatch repair. *Mol. Cell*. 50:323–332. doi:10.1016/j.molcel.2013.03.019.

Goodman, M.F., and R. Woodgate. 2013. Translesion DNA Polymerases. *Cold Spring Harb Perspect Biol*.

Grasby, J.A., L.D. Finger, S.E. Tsutakawa, J.M. Atack, and J.A. Tainer. 2012. Unpairing and gating: sequence-independent substrate recognition by FEN superfamily nucleases. *Trends Biochem Sci*. 37:74–84. doi:10.1016/j.tibs.2011.10.003.

Gratzner, H.G., R.C. Leif, D.J. Ingram, and A. Castro. 1975. The use of antibody specific for bromodeoxyuridine for the immunofluorescent determination of DNA replication in single cells and chromosomes. *Exp Cell Res*. 95:88–94.

Gregory, R.I., T.P. Chendrimada, N. Cooch, and R. Shiekhattar. 2005. Human RISC couples microRNA biogenesis and posttranscriptional gene silencing. *Cell*. 123:631–640. doi:10.1016/j.cell.2005.10.022.

Grundy, G.J., S.L. Rulten, Z. Zeng, R. Arribas-Bosacoma, N. Iles, K. Manley, A. Oliver, and K.W. Caldecott. 2013. APLF promotes the assembly and activity of non-homologous end joining protein complexes. *EMBO J.* 32:112–125. doi:10.1038/emboj.2012.304.

Guarne, A. 2012. The functions of MutL in mismatch repair: the power of multitasking. *Prog Mol Biol Transl Sci*. 110:41–70. doi:10.1016/B978-0-12-387665-2.00003-1.

GUO, G.Z., K. SASAI, N. OYA, T. SHIBATA, K. SHIBUYA, and M. HIRAOKA. 2009. A significant correlation between clonogenic radiosensitivity and the simultaneous assessment of micronucleus and apoptotic cell frequencies. *International Journal of Radiation Biology*. 75:857–864. doi:10.1080/095530099139917.

Gupta, R., and R.M. Brosh. 2008. Helicases as Prospective Targets for Anti-Cancer Therapy. *Anti-cancer agents in medicinal chemistry*. 8:390–401.

Han, J., Y. Lee, K.-H. Yeom, J.-W. Nam, I. Heo, J.-K. Rhee, S.Y. Sohn, Y. Cho, B.-T. Zhang, and V.N. Kim. 2006. Molecular basis for the recognition of primary microRNAs by the Drosha-DGCR8 complex. *Cell*. 125:887–901. doi:10.1016/j.cell.2006.03.043.

Han, K., E.E. Jeng, G.T. Hess, D.W. Morgens, A. Li, and M.C. Bassik. 2017. Synergistic drug combinations for cancer identified in a CRISPR screen for pairwise

genetic interactions. *Nat. Biotechnol.* 6:2781. doi:10.1038/nbt.3834.

Hanada, K., M. Budzowska, M. Modesti, A. Maas, C. Wyman, J. Essers, and R. Kanaar. 2006. The structure-specific endonuclease Mus81-Eme1 promotes conversion of interstrand DNA crosslinks into double-strands breaks. *EMBO J.* 25:4921–4932. doi:10.1038/sj.emboj.7601344.

Haran, T.E., and D.M. Crothers. 1988. Phased psoralen cross-links do not bend the DNA double helix. *Biochemistry*. 27:6967–6971.

Harrison, D.E., and C.P. Lerner. 1991. Most primitive hematopoietic stem cells are stimulated to cycle rapidly after treatment with 5-fluorouracil. *Blood*. 78:1237–1240.

Hartley, J.A., and D. Hochhauser. 2012. Small molecule drugs - optimizing DNA damaging agent-based therapeutics. *Curr Opin Pharmacol*. 12:398–402. doi:10.1016/j.coph.2012.03.008.

Hartley, J.A., and M.D. Wyatt. 1997. Determination of the DNA Sequence Specificity of Alkylation Damage Using Cleavage-Based Assays. *In* Drug-DNA Interaction Protocols. K.R. Fox, editor. Humana Press, Totowa, NJ. 147–156.

Hartley, J.M., V.J. Spanswick, and J.A. Hartley. 2011. Measurement of DNA Damage in Individual Cells Using the Single Cell Gel Electrophoresis (Comet) Assay. *In* Cancer Cell Culture. I.A. Cree, editor. Humana Press, Totowa, NJ. 309–320.

Hazra, T.K., J.W. Hill, T. Izumi, and S. Mitra. 2001. Multiple DNA glycosylases for repair of 8-oxoguanine and their potential in Vivo functions. *Progress in Nucleic Acid Research and Molecular Biology*. 68:193–205.

Hazrati, A., M. Ramis-Castelltort, S. Sarkar, L.J. Barber, C.J. Schofield, J.A. Hartley, and P.J. McHugh. 2008. Human SNM1A suppresses the DNA repair defects of yeast pso2 mutants. *DNA Repair (Amst)*. 7:230–238.

Hearst, J.E. 1981. Psoralen photochemistry. *Annu Rev Biophys Bioeng*. 10:69–86. doi:10.1146/annurev.bb.10.060181.000441.

Heil, F., H. Hemmi, H. Hochrein, F. Ampenberger, C. Kirschning, S. Akira, G. Lipford, H. Wagner, and S. Bauer. 2004. Species-specific recognition of single-stranded RNA via toll-like receptor 7 and 8. *Science*. 303:1526–1529.

Hemmati, H.D., I. Nakano, J.A. Lazareff, M. Masterman-Smith, D.H. Geschwind, M. Bronner-Fraser, and H.I. Kornblum. 2003. Cancerous stem cells can arise from pediatric brain tumors. *Proc. Natl. Acad. Sci. U.S.A.* 100:15178–15183.

Hickson, I.D., and A.L. Harris. 1988. Mammalian DNA repair--use of mutants hypersensitive to cytotoxic agents. *Trends Genet*. 4:101–106.

Higgins, G.S., R. Prevo, Y.-F. Lee, T. Helleday, R.J. Muschel, S. Taylor, M. Yoshimura, I.D. Hickson, E.J. Bernhard, and W.G. McKenna. 2010. A small interfering RNA screen of genes involved in DNA repair identifies tumor-specific

radiosensitization by POLQ knockdown. *Cancer Res*. 70:2984–2993. doi:10.1158/0008-5472.CAN-09-4040.

Hlavin, E.M., M.B. Smeaton, A.M. Noronha, C.J. Wilds, and P.S. Miller. 2010. Cross-link structure affects replication-independent DNA interstrand cross-link repair in mammalian cells. *Biochemistry*. 49:3977–3988. doi:10.1021/bi902169q.

Hoege, C., B. Pfander, G.-L. Moldovan, G. Pyrowolakis, and S. Jentsch. 2002. RAD6-dependent DNA repair is linked to modification of PCNA by ubiquitin and SUMO. *Nature*. 419:135–141.

Hohl, M., F. Thorel, S.G. Clarkson, and O.D. Schärer. 2003. Structural determinants for substrate binding and catalysis by the structure-specific endonuclease XPG. *J Biol Chem*. 278:19500–19508.

Horii, T., D. Tamura, S. Morita, M. Kimura, and I. Hatada. 2013. Generation of an ICF Syndrome Model by Efficient Genome Editing of Human Induced Pluripotent Stem Cells Using the CRISPR System. *International Journal of Molecular Sciences*. 14.

Hornung, V., M. Guenthner-Biller, C. Bourquin, A. Ablasser, M. Schlee, S. Uematsu, A. Noronha, M. Manoharan, S. Akira, A. de Fougerolles, S. Endres, and G. Hartmann. 2005. Sequence-specific potent induction of IFN-alpha by short interfering RNA in plasmacytoid dendritic cells through TLR7. *Nat Med*. 11:263–270. doi:10.1038/nm1191.

Hsu, H.L., L. Huang, J.T. Tsan, W. Funk, W.E. Wright, J.S. Hu, R.E. Kingston, and R. Baer. 1994. Preferred sequences for DNA recognition by the TAL1 helix-loop-helix proteins. *Mol. Cell. Biol.* 14:1256–1265.

Huang, H., L. Zhu, B.R. Reid, G.P. Drobny, and P.B. Hopkins. 1995. Solution structure of a cisplatin-induced DNA interstrand cross-link. *Science*. 270:1842–1845.

Huang, J., S. Liu, M. Bellani, A.K. Thazhathveetil, C. Ling, J.P. de Winter, Y. Wang, W. Wang, and M.M. Seidman. 2013. The DNA Translocase FANCM/MHF Promotes Replication Traverse of DNA Interstrand Crosslinks. *Mol. Cell*. 52:10.1016/j.molcel.2013.09.021.

Huang, M., R. Kennedy, A.M. Ali, L.A. Moreau, A.R. Meetei, A.D. D'Andrea, and C.C. Chen. 2011. Human MutS and FANCM complexes function as redundant DNA damage sensors in the Fanconi Anemia pathway. *DNA Repair (Amst)*. 10:1203–1212. doi:10.1016/j.dnarep.2011.09.006.

Huang, Y., and L. Li. 2013. DNA crosslinking damage and cancer - a tale of friend and foe. *Translational Cancer Research; Vol 2, No 3 (June 2013): Translational Cancer Research (DNA Damage and Repair)*.

Iliakis, G. 2009. Backup pathways of NHEJ in cells of higher eukaryotes: cell cycle dependence. *Radiother Oncol*. 92:310–315. doi:10.1016/j.radonc.2009.06.024.

Iorns, E., N.C. Turner, R. Elliott, N. Syed, O. Garrone, M. Gasco, A.N.J. Tutt, T. Crook, C.J. Lord, and A. Ashworth. 2008. Identification of CDK10 as an important determinant of resistance to endocrine therapy for breast cancer. *Cancer Cell*. 13:91–104. doi:10.1016/j.ccr.2008.01.001.

Ishiai, M., M. Kimura, K. Namikoshi, M. Yamazoe, K. Yamamoto, H. Arakawa, K. Agematsu, N. Matsushita, S. Takeda, J.-M. Buerstedde, and M. Takata. 2004. DNA cross-link repair protein SNM1A interacts with PIAS1 in nuclear focus formation. *Mol. Cell. Biol.* 24:10733–10741. doi:10.1128/MCB.24.24.10733-10741.2004.

Islas, A.L., J.M. Vos, and P.C. Hanawalt. 1991. Differential introduction and repair of psoralen photoadducts to DNA in specific human genes. *Cancer Res*. 51:2867–2873.

Ito, E., S. Yue, E.H. Moriyama, A.B. Hui, I. Kim, W. Shi, N.M. Alajez, N. Bhogal, G. Li, A. Datti, A.D. Schimmer, B.C. Wilson, P.P. Liu, D. Durocher, B.G. Neel, B. O'Sullivan, B. Cummings, R. Bristow, J. Wrana, and F.-F. Liu. 2011. Uroporphyrinogen decarboxylase is a radiosensitizing target for head and neck cancer. *Sci Transl Med*. 3:67ra7. doi:10.1126/scitranslmed.3001922.

Iversen, P.W., B.J. Eastwood, G.S. Sittampalam, and K.L. Cox. 2006. A comparison of assay performance measures in screening assays: signal window, Z' factor, and assay variability ratio. *J Biomol Screen*. 11:247–252. doi:10.1177/1087057105285610.

Iyama, T., and D.M. Wilson III. 2013. DNA repair mechanisms in dividing and non-dividing cells. *Genome maintenance in the Nervous system*. 12:620–636.

Jackson, A.L., J. Burchard, D. Leake, A. Reynolds, J. Schelter, J. Guo, J.M. Johnson, L. Lim, J. Karpilow, K. Nichols, W. Marshall, A. Khvorova, and P.S. Linsley. 2006a. Position-specific chemical modification of siRNAs reduces “off-target” transcript silencing. *RNA*. 12:1197–1205. doi:10.1261/rna.30706.

Jackson, A.L., J. Burchard, J. Schelter, B.N. Chau, M. Cleary, L. Lim, and P.S. Linsley. 2006b. Widespread siRNA “off-target” transcript silencing mediated by seed region sequence complementarity. *RNA*. 12:1179–1187. doi:10.1261/rna.25706.

Jackson, A.L., S.R. Bartz, J. Schelter, S.V. Kobayashi, J. Burchard, M. Mao, B. Li, G. Cavet, and P.S. Linsley. 2003. Expression profiling reveals off-target gene regulation by RNAi. *Nat. Biotechnol.* 21:635–637. doi:10.1038/nbt831.

Jackson, S.P., and J. Bartek. 2009. The DNA-damage response in human biology and disease. *Nature*. 461:1071–1078.

Jensen, R.B., A. Carreira, and S.C. Kowalczykowski. 2010. Purified human BRCA2 stimulates RAD51-mediated recombination. *Nature*. 467:678–683. doi:10.1038/nature09399.

Jinek, M., K. Chylinski, I. Fonfara, M. Hauer, J.A. Doudna, and E. Charpentier. 2012. A

Programmable Dual-RNA-Guided DNA Endonuclease in Adaptive Bacterial Immunity. *Science*. 337:816–821. doi:10.1126/science.1225829.

Johnson, R.E., M.T. Washington, L. Haracska, S. Prakash, and L. Prakash. 2000. Eukaryotic polymerases iota and zeta act sequentially to bypass DNA lesions. *Nature*. 406:1015–1019. doi:10.1038/35023030.

Jones, N.J., R. Cox, and J. Thacker. 1987. Isolation and cross-sensitivity of X-ray-sensitive mutants of V79-4 hamster cells. *Mutat. Res.* 183:279–286. doi:10.1016/0167-8817(87)90011-3.

Judge, A., and I. MacLachlan. 2008. Overcoming the innate immune response to small interfering RNA. *Hum Gene Ther*. 19:111–124. doi:10.1089/hum.2007.179.

Kannouche, P.L., J. Wing, and A.R. Lehmann. 2004. Interaction of human DNA polymerase eta with monoubiquitinated PCNA: a possible mechanism for the polymerase switch in response to DNA damage. *Mol. Cell*. 14:491–500.

Kartalou, M., and J.M. Essigmann. 2001. Recognition of cisplatin adducts by cellular proteins. *Mutat. Res.* 478:1–21.

Keeney, S., and M.J. Neale. 2006. Initiation of meiotic recombination by formation of DNA double-strand breaks: Mechanism and regulation. *Biochemical Society Transactions*. 34:523–525.

Keijzers, G., V.A. Bohr, and L.J. Rasmussen. 2015. Human exonuclease 1 (EXO1) activity characterization and its function on flap structures. *Bioscience Reports*. 35:e00206.

Kemp, L.M., S.G. Sedgwick, and P.A. Jeggo. 1984. X-ray sensitive mutants of Chinese hamster ovary cells defective in double-strand break rejoining. *Mutation Research/DNA Repair Reports*. 132:189–196.

Khan, A.A., D. Betel, M.L. Miller, C. Sander, C.S. Leslie, and D.S. Marks. 2009. Transfection of small RNAs globally perturbs gene regulation by endogenous microRNAs. *Nat. Biotechnol.* 27:549–555. doi:10.1038/nbt.1543.

Kim, J.M., Y. Kee, A. Gurtan, and A.D. D'Andrea. 2008. Cell cycle-dependent chromatin loading of the Fanconi anemia core complex by FANCM/FAAP24. *Blood*. 111:5215–5222. doi:10.1182/blood-2007-09-113092.

Kim, S., D. Kim, S.W. Cho, J. Kim, and J.-S. Kim. 2014. Highly efficient RNA-guided genome editing in human cells via delivery of purified Cas9 ribonucleoproteins. *Genome Res*. 24:1012–1019. doi:10.1101/gr.171322.113.

Kim, Y., F.P. Lach, R. Desetty, H. Hanenberg, A.D. Auerbach, and A. Smogorzewska. 2011. Mutations of the SLX4 gene in Fanconi anemia. *Nat Genet*. 43:142–146.

Kim, Y., G.S. Spitz, U. Veturi, F.P. Lach, A.D. Auerbach, and A. Smogorzewska. 2013. Regulation of multiple DNA repair pathways by the Fanconi anemia protein

SLX4. *Blood*. 121:54–63.

Kittler, R., V. Surendranath, A.-K. Heninger, M. Slabicki, M. Theis, G. Putz, K. Franke, A. Caldarelli, H. Grabner, K. Kozak, J. Wagner, E. Rees, B. Korn, C. Frenzel, C. Sachse, B. Sonnichsen, J. Guo, J. Schelter, J. Burchard, P.S. Linsley, A.L. Jackson, B. Habermann, and F. Buchholz. 2007. Genome-wide resources of endoribonuclease-prepared short interfering RNAs for specific loss-of-function studies. *Nat Methods*. 4:337–344. doi:10.1038/nmeth1025.

Klokov, D., S.M. MacPhail, J.P. Banath, J.P. Byrne, and P.L. Olive. 2006. Phosphorylated histone H2AX in relation to cell survival in tumor cells and xenografts exposed to single and fractionated doses of X-rays. *Radiother Oncol*. 80:223–229. doi:10.1016/j.radonc.2006.07.026.

Knipscheer, P., M. Räschle, A. Smogorzewska, M. Enoiu, T.V. Ho, O.D. Schärer, S.J. Elledge, and J.C. Walter. 2009. The Fanconi anemia pathway promotes replication-dependent DNA interstrand crosslink repair. *Science*. 326:1698–1701.

Kohn, K.W., C.L. Spears and P. Doty. 1966. Inter-strand crosslinking of DNA by nitrogen mustard. *J. Mol. Biol.* 19:266-88.

Kohn, K.W., J.A. Hartley, and W.B. Mattes. 1987. Mechanisms of DNA sequence selective alkylation of guanine-N7 positions by nitrogen mustards. *Nucleic Acids Res.* 15:10531–10549.

Kottakis, F., P. Foltopoulou, I. Sanidas, P. Keller, A. Wronski, B.T. Dake, S.A. Ezell, Z. Shen, S.P. Naber, P.W. Hinds, E. McNiel, C. Kuperwasser, and P.N. Tsichlis. 2014. NDY1/KDM2B Functions as a Master Regulator of Polycomb Complexes and Controls Self-Renewal of Breast Cancer Stem Cells. *Cancer Res*. 74:3935–3946. doi:10.1158/0008-5472.CAN-13-2733.

Kozekov, I.D., L.V. Nechev, A. Sanchez, C.M. Harris, R.S. Lloyd, and T.M. Harris. 2001. Interchain cross-linking of DNA mediated by the principal adduct of acrolein. *Chem. Res. Toxicol.* 14:1482–1485.

Kozekov, I.D., L.V. Nechev, M.S. Moseley, C.M. Harris, C.J. Rizzo, M.P. Stone, and T.M. Harris. 2003. DNA interchain cross-links formed by acrolein and crotonaldehyde. *J Am Chem Soc*. 125:50–61. doi:10.1021/ja020778f.

Kranz, D., and M. Boutros. 2014. A synthetic lethal screen identifies FAT1 as an antagonist of caspase-8 in extrinsic apoptosis. *EMBO J.* 33:181–197. doi:10.1002/embj.201385686.

Kratz, K., B. Schopf, S. Kaden, A. Sendoel, R. Eberhard, C. Lademann, E. Cannavo, A.A. Sartori, M.O. Hengartner, and J. Jiricny. 2010. Deficiency of FANCD2-associated nuclease KIAA1018/FAN1 sensitizes cells to interstrand crosslinking agents. *Cell*. 142:77–88. doi:10.1016/j.cell.2010.06.022.

Krishan, A. 1975. Rapid flow cytofluorometric analysis of mammalian cell cycle by propidium iodide staining. *J Cell Biol*. 66:188–193.

Kuchta, R.D., and G. Stengel. 2010. Mechanism and Evolution of DNA Primases. *Biochimica et biophysica acta*. 1804:1180–1189.

Kumari, A., I.G. Minko, M.B. Harbut, S.E. Finkel, M.F. Goodman, and R.S. Lloyd. 2008. Replication bypass of interstrand cross-link intermediates by Escherichia coli DNA polymerase IV. *J Biol Chem*. 283:27433–27437. doi:10.1074/jbc.M801237200.

Kunkel, T.A., and D.A. Erie. 2005. DNA mismatch repair. *Annu. Rev. Biochem.* 74:681–710. doi:10.1146/annurev.biochem.74.082803.133243.

Kuraoka, I., W.R. Kobertz, R.R. Ariza, M. Biggerstaff, J.M. Essigmann, and R.D. Wood. 2000. Repair of an interstrand DNA cross-link initiated by ERCC1-XPF repair/recombination nuclease. *J Biol Chem*. 275:26632–26636.

Kwon, Y., J.M. Daley, and P. Sung. 2017. Reconstituted System for the Examination of Repair DNA Synthesis in Homologous Recombination. *Methods Enzymol*. 591 IS -:307–325.

Lagerwaard, F.J., N.E. Verstegen, C.J.A. Haasbeek, B.J. Slotman, M.A. Paul, E.F. Smit, and S. Senan. Outcomes of Stereotactic Ablative Radiotherapy in Patients With Potentially Operable Stage I Non-Small Cell Lung Cancer. *International Journal of Radiation Oncology*Biology*Physics*. 83:348–353.

Lahaye, A., H. Stahl, D. Thines-Sempoux, and F. Foury. 1991. PIF1: a DNA helicase in yeast mitochondria. *EMBO J.* 10:997–1007.

Laine, J.-P., and J.-M. Egly. 2006. When transcription and repair meet: a complex system. *Trends Genet*. 22:430–436. doi:10.1016/j.tig.2006.06.006.

Landry, J.J.M., P.T. Pyl, T. Rausch, T. Zichner, M.M. Tekkedil, A.M. Stutz, A. Jauch, R.S. Aiyar, G. Pau, N. Delhomme, J. Gagneur, J.O. Korbel, W. Huber, and L.M. Steinmetz. 2013. The genomic and transcriptomic landscape of a HeLa cell line. *G3 (Bethesda)*. 3:1213–1224. doi:10.1534/g3.113.005777.

Langevin, F., G.P. Crossan, I.V. Rosado, M.J. Arends, and K.J. Patel. 2011. Fancd2 counteracts the toxic effects of naturally produced aldehydes in mice. *Nature*. 475:53–58. doi:10.1038/nature10192.

Larminat, F., W. Zhen, and V.A. Bohr. 1993. Gene-specific DNA repair of interstrand cross-links induced by chemotherapeutic agents can be preferential. *J Biol Chem*. 268:2649–2654.

Larsen, D.H., C. Poinsignon, T. Gudjonsson, C. Dinant, M.R. Payne, F.J. Hari, J.M.R. Danielsen, P. Menard, J.C. Sand, and M. Stucki. 2010. The chromatin-remodeling factor CHD4 coordinates signaling and repair after DNA damage. *J Cell Biol*. 190:731–740.

Lawley, P.D., and D.H. Phillips. 1996. DNA adducts from chemotherapeutic agents. *Mutat. Res.* 355:13–40.

Le Chalony, C., F. Hoffschir, L.R. Gauthier, J. Gross, D.S. Biard, F.D. Boussin, and V. Pennaneach. 2012. Partial complementation of a DNA ligase I deficiency by DNA ligase III and its impact on cell survival and telomere stability in mammalian cells. *Cell. Mol. Life Sci.* 69:2933–2949. doi:10.1007/s00018-012-0975-8.

Lehmann, A.R., A. Niimi, T. Ogi, S. Brown, S. Sabbioneda, J.F. Wing, P.L. Kannouche, and C.M. Green. 2007. Translesion synthesis: Y-family polymerases and the polymerase switch. *DNA Repair (Amst)*. 6:891–899. doi:10.1016/j.dnarep.2007.02.003.

Li, L., C.A. Peterson, X. Zhang, and R.J. Legerski. 2000. Requirement for PCNA and RPA in interstrand crosslink-induced DNA synthesis. *Nucleic Acids Res.* 28:1424–1427.

Li, S., S.-I. Kanno, R. Watanabe, H. Ogiwara, T. Kohno, G. Watanabe, A. Yasui, and M.R. Lieber. 2011. Polynucleotide kinase and aprataxin-like forkhead-associated protein (PALF) acts as both a single-stranded DNA endonuclease and a single-stranded DNA 3' exonuclease and can participate in DNA end joining in a biochemical system. *J Biol Chem*. 286:36368–36377. doi:10.1074/jbc.M111.287797.

Lieber, M.R. 2008. The mechanism of human nonhomologous DNA end joining. *J Biol Chem*. 283:1–5. doi:10.1074/jbc.R700039200.

Lieber, M.R. 2010. NHEJ and its backup pathways in chromosomal translocations. *Nat Struct Mol Biol*. 17:393–395. doi:10.1038/nsmb0410-393.

Lindahl, T., and D.E. Barnes. 2000. Repair of endogenous DNA damage. *Cold Spring Harb Symp Quant Biol*. 65:127–133.

Lindahl, T., and O. Karlstrom. 1973. Heat-induced depyrimidination of deoxyribonucleic acid in neutral solution. *Biochemistry*. 12:5151–5154.

Ling, C., J. Huang, Z. Yan, Y. Li, M. Ohzeki, M. Ishiai, D. Xu, M. Takata, M. Seidman, and W. Wang. Bloom syndrome complex promotes FANCM recruitment to stalled replication forks and facilitates both repair and traverse of DNA interstrand crosslinks JA . 2:16047 EP –. doi:10.1038/celldisc.2016.47.

Lippman, Z., and R. Martienssen. 2004. The role of RNA interference in heterochromatic silencing. *Nature*. 431:364–370. doi:10.1038/nature02875.

Liu, X., F. Jiang, S. Kalidas, D. Smith, and Q. Liu. 2006. Dicer-2 and R2D2 coordinately bind siRNA to promote assembly of the siRISC complexes. *RNA*. 12:1514–1520. doi:10.1261/rna.101606.

Liu, Z.-Z., W.-Y. Huang, X.-S. Li, J.-S. Lin, X.-K. Cai, K.-H. Lian, and H.-J. Zhou. 2005. Prediction value of radiosensitivity of hepatocarcinoma cells for apoptosis and micronucleus assay. *World J Gastroenterol*. 11:7036–7039.

Livneh, Z., O. Ziv, and S. Shachar. 2010. Multiple two-polymerase mechanisms in

mammalian translesion DNA synthesis. *Cell Cycle*. 9:729–735. doi:10.4161/cc.9.4.10727.

Lohman, P.H. 1999. Qualitative and quantitative procedures for health risk assessment. *Mutat. Res.* 428:237–254.

Long, D.T., V. Joukov, M. Budzowska, and J.C. Walter. 2014. BRCA1 promotes unloading of the CMG helicase from a stalled DNA replication fork. *Mol. Cell*. 56:174–185.

Lu, M., Q. Zhang, M. Deng, J. Miao, Y. Guo, W. Gao, and Q. Cui. 2008. An Analysis of Human MicroRNA and Disease Associations. *PLOS ONE*. 3:e3420. doi:10.1371/journal.pone.0003420.

Lujan, S.A., J.S. Williams, A.R. Clausen, A.B. Clark, and T.A. Kunkel. 2013. Ribonucleotides are signals for mismatch repair of leading-strand replication errors. *Mol. Cell*. 50:437–443. doi:10.1016/j.molcel.2013.03.017.

Lum, P.Y., C.D. Armour, S.B. Stepaniants, G. Cavet, M.K. Wolf, J.S. Butler, J.C. Hinshaw, P. Garnier, G.D. Prestwich, A. Leonardson, P. Garrett-Engele, C.M. Rush, M. Bard, G. Schimmack, J.W. Phillips, C.J. Roberts, and D.D. Shoemaker. 2004. Discovering modes of action for therapeutic compounds using a genome-wide screen of yeast heterozygotes. *Cell*. 116:121–137.

Lundholt, B.K., K.M. Scudder, and L. Pagliaro. 2003. A Simple Technique for Reducing Edge Effect in Cell-Based Assays. *J Biomol Screen*. 8:566–570. doi:10.1177/1087057103256465.

Lynch, H.T., and A. de la Chapelle. 1999. Genetic susceptibility to non-polyposis colorectal cancer. *J Med Genet*. 36:801–818.

MacKay, C., A.-C. Déclais, C. Lundin, A. Agostinho, A.J. Deans, T.J. MacArtney, K. Hofmann, A. Gartner, S.C. West, T. Helleday, D.M.J. Lilley, and J. Rouse. 2010. Identification of KIAA1018/FAN1, a DNA Repair Nuclease Recruited to DNA Damage by Monoubiquitinated FANCD2. *Cell*. 142:65–76. doi:10.1016/j.cell.2010.06.021.

MacRae, I.J., E. Ma, M. Zhou, C.V. Robinson, and J.A. Doudna. 2008. In vitro reconstitution of the human RISC-loading complex. *Proc. Natl. Acad. Sci. U.S.A.* 105:512–517. doi:10.1073/pnas.0710869105.

Madhusudan, S., and I.D. Hickson. 2005. DNA repair inhibition: a selective tumour targeting strategy. *Trends Mol Med*. 11:503–511. doi:10.1016/j.molmed.2005.09.004.

MAKINO, S. 1956. Further evidence favoring the concept of the stem cell in ascites tumors of rats. *Ann N Y Acad Sci*. 63:818–830.

Malinge, J.M., C. Pérez, and M. Leng. 1994. Base sequence-independent distorsions induced by interstrand cross-links in cis-diamminedichloroplatinum (II)-modified DNA. *Nucleic Acids Res.* 22:3834–3839.

Malivert, L., V. Ropars, M. Nunez, P. Drevet, S. Miron, G. Faure, R. Guerois, J.-P. Mornon, P. Revy, J.-B. Charbonnier, I. Callebaut, and J.-P. de Villartay. 2010. Delineation of the Xrcc4-interacting Region in the Globular Head Domain of Cernunnos/XLF. *Journal of Biological Chemistry*. 285:26475–26483.

Malo, N., J.A. Hanley, S. Cerquozzi, J. Pelletier, and R. Nadon. 2006. Statistical practice in high-throughput screening data analysis. *Nat. Biotechnol.* 24:167–175. doi:10.1038/nbt1186.

Maor-Shoshani, A., L.B. Meira, X. Yang, and L.D. Samson. 2008. 3-Methyladenine DNA glycosylase is important for cellular resistance to psoralen interstrand cross-links. *DNA Repair (Amst)*. 7:1399–1406.

Mari, P.-O., B.I. Florea, S.P. Persengiev, N.S. Verkaik, H.T. Bruggenwirth, M. Modesti, G. Giglia-Mari, K. Bezstarosti, J.A.A. Demmers, T.M. Luider, A.B. Houtsmuller, and D.C. van Gent. 2006. Dynamic assembly of end-joining complexes requires interaction between Ku70/80 and XRCC4. *Proc. Natl. Acad. Sci. U.S.A.* 103:18597–18602. doi:10.1073/pnas.0609061103.

Marraffini, L.A., and E.J. Sontheimer. 2010. Self versus non-self discrimination during CRISPR RNA-directed immunity. *Nature*. 463:568–571. doi:10.1038/nature08703.

Marteijn, J.A., H. Lans, W. Vermeulen, and J.H.J. Hoeijmakers. 2014. Understanding nucleotide excision repair and its roles in cancer and ageing. *Nat Rev Mol Cell Biol*. 15:465–481. doi:10.1038/nrm3822.

Martinez-Jimenez, M.I., S. Garcia-Gomez, K. Bebenek, G. Sastre-Moreno, P.A. Calvo, A. Diaz-Talavera, T.A. Kunkel, and L. Blanco. 2015. Alternative solutions and new scenarios for translesion DNA synthesis by human PrimPol. *DNA Repair (Amst)*. 29:127–138. doi:10.1016/j.dnarep.2015.02.013.

Masutani, C., K. Sugasawa, J. Yanagisawa, T. Sonoyama, M. Ui, T. Enomoto, K. Takio, K. Tanaka, P.J. van der Spek, and D. Bootsma. 1994. Purification and cloning of a nucleotide excision repair complex involving the xeroderma pigmentosum group C protein and a human homologue of yeast RAD23. *EMBO J.* 13:1831–1843.

Mateos-Gomez, P.A., F. Gong, N. Nair, K.M. Miller, E. Lazzerini-Denchi, and A. Sfeir. 2015. Mammalian polymerase ? promotes alternative NHEJ and suppresses recombination. *Nature*. 518:254–257. doi:10.1038/nature14157.

Mathieu, N., N. Kaczmarek, P. Ruthemann, A. Luch, and H. Naegeli. 2013. DNA quality control by a lesion sensor pocket of the xeroderma pigmentosum group D helicase subunit of TFIIH. *Curr Biol*. 23:204–212. doi:10.1016/j.cub.2012.12.032.

Matsuda, T., M. Kawanishi, T. Yagi, S. Matsui, and H. Takebe. 1998. Specific tandem GG to TT base substitutions induced by acetaldehyde are due to intra-strand crosslinks between adjacent guanine bases. *Nucleic Acids Res.* 26:1769–1774.

McHugh, P.J., and S. Sarkar. 2006. DNA interstrand cross-link repair in the cell cycle: a critical role for polymerase zeta in G1 phase. *Cell Cycle*. 5:1044–1047. doi:10.4161/cc.5.10.2763.

McHugh, P.J., V.J. Spanswick, and J.A. Hartley. 2001. Repair of DNA interstrand crosslinks: molecular mechanisms and clinical relevance. *Lancet Oncol.* 2:483–490. doi:10.1016/S1470-2045(01)00454-5.

McHugh, P.J., W.R. Sones, and J.A. Hartley. 2000. Repair of intermediate structures produced at DNA interstrand cross-links in Saccharomyces cerevisiae. *Mol. Cell. Biol.* 20:3425–3433.

McKinnon, P.J. 2009. DNA repair deficiency and neurological disease. *Nature Reviews Neuroscience*. 10:100–112.

McMurdie, K.E., J. Little, J. Sielge, and S. Dunaway. 2010. Elucidating the Role of the DNA Helicase Pfh1 in DNA Repair in Fission Yeast. *The FASEB Journal*. 24:875.3.

Mendelsohn, M.L., D.H.2. Moore, and P.H. Lohman. 1992. International Commission for Protection Against Environmental Mutagens and Carcinogens. A method for comparing and combining short-term genotoxicity test data: results and interpretation. *Mutat. Res.* 266:43–60.

Miętus, M., E. Nowak, M. Jaciuk, P. Kustosz, J. Studnicka, and M. Nowotny. 2014. Crystal structure of the catalytic core of Rad2: insights into the mechanism of substrate binding. *Nucleic Acids Res.* 42:10762–10775.

Mimitou, E.P., and L.S. Symington. 2008. Sae2, Exo1 and Sgs1 collaborate in DNA double-strand break processing. *Nature*. 455:770–774. doi:10.1038/nature07312.

Mimori, T., and J.A. Hardin. 1986. Mechanism of interaction between Ku protein and DNA. *J Biol Chem*. 261:10375–10379.

Min, J.-H., and N.P. Pavletich. 2007. Recognition of DNA damage by the Rad4 nucleotide excision repair protein. *Nature*. 449:570–575. doi:10.1038/nature06155.

Minko, I.G., M.B. Harbut, I.D. Kozekov, A. Kozekova, P.M. Jakobs, S.B. Olson, R.E. Moses, T.M. Harris, C.J. Rizzo, and R.S. Lloyd. 2008. Role for DNA polymerase kappa in the processing of N2-N2-guanine interstrand cross-links. *J Biol Chem*. 283:17075–17082. doi:10.1074/jbc.M801238200.

Modrich, P., and R. Lahue. 1996. Mismatch repair in replication fidelity, genetic recombination, and cancer biology. *Annu. Rev. Biochem.* 65:101–133. doi:10.1146/annurev.bi.65.070196.000533.

Mogi, S., C.E. Butcher, and D.H. Oh. 2008. DNA polymerase η reduces the γ-H2AX response to psoralen interstrand crosslinks in human cells. *Exp Cell Res*. 314:887–895.

Mok, T.S., Y.-L. Wu, S. Thongprasert, C.-H. Yang, D.-T. Chu, N. Saijo, P. Sunpaweravong, B. Han, B. Margono, Y. Ichinose, Y. Nishiwaki, Y. Ohe, J.-J. Yang, B. Chewaskulyong, H. Jiang, E.L. Duffield, C.L. Watkins, A.A. Armour, and M. Fukuoka. 2009. Gefitinib or carboplatin-paclitaxel in pulmonary adenocarcinoma. *N Engl J Med*. 361:947–957. doi:10.1056/NEJMoa0810699.

Moldovan, G.-L., M.V. Madhavan, K.D. Mirchandani, R.M. McCaffrey, P. Vinciguerra, and A.D. D'Andrea. 2010. DNA polymerase POLN participates in cross-link repair and homologous recombination. *Mol. Cell. Biol.* 30:1088–1096. doi:10.1128/MCB.01124-09.

Mony, B.M., P. MacGregor, A. Ivens, F. Rojas, A. Cowton, J. Young, D. Horn, and K. Matthews. 2014. Genome-wide dissection of the quorum sensing signalling pathway in Trypanosoma brucei. *Nature*. 505:681–685. doi:10.1038/nature12864.

Moser, J., H. Kool, I. Giakzidis, K. Caldecott, L.H.F. Mullenders, and M.I. Fousteri. 2007. Sealing of chromosomal DNA nicks during nucleotide excision repair requires XRCC1 and DNA ligase III alpha in a cell-cycle-specific manner. *Mol. Cell*. 27:311–323. doi:10.1016/j.molcel.2007.06.014.

Moshous, D., I. Callebaut, R. de Chasseval, B. Corneo, M. Cavazzana-Calvo, F. Le Deist, I. Tezcan, O. Sanal, Y. Bertrand, N. Philippe, A. Fischer, and J.P. de Villartay. 2001. Artemis, a novel DNA double-strand break repair/V(D)J recombination protein, is mutated in human severe combined immune deficiency. *Cell*. 105:177–186.

Mosmann, T. 1983. Rapid colorimetric assay for cellular growth and survival: application to proliferation and cytotoxicity assays. *J Immunol Methods*. 65:55–63.

Moynahan, M.E., and M. Jasin. 2010. Mitotic homologous recombination maintains genomic stability and suppresses tumorigenesis. *Nat Rev Mol Cell Biol*. 11:196–207. doi:10.1038/nrm2851.

Moynahan, M.E., T.Y. Cui, and M. Jasin. 2001. Homology-directed dna repair, mitomycin-c resistance, and chromosome stability is restored with correction of a Brca1 mutation. *Cancer Res*. 61:4842–4850.

Muniandy, P.A., D. Thapa, A.K. Thazhathveetil, S.-T. Liu, and M.M. Seidman. 2009. Repair of laser-localized DNA interstrand cross-links in G1 phase mammalian cells. *J Biol Chem*. 284:27908–27917. doi:10.1074/jbc.M109.029025.

Munshi, A., M. Hobbs, and R.E. Meyn. 2005. Clonogenic cell survival assay. *Methods Mol Med*. 110:21–28. doi:10.1385/1-59259-869-2:021.

Nagel, R., M. Stigter-van Walsum, M. Buijze, J. van den Berg, I.H. van der Meulen, J. Hodzic, S.R. Piersma, T.V. Pham, C.R. Jiménez, V.W. van Beusechem, and R.H. Brakenhoff. 2015. Genome-wide siRNA Screen Identifies the Radiosensitizing Effect of Downregulation of MASTL and FOXM1 in NSCLC. *Molecular Cancer Therapeutics*. 14:1434–1444. doi:10.1158/1535-7163.MCT-14-0846.

Nakanishi, K., F. Cavallo, L. Perrouault, C. Giovannangeli, M.E. Moynahan, M. Barchi, E. Brunet, and M. Jasin. 2011. Homology-directed Fanconi anemia pathway crosslink repair is dependent on DNA replication. *Nat Struct Mol Biol*. 18:500–503.

Ni, X., Y. Zhang, J. Ribas, W.H. Chowdhury, M. Castanares, Z. Zhang, M. Laiho, T.L. DeWeese, and S.E. Lupold. 2011. Prostate-targeted radiosensitization via aptamer-shRNA chimeras in human tumor xenografts. *J Clin Invest*. 121:2383–2390. doi:10.1172/JCI45109.

Nicolas, N., D. Moshous, M. Cavazzana-Calvo, D. Papadopoulo, R. de Chasseval, F. Le Deist, A. Fischer, and J.P. de Villartay. 1998. A human severe combined immunodeficiency (SCID) condition with increased sensitivity to ionizing radiations and impaired V(D)J rearrangements defines a new DNA recombination/repair deficiency. *J Exp Med*. 188:627–634.

Niedernhofer, L.J., A.S. Lalai, and J.H.J. Hoeijmakers. 2005. Fanconi anemia (cross)linked to DNA repair. *Cell*. 123:1191–1198. doi:10.1016/j.cell.2005.12.009.

Nijwening, J.H., H.J. Kuiken, and R.L. Beijersbergen. 2011. Screening for modulators of cisplatin sensitivity: unbiased screens reveal common themes. *Cell Cycle*. 10:380–386. doi:10.4161/cc.10.3.14642.

Nimonkar, A.V., J. Genschel, E. Kinoshita, P. Polaczek, J.L. Campbell, C. Wyman, P. Modrich, and S.C. Kowalczykowski. 2011. BLM-DNA2-RPA-MRN and EXO1-BLM-RPA-MRN constitute two DNA end resection machineries for human DNA break repair. *Genes Dev.* 25:350–362. doi:10.1101/gad.2003811.

Nishi, R., Y. Okuda, E. Watanabe, T. Mori, S. Iwai, C. Masutani, K. Sugasawa, and F. Hanaoka. 2005. Centrin 2 stimulates nucleotide excision repair by interacting with xeroderma pigmentosum group C protein. *Mol. Cell. Biol.* 25:5664–5674. doi:10.1128/MCB.25.13.5664-5674.2005.

Nojima, K., H. Hochegger, A. Saberi, T. Fukushima, K. Kikuchi, M. Yoshimura, B.J. Orelli, D.K. Bishop, S. Hirano, M. Ohzeki, M. Ishiai, K. Yamamoto, M. Takata, H. Arakawa, J.-M. Buerstedde, M. Yamazoe, T. Kawamoto, K. Araki, J.A. Takahashi, N. Hashimoto, S. Takeda, and E. Sonoda. 2005. Multiple repair pathways mediate tolerance to chemotherapeutic cross-linking agents in vertebrate cells. *Cancer Res*. 65:11704–11711. doi:10.1158/0008-5472.CAN-05-1214.

Noll, D.M., T.M. Mason, and P.S. Miller. 2006. Formation and Repair of Interstrand Cross-Links in DNA. *Chem Rev*. 106:277–301.

Norman, D., D. Live, M. Sastry, R. Lipman, B.E. Hingerty, M. Tomasz, S. Broyde, and D.J. Patel. 1990. NMR and computational characterization of mitomycin cross-linked to adjacent deoxyguanosines in the minor groove of the d(T-A-C-G-T-A).d(T-A-C-G-T-A) duplex. *Biochemistry*. 29:2861–2875.

Ochi, T., A.N. Blackford, J. Coates, S. Jhujh, S. Mehmood, N. Tamura, J. Travers, Q. Wu, V.M. Draviam, C.V. Robinson, T.L. Blundell, and S.P. Jackson. 2015. DNA

repair. PAXX, a paralog of XRCC4 and XLF, interacts with Ku to promote DNA double-strand break repair. *Science*. 347:185–188. doi:10.1126/science.1261971.

Ogi, T., S. Limsirichaikul, R.M. Overmeer, M. Volker, K. Takenaka, R. Cloney, Y. Nakazawa, A. Niimi, Y. Miki, N.G. Jaspers, L.H.F. Mullenders, S. Yamashita, M.I. Fousteri, and A.R. Lehmann. 2010. Three DNA polymerases, recruited by different mechanisms, carry out NER repair synthesis in human cells. *Mol. Cell*. 37:714–727. doi:10.1016/j.molcel.2010.02.009.

Ohmori, H., E.C. Friedberg, R.P. Fuchs, M.F. Goodman, F. Hanaoka, D. Hinkle, T.A. Kunkel, C.W. Lawrence, Z. Livneh, T. Nohmi, L. Prakash, S. Prakash, T. Todo, G.C. Walker, Z. Wang, and R. Woodgate. 2001. The Y-family of DNA polymerases. *Mol. Cell*. 8:7–8.

Ojwang, J.O., D.A. Grueneberg, and E.L. Loechler. 1989. Synthesis of a duplex oligonucleotide containing a nitrogen mustard interstrand DNA-DNA cross-link. *Cancer Res*. 49:6529–6537.

Olive, P.L., J.P. Banath and R.E. Durand. 1990. Heterogeneity in radiation-induced DNA damage and repair in tumour and normal cells measured using the "comet" assay. *Radiat Res.* 122:86-94.

Oliver, D.G., A.H. Sanders, R.D. Hogg, and J.W. Hellman. 1981. Thermal gradients in microtitration plates. Effects on enzyme-linked immunoassay. *J Immunol Methods*. 42:195–201.

Osawa, T., D. Davies, and J.A. Hartley. 2011. Mechanism of cell death resulting from DNA interstrand cross-linking in mammalian cells. *Cell Death Dis*. 2:e187. doi:10.1038/cddis.2011.70.

Ostling, O., and K.J. Johanson. 1984. Microelectrophoretic study of radiation-induced DNA damages in individual mammalian cells. *Biochem Biophys Res Commun*. 123:291–298.

Overmeer, R.M., J. Moser, M. Volker, H. Kool, A.E. Tomkinson, A.A. van Zeeland, L.H.F. Mullenders, and M. Fousteri. 2011. Replication protein A safeguards genome integrity by controlling NER incision events. *J Cell Biol*. 192:401–415. doi:10.1083/jcb.201006011.

Paeschke, K., M.L. Bochman, P.D. Garcia, P. Cejka, K.L. Friedman, S.C. Kowalczykowski, and V.A. Zakian. 2013. Pif1 family helicases suppress genome instability at G-quadruplex motifs. *Nature*. 497:458–462. doi:10.1038/nature12149.

Palombo, F., I. Iaccarino, E. Nakajima, M. Ikejima, T. Shimada, and J. Jiricny. 1996. hMutSbeta, a heterodimer of hMSH2 and hMSH3, binds to insertion/deletion loops in DNA. *Curr Biol*. 6:1181–1184.

Pang, D., S. Yoo, W.S. Dynan, M. Jung, and A. Dritschilo. 1997. Ku proteins join DNA fragments as shown by atomic force microscopy. *Cancer Res*. 57:1412–1415.

Park, C.H., D.E. Bergsagel, and E.A. McCulloch. 1971. Mouse myeloma tumor stem cells: a primary cell culture assay. *J. Natl. Cancer Inst.* 46:411–422.

Passegue, E., C.H.M. Jamieson, L.E. Ailles, and I.L. Weissman. 2003. Normal and leukemic hematopoiesis: are leukemias a stem cell disorder or a reacquisition of stem cell characteristics? *Proc. Natl. Acad. Sci. U.S.A.* 100 Suppl 1:11842–11849.

Pepe, A., and S.C. West. 2014. Substrate specificity of the MUS81-EME2 structure selective endonuclease. *Nucleic Acids Res.* 42:3833–3845. doi:10.1093/nar/gkt1333.

Perrimon, N., J.-Q. Ni, and L. Perkins. 2010. In vivo RNAi: today and tomorrow. *Cold Spring Harb Perspect Biol*. 2:a003640. doi:10.1101/cshperspect.a003640.

Persengiev, S.P., X. Zhu, and M.R. Green. 2004. Nonspecific, concentration-dependent stimulation and repression of mammalian gene expression by small interfering RNAs (siRNAs). *RNA*. 10:12–18.

Pfeiffer, P., W. Goedecke, and G. Obe. 2000. Mechanisms of DNA double-strand break repair and their potential to induce chromosomal aberrations. *Mutagenesis*. 15:289–302.

Pizzolato, J., S. Mukherjee, O.D. Schärer, and J. Jiricny. 2015. FANCD2-associated nuclease 1, but not exonuclease 1 or flap endonuclease 1, is able to unhook DNA interstrand cross-links in vitro. *J Biol Chem*. 290:22602–22611. doi:10.1074/jbc.M115.663666.

Pluciennik, A., L. Dzantiev, R.R. Iyer, N. Constantin, F.A. Kadyrov, and P. Modrich. 2010. PCNA function in the activation and strand direction of MutLalpha endonuclease in mismatch repair. *Proc. Natl. Acad. Sci. U.S.A.* 107:16066–16071. doi:10.1073/pnas.1010662107.

Poe, J.A., L. Vollmer, A. Vogt, and T.E. Smithgall. 2014. Development and validation of a high-content bimolecular fluorescence complementation assay for small-molecule inhibitors of HIV-1 Nef dimerization. *J Biomol Screen*. 19:556–565. doi:10.1177/1087057113513640.

Polo, S.E., A. Kaidi, L. Baskcomb, Y. Galanty, and S.P. Jackson. 2010. Regulation of DNA-damage responses and cell-cycle progression by the chromatin remodelling factor CHD4. *EMBO J.* 29:3130–3139.

Pontel, L.B., I.V. Rosado, G. Burgos-Barragan, J.I. Garaycoechea, R. Yu, M.J. Arends, G. Chandrasekaran, V. Broecker, W. Wei, L. Liu, J.A. Swenberg, G.P. Crossan, and K.J. Patel. 2015. Endogenous Formaldehyde Is a Hematopoietic Stem Cell Genotoxin and Metabolic Carcinogen. *Mol. Cell*. 60:177–188. doi:10.1016/j.molcel.2015.08.020.

Postel-Vinay, S., I. Bajrami, L. Friboulet, R. Elliott, Y. Fontebasso, N. Dorvault, K.A. Olaussen, F. André, J.-C. Soria, C.J. Lord, and A. Ashworth. 2013. A high-throughput screen identifies PARP1/2 inhibitors as a potential therapy for

ERCC1-deficient non-small cell lung cancer. *Oncogene*. 32:5377–5387. doi:10.1038/onc.2013.311.

Prakash, L., R.E. Johnson, M.T. Washington, L. Haracska, and S. Prakash. 2000. Eukaryotic polymerases [iota] and [zeta] act sequentially to bypass DNA lesions. *Nature*. 406:1015–1019. doi:10.1038/35023030.

Prakash, S., and L. Prakash. 2002. Translesion DNA synthesis in eukaryotes: a one- or two-polymerase affair. *Genes Dev.* 16:1872–1883. doi:10.1101/gad.1009802.

Price, P., and T.J. McMillan. 1990. Use of the tetrazolium assay in measuring the response of human tumor cells to ionizing radiation. *Cancer Res*. 50:1392–1396.

Qiu, J., Y. Qian, V. Chen, M.X. Guan, and B. Shen. 1999. Human exonuclease 1 functionally complements its yeast homologues in DNA recombination, RNA primer removal, and mutation avoidance. *J Biol Chem*. 274:17893–17900.

Quan, J., and T. Yusufzai. 2014. The tumor suppressor chromodomain helicase DNA-binding protein 5 (CHD5) remodels nucleosomes by unwrapping. *J Biol Chem*. 289:20717–20726. doi:10.1074/jbc.M114.568568.

Rajski, S.R., and R.M. Williams. 1998. DNA Cross-Linking Agents as Antitumor Drugs. *Chem Rev*. 98:2723–2796.

Rass, E., A. Grabarz, I. Plo, J. Gautier, P. Bertrand, and B.S. Lopez. 2009. Role of Mre11 in chromosomal nonhomologous end joining in mammalian cells. *Nat Struct Mol Biol*. 16:819–824. doi:10.1038/nsmb.1641.

Räschle, M., P. Knipscheer, P. Knipsheer, M. Enoiu, T. Angelov, J. Sun, J.D. Griffith, T.E. Ellenberger, O.D. Schärer, and J.C. Walter. 2008. Mechanism of replication-coupled DNA interstrand crosslink repair. *Cell*. 134:969–980. doi:10.1016/j.cell.2008.08.030.

Reardon, J.T., and A. Sancar. 2003. Recognition and repair of the cyclobutane thymine dimer, a major cause of skin cancers, by the human excision nuclease. *Genes Dev.* 17:2539–2551.

Rhodes, D.R., S. Kalyana-Sundaram, V. Mahavisno, R. Varambally, J. Yu, B.B. Briggs, T.R. Barrette, M.J. Anstet, C. Kincead-Beal, P. Kulkarni, S. Varambally, D. Ghosh, and A.M. Chinnaiyan. 2007. Oncomine 3.0: genes, pathways, and networks in a collection of 18,000 cancer gene expression profiles. *Neoplasia*. 9:166–180.

Ribeyre, C., J. Lopes, J.-B. Boule, A. Piazza, A. Guedin, V.A. Zakian, J.-L. Mergny, and A. Nicolas. 2009. The yeast Pif1 helicase prevents genomic instability caused by G-quadruplex-forming CEB1 sequences in vivo. *PLoS Genet.* 5:e1000475. doi:10.1371/journal.pgen.1000475.

Riedl, T., F. Hanaoka, and J.-M. Egly. 2003. The comings and goings of nucleotide excision repair factors on damaged DNA. *EMBO J.* 22:5293–5303.

doi:10.1093/emboj/cdg489.

Rink, S.M., and P.B. Hopkins. 1995. A mechlorethamine-induced DNA interstrand cross-link bends duplex DNA. *Biochemistry*. 34:1439–1445.

Rink, S.M., R. Lipman, S.C. Alley, P.B. Hopkins, and M. Tomasz. 1996. Bending of DNA by the mitomycin C-induced, GpG intrastrand cross-link. *Chem. Res. Toxicol.* 9:382–389.

Rohleder, F., J. Huang, Y. Xue, J. Kuper, A. Round, M. Seidman, W. Wang, and C. Kisker. 2016. FANCM interacts with PCNA to promote replication traverse of DNA interstrand crosslinks. *Nucleic Acids Res.* 44:3219–3232.

Rosado, I.V., W. Niedzwiedz, A.F. Alpi, and K.J. Patel. 2009. The Walker B motif in avian FANCM is required to limit sister chromatid exchanges but is dispensable for DNA crosslink repair. *Nucleic Acids Res.* 37:4360–4370. doi:10.1093/nar/gkp365.

Rosell, R., R.V.N. Lord, M. Taron, and N. Reguart. 2002. DNA repair and cisplatin resistance in non-small-cell lung cancer. *Lung Cancer*. 38:217–227.

ROSENBERG, B., L. Van Camp, E.B. Grimley, and A.J. Thomson. 1967. The inhibition of growth or cell division in Escherichia coli by different ionic species of platinum(IV) complexes. *J Biol Chem*. 242:1347–1352.

ROSENBERG, B., L. VANCAMP, and T. KRIGAS. 1965. INHIBITION OF CELL DIVISION IN ESCHERICHIA COLI BY ELECTROLYSIS PRODUCTS FROM A PLATINUM ELECTRODE. *Nature*. 205:698–699.

ROSENBERG, B., L. VANCAMP, J.E. Trosko, and V.H. Mansour. 1969. Platinum compounds: a new class of potent antitumour agents. *Nature*. 222:385–386.

Rosner, M., K. Schipany, and M. Hengstschläger. 2013. Merging high-quality biochemical fractionation with a refined flow cytometry approach to monitor nucleocytoplasmic protein expression throughout the unperturbed mammalian cell cycle. *Nat. Protocols*. 8:602–626. doi:10.1038/nprot.2013.011.

Rothfuss, A., and M. Grompe. 2004. Repair kinetics of genomic interstrand DNA cross-links: evidence for DNA double-strand break-dependent activation of the Fanconi anemia/BRCA pathway. *Mol. Cell. Biol.* 24:123–134.

Rothkamm, K., I. Krüger, L.H. Thompson, and M. Löbrich. 2003. Pathways of DNA Double-Strand Break Repair during the Mammalian Cell Cycle. *Mol. Cell. Biol.* 23:5706–5715.

Rupp, W.D., and P. Howard-Flanders. 1968. Discontinuities in the DNA synthesized in an excision-defective strain of Escherichia coli following ultraviolet irradiation. *J Mol Biol*. 31:291–304.

Saini, H.K., S. Griffiths-Jones, and A.J. Enright. 2007. Genomic analysis of human microRNA transcripts. *Proc. Natl. Acad. Sci. U.S.A.* 104:17719–17724.

doi:10.1073/pnas.0703890104.

Sale, J.E. 2013. Translesion DNA synthesis and mutagenesis in eukaryotes. *Cold Spring Harb Perspect Biol*. 5:a012708. doi:10.1101/cshperspect.a012708.

Sallmyr, A., A.E. Tomkinson, and F.V. Rassool. 2008. Up-regulation of WRN and DNA ligase III in chronic myeloid leukemia: consequences for the repair of DNA double-strand breaks. *Blood*. 112:1413–1423. doi:10.1182/blood-2007-07-104257.

Sancar, A. 2003. Structure and function of DNA photolyase and cryptochrome blue-light photoreceptors. *Chem Rev*. 103:2203–2237. doi:10.1021/cr0204348.

Sanders, C.M. 2010. Human Pif1 helicase is a G-quadruplex DNA-binding protein with G-quadruplex DNA-unwinding activity. *Biochem J*. 430:119–128. doi:10.1042/BJ20100612.

Sanderson, B.J., and A.J. Shield. 1996. Mutagenic damage to mammalian cells by therapeutic alkylating agents. *Mutat. Res.* 355:41–57.

Sarkar, S., A.A. Davies, H.D. Ulrich, and P.J. McHugh. 2006. DNA interstrand crosslink repair during G1 involves nucleotide excision repair and DNA polymerase zeta. *EMBO J.* 25:1285–1294. doi:10.1038/sj.emboj.7600993.

Schärer, O.D. 2005. DNA interstrand crosslinks: natural and drug-induced DNA adducts that induce unique cellular responses. *Chembiochem*. 6:27–32. doi:10.1002/cbic.200400287.

Schulz, V.P., and V.A. Zakian. 1994. The saccharomyces PIF1 DNA helicase inhibits telomere elongation and de novo telomere formation. *Cell*. 76:145–155.

Schwacha, A., and N. Kleckner. 1995. Identification of double Holliday junctions as intermediates in meiotic recombination. *Cell*. 83:783–791.

Schwertman, P., A. Lagarou, D.H.W. Dekkers, A. Raams, A.C. van der Hoek, C. Laffeber, J.H.J. Hoeijmakers, J.A.A. Demmers, M. Fousteri, W. Vermeulen, and J.A. Marteijn. 2012. UV-sensitive syndrome protein UVSSA recruits USP7 to regulate transcription-coupled repair. *Nat Genet*. 44:598–602. doi:10.1038/ng.2230.

Semlow, D.R., J. Zhang, M. Budzowska, A.C. Drohat, and J.C. Walter. 2016. Replication-Dependent Unhooking of DNA Interstrand Cross-Links by the NEIL3 Glycosylase. *Cell*. 167:498–511.e14. doi:10.1016/j.cell.2016.09.008.

Sengerová, B., C.K. Allerston, M. Abu, S.Y. Lee, J. Hartley, K. Kiakos, C.J. Schofield, J.A. Hartley, O. Gileadi, and P.J. McHugh. 2012. Characterization of the human SNM1A and SNM1B/Apollo DNA repair exonucleases. *J Biol Chem*. 287:26254–26267. doi:10.1074/jbc.M112.367243.

Shachar, S., O. Ziv, S. Avkin, S. Adar, J. Wittschieben, T. Reissner, S. Chaney, E.C. Friedberg, Z. Wang, T. Carell, N. Geacintov, and Z. Livneh. 2009. Two-

polymerase mechanisms dictate error-free and error-prone translesion DNA synthesis in mammals. *EMBO J.* 28:383–393. doi:10.1038/emboj.2008.281.

Shalem, O., N.E. Sanjana, E. Hartenian, X. Shi, D.A. Scott, T.S. Mikkelsen, D. Heckl, B.L. Ebert, D.E. Root, J.G. Doench, and F. Zhang. 2014. Genome-Scale CRISPR-Cas9 Knockout Screening in Human Cells. *Science*. 343:84–87. doi:10.1126/science.1247005.

Shaw, A.T., D.-W. Kim, K. Nakagawa, T. Seto, L. Crinó, M.-J. Ahn, T. De Pas, B. Besse, B.J. Solomon, F. Blackhall, Y.-L. Wu, M. Thomas, K.J. O'Byrne, D. Moro-Sibilot, D.R. Camidge, T. Mok, V. Hirsh, G.J. Riely, S. Iyer, V. Tassell, A. Polli, K.D. Wilner, and P.A. Jänne. 2013. Crizotinib versus Chemotherapy in Advanced ALK-Positive Lung Cancer. *N Engl J Med*. 368:2385–2394. doi:10.1056/NEJMoa1214886.

Shen, X., S. Jun, L.E. O'Neal, E. Sonoda, M. Bemark, J.E. Sale, and L. Li. 2006. REV3 and REV1 Play Major Roles in Recombination-independent Repair of DNA Interstrand Cross-links Mediated by Monoubiquitinated Proliferating Cell Nuclear Antigen (PCNA). *Journal of Biological Chemistry*. 281:13869–13872.

Sigoillot, F.D., and R.W. King. 2011. Vigilance and validation: Keys to success in RNAi screening. *ACS Chem Biol*. 6:47–60. doi:10.1021/cb100358f.

Sigurdsson, S., A.B. Dirac-Svejstrup, and J.Q. Svejstrup. 2010. Evidence that transcript cleavage is essential for RNA polymerase II transcription and cell viability. *Mol. Cell*. 38:202–210. doi:10.1016/j.molcel.2010.02.026.

Sijbers, A.M., W.L. de Laat, R.R. Ariza, M. Biggerstaff, Y.F. Wei, J.G. Moggs, K.C. Carter, B.K. Shell, E. Evans, M.C. de Jong, S. Rademakers, J. de Rooij, N.G. Jaspers, J.H. Hoeijmakers, and R.D. Wood. 1996. Xeroderma pigmentosum group F caused by a defect in a structure-specific DNA repair endonuclease. *Cell*. 86:811–822. doi:10.1016/S0092-8674(00)80155-5.

Simon, J.A., P. Szankasi, D.K. Nguyen, C. Ludlow, H.M. Dunstan, C.J. Roberts, E.L. Jensen, L.H. Hartwell, and S.H. Friend. 2000. Differential toxicities of anticancer agents among DNA repair and checkpoint mutants of Saccharomyces cerevisiae. *Cancer Res*. 60:328–333.

Sin, O., H. Michels, and E.A.A. Nollen. 2014. Genetic screens in Caenorhabditis elegans models for neurodegenerative diseases. *From genome to function*. 1842:1951–1959.

Singh, S.K., I.D. Clarke, M. Terasaki, V.E. Bonn, C. Hawkins, J. Squire, and P.B. Dirks. 2003. Identification of a cancer stem cell in human brain tumors. *Cancer Res*. 63:5821–5828.

Singh, T.R., S.T. Bakker, S. Agarwal, M. Jansen, E. Grassman, B.C. Godthelp, A.M. Ali, C.-H. Du, M.A. Rooimans, Q. Fan, K. Wahengbam, J. Steltenpool, P.R. Andreassen, D.A. Williams, H. Joenje, J.P. de Winter, and A.R. Meetei. 2009. Impaired FANCD2 monoubiquitination and hypersensitivity to camptothecin uniquely characterize Fanconi anemia complementation group M. *Blood*. 114:174–180.

doi:10.1182/blood-2009-02-207811.

Sinha, R.P., and D.P. Hader. 2002. UV-induced DNA damage and repair: a review. *Photochem Photobiol Sci*. 1:225–236.

Sioud, M. 2005. Induction of inflammatory cytokines and interferon responses by double-stranded and single-stranded siRNAs is sequence-dependent and requires endosomal localization. *J Mol Biol*. 348:1079–1090. doi:10.1016/j.jmb.2005.03.013.

Sladek, F.M., M.M. Munn, W.D. Rupp, and P. Howard-Flanders. 1989. In vitro repair of psoralen-DNA cross-links by RecA, UvrABC, and the 5'-exonuclease of DNA polymerase I. *J Biol Chem*. 264:6755–6765.

Smeaton, M.B., E.M. Hlavin, T. McGregor Mason, A.M. Noronha, C.J. Wilds, and P.S. Miller. 2008. Distortion-Dependent Unhooking of Interstrand Cross-Links in Mammalian Cell Extracts ? *Biochemistry*. 47:9920–9930. doi:10.1021/bi800925e.

Smogorzewska, A., R. Desetty, T.T. Saito, M. Schlabach, F.P. Lach, M.E. Sowa, A.B. Clark, T.A. Kunkel, J.W. Harper, M.P. Colaiácovo, and S.J. Elledge. 2010. A genetic screen identifies FAN1, a Fanconi anemia associated nuclease necessary for DNA interstrand crosslink repair. *Mol. Cell*. 39:36–47.

Sollier, J., and K.A. Cimprich. 2015. Breaking bad: R-loops and genome integrity. *Trends Cell Biol*. 25:514–522. doi:10.1016/j.tcb.2015.05.003.

Sorensen, C.S., L.T. Hansen, J. Dziegielewski, R.G. Syljuasen, C. Lundin, J. Bartek, and T. Helleday. 2005. The cell-cycle checkpoint kinase Chk1 is required for mammalian homologous recombination repair. *Nat Cell Biol*. 7:195–201. doi:10.1038/ncb1212.

Spangrude, G.J., S. Heimfeld, and I.L. Weissman. 1988. Purification and characterization of mouse hematopoietic stem cells. *Science*. 241:58–62. doi:10.1126/science.2898810.

Spanswick, V.J., J.M. Hartley, and J.A. Hartley. 2010. Measurement of DNA interstrand crosslinking in individual cells using the Single Cell Gel Electrophoresis (Comet) assay. *Methods Mol Biol*. 613:267–282. doi:10.1007/978-1-60327-418-0_17.

Statistical Bulletin. 2016. Statistical Bulletin. 1–17.

Stern, R.S. 2007. Psoralen and Ultraviolet A Light Therapy for Psoriasis. *N Engl J Med*. 357:682–690. doi:10.1056/NEJMct072317.

Stone, M.P., Y.-J. Cho, H. Huang, H.-Y. Kim, I.D. Kozekov, A. Kozekova, H. Wang, I.G. Minko, R.S. Lloyd, T.M. Harris, and C.J. Rizzo. 2008. Interstrand DNA cross-links induced by alpha,beta-unsaturated aldehydes derived from lipid peroxidation and environmental sources. *Acc. Chem. Res.* 41:793–804. doi:10.1021/ar700246x.

Sun, D., R. Urrabaz, M. Nguyen, J. Marty, S. Stringer, E. Cruz, L. Medina-Gundrum, and S. Weitman. 2001. Elevated expression of DNA ligase I in human cancers. *Clin Cancer Res*. 7:4143–4148.

Swanton, C., M. Marani, O. Pardo, P.H. Warne, G. Kelly, E. Sahai, F. Elustondo, J. Chang, J. Temple, A.A. Ahmed, J.D. Brenton, J. Downward, and B. Nicke. 2007. Regulators of mitotic arrest and ceramide metabolism are determinants of sensitivity to paclitaxel and other chemotherapeutic drugs. *Cancer Cell*. 11:498–512. doi:10.1016/j.ccr.2007.04.011.

Symington, L.S., and J. Gautier. 2011. Double-strand break end resection and repair pathway choice. *Annu Rev Genet*. 45:247–271. doi:10.1146/annurev-genet-110410-132435.

Taccioli, G.E., T.M. Gottlieb, T. Blunt, A. Priestley, J. Demengeot, R. Mizuta, A.R. Lehmann, F.W. Alt, S.P. Jackson, and P.A. Jeggo. 1994. Ku80: product of the XRCC5 gene and its role in DNA repair and V(D)J recombination. *Science*. 265:1442–1445.

Tapias, A., J. Auriol, D. Forget, J.H. Enzlin, O.D. Schärer, F. Coin, B. Coulombe, and J.-M. Egly. 2004. Ordered conformational changes in damaged DNA induced by nucleotide excision repair factors. *J Biol Chem*. 279:19074–19083.

Tiraby, J.G., and M.S. Fox. 1973. Marker discrimination in transformation and mutation of pneumococcus. *Proc. Natl. Acad. Sci. U.S.A.* 70:3541–3545.

Tiwana, G.S., R. Prevo, F.M. Buffa, S. Yu, D.V. Ebner, A. Howarth, L.K. Folkes, B. Budwal, K.-Y. Chu, L. Durrant, R.J. Muschel, W.G. McKenna, and G.S. Higgins. 2015. Identification of vitamin B1 metabolism as a tumor-specific radiosensitizing pathway using a high-throughput colony formation screen. *Oncotarget; Vol 6, No 8*.

Tobey, R.A., and H.A. Crissman. 1972. Preparation of large quantities of synchronized mammalian cells in late G1 in the pre-DNA replicative phase of the cell cycle. *Exp Cell Res*. 75:460–464.

Tobin, L.A., C. Robert, A.P. Rapoport, I. Gojo, M.R. Baer, A.E. Tomkinson, and F.V. Rassool. 2013. Targeting abnormal DNA double-strand break repair in tyrosine kinase inhibitor-resistant chronic myeloid leukemias. *Oncogene*. 32:1784–1793. doi:10.1038/onc.2012.203.

Tokuda, K., and W.J. Bodell. 1987. Cytotoxicity and sister chromatid exchanges in 9L cells treated with monofunctional and bifunctional nitrogen mustards. *Carcinogenesis*. 8:1697–1701.

Tomkinson, A.E., and Z.B. Mackey. 1998. Structure and function of mammalian DNA ligases. *Mutat. Res.* 407:1–9.

Tomkinson, A.E., L. Chen, Z. Dong, J.B. Leppard, D.S. Levin, Z.B. Mackey, and T.A. Motycka. 2001. Completion of base excision repair by mammalian DNA ligases. 68. 14 pp.

Trakselis, M.A., M.M. Seidman, and R.M. Brosh Jr. Mechanistic insights into how CMG helicase facilitates replication past DNA roadblocks. *Genome maintenance in the Nervous system*. 55 IS -:76–82.

Travis, L.B., E.J. Holowaty, K. Bergfeldt, C.F. Lynch, B.A. Kohler, T. Wiklund, R.E. Curtis, P. Hall, M. Andersson, E. Pukkala, J. Sturgeon, and M. Stovall. 1999. Risk of leukemia after platinum-based chemotherapy for ovarian cancer. *N Engl J Med*. 340:351–357. doi:10.1056/NEJM199902043400504.

Tuschl, T., P.D. Zamore, R. Lehmann, D.P. Bartel, and P.A. Sharp. 1999. Targeted mRNA degradation by double-stranded RNA in vitro. *Genes Dev.* 13:3191–3197.

Tzatsos, A., P. Paskaleva, F. Ferrari, V. Deshpande, S. Stoykova, G. Contino, K.-K. Wong, F. Lan, P. Trojer, and P.J. Park. 2013. KDM2B promotes pancreatic cancer via Polycomb-dependent and-independent transcriptional programs. *J Clin Invest*. 123:727–739.

Tzatsos, A., R. Pfau, S.C. Kampranis, and P.N. Tsichlis. 2009. Ndy1/KDM2B immortalizes mouse embryonic fibroblasts by repressing the Ink4a/Arf locus. *Proc. Natl. Acad. Sci. U.S.A.* 106:2641–2646.

Uematsu, N., E. Weterings, K.-I. Yano, K. Morotomi-Yano, B. Jakob, G. Taucher-Scholz, P.-O. Mari, D.C. van Gent, B.P.C. Chen, and D.J. Chen. 2007. Autophosphorylation of DNA-PKCS regulates its dynamics at DNA double-strand breaks. *J Cell Biol*. 177:219–229. doi:10.1083/jcb.200608077.

Van Houten, B., H. Gamper, J.E. Hearst, and A. Sancar. 1986a. Construction of DNA substrates modified with psoralen at a unique site and study of the action mechanism of ABC excinuclease on these uniformly modified substrates. *J Biol Chem*. 261:14135–14141.

Van Houten, B., H. Gamper, S.R. Holbrook, J.E. Hearst, and A. Sancar. 1986b. Action mechanism of ABC excision nuclease on a DNA substrate containing a psoralen crosslink at a defined position. *Proc. Natl. Acad. Sci. U.S.A.* 83:8077–8081.

Vogel, E.W., A. Barbin, M.J. Nivard, H.F. Stack, M.D. Waters, and P.H. Lohman. 1998. Heritable and cancer risks of exposures to anticancer drugs: inter-species comparisons of covalent deoxyribonucleic acid-binding agents. *Mutat. Res.* 400:509–540.

Vogel, E.W., M.J. Nivard, L.A. Ballering, H. Bartsch, A. Barbin, J. Nair, M.A. Comendador, L.M. Sierra, I. Aguirrezabalaga, L. Tosal, L. Ehrenberg, R.P. Fuchs, R. Janel-Bintz, G. Maenhaut-Michel, R. Montesano, J. Hall, H. Kang, M. Miele, J. Thomale, K. Bender, J. Engelbergs, and M.F. Rajewsky. 1996. DNA damage and repair in mutagenesis and carcinogenesis: implications of structure-activity relationships for cross-species extrapolation. *Mutat. Res.* 353:177–218.

Vogelstein, B., E.R. Fearon, S.R. Hamilton, S.E. Kern, A.C. Preisinger, M. Leppert, Y. Nakamura, R. White, A.M. Smits, and J.L. Bos. 1988. Genetic alterations during colorectal-tumor development. *N Engl J Med*. 319:525–532.

doi:10.1056/NEJM198809013190901.

Voulgaridou, G.-P., I. Anestopoulos, R. Franco, M.I. Panayiotidis, and A. Pappa. 2011. DNA damage induced by endogenous aldehydes: current state of knowledge. *Mutat. Res.* 711:13–27. doi:10.1016/j.mrfmmm.2011.03.006.

Wagner, R., Jr, and M. Meselson. 1976. Repair tracts in mismatched DNA heteroduplexes. *Proc. Natl. Acad. Sci. U.S.A.* 73:4135–4139.

Wakasugi, M., A. Kawashima, H. Morioka, S. Linn, A. Sancar, T. Mori, O. Nikaido, and T. Matsunaga. 2002. DDB accumulates at DNA damage sites immediately after UV irradiation and directly stimulates nucleotide excision repair. *J Biol Chem*. 277:1637–1640.

Wang, A.T., B. Sengerová, E. Cattell, T. Inagawa, J.M. Hartley, K. Kiakos, N.A. Burgess-Brown, L.P. Swift, J.H. Enzlin, C.J. Schofield, O. Gileadi, J.A. Hartley, and P.J. McHugh. 2011. Human SNM1A and XPF-ERCC1 collaborate to initiate DNA interstrand cross-link repair. *Genes Dev.* 25:1859–1870. doi:10.1101/gad.15699211.

Wang, H. 2005. DNA Ligase III as a Candidate Component of Backup Pathways of Nonhomologous End Joining. *Cancer Res*. 65:4020–4030. doi:10.1158/0008-5472.CAN-04-3055.

Wang, H., A.R. Perrault, Y. Takeda, W. Qin, H. Wang, and G. Iliakis. 2003. Biochemical evidence for Ku-independent backup pathways of NHEJ. *Nucleic Acids Res.* 31:5377–5388.

Wang, M., E.J. McIntee, G. Cheng, Y. Shi, P.W. Villalta, and S.S. Hecht. 2000. Identification of DNA adducts of acetaldehyde. *Chem. Res. Toxicol.* 13:1149–1157.

Wang, T., J.J. Wei, D.M. Sabatini, and E.S. Lander. 2014. Genetic Screens in Human Cells Using the CRISPR-Cas9 System. *Science*. 343:80–84. doi:10.1126/science.1246981.

Wang, X., C.A. Peterson, H. Zheng, R.S. Nairn, R.J. Legerski, and L. Li. 2001a. Involvement of nucleotide excision repair in a recombination-independent and error-prone pathway of DNA interstrand cross-link repair. *Mol. Cell. Biol.* 21:713–720. doi:10.1128/MCB.21.3.713-720.2001.

Wang, X., C.A. Peterson, H. Zheng, R.S. Nairn, R.J. Legerski, and L. Li. 2001b. Involvement of Nucleotide Excision Repair in a Recombination-Independent and Error-Prone Pathway of DNA Interstrand Cross-Link Repair. *Mol. Cell. Biol.* 21:713–720.

Wang, Y., J.W. Leung, Y. Jiang, M.G. Lowery, H. Do, K.M. Vasquez, J. Chen, W. Wang, and L. Li. 2013. FANCM and FAAP24 maintain genome stability via cooperative as well as unique functions. *Mol. Cell*. 49:997–1009. doi:10.1016/j.molcel.2012.12.010.

Warren, J.J., T.J. Pohlhaus, A. Changela, R.R. Iyer, P.L. Modrich, and L.S. Beese. 2007. Structure of the human MutSalpha DNA lesion recognition complex. *Mol. Cell*. 26:579–592. doi:10.1016/j.molcel.2007.04.018.

Watanabe, N., D.A. Dickinson, R.-M. Liu, and H.J. Forman. 2004. Quinones and glutathione metabolism. *Methods Enzymol*. 378:319–340.

Watanabe, T., Y. Totoki, A. Toyoda, M. Kaneda, S. Kuramochi-Miyagawa, Y. Obata, H. Chiba, Y. Kohara, T. Kono, T. Nakano, M.A. Surani, Y. Sakaki, and H. Sasaki. 2008. Endogenous siRNAs from naturally formed dsRNAs regulate transcripts in mouse oocytes. *Nature*. 453:539–543. doi:10.1038/nature06908.

Wiederhold, L., J.B. Leppard, P. Kedar, F. Karimi-Busheri, A. Rasouli-Nia, M. Weinfeld, A.E. Tomkinson, T. Izumi, R. Prasad, S.H. Wilson, S. Mitra, and T.K. Hazra. 2004. AP endonuclease-independent DNA base excision repair in human cells. *Mol. Cell*. 15:209–220.

Wijen, J.P., M.J. Nivard, and E.W. Vogel. 2000. The in vivo genetic activity profile of the monofunctional nitrogen mustard 2-chloroethylamine differs drastically from its bifunctional counterpart mechlorethamine. *Carcinogenesis*. 21:1859–1867.

Williams, H.L., M.E. Gottesman, and J. Gautier. 2012. Replication-independent repair of DNA interstrand crosslinks. *Mol. Cell*. 47:140–147. doi:10.1016/j.molcel.2012.05.001.

Williamson, C.E., and B. Witten. 1967. Reaction mechanism of some aromatic nitrogen mustards. *Cancer Res*. 27:33–38.

Wilson, M.A., Y. Kwon, Y. Xu, W.-H. Chung, P. Chi, H. Niu, R. Mayle, X. Chen, A. Malkova, P. Sung, and G. Ira. 2013. Pif1 helicase and Polδ promote recombination-coupled DNA synthesis via bubble migration. *Nature*. 502:393–396. doi:10.1038/nature12585.

Wilson, S.H. 1998. Mammalian base excision repair and DNA polymerase beta. *Mutation Research/DNA Repair*. 407:203–215.

Wilson, S.H., and T.A. Kunkel. 2000. Passing the baton in base excision repair. *Nature Structural Biology*. 7:176–178.

Wolski, S.C., J. Kuper, P. Hanzelmann, J.J. Truglio, D.L. Croteau, B. Van Houten, and C. Kisker. 2008. Crystal structure of the FeS cluster-containing nucleotide excision repair helicase XPD. *PLoS Biol*. 6:e149. doi:10.1371/journal.pbio.0060149.

Woodbine, L., H. Brunton, A.A. Goodarzi, A. Shibata, and P.A. Jeggo. 2011. Endogenously induced DNA double strand breaks arise in heterochromatic DNA regions and require ataxia telangiectasia mutated and Artemis for their repair. *Nucleic Acids Res.* 39:6986–6997. doi:10.1093/nar/gkr331.

Woodgate, R. 2001. Evolution of the two-step model for UV-mutagenesis. *Mutat.*

*Res.* 485:83–92.

Wu, H.I., J.A. Brown, M.J. Dorie, L. Lazzeroni, and J.M. Brown. 2004. Genome-wide identification of genes conferring resistance to the anticancer agents cisplatin, oxaliplatin, and mitomycin C. *Cancer Res*. 64:3940–3948.

Wu, L., and I.D. Hickson. 2003. The Bloom's syndrome helicase suppresses crossing over during homologous recombination. *Nature*. 426:870–874. doi:10.1038/nature02253.

Wu, Q., L.A. Christensen, R.J. Legerski, and K.M. Vasquez. 2005. Mismatch repair participates in error-free processing of DNA interstrand crosslinks in human cells. *EMBO Rep*. 6:551–556.

Wu, W., M. Wang, T. Mussfeldt, and G. Iliakis. 2008a. Enhanced use of backup pathways of NHEJ in G2 in Chinese hamster mutant cells with defects in the classical pathway of NHEJ. *Radiat Res*. 170:512–520.

Wu, W., M. Wang, W. Wu, S.K. Singh, T. Mussfeldt, and G. Iliakis. 2008b. Repair of radiation induced DNA double strand breaks by backup NHEJ is enhanced in G2. *DNA Repair (Amst)*. 7:329–338. doi:10.1016/j.dnarep.2007.11.008.

Wynne, P., C. Newton, J.A. Ledermann, A. Olaitan, T.A. Mould, and J.A. Hartley. 2007. Enhanced repair of DNA interstrand crosslinking in ovarian cancer cells from patients following treatment with platinum-based chemotherapy. *Br. J. Cancer*. 97:927–933. doi:10.1038/sj.bjc.6603973.

Yaghi, B.M., P.M. Turner, W.A. Denny, P.R. Turner, C.J. O'Connor, and L.R. Ferguson. 1998. Comparative mutational spectra of the nitrogen mustard chlorambucil and its half-mustard analogue in Chinese hamster AS52 cells. *Mutat. Res.* 401:153–164.

Yamamoto, K.N., S. Kobayashi, M. Tsuda, H. Kurumizaka, M. Takata, K. Kono, J. Jiricny, S. Takeda, and K. Hirota. 2011. Involvement of SLX4 in interstrand cross-link repair is regulated by the Fanconi anemia pathway. *Proc. Natl. Acad. Sci. U.S.A.* 108:6492–6496.

Yan, Z., M. Delannoy, C. Ling, D. Daee, F. Osman, P.A. Muniandy, X. Shen, A.B. Oostra, H. Du, J. Steltenpool, T. Lin, B. Schuster, C. Decaillet, A. Stasiak, A.Z. Stasiak, S. Stone, M.E. Hoatlin, D. Schindler, C.L. Woodcock, H. Joenje, R. Sen, J.P. de Winter, L. Li, M.M. Seidman, M.C. Whitby, K. Myung, A. Constantinou, and W. Wang. 2010. A histone-fold complex and FANCM form a conserved DNA-remodeling complex to maintain genome stability. *Mol. Cell*. 37:865–878. doi:10.1016/j.molcel.2010.01.039.

Yaneva, M., T. Kowalewski, and M.R. Lieber. 1997. Interaction of DNA-dependent protein kinase with DNA and with Ku: biochemical and atomic-force microscopy studies. *EMBO J.* 16:5098–5112. doi:10.1093/emboj/16.16.5098.

Yang, Z., M.I. Nejad, J.G. Varela, N.E. Price, Y. Wang, and K.S. Gates. 2017. A role for the base excision repair enzyme NEIL3 in replication-dependent repair of

interstrand DNA cross-links derived from psoralen and abasic sites. *DNA Repair (Amst)*. 52:1–11. doi:10.1016/j.dnarep.2017.02.011.

Yano, K.-I., and D.J. Chen. 2014. Live cell imaging of XLF and XRCC4 reveals a novel view of protein assembly in the non-homologous end-joining pathway. *Cell Cycle*. 7:1321–1325. doi:10.4161/cc.7.10.5898.

Yano, K.-I., K. Morotomi-Yano, K.-J. Lee, and D.J. Chen. Functional significance of the interaction with Ku in DNA double-strand break recognition of XLF. *FEBS Letters*. 585:841–846.

Yano, K.-I., K. Morotomi-Yano, S.-Y. Wang, N. Uematsu, K.-J. Lee, A. Asaithamby, E. Weterings, and D.J. Chen. 2008. Ku recruits XLF to DNA double-strand breaks. *EMBO Rep*. 9:91–96. doi:10.1038/sj.embor.7401137.

Yardimci, H., X. Wang, A.B. Loveland, I. Tappin, D.Z. Rudner, J. Hurwitz, A.M. van Oijen, and J.C. Walter. 2012. Bypass of a protein barrier by a replicative DNA helicase. *Nature*. 492:205–209. doi:10.1038/nature11730.

Yokoi, M., C. Masutani, T. Maekawa, K. Sugasawa, Y. Ohkuma, and F. Hanaoka. 2000. The xeroderma pigmentosum group C protein complex XPC-HR23B plays an important role in the recruitment of transcription factor IIH to damaged DNA. *J Biol Chem*. 275:9870–9875.

Zhang, Chung, Oldenburg. 1999. A Simple Statistical Parameter for Use in Evaluation and Validation of High Throughput Screening Assays. *J Biomol Screen*. 4:67–73. doi:10.1177/108705719900400206.

Zhang, D.-H., B. Zhou, Y. Huang, L.-X. Xu, and J.-Q. Zhou. 2006. The human Pif1 helicase, a potential Escherichia coli RecD homologue, inhibits telomerase activity. *Nucleic Acids Res.* 34:1393–1404. doi:10.1093/nar/gkl029.

Zhang, N., X. Lu, and R.J. Legerski. Partial reconstitution of human interstrand cross-link repair in vitro: characterization of the roles of RPA and PCNA. *Biochem Biophys Res Commun*. 309:71–78.

Zhang, N., X. Lu, X. Zhang, C.A. Peterson, and R.J. Legerski. 2002. hMutSbeta is required for the recognition and uncoupling of psoralen interstrand cross-links in vitro. *Mol. Cell. Biol.* 22:2388–2397.

Zhang, Z., W. Hu, L. Cano, T.D. Lee, D.J. Chen, and Y. Chen. Solution Structure of the C-Terminal Domain of Ku80 Suggests Important Sites for Protein-Protein Interactions. *Structure*. 12:495–502.

Zhao, J., A. Jain, R.R. Iyer, P.L. Modrich, and K.M. Vasquez. 2009. Mismatch repair and nucleotide excision repair proteins cooperate in the recognition of DNA interstrand crosslinks. *Nucleic Acids Res.* 37:4420–4429. doi:10.1093/nar/gkp399.

Zheng, H., X. Wang, A.J. Warren, R.J. Legerski, R.S. Nairn, J.W. Hamilton, and L. Li. 2003. Nucleotide excision repair- and polymerase eta-mediated error-prone

removal of mitomycin C interstrand cross-links. *Mol. Cell. Biol.* 23:754–761.

Zheng, M., S.E. Morgan-Lappe, J. Yang, K.M. Bockbrader, D. Pamarthy, D. Thomas, S.W. Fesik, and Y. Sun. 2008. Growth inhibition and radiosensitization of glioblastoma and lung cancer cells by small interfering RNA silencing of tumor necrosis factor receptor-associated factor 2. *Cancer Res*. 68:7570–7578. doi:10.1158/0008-5472.CAN-08-0632.

Zhou, H., M. Xu, Q. Huang, A.T. Gates, X.D. Zhang, J.C. Castle, E. Stec, M. Ferrer, B. Strulovici, D.J. Hazuda, and A.S. Espeseth. 2008. Genome-Scale RNAi Screen for Host Factors Required for HIV Replication. *Cell Host & Microbe*. 4:495–504. doi:10.1016/j.chom.2008.10.004.

Zhu, G., and S.J. Lippard. 2009. Photoaffinity labeling reveals nuclear proteins that uniquely recognize cisplatin-DNA interstrand cross-links. *Biochemistry*. 48:4916–4925. doi:10.1021/bi900389b.

Zietlow, L., L.A. Smith, M. Bessho, and T. Bessho. 2009. Evidence for the involvement of human DNA polymerase N in the repair of DNA interstrand cross-links. *Biochemistry*. 48:11817–11824. doi:10.1021/bi9015346.